MITOCHONDRIAL REGULATION OF APOPTOSIS DURING B CELL SELECTION

by

Elad Katz

A thesis submitted to the University of Glasgow
for the degree of Doctor of Philosophy

Faculty of Medicine, University of Glasgow

Department of Immunology
Western Infirmary
Glasgow G11 6NT

Submitted: October 2000

ProQuest LLC.
789 East Eisenhower Parkway
P.O. Box 1346
Ann Arbor, MI 48106 – 1346

Table of contents

List of figures and tables

Acknowledgements

It is a pleasure to thank Dr. Maggie Harnett for having me in her lab for the duration of this PhD work, investing a long time in getting the work (and me) right. I would also like to thank members, past and present, of the lab for their help regarding science and otherwise and especially to Sandra Seatter and Caroline Lord who conducted some of the experiments with me. Special thanks go to Maureen Deehan, who apart for being great to work with and a good friend also contributed to making this thesis clearer.

Many people in the Department of Immunology in University of Glasgow have helped during the course of the work in reagents and advise: Claire Adams, Jim Brewer, Ehsan Esfandiari and Karen Smith. Thanks, too, to Dr. Billy Harnett's lab in University of Strathclyde, especially to Emma Wilson who helped with all things relating to ES-62. I would like also to thank Dr. Matt van der Heiden (now at University of Chicago) for his help and advice in mitochondrial matters. It is also an honour to thank Prof. John Monroe (University of Pennsylvania) for the unique opportunity to discuss in length the context of my immature B cells results.

Lastly, I would like to thank my family and friends, here and abroad, for their belief in my abilities, which in many cases override my own doubts.

This work received the financial support of Tenovus (Scotland), The Overseas Research Students Awards Scheme, University of Glasgow Clinical Medicine Planning Unit and B'nai B'rith (London).

Summary

This thesis has focused on identifying key signalling events during antigen-driven B cell development, particularly those concerned with the regulation and commitment to apoptosis. The research comprised both biochemical and physiological aspects of cell fate decisions, mainly focusing on the immature-mature B cell transition, as well as other later selection events in the spleen, lymph nodes and the peritoneal cavity. With respect to the molecular aspects, the work has concentrated mainly on identifying mitochondria-related changes and the role of cell cycle proteins in the events downstream of B cell receptor (BCR) ligation which lead to apoptosis. A novel phospholipase A_2-dependent mechanism of mitochondrial disruption was identified as being responsible for the transduction of antigen receptor-mediated apoptosis of an immature B cell line, WEHI-231. The product of phospholipase A_2, arachidonic acid, rather than one of its metabolites, directly causes a collapse in the mitochondrial potential which results in apoptosis. Regulation of this mitochondrial dysfunction also involves the Bcl-2 family. Pro-apoptotic and anti-apoptotic members of this family are both elevated in response to BCR stimulation. Nonetheless, a rescue signal via CD40 elevates Bcl-x_L expression and prevents Bid and Bad from translocating to the mitochondria. Indeed, Bcl-x_L overexpression is sufficient to reverse both BCR and arachidonic acid-induced apoptosis in WEHI-231 cells. Intriguingly, this novel cPLA$_2$-dependent pathway of BCR-induced apoptosis in WEHI-231 is executed in a Caspase-independent manner and hence differs from the classical description of apoptosis. This novel form of apoptosis appears to be excuted by Cathepsin B which appears to act as an alternative killer protease to exert the destruction of cell components.

In order to address the physiological relevance of these findings, an *ex vivo* model has also been devised to study the development of immature B cells in the bone marrow. This model has been used to identify the major cellular intermediates in this process and to observe some of the signals required for immature and transitional B cell selection. The detection of different B cell populations and determination of their cell cycle profiles, after BCR stimulation, has allowed the determination of sequence of events during B cell selection. For example, immature B cell apoptosis bears some of the hallmarks of the mechanisms identified in WEHI-231 B cells. In addition, this model has made it possible to examine the key factors regulating transitional B cell deletion. Interestingly, the use of *Xid* mice, which are defient in the PTK Btk, showed that Btk was essential for the maturation of transitional B cells in response to BCR stimulation. Moreover, it was shown that transitional B cells can undergo apoptosis in response to anti-Fas treatment and this may involve also a collapse in the mitochondrial potential. Further work with cells from mice immunocompromised by a parasite-derived molecule, ES-62 which is capable of desensitising BCR stimulation *in vivo*, showed that such proteins can also compromise the maturation of B cells in the bone marrow. This results in the breaking of tolerance and greater rates of B cell maturation, presumably as a consequence of ES-62 raising the threshold of apoptosis. Taken together, these observations challenge the instructive model for B cell selection, which relies on BCR-specificity being the sole determinant of cell fate decisions. This new evidence suggests that B cell selection may also be dependent on stochastic parameters such as Fas expression, cell density or other environmental factors.

Similar investigations were performed on B cells from the periphery, which are involved in cell fate determination, in particular, B cells from Germinal Centres and the peritoneal cavity. It was established that apoptosis and proliferation of B cells differed depending on their maturation and activation status.

These novel observations tracked the formation of Germinal Centres, at both sites, *ex vivo*. The molecular mechanisms regulating the responses of Germinal Centre B cells were also explored. Two main observations were made. Firstly, $Btk^{-/-}$ Germinal Centre B cells were found to be hyperproliferative in response to BCR stimulation, whilst non-Germinal Centre B cells were found to be hyposensitive. Secondly, BCR-induced apoptosis of Germinal Centre B cells appeared to be Caspase-dependent, similarly to that observed for transitional B cells. Furthermore, using HEL-BCR transgenic mice, it was shown that the primary and secondary responses to antigen are different in the spleen and in the lymph nodes.

Finally, B-1 cells from the peritoneal cavity were shown to exhibit restricted proliferative responses and did not respond strongly to a secondary stimulation via the BCR. In addition, and in contrast to the situation in immature B cells, but similar to Germinal Centre B cells, BCR-induced apoptosis of B-1 cells appears Caspase-dependent.

Et ignotas animum dimittit in artes.

- *Ovid*, *Metamorphoses*, VIII, 188

List of abbreviations

AA	arachidonic acid
Ab	antibody
Ac-DEVD-CHO	Acetyl-Asp(OMe)-Glu-Val-Asp(OMe)-aldehyde
Ag	antigen
AICR	activation-induced cell death
ANT	adenine nucleotide transferase
APC	allophytocyanin
ATM	(gene) mutated in ataxia-telangiectasia
BCR	B cell receptor
Btk	Bruton's tyrosine kinase
CARD	caspase activation and recruitment domain
cdk	cyclin dependent kinase
CFSE	5-/6-carboxyfluorescein diacetate, succinimidyl ester
cki	cyclin dependent kinase inhibitor
COX	cyclooxygenase
$cPLA_2$	cytosolic phospholipase A_2
CsA	cyclosporin A
DAG	diacylglycerol
DC	dendritic cell
DD	death domain
DED	death effector domain
DEL	duck egg lysozyme
$DiOC_6$ (3)	3.3'-dihexyloxacarbocyanine iodide
$\Delta\Psi_m$	mitochondrial inner membrane potential
ER	endoplasmic reticulum
ES-62	excretory-secretory product of 62kDa

FCS	foetal calf serum
FITC	fluorescein isothiocyanate
GC	germinal centre
HDAC-1	histone deacetylase 1
HEL	chicken (hen) egg lysozyme
HRP	horseradish peroxide
Ig	immunoglobulin
IL-4	interleukin 4
IP_3	inositol tri-phosphate
ITAM	immunoreceptor tyrosine-base activation motif
kDa	kilodalton
KO	knock out
L-NIL	L-N^6-(1-Iminoethyl)lysine
L-NMMA	N^G-Monomethyl-L-Arginine
LOX	lipooxygenase
LPS	lipopolysaccharides
MAPK	mitogen activated protein kinase
Mdm2	murine double minute 2
MHC	major histocompatibility complex
PARP	poly(ADP-ribose) polymerase
PE	R-phycoerytherin
PerCP	peridinin chlorophyll-*a* protein
PG	prostaglandins
PHA	phytohemagglutinin
PI	propidium iodide
PI-3K	phosphatidylinositol-3 kinase
PIP_3	phosphatidylinositol tris-phosphate
PKC	protein kinase C

PLA_2	phospholipase A_2
PLC	phospholipase C
PNA	Peanut agglutinin
PTP	(mitochondrial) permeability transition pore
RAG	recombinase activator gene
Rb	retinoblastoma susceptibility protein
ROS	reactive oxygen species
RT-PCR	reverse transcriptase-polymerase chain reaction
sIg	surface immunoglobulin
TCR	T cell receptor
Th(2)	T helper cell-mediated reaction (type 2)
TLCK	Nα-p-Tosyl-L-lysine chloromethyl ketone
TNF	Tumour necrosis factor
WT	wild type
Xid	X-linked immunodeficiency
zVAD-fmk	N-benzyl-oxycarbonyl-Val-Ala-Asp(OMe)-fluoromethylketone
zVEID-fmk	N-benzyloxycarbonyl-Val-Glu-Ile-Asp(OMe)-fluoromethylketone

27/10/00

Declaration

I declare that this work has been written by myself and is a record of work performed by myself.

Elad Katz

Chapter 1. INTRODUCTION

1.1 B cells in the humoral immune response

B cells are the principal component of the humoral immune response. These cells can produce specific antibodies to foreign antigens after a carefully conducted mechanism of B cell development. During this process, B cells arise from the pluripotent stem cells generating a population of antibody-secreting cells with a diverse repertoire of specificities. In order to achieve this diversity, B cells undergo three processes: lineage commitment, proliferative expansion and cell selection [1-3].

In addition to the generation of antibodies, B cells have other functions. First, they can act as antigen presenting cells and activate T helper cells. In this context, B cells can play a part, together with other antigen presenting cells, in the Th type responses.

Second, memory B cells respond rapidly to a secondary challenge by antigen. In parallel to the primary antibody production, B cells in the Germinal Centres achieve a higher affinity to antigen due to somatic mutations within their immunoglobulin (Ig) genes and Ig isotype switching. In the secondary response, specific memory B cells will respond more quickly to antigen, differentiate into plasma cells and secrete large quantities of highly specific antibodies. This phenomena of enhanced secondary humoral response enables vaccination as a preventive step against pathogens.

1.2 Determination of B cell repertoire

1.2.1 Development of immature B cells

B cell development can be divided into two stages: an antigen-independent stage which is carried out entirely in the bone-marrow (or foetal liver); and an antigen-dependent stage which starts in the bone marrow and continues in the peripheral lymphoid organs such as the lymph nodes and the spleen (fig. 1).

The lineage commitment of B cells starts from the recently identified common lymphoid progenitor and continues though multiple stages. B cell markers (B220 and CD19) are expressed for the first time on pro-B cells. Soon after the generation of pro-B cells, they express the recombination activator proteins RAG-1 and -2, which are required for Ig gene rearrangement. RAG-1 and -2 expression is essential for the development of a later stage of pro-B cells (sometimes called pre-BI), when DJ rearrangements of the Ig heavy chain occur. This is illustrated by knock out mice for RAG-1 or -2, which do not develop B cells beyond the early pro-B cells. Late pro-B cells express on their surface the accessory components of the B cell receptor (BCR), Igα and Igβ, together with the chaperone protein calnexin. Igα and Igβ transduce a constitutive signal which is essential for B cell survival in pro-B and pre-B cells (fig. 2).

Late pro-B cells develop to pre-B cells, which express on their surface a pre-B cell receptor. The pre-BCR comprimises a fully arranged mu (μ) heavy chain (V(D)J) together with surrogate light chains made of VpreB and λ5. This functional BCR has a crucial role in B cell development, as knock out studies revealed not only that VpreB and λ5 are essential for pre-B stage of development, but also the lineage-restricted transcription factor Pax5, Igβ, and maybe most importantly the mu chain itself. Knock-out mice which are deficient in the transmembrane domain of the mu chain (termed μm(TM) knock out), lack all peripheral B cells [4]. It seems, though, that the requirement is simply for a functional heavy chain at this stage, since knock-out mice in which mu chain has been replaced by delta chain, have apparently normal B cell development [5]. Supporting

evidence in this context is provided by $Syk^{-/-}$ mice, which do not progress into the pre-B cell stage either as Syk, a tyrosine kinase, has a non-redundant role in transducing signals from the BCR into the cell. Finally, by the end of pre-B cell stage, both heavy and light chains are rearranged. Surface IgM is expressed as the clonatypic component of the BCR, in association with Igα and Igβ. Only one of the alternative alleles for each Ig chain is expressed in an allelic exclusion process which ensures that only one type of IgM is expressed on each individual immature B cell.

1.2.2 Selection into the naive B cell pool

Out of the $2x10^7$ IgM^+ B cells that develop daily in the bone marrow of the mouse, about 10% reach the spleen and only 1-3% enter the mature B cell pool [6]. A comparison of the heavy chain repertoire in pre-B cells and mature B cells shows clearly that the repertoire in the bone marrow is much broader than in the periphery [7]. Immature B cells emerge from the pre-B cell stage with a wide variety of specificities of their surface IgM. This variety is due to the random usage of VDJ domains in the Ig rearrangements of pre-B cells. In the pre-BCR stage, a functional BCR is needed in order to assure the cell that it can develop further [3]. However, immature B cells are negatively selected in order to avoid self-reactivity. Generation of self-reactive B cells is avoided by one (or more) mechanisms:

(i) clonal deletion - the self-reactive immature B cell undergoes programmed cell death (apoptosis).

(ii) anergy - the self-reactive immature B cell becomes non-responsive and is unable to differentiate.

(iii) receptor editing - the self-reactive immature B cell downregulates its BCR and rearranges its Ig genes using RAG proteins, once again, in a manner similar to pre-B cells.

It was long thought that the variety in newly formed B cells in the periphery reflects these selection mechanisms. Recently, however, another phenotype of selection-sensitive B cells were identified as an intermediate stage (or stages) between immature and mature B cells ([8]

and fig. 2). These cells, known as transitional B cells, are IgM^+ $CD24/HSA^{+++}$ as are immature B cells, but they express higher levels of B220 and Bcl-2 together with low expression of IgD on their surface [6]. It is also known that transitional B cells can emigrate from the bone marrow to the periphery [9].

The discovery of transitional B cells has provided a new model for the effects of surface Ig cross-linking on immature and transitional B cells: When immature B cells encounter sufficient BCR stimulation, reflecting self-reactivity, nearly half of them may undergo receptor editing [10, 11]. The strength of signal needed to induce receptor editing is disputable and this mechanism does not produce a full explanation for the evidence known regarding immature B cell selection. Firstly, a large number of immature B cells are lost before they reach the periphery as transitional B cells. Moreover, it is well documented that immature B cells can be induced to undergo apoptosis in response to BCR cross-linking. More recently, it was shown that the bone marrow environment, and more specifically $Thy\text{-}1^{dull}$ cells (of unknown lineage), can protect immature B cells from apoptosis [12]. Therefore, the question of the extent of deletion of immature B cells by antigen in the bone marrow *in vivo* remains open. Thus, cells targeted for deletion by self-antigens may be transitional B cells in the bone marrow and the spleen rather than the immature B cell population in the bone marrow [13-15]. Furthermore, since transitional B cells are Fas^+, it is feasible that they could be deleted not only directly by antigen but also by cells expressing FasL [8]. Although it was shown that transitional B cells in the spleen depend on BCR stimulation for survival, some questions remain unsolved [16]. The view that only a small proportion of immature B cells might be deleted by negative selection, implies that BCR-driven B cell maturation may involve a positive selection event. Such an event may enable a restricted number of transitional B cells to fully develop [17]. It is hard conceptually to understand a mechanism of negative selection which occurs in the periphery. Because transitional B cells in the periphery may encounter both self and nonself antigens, it is not clear how these types of antigens can be discriminated. Moreover, the roles for T cell help and Fas-induced deletion, which may help to explain negative selection in the periphery,

have not been resolved as well [9]. Thus, T cells may provide a rescue signal (CD40L, IL-4) to transitional B cells, but equally may provide death signals (via FasL).

Once the B cell survives the selction processes, it is recruited to the naive B cell pool in the periphery. Naive B cells are activated by antigens through their BCR receptor and then proliferate in what is usually described as clonal expansion [18]. Although activation depends on the BCR, T cell-derived factors can promote B cell survival and even proliferation in this stage, namely CD40 and IL-4 receptor ligation [19]. In the spleen, B cells exist in three zones: the follicles, the Germinal Centres (within the follicles) and the marginal zones (which do not exist in the lymph nodes). The naive pool consists of recirculating B cells and is activated in the follicles. Some cells will enter the Germinal Centres, where they will undergo somatic mutation and class switching from IgM to IgG or other isotypes and become either memory cells or antibody-secreting plasma cells [20]. The Germinal Centre reaction is discussed in further detail below. The function of marginal zone B cells, together with the way they are generated, is still under dispute. In some aspects, they are reminiscent of B-1 cells [21], a particular sub-lineage of B cell whose development is discussed separately, in section 1.2.4.

1.2.3 The Germinal Centre and B cell memory

Memory B cell generation represents a biological phenomenon in which somatic mutation of immunoglobulin molecules occurs within days to weeks of antigen encounter. Germinal Centres (GC) within the follicles of peripheral lymphoid organs have a critical role in the cellular and molecular events that underlie memory B cell generation. This is especially true for somatic mutations which are part of affinity maturation of peripheral B cells (reviewed in [20, 22]). Nonetheless, many of the most crucial aspects of memory B cell generation remain highly controversial, including the mechanism of somatic mutation and the means by which B cells with increased affinity are selected.

A primary encounter with antigen stimulates specific B cells not only to differentiate into antibody-forming cells (AFCs), but also to give rise to a

population of memory cells [14, 15, 23]. Memory B cells are thought to be solely derived from GC B cells. In the primary response, GCs first appear at day 4–5 after immunization, achieve their maximum cell number by day 10–11, and decline after about three weeks. After immunization, activated antigen-specific splenic B lymphocytes first proliferate in the T cell zone of the white pulp in the spleen, where antigen-activated T and B cells make physical contact, during T cell-dependent immune responses (fig. 3). Most of the activated B cells develop locally into foci for AFCs, while a minority of antigen-specific B cells migrate back into the lymphoid follicles to form GCs. Although neighbouring AFC and GC B cells are frequently descended from the same parental cells, only the cells that enter the GC microenvironment become memory cells. Memory B cell differentiation takes place in two phases: (i) in centroblasts, which populate the dark zone of the GC, somatic mutations occur in the V region of rearranged Ig genes; (ii) The selection of B cells expressing antigen receptors with high affinity for the antigen ligand occurs later in the light zone, by immune complexes captured on follicular dendritic cells.

Although it is now generally accepted that the GC reaction is central to memory B cell generation, memory B cell generation in the absence of GC has been observed [22]. Nonetheless, understanding the cellular interactions within GC that are responsible for memory B cell generation and survival remains an aim for future research. While it is clear that the CD40–CD40L interaction is essential, the timing of these interactions as well as the role of other molecular interactions and cytokines remains controversial [24, 25]. It is clear that besides B-T cell interactions, GC dendritic cells are required for the GC reaction although the nature of their involvement is still largely obscure [26]. Recently, it was demonstrated that T cells are essential for class switching of centroblasts to certain isotypes of Ig [27].

In mouse and man, it is now possible to use cell surface markers to identify, isolate and analyse cells at each of the progressive stages from entry to exit from GC [17, 28]. It has been possible to isolate from follicles small, resting, unmutated cells with an early GC phenotype, which are the likely originators of GC B cell clones. Furthermore, the various

progressive GC-derived subsets can be shown to differ in their stimulatory requisites and susceptibility to apoptosis [17, 22, 28]. Indeed, in the course of their generation GC cells can re-express the RAG-1 and -2 proteins which are required for gene rearrangements [22]. Finally, GC cells that survive and mature, ultimately leave the follicles, however, their exact fate and longevity remain controversial [26, 29]. Indeed, it appears that there may be distinct subsets of memory B cells wherein peripheral localization and longevity may be interrelated.

1.2.4 The B-1 cell lineage

B-1 cells were first decribed in 1983 as Ly-1$^+$ B cells [30]. In the mouse, this subset of self-renewing B cells is found primarily in the peritoneal cavity although smaller numbers of B-1 lymphocytes populate the spleens and lymph nodes of adult mice [31]. The B-1 subset exhibits high frequencies of cells bearing receptors specific for multivalent self-antigens. The restricted diversity of B-1 cells include broad specificities for phosphatidylcholine, immunoglobulins, DNA, membrane proteins on erythrocytes and thymocytes, as well as environmental antigens and common pathogens such as lipopolysaccharides and phosphorylcholine. B-1 cells secrete large quantities of IgM, IgG3, and IgA and are presumed to be responsible for natural immunity. B-1 cells are therefore especially important in newborns where adaptive B-2 cells only start to develop (see below). B-1 cells are also involved, both in mouse and man, in the generation of some disease-associated autoantibodies. The level of multivalent antibodies (i.e. antibodies to common antigens) may be regulated by controlling the numbers of these intrinsically activated, self-regenerating B-1 cells [32].

B-1 cells are categorized as either B-1a cells, which express CD5, or B-1b cells, which are very similar to B-1a cells but do not express CD5. Both B-1a and B-1b cells are phenotypically IgM^{hi} IgD$^-$ CD23$^-$ Mac-1$^+$ [6]. The mechanism of generation of B-1 cells from B cell progenitors was for a long time unclear [33]. Only recently, a comprehensive model for the development of B-1 cells has emerged (reviewed in [32]). According to this model, positive selection in the foetal bone marrow gives rise to both B-1a

and B-1b cells. In order to achieve that, particular mu heavy chains specific to multivalent antigens are used in the gene rearrangements of the BCR. The same antigen can induce negative selection in B-2 cells and positive selection in B-1 cells at the same time, and *vice versa* if the specificity to antigen is different as a result of distinct mu chain usage in each lineage [33, 34].

In the adult, the picture of B-1 development is still somewhat muddled. There is evidence that B-2 cells can be converted to B-1b cells [32]. The means by which this process occurs are poorly understood. It is well documented, though, that in certain knock out mice, such as $Lyn^{-/-}$ and $CD19^{-/-}$, the numerical balance between B-1 and B-2 populations is disturbed. In Lyn knock out mice, B-1 cell number is higher than normal although peripheral B-2 cell are absent [35]. In contrast, in $CD19^{-/-}$ mice B-1 cells are absent whilst B-2 cells expand [36]. It is likely that this evidence reflect a different role for these specific B cell components in each developmental process [37] and in other responses such as proliferation in response to BCR cross-linking [38].

1.3 Known mediators of apoptosis

1.3.1 The mitochondria is at the centre of the cell death programme

Cell death can occur through apoptosis or necrotic death pathways. In contrast to necrosis, which is a disorderly mode of cell death, apoptosis is an orderly process that proceeds through several morphological phases [38a]. Necrotic cells tend to swell and burst, a process which can induce inflammation. In contrast, cells undergoing programmed cell death go through changes which ensure release of condensed bodies which are phagocytosed by other cells. First, cells which undergo apoptosis release contact with neighbouring cells and become detached from the surrounding tissue [39]. There is then a marked condensation of both the nucleus and the cytoplasm, causing the cells to shrink significantly in size. The nuclear envelope and the nucleolus break apart as chromatin condenses and is cleaved in the nucleus into multiple fragments of ~180

base pairs. The plasma membrane also begins to bleb, and the blebs can divide the cells into smaller apoptotic bodies. Finally, apoptotic bodies are rapidly phagocytosed by the surrounding cells and degraded in lysosomes.

In the past several years, mitochondria have been found to play a key role in apoptosis, beyond its traditional role as the energy supplier of the cell. In some cases, mitochondria release cytochrome C and other proteins, such as apoptosis inducing factor (AIF), into the cytoplasm. The mitochondria also undergo a loss of inner membrane potential ($\Delta\Psi_m$) and mitochondrial permeability transition occurs. It has also become clear that in concert with mitochondrial function, proteins from the Bcl-2 and Caspase families largely determine the fate of the cell (fig. 4). Hence, in most cases of apoptotic cell death, decision of cell fate is dependent on mitochondrial events. These events can be divided into four types:

(i) Morphological changes and redistribution of mitochondria - early in apoptosis, the mitochondria will redistribute in the cytosol in a manner which is cell dependent, but usually consists of some condensation visible under the microscope [38a]. There are further internal changes in the inner mitochondrial membrane, including depolarisation of the mitochondrial membrane potential, $\Delta\Psi_m$. One crucial event is opening of the mitochondrial permeability transition pore (PTP), which is located in the membrane junctions of the mitochondria. Although this event is poorly charecterised, it is widely thought that upon opening of the channel, the cell is sentenced to die [40].

(ii) Bcl-2 family proteins target the mitochondria - the mitochondria is a main site for the activity of Bcl-2 family proteins, although the nature of their action is largely undetermined (see below).

(iii) Reactive oxygen species (ROS) are generated in the mitochondria - the participation of various ROS in apoptotic events is observed in many systems [41, 42]. The regulation of these phenomena in the cell death context is still obscure, although our knowledge about how ROS are generated has expanded considerably [43]. There is also some indirect evidence that Bcl-2 family members, such as Bcl-2 and Bcl-x_L, participate in this regulatory mechanism [44]. It is however, unclear

what is the involvement of ROS in the energetic imbalance resulting from apoptosis-related mitochondrial dysfunction [45, 46].
(iv) Caspases act both upstream and downstream of the mitochondria - initiator Caspases are proteases that mainly mediate the targeting of pro-apoptotic proteins (such as Bid) to the mitochondria. Effector Caspases are activated downstream of mitochondrial events such as the release of cytochome C (see below). Caspase-2 and -9 may also be released from the mitochondria itself during apoptosis [47].

There is a bi-directional and complex interaction between apoptosis and the cell cycle machinery. On one hand, it is well-documented that many components which control the progress of cell cycle also have a role in regulating cell death. These include mainly regulators of the G_1 and G_2 checkpoints, such as p53, Rb and E2F (see section 1.3.4). These proteins have also been shown to be involved when the cell cannot overcome stress and it decides to initiate the cell death programme. On the other hand, many proteins which are usually regarded as restricted to the regulation of apoptosis, such as those belonging to the Bcl-2 and Caspase families, have recently been shown to interact with the cell cycle machinery. The full description of this side of the equation is still lacking, but some important observations have been made. These include enforcement of cell cycle arrest by over-expression of Bcl-2 [48] and cleavage of many cell cycle proteins, such as Rb, by Caspases [49, 50]. The significance of the latter phenomenon is unclear because caspase cleavage can either activate or deactivate proteins, depending on their structure.
Lastly, an interesting link was suggested between the cell cycle regulating machinery and the mitochondria. Although it has been known for some time that certain proteins transactivated by p53 are mitochondrial [51], it now has being shown that p53 itself can translocate to the mitochondria [52]. The outcome of this event remain obscure.

1.3.2 Bcl-2 family of proteins

The Bcl-2 gene family comprises structurally related proteins which form homo- or heterodimers and act either to promote or antagonise apoptosis by acting on the mitochondria and other sites in the cell.

The pro-apoptotic members of the Bcl-2 family (Bad, Bak, Bid, Bax) have been proposed to act by inactivating dimers of anti-apoptotic Bcl-2 family members such as Bcl-2, Bcl-x_L and Mcl-1 [53], which act to preserve mitochondrial integrity. Bad activation generally appears to be controlled by the protein kinase Akt [54]. Alternatively, Bcl-2 has been shown to target Raf-1 to the mitochondrial membrane in order to phosphorylate Bad [55]. Phosphorylation of Bad leads to its interaction with 14-3-3 proteins and therefore, as it can no longer complex with Bcl-2, renders it inactivated. In addition, Bax and Bak have also been recently proposed to mediate Bcl-2/Bcl-x_L-independent mechanisms of apoptosis [56].

Bcl-2 family members have generally been shown to be located in the mitochondrial membrane and nuclear envelope of cells, and are known to have anti-oxidant properties and prevent leakage of cytochrome C from the mitochondria. Nonetheless, their exact mode of action is still unclear (reviewed in [57]). Based on structural similarities and differences the following model has, however, emerged: the anti-apoptotic members of the Bcl-2 family all share 4 homology domains (denoted BH1 to BH4). In contrast, the pro-apoptotic members lack at least one domain and some (such as Bad and Bid) have only a BH3 domain. This domain, however, is regarded as being required for interactions between different Bcl-2 family members [50]. Following apoptotic signals, pro-apoptotic proteins such as Bax heterodimerise with anti-apoptotic proteins such as Bcl-2 at the mitochondrial membrane [58]. The interaction blocks the anti-apoptotic capabilities of the Bcl-2-like proteins. The actual means by this is achieved are still to be elucidated, but they could be related to the proposed function of these proteins as ion channels [59, 60]. Thus, the overall structure created by the BH domains is reminiscence of diphteria toxin [61] and studies in artifical lipid membranes have shown that Bcl-2 family proteins can form ion channels with different affinities to anions and cations [62, 63].

Two observations, however, have questioned whether all Bcl-2 family function can be attributed to channel formation:

(i) Upon its cleavage by Caspases, Bid has been shown to activate Bax by inducing its translocation to the mitochondrial membrane [64]. After its activation by Bid, Bax oligomerises and triggers the release of cytochrome C. Hence, Bid may not posses any intrinsic ion channel abilities of its own.

(ii) Bax is known to associate with the mitochondrial PTP and to influence its state via unknown mechanism, which is thought not to require ion transport through Bax itself [62].

Indeed, the Bcl-2 family have some other capabilities in exerting anti- and pro-apoptotic functions, by inducing regulation of cellular homeostasis in terms of controlling pH, Ca^{2+} and other factors regarding not only the mitochondria but also the ER [65]. Furthermore, their interaction with the cell cycle machinery remains obscure. For example, Bcl-2 proteins can rescue cells from apoptosis, but not from growth arrest which usually accompanies it [58, 66]. Nonetheless, their phosphorylation state changes with cell cycle progression, suggesting that they have a protective role during these vulnerable times [67]. This evidence points again to a connection between maintenance of mitochondrial energetic balance and cell survival.

1.3.3 Caspases and other killer proteases

Caspases are an important group of cysteinyl aspartate-specific proteases which were identified as homologues of the cell death protein, CED-3 from the nematode *C. elegans*. Caspases act by cleaving key target proteins resulting in the systematic disassembly of the apoptotic cell by (i) halting cell cycle progression; (ii) disabling homeostatic and repair mechanisms; (iii) initiating the detachment of the cell from its surrounding tissue structures; (iv) dismantling structural components such as the cytoskeleton and (v) flag the dying cell for phagocytosis (reviewed in [68, 69]). Indeed, over-expression of active Caspases is sufficient to cause cellular apoptosis [69]. The Caspase family contains 14 different members, which are able to recognise and cleave similar, but not identical, four amino acids sequences ([50]; table 1). Caspases are

expressed as inactive pro-Caspases and Caspase activation occurs in a cascade fashion with the initial activation of an initiator Caspase serving to activate downstream effector Caspases by proteolysis ([50] and fig. 4). All pro-Caspases consist of a large and small subunit and a pro-domain. The pro-domains of Caspases possess two types of adaptor motifs, which serve them in their interactions with other proteins (reviewed in [68, 70]): the Caspase activation and recruitment (CARD) or the death effector domain (DED). These motifs are essential for interactions with death domain (DD) proteins which are downstream of certain death receptors (see below) and crucial for the activation of initiator Caspases. In a fully processed and activated Caspase, the large subunit and small subunit are covalently linked and the pro-domain is cleaved out ([50] and fig. 4).

Although the precise molecular mechanisms of effector Caspase activation are as yet unknown, it has recently been observed that proteolysis and activation of effector Caspases is facilitated by binding to cytochrome C which is released from the mitochondria during the process of apoptosis. The exit of cytochrome C from the mitochondria is controlled by the Bcl-2 family of apoptosis regulators, and causes the indirect activation of these caspases [71]. Cytochrome C, together with dATP and a cytosolic factor termed Apaf-1, assemble an initiator complex called the apoptosome [72]. This complex initiates the cleavage of Caspase-9 into a mature active form. This active protease, in turn, initiates a series of effector Caspases [73]. This initiation is regarded as "point of no return", where cell disassembly cannot be reversed due to the ensuing quick and broad destruction of cell components [73]. The central effector Caspase, Caspase-3, normally exists as a 32kDa inactive protein precursor that is converted proteolytically to a 20kDa and a 10kDa activated heterodimer by both Caspase-9 and Caspase-6. In addition, Caspase-3 is also able to cleave and activate Caspase-6, a process which amplifies Caspase-cascade events [73]. Downstream targets of Caspase-3 are: (1) DNA fragmentation factor (DFF40/CAD), a heterodimer that functions to trigger fragmentation of genomic DNA into nucleosomal segments; (2) PKCδ, which is activated by its cleavage; (3) the DNA

repair enzyme poly(ADP ribose) polymerase (PARP); as well as many other proteins [50].

Cell death receptors such as Tumour Necrosis Factor-α and Fas, mediate rapid apoptotic cell death pathways in a number of cell types but particularly in cells of the immune system. TNF-α and Fas utilise a specific initiator Caspase, Caspase-8, to activate the effector Caspases. Apoptosis is initiated by directly recruiting pro-Caspase-8 to the accessory death domain transducing molecules (such as FADD, TRADD, RIP and RAIDD), which are associated with these receptors [50]. Caspase-8 is cleaved to its mature form during the death receptor ligation, as a result of its interaction with the death domain proteins [68]. Mature Capsase-8 acts in two ways: firstly, it directly cleaves Caspase-3; Secondly, it cleaves Bid, which in turn translocates to the mitochondria to activate the cytochrome C cascade ([64] and see above).

Although for some time, Caspase activation was regarded as absolute requirement for cell death, this has been disputed recently. The existance of alternative mechanisms has emerged. Borner and Monney [74] suggested that these alternative mechanisms may utilise other cysteine and serine proteases and calpains. There is a growing number of reports of Caspase-independent death pathways [75, 76], along with some evidence relating to the participation of alternative proteases in apoptosis is documented [77, 78]. An apoptotic process which utilises exclusively non-Caspase proteases to achieve full execution of the cell has not been described yet.

1.3.4 The cell cycle machinery

The cell cycle is the elaborate mechanism by which the eukaryotic cell divides into two daughter cells. The cell cycle comprises multiple stages with many safeguards to assure precise division with unchanged DNA. These stages, commonly known as phases, are closely regulated by pairs of proteins - cyclins and their dependent-kinases (cdks) ([79] and fig. 5). When a cell exits its quiescent stage (called G_0), it enters a preparatory phase known as G_1. In this phase, controlled by cyclins of the D-type and cdk-4 and -6, the cell grows to a sufficient size and synthesises the

proteins needed for RNA and DNA synthesis and division. Cells can arrest in G_1 if any of these requirements are not met (see below). If cleared past the checkpoint, the cell will then progress into DNA synthesis, known as S phase, which is regulated by cyclins A and E and cdk2. When synthesis is completed the cell enters a second preparatory phase, G_2. Here the cell checks that all copies of DNA are unchanged before it can divide. Finally the cell undergo mitosis, phase M, and divides into two cells. Phases G_2 and M are regulated by cyclin B and cdc2.

Cells can be arrested in both G_1 and G_2. In many cases, lengthy arrest leads to apoptosis and certain components of the cell cycle machinery (such as p21 and p53; see below) are required for this transition. In some cases, growth arrest is also a requirement for apoptosis [80]. The G_1 checkpoint (also known as Start restriction point), approximately two-thirds into this phase, is regarded as crucial for cell fate decisions [81]. This checkpoint is regulated by the retinoblastoma susceptibility protein pRb and a series of cdk inhibitors (ckis): p15, p16, p18, p19 and p21 (reviewed in [82, 83]). p21 function is well characterised and it is thought to be important mainly in the regulation of differentiation induction in concert with growth arrest [84, 85]. $p19^{ARF}$ stabilises the p53 protein by blocking nucleo-cytoplasmic shuttling of Mdm2, which degrades p53 ([86, 87] and fig. 6). Little is known about the function of p15 and p18 [88]. p16 appears to act to prevent cell cycle progression. This activity can by reversed by the transcription factors from the E2F family and is thought to be crucial to cancer development [88, 89].

Commitment to apoptosis requires the activation of the E2F and DP families of transcription factors [90]. All E2F/DP dimers interact with similar, but not identical, DNA consensus sequenses [91]. E2F factors usually cooperate with p53 in activating various apoptosis-related genes ([92, 93] and see below), through the co-activator p300 [94]. Some evidence, though, exists for p53-independent activity of E2F factors [95, 96]. Another family of proteins which interact with E2F transcription factors is the pRb family of "pocket" proteins. The pRb proteins are active only while they are not phosphorylated by cdks or tyrosine kinases [97].

The interaction of E2F and DP factors with DNA is either inhibited by proteins from the pRb family [98] or altered by them [91]. E2F-1, -2 and -3

form dimers with the transcription factor DP-1 [99]. DP-1 dimers are up-regulated during G_1 [100] and are controlled by pRB [79]. E2F-4 and -5 complex with DP-2 and persist during G_0 [100]. DP-2 dimers are regulated by the pRb related proteins, p107 and p130 [99]. These proteins displayed in some cases a pRb-independent activity [101, 102], when p107 closely imitates repression by pRb of E2F via HDAC-1 (Histone deacetylase-1) [103].

The tumor supressor p53 sits in the centre of a complicated network, which responds to a variety of stimuli and exerts a whole range of actions ([104] and fig. 6). Investigations of DNA damage checkpoints revealed that p53 is the main "gatekeeper" in the repair or death decisions in the cell (reviewed in [105, 106]). Recently, however, some of the activities of p53 have been attributed to its close homologues, p63 and p73 [107, 108]. All of the members of the p53 family share the same DNA binding consensus sequence. Thus, these proteins were shown to play a part in both apoptosis [109, 110] and development [109, 111].

The p53-mediated stress response includes three stages:

(a) stabilisation of p53 protein [112] and its action as an anti-oxidant [113].

(b) translocation to the nucleus [114].

(c) activation and suppression of p53-responsive genes [115]. The mechanisms involved in this stage are still elusive but phosphorylation of Ser-15 on p53 is considered as the minimal requirment for its transactivation [116, 117].

Numerous genes contain p53 response elements and p53 activity is, in fact, executed by different p53 containing complexes [115]. A few proteins have been suggested to "cross talk" with p53 in this, including NF-κB in association with p300 [118]. Similarly, the cell cycle regulator ATM is thought to be necessary for both growth arrest and apoptosis mediated by p53 [80, 119]. Both NF-κB and ATM themselves have a role in cell fate decisions and integration between all of these factors is likely to be at the DNA transcription level.

p53 has also been linked to mitochondrial function and through this to determining the fate of the cell. For example, p53 appears to regulate the

transcription of both Bcl-2 [120, 121] and Bax [122] and hence can control the levels of pro- and anti-apoptotic complexes made of Bcl-2 family members. p53 can also induce a rise in ROS content [123, 124], leading to an oxidative degradation of mitochondrial components [51]. In addition, it has been shown that p53 can inhibit the expression of COX-2, an inducible enzyme responsible for prostaglandin production ([125] and see section 1.4.2.3) which may influence further intercellular phenomena. Moreover, p53 has been recently shown to translocate to the mitochondria [126], presumably to directly exert these actions. Interestingly, a Caspase substrate, the DNA repair protein PARP, alters p53 DNA binding by an unknown yet mechanism [127].

Mdm2 is an oncogene which regulates p53 activity. Although p53 itself regulates Mdm2 transcription [128], Mdm2 drives p53 to ubiquitin-mediated degradation [129]. Interestingly, using a proteosome inhibitor, lactacystin [130], it was shown that both Mdm2 and Bax are degraded by ubiquitination [131]. Moreover, the proteasome has been proposed to play a key role in the regulation of p53-mediated apoptosis in lymphocytes [132]. p53 has also been suggested to interact with the E2F/pRb mechanism [92], presumably via direct interaction between Mdm2 and pRb [97]. A related event to this interation is the cleavage of pRb by Caspase activity [133], which was may also be mediated by p53 [49].

1.4 Apoptosis of B cells

The first observations that different responses to antigen, via the BCR, occur at distinct stages in development were dependent on immature animal models and neonatal antigen exposure [14, 134]. The difference between the responses of immature and of mature B cells to antigen receptor ligation was the first example, and perhaps best example, of the role development plays in governing lymphocyte responses [135].

Cross-linking B cell receptors on immature B cells aborts B cell development *in vivo*. The BCR also transmits a signal that is sensitive to metabolic inhibitors and that preferentially inactivates immature B cells *in vitro* [136, 137]. *In vitro*, stimulation of mature B cells with anti-IgM

antibodies triggers a mitogenic response that is affected by the degree of cross-linking and the presence of co-stimuli, such as CD40 ligation. Experiments tracking antigen-specific monoclonal B cells in transgenic mice have reinforced the notion of different responses to the same antigen by immature and mature B cells [138]. A parallel situation exists in T cells, where extensive receptor cross-linking by anti-CD3, superantigens, alloantigens, or viral antigens triggers apoptotic deletion of immature thymocytes but triggers proliferation of mature T cells [139, 140].

1.4.1 The B cell receptor and its immediate signalling mediators

Cross linking of the B cell receptor leads to activation of multiple pathways. Numerous signalling events induced by the BCR were investigated in the last decade, due to their importance in B cell development (reviewed in [3, 12, 18]; see section 1.3). The BCR comprises two components: clonatypic surface Ig (heavy and light chains) and the accessory moleules, Igα and Igβ. While surface Ig has antigen binding ability but no signalling capacity, the accessory molecules contain immunoreceptor tyrosine-based activation motifs (ITAM). These motifs mediate the signal transduced by the BCR through the tyrosine kinases from the Src-family, such as Syk and Lyn [141]. These kinases are responsible for the activation of a number of key pathways:

(i) The PI-3K pathway: this pathway is activated directly by Syk and indirectly by Ras to convert PIP_2 into PIP_3. This event serves to activate many PH-containing proteins such as Vav, Akt, PLCγ and Btk [142].

(ii) Activation of phospholipase C (PLC)-γ and Calcium mobilisation: activation of tyrosine kinase Btk triggers PLCγ to produce IP_3 and DAG. IP_3 ligates its receptors on the ER, which mobilise Ca^{2+} in response. Calcium mobilisation has many effects such as activation of the calcium sensitive protein Calcineurin and NF-κB. Calcium and IP_3 activates the conventional (α, β, γ) isoforms of protein kinase C (PKC) [143]. DAG is sufficient to activate the novel (δ, ε, θ, η) PKC isoforms [144].

(iii) The Ras pathway: activation of the Grb2:Sos protein complex leads to activation of Ras. Downstream of Ras, the classical MAPK/ERK pathway is activated through Raf-1 [145]. In addition, Ras activates the PI-3K pathway.

(iv) Phosphorylation of the Guanine exchange factor Vav activates the Rho family of GTPases (such as Rac and cdc42), which in turn activate the MAPKs p38 and JNK and ultimately, actin polymerisation [18].

All pathways were shown to deliver the BCR signal to a variety of transcription factors in the nucleus in order to execute the transcription of a variety of genes. Furthermore, investigation into their collaborative nature has elucidated the importance of adaptor molecules such as BLNK/SLP-65. For example, BLNK was shown to interact in parallel with Grb2, Vav and PLCγ together with Nck, an activator of NF-κB [146].

1.4.1.1 Bruton's kinase (Btk) and Xid phenotype

The X-chromosome linked immunodeficiencies in CBA/N mice (Xid) and man (XLA) are genetic diseases caused by alterations of the structure of the protein tyrosine kinase Btk. Both Xid and XLA defects are intrinsic to the B cell lineage and are characterised by a partial block in pre-B-cell development in the bone marrow, a moderate (Xid) or severe (XLA) reduction in mature B cell numbers in the peripheral lymphoid organs and low titers of circulating antibodies (reviewed in [147]). Btk, a member of the Tec family of protein tyrosine kinases, was shown to be essential for both PLCγ activation and calcium signalling [3, 142] and therefore represent a crucial component of the BCR-sensitive pathways. The mature B cells from Xid mice exhibit poor activation in response to BCR stimulation, because of their failure to activate Akt [142]. The dual role of Btk in both selection of immature B cells and activation of peripheral B cells pinpoints it as crucial regulator of B cell fate [148-152].

1.4.2 The WEHI-231 model and developmental-stage dependent BCR signalling

Little is known about BCR induced signalling events in immature B cells, especially *in vivo*. Attempts to resolve this question by *ex vivo* experiments with primary cells provided contradictory evidence (reviewed in [9]). For example, while in some systems BCR cross-linking induced mainly receptor editing [7], other studies sugested that deletion of immature (or transitional) B cells is the principal mechanism for B cell selection [12, 153].

A widely used model for tolerance susceptibility in immature B cells is the murine lymphoma B cell line WEHI-231. It is well established that this IgM^+ IgD^{lo} B cell line undergoes apoptosis when stimulated via its BCR [154, 155]. This cell line can be rescued by Th2 type response as demonstrated by using either Th2 clone, D10.G4 [156], anti-CD40 antibodies [157, 158] or IL-4 treatment [157, 159]. Hence, the WEHI-231 model is used to investigate how the balance between the death and rescue processes is achieved.

1.4.2.1 Calcium mobilisation and PLCγ activation

Calcium mobilisation from internal stores is a well documented apoptotic event in immature B cell lines stimulated via their BCR [160-163]. Release of calcium from internal stores is induced by the production of the second messenger IP_3 by the BCR-coupled PLCγ [159] and can induce multiple events in the cell [43, 63, 164-166]. It is unclear which of these events are in fact developmental stage dependent, since the BCR utilises calcium mobilisation also in mature B cells [43, 167]. An intriguing possibility is the involvement of PKC isoforms, some of them known to be calcium dependent (α, β, and γ; for review see [144]). Overall PKC activation was suggested to have a role in the growth inhibition of immature B cells [134, 136, 161, 168]. The other second messenger produced by PLCγ, DAG, can act alone on novel PKC isoforms (δ, ε, η, and θ; [154]). Many other possible candidates for calcium-related signalling in B cell development are awaiting exploration. One such pathway involves the phospholipase $cPLA_2$ [169, 170]. This protein is calcium dependent and has been shown to be expressed in B cells when BCR

signalling leads to cell death [171]. Therefore, $cPLA_2$ may provide a component of development-specific calcium response (see below).

1.4.2.2 $cPLA_2$ and its role in lymphocyte selection

The major source of eicosanoid and related compounds in mammals is the arachidonic acid (AA) cascade. Upon cell stimulation, AA, or under certain circumstances other precursor fatty acids, are liberated from the membrane phospholipids via activation of lipid-cleaving enzymes, such as phospholipase A_2 (for review see [172]).

The phospholipase A_2 (PLA_2) enzymes hydrolyse fatty acid from the *sn*-2 position of phospholipid with the concomitant production of lyso-phospholipid. Mammalian cells contain structurally diverse forms of PLA_2 including secretory PLA_2 ($sPLA_2$), calcium-independent PLA_2 ($iPLA_2$), and the 85-kDa cytosolic PLA_2 ($cPLA_2$) [173, 174]. $cPLA_2$ shares no homology with other PLA_2 enzymes and is the only well characterized PLA_2 that preferentially hydrolyses *sn*-2 arachidonic acid. It should be noted, however, that although $sPLA_2$ and $iPLA_2$ do not exhibit acyl chain specificity they can also mediate arachidonic acid release depending on the cell type and agonist involved [175-178]. Arachidonic acid is itself an important regulator of specific cellular processes including regulation of PKC and PLCγ and modulation of Ca^{2+} transients. Arachidonic acid can also be converted to eicosanoids, potent inflammatory lipid mediators. This can occur enzymatically through the lipoxygenase or cyclooxygenase pathways for the production of leukotrienes, lipoxins, thromboxanes, or prostaglandins. Arachidonic acid is also subject to non-enzymatic, free radical oxidation to bioactive isoprostanes and isoleukotrienes. The important role of arachidonic acid in cellular activation ensures that its levels are tightly controlled.

$cPLA_2$ plays a role in maintaining arachidonate levels and is subject to complex mechanisms of regulation at both the transcriptional and post-translational levels [179]. An increase in intracellular calcium is necessary for $cPLA_2$ translocation, and $cPLA_2$ phosphorylation, all of these enhance enzymatic activity and can act together to fully activate $cPLA_2$ (reviewed in [180]). Interestingly, phosphorylation of $cPLA_2$ must

precede the increase in intracellular Ca^{2+} to fully activate the enzyme for arachidonic acid release in HER14 cells, and this suggests that $cPLA_2$ may not be available for phosphorylation if it is first translocated to membrane. However, there is evidence suggesting alternative pathways for regulation of $cPLA_2$ activation and arachidonic acid release. In macrophages and neutrophils, PMA can induce an increase in phosphorylation and catalytic activity of $cPLA_2$ as well as arachidonic acid release, and this occurs without an increase in intracellular calcium. The properties of $cPLA_2$ are consistent with the enzyme being cytoplasmic in resting cells at 50–100 nM calcium and translocating to the membrane when intracellular calcium levels increase. It is well documented that arachidonic acid release is triggered in cells by many calcium-mobilizing agonists.

The $cPLA_2$ activation pathway involves also an agonist-induced phosphorylation of $cPLA_2$ at Ser-505 by mitogen-activated protein kinases (MAPKs) and calcium-dependent translocation of $cPLA_2$ form cytosol to membranes where the substrate is localised. Phosphorylation of Ser-505 is important in the activation of $cPLA_2$ *in vivo* since over-expression of mutant $cPLA_2$ (S505A) in Chinese hamster ovary cells fails to enhance agonist-induced arachidonic acid release as seen when wild type enzyme is expressed [181]. Other kinases such as PKC and protein kinase A can phosphorylate $cPLA_2$ *in vitro*, but this does not result in a significant increase in $cPLA_2$ activity or a gel shift [180]. However, there is evidence for a role for PKC in the activation of PLA_2 and regulation of arachidonic acid release. PKC activation can play a role by triggering a kinase cascade leading to MAPK activation [171]. However, there is no evidence that PKC directly phosphorylates $cPLA_2$ *in vivo*.

Cellular oxidants have also been shown to activate $cPLA_2$ [182, 183]. In vascular smooth muscle cells, hydrogen peroxide (H_2O_2) induces serine phosphorylation and activation of $cPLA_2$. In this system, $cPLA_2$ activation and arachidonic acid production are implicated in the induction of c-fos and c-jun and the mitogenic response induced by H_2O_2. In contrast, treatment of kidney epithelial cells with H_2O_2 has been shown to activate $cPLA_2$, which contributes to oxidant-induced cytotoxicity.

$cPLA_2$ is a widely distributed enzyme, and the transcript is expressed at a fairly constant level in all human tissues with somewhat elevated levels in lung and the hippocampus. At the cellular level, $cPLA_2$ is enriched in mononuclear phagocytes but has been found in most cells [172]. One notable exception is that most mature T and B lymphocytes do not contain $cPLA_2$, whereas it is present in thymocytes, immature and GC B cells [171]. The antigen receptors on mature B and T cells are not coupled to the activation of $cPLA_2$ and arachidonic acid release. Moreover, phorbol esters such as PMA, which can activate $cPLA_2$ via MAP kinase in most cell types, also failed to induce the release of arachidonate from mature lymphocytes, suggesting that $cPLA_2$ pathway may not be functional in these cells. Interestingly, western blot analysis revealed that $cPLA_2$ is not expressed in mature B or T cells and that $cPLA_2$ expression could not be up-regulated in lymphocytes following culture with a range of cytokines most likely to be involved in an immune response. In contrast, $cPLA_2$ was shown to be expressed and activated in thymocytes and immature B cells under conditions in which ligation of the antigen receptors led to growth arrest and/or apoptosis. Taken together, these data suggest that $cPLA_2$ does not play a role in antigen receptor mediated lymphocyte activation, but may be involved in the molecular mechanisms underlying lymphocyte maturation and/or self tolerance by clonal deletion.

1.4.2.3 Further processing of arachidonic acid

Arachidonic acid, which contains four double bonds, is converted via the COX pathway into the prostaglandins of the 2-series (PDG_2, PGE_2, PGF_{2a}, PGI_2, TXA_2). During the COX reaction two molecules of the dioxygen are introduced, one at C_{11} and the second at the C_{15} of the AA backbone.

Both COX-1 and COX-2 are located within the ER and the nuclear envelope. COX-2 is, however, more concentrated in the nuclear envelope than COX-1. This observation suggests that COX-1 and COX-2 in the ER and COX-2 in the nuclear envelope constitute independent prostanoid biosynthetic systems [172]. COX-2 is especially important because it is upregulated in certain types of cancer and is thought to support their proliferation [184].

Lipoxygenases (LOXs) catalyse the oxygenation of polyunsaturated fatty acids containing at least one 1,4-pentadienyl system to their corresponding 1-hydroperoxy derivatives [172]. LOXs are classified with respect to their positioned specificity of AA oxygenation. In mammalian cells, there are three major types of LOXs: 5-LOX, 12-LOX and 15-LOX. Interestingly, the main product of COX-2, PGE_2, acts through G-protein receptors of B cells to induce cAMP-mediated apoptosis [185]. The function of PGE_2 was suggested to be biphasic, causing growth inhibition at low concentrations and apoptosis at higher concentrations [186]. Over-expression of Bcl-2 in immature B cells failed to stop PGE_2-induced apoptosis [185]. In thymocytes, PGE_2 was shown to cause apoptosis by stabilization of c-Myc, but without any effect on Bcl-2 expression [187]. Interestingly, Bcl-2 expression in CH31 B cells inhibited PGE_2-induced apoptosis [185]. In contrary, PGE_2 abolished apoptosis caused by COX-2 inhibition, in colon cancer cells, by modulating Bcl-2 expression [188].
Although LOXs are present in B cells, there is no evidence yet of their involvement in cell signalling of these cells [179, 189].

1.4.2.4 Ceramide production downstream of BCR stimulation

The sphingomyelin pathway is initiated by hydrolysis of the phospholipid sphingomyelin (N-acylsphingosine-1-phosphocholine) which is preferentially concentrated in the plasma membrane of mammalian cells. Ceramide, generated by sphingomyelin hydrolysis, acts as a second messenger and initiates cell type specific signalling [190]. Apoptosis is only one of many reported effects in response to ceramide generation although it is a commonly reported event (for review see: [191]). Moreover, a number of cellular sphingomyelinases have been characterised and they are defined by their pH optima as either neutral or acid. Neutral sphingomyelinase is found in many, if not all, tissues. Neutral sphingomyelinase displays a pH optimum of 7.4, while acid sphingomyelinase, posses optimum pH between 4.5-5.5. A synthetic mechanism also exists for the generation of ceramide, which under some circumstances can be regulated for induction of apoptosis.
Early studies suggested that ceramide mediates the apoptotic response of WEHI-231 cells to anti-IgM, corticosteroids and irradiation [192].

Furthermore, resistance to anti-IgM-induced apoptosis in a WEHI-231 subline was found to be due to insufficient production of ceramide [193]. In WEHI-231 cells, neutral sphingomyelinase was long thought to be to source for BCR-induced ceramide [194]. Conflicting studies, however, suggested that apoptosis in WEHI-231 cells is mediated by either ceramide production *de novo* from palmitate [195] or acid sphingomyelinase [194]. Studies in WEHI-231 cells suggested PKC inhibition combined with ceramide production synergise to promote apoptosis [196]. Moreover, PKC inhibition in these cells increased ceramide production over baseline levels with a concurrent decrease in sphingomyelin due to activation of neutral sphingomyelinase [197]. In contrast, in other systems, activation of PKC was shown to block radiation-induced generation of ceramide and apoptosis [198].

In a number of systems, other than lymphocytes, ceramide was linked to the arachidonic acid cascade. Ceramide stimulates the transcription of COX-2 and $cPLA_2$ [199]. It is possible that ceramide acts to amplify the magnitude of signals downstream of the $cPLA_2$ pathway. Furthermore, sphingosine generation has been shown to synergise with TNFα signalling to effect $cPLA_2$ activity [200]. In contrast, membrane soluble ceramide (c_2-ceramide) and one of its metabolites were shown to increase COX-2 levels in fibroblasts but not to influence $cPLA_2$ [201].

1.4.2.5 Cell cycle related events in the apoptosis and rescue of WEHI-231 cells

A network of nuclear proteins was suggested to mediate the downstream effects of IgM cross-linking in WEHI-231 cells (for review see [98]). It is unclear, though, how BCR-induced growth arrest and apoptosis are controlled by this network [202]. Proteins linked to apoptosis, such as Bcl-2 family members, may also influence the transcriptional regulation during the cell cycle [203, 204], a suggestion which was also raised for BCR-induced cell death of WEHI-231 cells [159]. Another important link between the cell cycle and apoptosis is that an abortive entry into the cell cycle may be a primary reason for apoptosis [205].

The signalling events following BCR stimulation of immature phenotype B lymphomas are very diverse. While apoptosis of various cell types through the TNF and TNF-R receptor families is relatively fast (about 4 hours until DNA ladders appear), the programmed cell death of immature B cells takes substantially longer (at least 24 hours in WEHI-231 cells). This may reflect a difference in the regulation of BCR induced apoptosis. A few attempts have been made to establish an explanation for how this regulation is achieved. An important suggestion is that apoptosis of immature B cells requires growth arrest and that the rescue process is essentially the reversal of this arrest ([154, 156, 157, 159, 206] and see below). This theory is supported by the involvement of two phenomena observed downstream of BCR-induced apoptosis: destabilisation of the transcription factor c-myc, a crucial mediator of cell fate decisions [206-208] and the involvement of G_1 cyclin-cdk complexes in this process [159, 209].

Stimulation of the BCR on of WEHI-231 cells leads to a transient increase in c-myc transcription, followed within hours by a drop in c-myc mRNA levels to below background [98]. This evidence suggest that elevation of c-myc expression predisposes immature B cells to apoptosis, as shown in other systems [210]. Surprisingly, treatment with anti-sense to c-myc mRNA stabilises it and in fact blocks both growth arrest and apoptosis in WEHI-231 cells. It was suggested that maintenance of c-myc levels is therefore essential for normal cell survival in these cells. Therefore, disturbance of c-myc mRNA levels leads to cell death [98]. This view is supported by studies showing that increase in c-myc expression can lead to susceptibility to cell death [83].

Evidence from different groups regarding the role of cyclins and their counterpart kinases (Cdks) in BCR signalling is incomplete and sometimes contradictory. For example, an important study reported that immature B cells enter but do not progress beyond the early G_1 phase of the cell cycle in response to antigen receptor signalling [159]. Nonetheless, both immature and mature B cells showed BCR-induced increase in Cyclin D2 and Cdk4, which are essential for early G_1 phase progress. In contrast, whilst cross-linking of sIg on WEHI-231 cells also reduced the Cyclin A:Cdk2 complex activity [98, 209], in mature B cells

such a signal caused an increase in Cyclin A [211], Cyclin E and Cdk2 levels [159]. In contrast to this evidence, observations of CD40 signalling in WEHI-231 cells suggested that rescue signals are actually mediated by both re-induction of Cdk4 and Cdk6 to resume their normal expression levels and this is sufficient for passing the G_1 restriction point even in the presence of apoptotic signals mediated by IgM [212].

Until recently, apoptosis in immature B cells was generally considered to be p53-independent [98]. However, new data has showed that p53 expression peaks 6hr after anti-IgM stimulation [114]. However, this experiment was restricted to only a 12hr time-course and involved exogenous p53 being microinjected under serum-starvation stress. Moreover, it was recently reported that during BCR-induced apoptosis, p53 disassociates from NF-κB [213], in contrast to the expected participation of the latter in growth arrest and cell death. This has raised new doubts about the importance of p53 in inducing this type of apoptosis.

Some studies illustrate a crucial role for two cyclin inhibitors, p21 and p27, in B cell signalling. This is a significant observation since these inhibitors mediate many of p53 interactions with the cell cycle machinery and the pRb family [82, 105, 214], alongside some p53-indepedent activities [215, 216]. The cell cycle arrest accompanying apoptosis in WEHI-231 cells was suggested to be mediated by both p21 and p27 [114, 217, 218]. Furthermore, p27 is capable of inhibiting cyclin A:cdk2 complexes, which were shown to be essential for BCR signalling in WEHI-231 cells [217]. p27 levels were also reported to be down-regulated by CD40 signalling in WEHI-231 cells [218]. However, p27 knock out mice did not show any defects in lymphocyte differentiation[1]. Dysfunction of other cyclin inhibitors, p15, p16 and p19, was observed in diffuse large B cell lymphomas [88].

The cell cycle arrest of WEHI-231 cells after IgM cross-linking was also shown to correlate with the dephosphorylation of pRb [98, 217], which denies exit from G_1 [209]. Interestingly, pRb is dephosphorylated, as well, by sphingosine, a ceramide metabolite [219]. Although it has long been

[1] J. M. Roberts, Fred Hutchinson Cancer Research Center, Seattle, personal communication.

assumed that pRb/E2F complexes play their classical role in modulating apoptosis/survival decisions in B cells [98], there has been very little evidence to support this assumption. In Bcl-x_L transfected WEHI-231 cells, BCR stimulation, induces growth arrest but does not kill. Recently, it was shown that in these cells, p130 replaced p107 in E2F-1/DP-1 complexes This effect was reversed by CD40 ligation [220]. Although this study did not find any role for pRb, quiescence in human B cells was shown to be maintained by pRb/E2F-4/DP-1 complexes [221]. This evidence suggest that different pocket-protein/E2F/DP complexes may determine the fate of B cells during their development.

Taken together, it seems likely that growth arrest of immature B cells would be the crucial point when they could be still rescued after BCR cross-linking. Importantly, over-expression of Bcl-2 in immature B cells rescues them from apoptosis, but fails to initiate cell cycle progression [222]. This evidence suggests two independent mechanisms of BCR-induced apoptosis of immature B cells, one for growth arrest and second for death. In other systems, it was shown that catastrophically high cdk activity is sufficient for the induction of apoptosis [204]. Therefore the possibility that the mechanisms of growth arrest and apoptosis in WEHI-231 cells are closely linked cannot be entirely excluded (for review see [98]).

1.5 Aims

This study had three closely related aims:

(i) To establish the involvement of mitochondrial and cell cycle related events in BCR-mediated apoptosis of WEHI-231 immature B cells.

(ii) To extend this knowledge into primary immature and transitional B cells with emphasis on the factors required for their development.

(iii) To draw parallels between selection of B cells in the bone marrow and that of B cells in the Germinal Centres and in the peritoneal cavity.

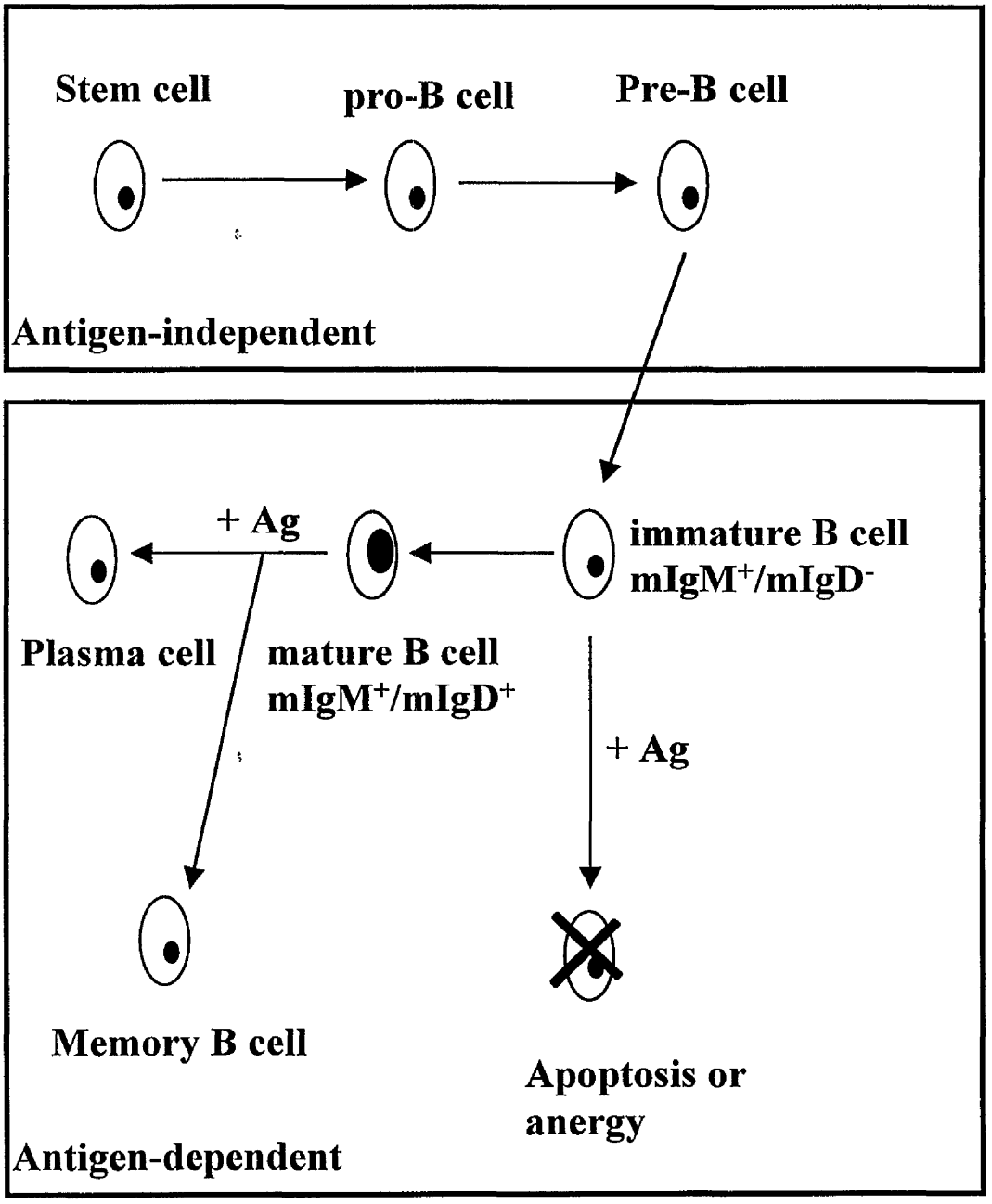
Stem cell
pro-B cell
Pre-B cell
Antigen-independent
+ Ag
immature B cell
mIgM+/mIgD-
Plasma cell
mature B cell
mIgM+/mIgD+
+ Ag
Memory B cell
Apoptosis or
anergy
Antigen-dependent

Fig. 1

Figure 1: The classical model for B cell development. The development of B cells can be divided into two stages: antigen-independent and and antigen-dependent. The first positive selection checkpoint is at the pro-B to pre-B transition, and cells that express the pre-BCR expand. At the immature B cell stage in the bone marrow, cells may be eliminated, their receptors may be edited, or they may be otherwise anergised by self-antigens. These immature B cells may also be positively selected to emigrate to the periphery. B cells emerge from the bone marrow into the periphery where they enter the follicles and acquire the ability to enter the recirculating naive B cell pool. BCR-mediated signalling permits the maintenance of peripheral B cells. A secondary selection process during affinity maturation occurs in the Geminal Centres (see fig. 3).

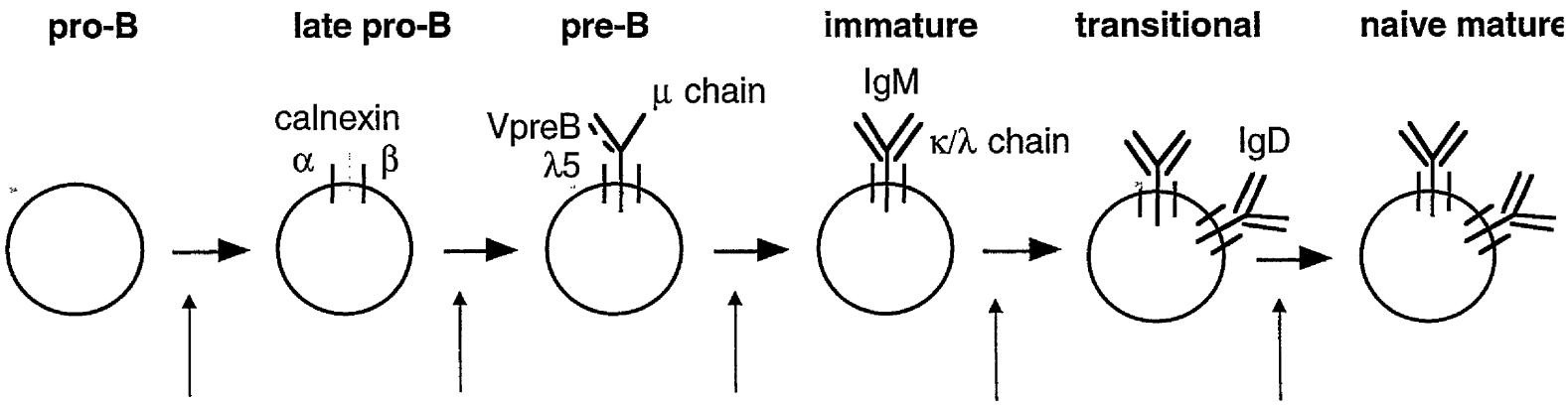

block in knockout models: RAG-1/2$^{-/-}$ Igβ, Syk$^{-/-}$ λ5, μm(TM)$^{-/-}$ Igα$^{-/-}$ Btk$^{-/-}$

BCR expression:	-	-	pre-BCR	IgM	IgM IgD^{lo}	IgM IgD^{hi}
Ig heavy chain:	germline	DJ rearrangement	VDJ rearrangement			
Ig light chain:	germline	germline	VJ rearrangement			
Surface markers:	B220^{+}	B220^{+}	B220^{+}	B220^{+}	B220^{+}	B220^{+}
	CD19^{+}	CD19^{+}	CD19^{+}	CD19^{+}	CD19^{+}	CD19^{++}
	CD43^{+}	CD43^{+}	CD43$^{+/-}$	CD43^{-}	CD43^{-}	CD43^{-}
	CD24^{-}	CD24^{+}	CD24^{++}	CD24^{++}	CD24^{+++}	CD24^{+}
	CD25^{-}	CD25^{-}	CD25^{+}	CD25^{+}	CD25^{-}	CD25^{-}
	CD23^{-}	CD23^{-}	CD23^{-}	CD23^{-}	CD23$^{+/-}$	CD23^{+}

Fig. 2

Figure 2: Changes in surface expression and receptor rearrangement during B cell development. The various stages of B cell development in the bone marrow can be identified by various cell markers. Pan B-cell markers, CD19 and B220/CD45R, appear on the cell surface as early as the pre-B stage. A mature form of surface IgM appears in immature B cells and directs their negative selection. IgD is firstly expressed on transitional B cells and enables them to emigrate to the periphery and there to undergo further selection. Peripheral mature B cells also co-express IgM and IgD.

Arrows indicate arrests in development of various knock-out mice models. These observations are useful in assesing the role of different molecules in B cell development.

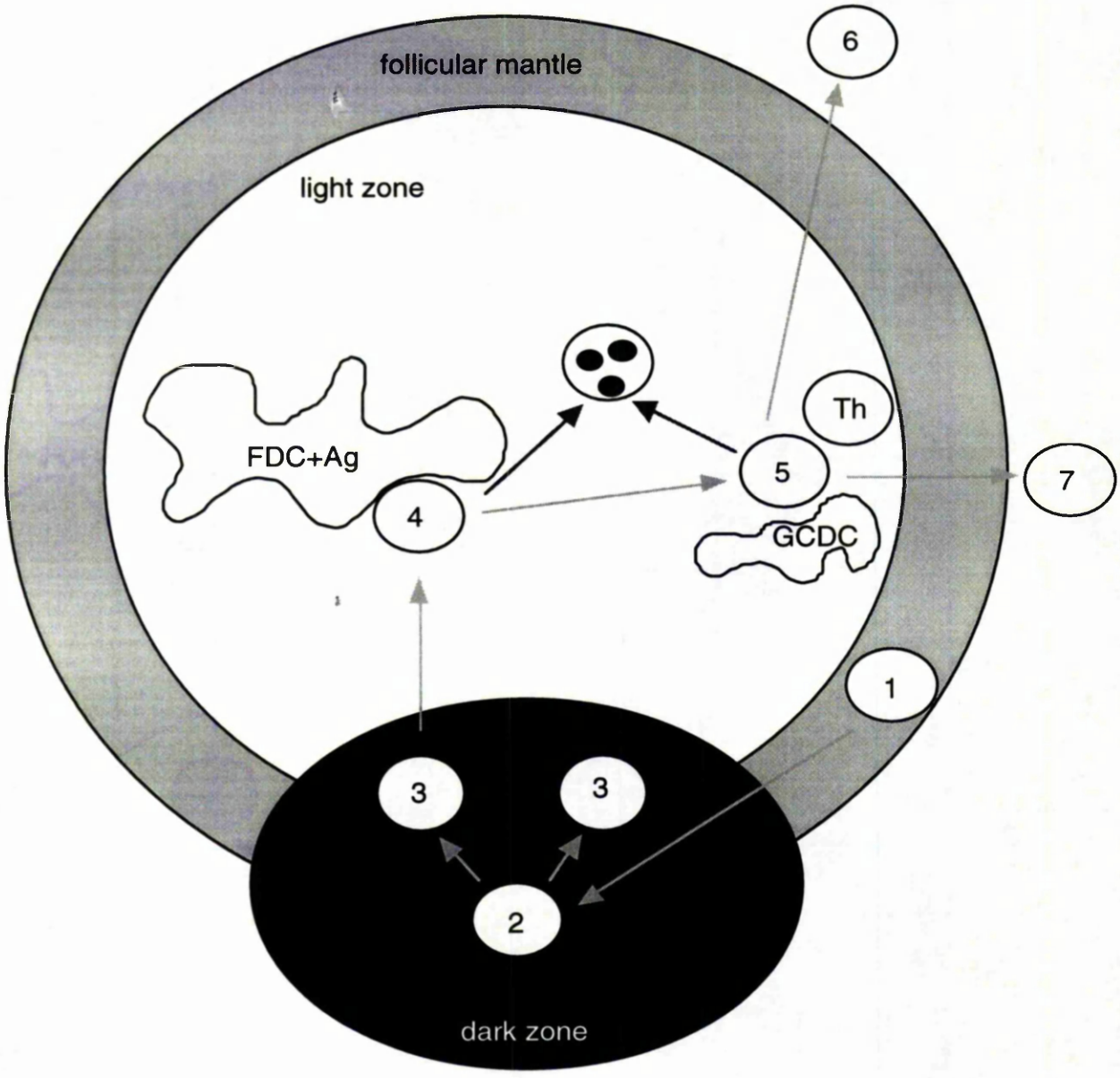
follicular mantle
light zone
6
Th
FDC+Ag
5
7
4
GCDC
1
3
3
2
dark zone

Fig. 3

Figure 3: Mature B cell development in Germinal Centre. Resting unmutated naive B cells (1) in the follicular mantle are activated in a T cell dependent manner, then migrate into B cell follicles (2), where they differentiate into proliferating centroblasts (3); there they form the GC dark zone, where somatic mutation in the variable region of the Ig genes occurs. The centroblasts differentiate into centrocytes (4) that undergo positive selection depending on the affinity of their mutated antigen receptors in the GC light zone. Low affinity and autoreactive centroblasts (4) that are not selected undergo spontaneous apoptosis. The positively selected high-affinity centrocytes (5) may undergo CD40-induced isotype switching, become protected from Fas-induced apoptosis, and differentiate into either plasma cells (6) or into memory B cells (7).

Caspase (Zymogen length in kDa)	**Prodomain length and motif**	**Active subunits in kDa**	**Activation adapter**	**Tetra-peptide preference**
Apoptotic initiators				
Caspase-2 (51)	Long, CARD	20 /12	RAIDD	DXXD
Caspase-8 (55)	Long, DED	18 /11	FADD	(L/V/D)EXD
Caspase-9 (45)	Long, CARD	17 /10	APAF-1	(I/V/L)EHD
Caspase-10 (55)	Long, DED	17 /12	FADD	Unknown
Apoptotic effectors				
Caspase-3 (32)	Short	17 /12	NA	DEXD
Caspase-6 (34)	Short	18 /11	NA	(V/T/I)EXD
Caspase-7 (35)	Short	20 /12	NA	DEXD
Cytokine processors				
Caspase-1 (45)	Long, CARD	20 /10	?CARDIAK	(W/Y/F)EHD
Caspase-4 (43)	Long, CARD	20 /10	Unknown	(W/L/F)EHD
Caspase-5 (48)	Long	20 /10	Unknown	(W/L/F)EHD
Caspase-11 (42)	Long	20 /10	Unknown	Unknown
Caspase-12 (50)	Long	20 /10	Unknown	Unknown
Caspase-13 (43)	Long	20 /10	Unknown	Unknown
Caspase-14 (30)	Short	20 /10	NA	

Table 1: Caspase characteristics and activation. adapted from [223].

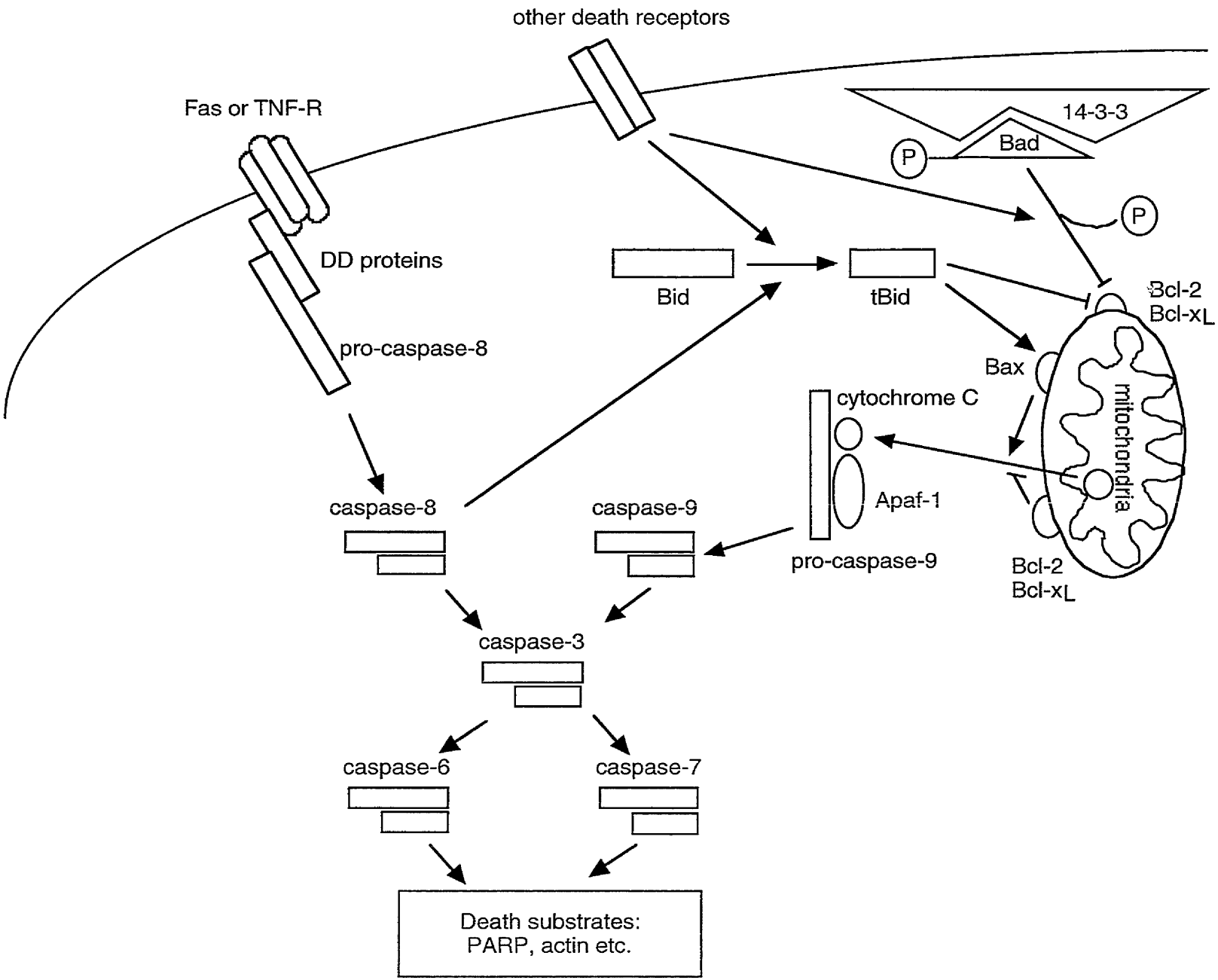
other death receptors
Fas or TNF-R
14-3-3
Bad
P
P
DD proteins
Bid
tBid
Bcl-2
Bcl-xL
pro-caspase-8
Bax
cytochrome C
mitochondria
caspase-8
caspase-9
Apaf-1
pro-caspase-9
Bcl-2
Bcl-xL
caspase-3
caspase-6
caspase-7
Death substrates:
PARP, actin etc.

Fig. 4

Figure 4: Two Principal Signalling Pathways of Apoptosis. One pathway involves ligation of death receptors, resulting in the recruitment of the adaptor protein FADD through interaction between the death domains (DD) of both molecules. The death effector domain (DED) of FADD in turn recruits pro-Caspase-8, which is cleaved and activated at the receptor complex. Another pathway, which is triggered by many apoptotic stimuli, is initiated at the mitochondria. An early, not well-understood step is the mitochondrial release of cytochrome C into the cytosol which, together with dATP, binds to the CED-4 homolog Apaf1. This event unmasks the CARD motif in Apaf1 and allows binding of pro-Caspase-9 through CARD/CARD interaction. The mitochondrial but not the death receptor pathway is inhibited by Bcl-2. Antiapoptotic members of the Bcl-2 family may interfere with the relocalization of cytochrome C or with the binding of cytochrome C to Apaf-1. Following activation of the initiator caspase Caspase-8 or Caspase-9, the two pathways converge on the activation of effector Caspase-3, -6, and -7, which finally cleave various death substrates. Because Caspase-8 cleaves Bid and generates a truncated, proapoptotic BH3-containing fragment (tBid) that induces cytochrome C release, both pathways cross-communicate. Caspase-8, in turn, can be also activated by Caspase-6 following Caspase-9 cleavage, thereby amplifying the apoptotic signal.

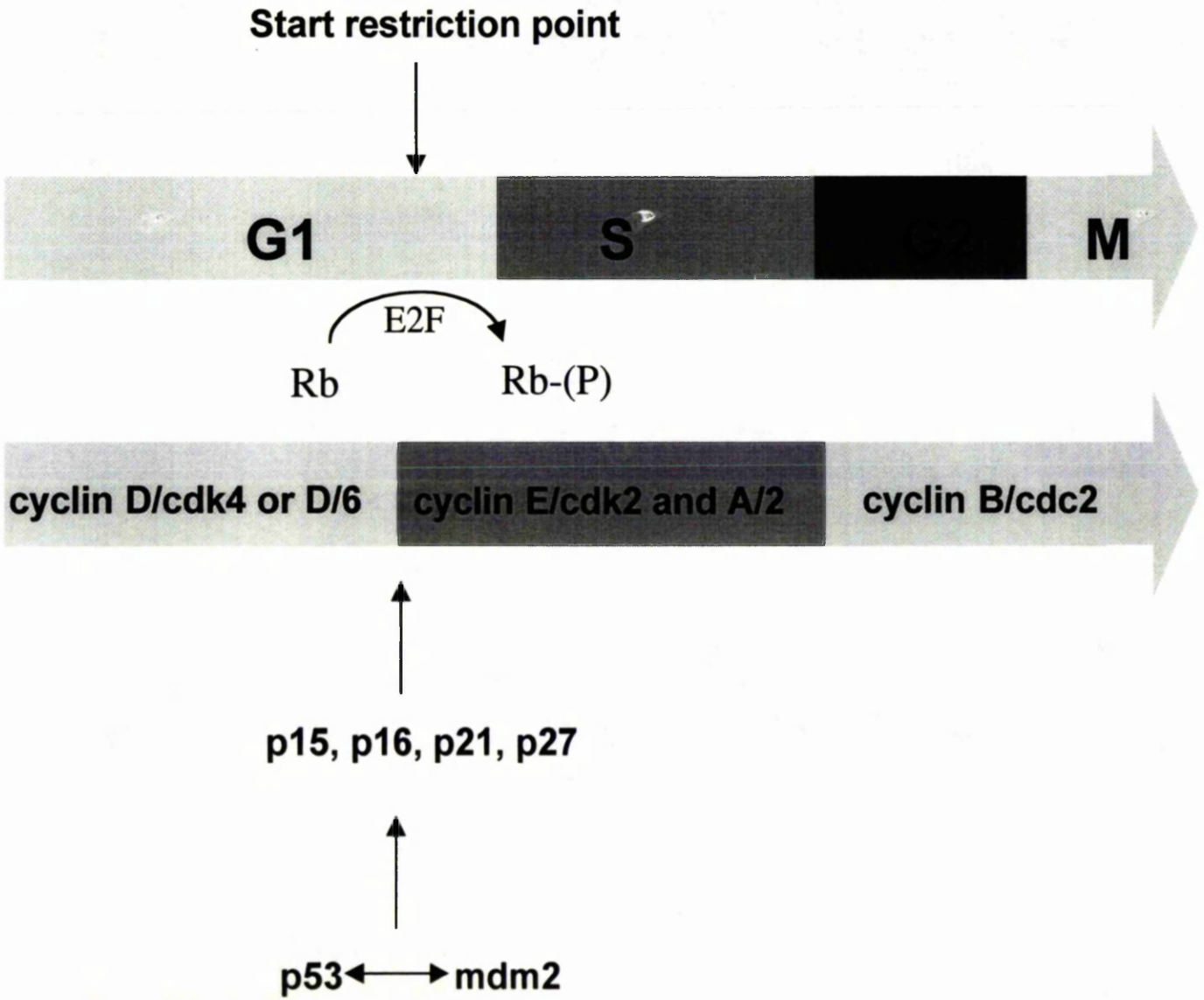
Start restriction point
G1
S
M
E2F
Rb
Rb-(P)
cyclin D/cdk4 or D/6
cyclin E/cdk2 and A/2
cyclin B/cdc2
p15, p16, p21, p27
p53
mdm2

Fig. 5

Figure 5: Progession of the cell cycle. Many cell fate decision are taken at the Start restriction point, two thirds into G_1 phase. In order to pass this point Rb has to be phosphorylated to allow E2F DNA binding. Inhibitors downstream of p53, such as p21 and p27, also regulate this restriction by binding to Cdks and inhibiting the catalytic activity of Ckis (see also fig. 6).

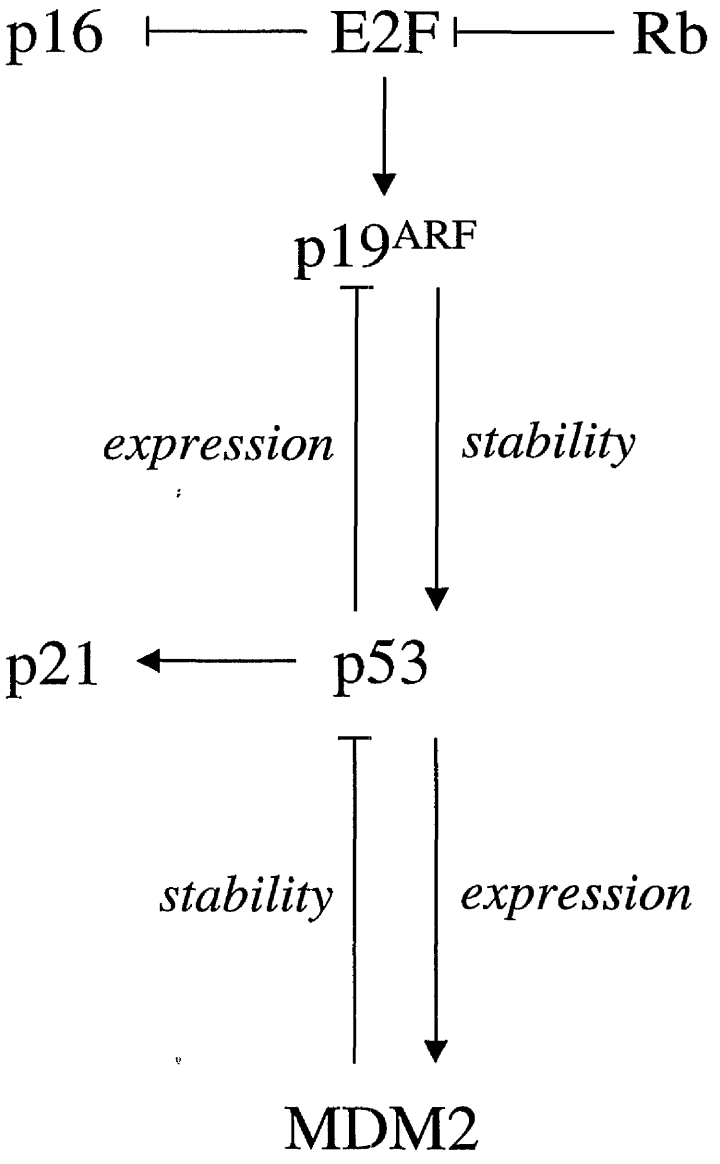
p16
E2F
Rb
p19ARF
expression
stability
p21
p53
stability
expression
MDM2

Fig. 6

Figure 6: The p53/Rb network. The balance between components of the Rb/p53 network decide whether the cell will progress to S phase and will ultimately divide. p53 is at the centre of this network, regulating the expression of many components not shown here such as Bcl-2 family members, mitochondrial proteins and others. Mdm2 binding to p53 casues the degradation of the latter and $p19^{ARF}$ stabilizes p53 by blocking nucleo-cytoplasmic shuttling of Mdm2 [86].

Chapter 2. MATERIALS AND METHODS

2.1 Antibodies and protein conjugates

2.1.1 Non-conjugated antibodies

Protein[2]	Source	Host	Clone or ID	Dilution	Usage[3]
A1	Santa Cruz	goat	T-18	1:500	WB
ANT[4]	Gift from Dr. P. Schmid, Hormel Inst., University of Minnesota	rabbit		1:2000	WB
BAD	Transduction Laboratories	mouse	32	1:500	WB
pSer112-BAD	New England BioLabs	rabbit	9291	1:1000	WB
pSer136-BAD	New England BioLabs	rabbit	9295	1:1000	WB
Bak[3]	Oncogene	mouse	TC102	1:500	WB/IP
Bax[3]	PharMingen	mouse	6A7	1:500	WB
Bcl-2[3]	Transduction Laboratories	mouse	7	1:500	WB
Bcl-x[3]	Transduction Laboratories	rabbit	B22630	1:1000	WB
Bcl-x_L[3]	Zymed	mouse	2H12		IP
BID	Santa Cruz	goat	M-20	1:500	WB
CD40	-	rat[5]	FGK.45		Stimul.
cdk4	Santa Cruz	rabbit	C-22	1:1000	WB

[2] Antibodies were origanlly raised against the murine form of the protein unless indicated.
[3] Abbreviations: WB: Western Blotting; IP: Immunoprecipitation; Stimul.: Stimulation; IF: immunofluorescence.
[4] Raised against the human form of the protein. Crossreactive with mouse.
[5] From hybridoma cell line, see antibody purification, section 2.3.9.

Protein[2]	Source	Host	Clone or ID	Dilution	Usage[3]
$cPLA_2$[3]	Diagnostics Scotland	sheep	S572	10µl	IP
$cPLA_2$[3]	The Binding Site	sheep		1µl	IF
cytochrome C[3]	PharMingen	mouse	7H8. 2C12	1:500	WB
cytochrome C[6]	Santa Cruz	rabbit	H-104	1:1000	WB
$F(ab')_2$ fragment anti-IgG+ IgM (H+L)	Jackson Laboratories	goat			Stimul.
HDAC-1[3]	Santa Cruz	rabbit	H-51	1:500	WB
Mcl-1[3]	Transduction Laboratories	mouse	11	1:1000	WB
mdm2[3]	Santa Cruz	mouse	SMP14	1:500	WB
Ig mu chain	-	rat[4]	B7.6		Stimul.
p16	Santa Cruz	rabbit	M-156	1:500	WB
p53[3]	Oncogene	mouse	Pab421	NA	IP
p53[3]	Santa Cruz	rabbit	FL-393	1:500	WB
p53[3]	Diagnostics Scotland	rabbit	S238-120	1:1000	WB
pSer15-p53[3]	New England BioLabs	rabbit		1:1000	WB
p130[3]	Santa Cruz	rabbit	C-20	1:500	WB
PARP[3]	Santa Cruz	goat	N-20	1:1000	WB
cleaved PARP	New England BioLabs	rabbit		1µl	IF
RAG-1	Santa Cruz	rabbit	K-20	5µl	IF
Rb[3]	PharMingen	mouse	G3-245	1:500	WB/IP

Secondary antibodies and streptavidin conjugates:

Proteins	Host	Conjugate	Source
goat/sheep IgG	donkey	HRP	Diagnostics Scotland
mouse IgG	goat	HRP	Diagnostics Scotland
rabbit IgG	donkey	HRP	Diagnostics Scotland
streptavidin	-	HRP	Diagnostics Scotland

2.1.2 Flow cytometry and cell separation

All antibodies were titrated per batch and used accordingly (fig. 7). The magnetic beads were used according to the manufacturer's instructions (see section 2.3.5.1).

Protein	Conjugate	Source	Host	Clone
Annexin V[7]	Biotin	Roche	-	
B220 (CD45R)	Allophyto-cyanin (APC)	PharMingen	rat	RA3-6B2
CD11b	PE	PharMingen	rat	M1/70
CD19	-	PharMingen	rat	1D3
CD43	Magnetic beads	Miltenyi Biotech	rat	
CD44	FITC	PharMingen	rat	1M7
CD5	PE	Serotec	mouse	KT25
Fas (CD95)[4]	-	Serotec	mouse	LOB3
Fas[4]	Biotin	PharMingen	hamster	Jo2
FITC	Magnetic beads	Miltenyi Biotech	mouse	
HEL[8]	FITC	Gift from Dr. P. Garside, Dept. of Immunology, Uni. of Glasgow	-	

[6] Raised against the horse form of the protein. Crossreactive with mouse.
[7] Conjugated protein for the detection of apoptotic cells, see section 2.3.11.2.
[8] Protein conjugate for the detection of B cells bearing BCR specific for chicken egg lysosyme (HEL)

Protein	Conjugate	Source	Host	Clone
Ig delta-chain	-	Hybridoma cell line	-	1.19
Ig kappa-chain	Biotin	Serotec	rat	MRC OX-20
Ig kappa-chain	Biotin	Zymed	rat	LO-MK-1
Peanut Agglutinin (PNA)[9]	Biotin	Pierce	-	
PNA	FITC	Sigma	-	

Secondary antibodies and streptavidin conjugates:

Proteins	Host	Conjugate	Source
goat/sheep IgG	donkey	Biotin	Diagnostics Scotland
mouse Ig gamma chain	goat	Biotin	Sigma
rabbit IgG	donkey	Biotin	Diagnostics Scotland
rabbit IgG	donkey	FITC	Diagnostics Scotland
rat Ig	rabbit	FITC	DAKO
rat Ig	goat	FITC	PharMingen
rat IgG	goat	APC	Caltag
streptavidin	-	APC	PharMingen
streptavidin	-	FITC	Pierce
streptavidin	-	Peridinin Chlorophyll-*a* Protein (PerCP)	PharMingen
streptavidin	-	Texas Red	Vector

from MD4 transgenic mice. See section 2.3.1.

[9] Protein conjugate for the detection of Germinal Centre B cells (section 5.4).

2.2 Other reagents

Description [common name]	Source
3.3'-dihexyloxacarbocyanine iodide [$DiOC_6$ (3)]	Molecular Probes
5,6,7-trihydroxyflavone [Baicalein, 12-LOX inhibitor]	Alexis
5-/6-carboxyfluorescein diacetate, succinimidyl ester [CFSE]	Molecular Probes
Ac-Asp-Glu-Val-Asp-CHO [Ac-DEVD-CHO, Caspase-3 inhibitor]	Calbiochem
Acrylamide/Bis Solution, 29:1	Bio-Rad
Antimycin A [Respiratory chain complex IV inhibitor]	Calbiochem
Carbobenzoxy-L-leucyl-L-leucyl-L-Leucinal [MG-132, Proteosome inhibitor]	Calbiochem
Cyclosporin A	Calbiochem
cytosolic Phospholipase A_2 assay kit	Cayman
Duck egg lysosome [DEL]	Gift from Dr. P. Garside, Dept. of Immunology, Uni. of Glasgow
E64d [EST, Pan Cathepsin inhibitor]	Calbiochem
ECL western blotting reagent	Amersham
Ethyl 3,4-dihydroxybenzylidenecyanoacetate [Pan LOX inhibitor]	Alexis
Foetal Calf Serum [FCS]	Gibco
Fumonisin B_1 [FB_1, Ceramide synthase inhibitor]	Calbiochem
Glutamine	Gibco
L-N^6-(1-Iminoethyl)lysine [L-NIL, iNOX inhibitor]	Alexis
Lactacystin [Proteosome inhibitor]	Calbiochem
MEM non-essential amino acids	Gibco

Description [common name]	Source
MicroBCA protein assay	Pierce
MitoTracker Green	Molecular Probes
N-(2-Cyclohexyloxy-4-nitro-phenyl)methanesulfonamide [NS-398, COX-2 inhibitor]	Calbiochem
N-Acetyl-Asp-Glu-Val-Asp- *p*NA [Caspase 3 substrate]	Calbiochem
N-Acetylsphingosine [c_2-ceramide]	BioMol
N-benzyl-oxycarbonyl-Arg-Arg- *p*NA [Cathespin B substrate]	Calbiochem
N-benzyl-oxycarbonyl-Val-Ala-Asp(OMe)-fluoromethylketone [zVAD-fmk, Pan Caspase inhibitor]	Calbiochem
N-benzyl-oxycarbonyl-Val-Glu(OMe)-Ile-Asp(OMe) -fluoromethylketone [zVEID-fmk, Caspase-6 inhibitor]	Calbiochem
N^G-Monomethyl-L-Arginine [L-NMMA, All NOS inhibitor]	Calbiochem
Nifluril, 2-[[3-(Trifluoro-methyl)phenyl]-amino]-3-pyridinecarboxylic acid [Niflumic Acid, COX-2 inhibitor]	Alexis
Oligomycin [Respiratory chain complex V inhibitor]	Calbiochem
p53 western blotting standard	Calbiochem
Penicillin/Streptomycin	Gibco
Propidium Iodide	Calbiochem
Rhodamine 123	Molecular Probes
RPMI-1640 media	Gibco
Sodium Pyruvate	Gibco
SP Sepharose FastFlow	Amersham
ViaLight HS ATP kit	Lumitech
[^{3}H]-Thymidine	Amersham

All other reagents purchased from Sigma and were at the highest grade available.

2.3 Methods

2.3.1 Animals

BALB/c mice aged 8-12 weeks were used unless otherwise stated. These mice, as well as $IgM^{-/-}$ BALB/c (gift from Prof. F. Brombacher, University of Cape Town, South Africa), Xid (CBA/N) and ES-62 treated BALB/c, were kept in the animal facility of Department of Immunology, University of Strathclyde, Glasgow. $IgM^{-/-}$ BALB/c and Xid (CBA/N) mice were kept at the barrier facility until sacrifice. MD4 (BCR-HEL, C57/CBA) and *lpr* mice were kept in the animal facility of University of Glasgow and were provided by Dr. P. Garside and Prof. F. Y. Liew from the Department of Immunology. These mice were used at the age of 10-18 weeks.

2.3.2 ES-62 minipumps

The following procedures were preformed by Dr. Maureen Deehan and were designed to mimic the *in vivo* release of parasite-derived immunomodulatory molecule, ES-62 by the rodent flarial nematode *A. viteae*.

2.3.2.1 Priming of osmotic mini-pumps

Alzet Osmotic Mini-Pumps model 2002 (Alza) were loaded with 200µl of either 10µg, 20µg, 40µg, 80µg ES-62 or PBS pH 7.4 and were left overnight at room temperature submerged in sterile 0.9% saline solution, according to the manufaturer's instructions.

2.3.2.2 Surgical implantation of osmotic mini-pump

Five groups of male BALB/c mice of at least 20g and 6-8 weeks old were anaesthetised with Halothane-RM (Aventis Pasteur MSD) in a O_2/N_2O mix, under sterile conditions. The back of the neck was swabbed with

disinfectant (0.1% benzalkonium chloride) and the area shaved. A mid-scapular incision was made and the connective tissue severed to create a pocket to insert the minipump. The pump was placed, according to manufacturer's instructions with the flow moderator inserted first. The wound was sutured and the animal observed until consciousness was regained. All animals were housed individually. Animals were sacrificed on day 14 by cardiac puncture. Once sacrificed, spleen, lymph nodes and peritoneal cells were harvested from each mouse.

2.3.3 Pre-immunisation of MD4 mice

The following procedure was preformed by Karen Smith. MD4 HEL-BCR mice were injected subcutaneously with either PBS, 100µg DEL (+Freund's complete adjuvant) or 100µg HEL (+Freund's complete adjuvant). The animals were sacrificed after 8d.

2.3.4 Cell maintenance and stimulations

The murine B cell lymphoma, WEHI-231 and the human leukemia T cell line Jurkat were purchased from ECACC and frozen stocks were kept in cryostorage. All cells were cultured in RPMI-1640 medium containing 5% foetal calf serum, L-glutamine (2mM), penicillin (100U/ml) and streptomycin (100 µg/ml) (RPMI complete) at 37°C in 5% CO_2. RPMI complete media for WEHI-231 cells and primary cells was supplemented with 2-mercaptoethanol (50µM). For DNA synthsis assays the media was supplemented with MEM non-essential amino acids (1:100) and sodium pyruvate (0.1mM).

Cells were seeded at the following densities for stimulation: 0.5-1x10^6 cells for WEHI-231 and Jurkat cells and 0.5-5x10^6 cells for primary cells. Stimulations lasted 2 days (42-48h, unless indicated otherwise in text) and were terminated by a wash in cold PBS (1.37M NaCl, 3mM KCl, 10mM Na_2HPO_4, 2mM KH_2PO_4).

2.3.5 Primary cell purification

For bone marrow cultures the bone marrow was flushed with RPMI-1640 media out of the femur bones. The brachial, axial, inguinal and mesenteric lymph nodes were pooled together for lymph node cultures.
Bone marrow, lymph nodes and spleens were mashed through a wire mesh, in RPMI-1640 media. The resultant single cell suspensions were underlaid by 1ml cold FCS and left for 5min on ice to remove fat. The upper layers were transferred to fresh tubes and centrifuged through another layer of FCS (1ml). Cells were recovered from the pellet, resuspended and cultured.
Peritoneal B cells were retrieved from peritoneal cavity washes (7ml from each mice). The washes were incubated in culture flasks for 1h at 37°C. The incubation was repeated once more and the non-adherent cells were collected (typically ~70% B cells by flow cytometry).

2.3.5.1 Purification of B cells from spleens or lymph nodes

Single cell suspension (6ml; equivalent to 2 spleens or lymph node sets) were layered over Hystopaque-1077 cushions (3ml) and centrifuged at 400g, for 30min at 20°C. Cells at the interface were removed and diluted out with media to 50ml and then centrifuged at 630g for 10min at 4°C. The supernatant was discarded and cells were resuspended in 50ml cold MACS buffer (PBS/0.5% Bovine Serum Albumin/2mM EDTA). The cells were centrifuged at 430g, for 5min at 4°C and resuspended in 50ml cold MACS buffer and counted. The cells were centrifuged again before resuspending in cold MACS buffer ($2x10^8$ cells/ml), and passing through gauze, to remove clumps. Cells were incubated for 20min at 4°C with anti-CD43 beads (100µl $CD43^+$ beads/$2x10^8$ cells) and then allowed to pass through a CS-type depletion magnetic column (Miltenyi Biotec). Purified mature B cells, which are $CD43^-$, were collected from the first 10-15ml of buffer. Purity (as determined by B220 staining) was at least 95% B cells.

2.3.5.2 Depletion of IgD^{hi} B cells

A similar protocol to B cell isolation was employed with minor changes. Bone marrow cells were incubated with anti-delta chain (1:50) and anti-rat-IgG-FITC (1:100) according to flow cytomentry protocol (section 2.3.11). Immediately afterwards, the cells were incubated with anti-FITC magnetic beads, according to the manufacturer's instructions. A positive depletion was performed on a RS-type selection magnetic column (Miltenyi Biotec), and negative cells collected as run-through. Due to the lack of sensitivity of this method, only highly expressing cells (such as IgD^{hi} B cells) are trapped on the column, as verified by flow cytometry.

2.3.6 DNA Synthesis ([^{3}H] thymidine uptake)

Exponentially growing cells ($5x10^4$ cells/well for WEHI-231 cells, $5x10^5$ cells/well for primary cells) in RPMI-1640 complete medium (supplemented with sodium pyruvate and non-essential amino acids) were stimulated for 44h at 37°C in 5% CO_2. At 44h, the cells were pulsed with 0.5µCi/well of [^{3}H]-thymidine before culturing for a further 4h. The cells were harvested and the level of [^{3}H]-thymidine incorporated into DNA measured by liquid scintillation counting, using a Wallac 1205 Betaplate reader.

2.3.7 Lysate Preparation

WEHI-231 cells (10^7 cells) were stimulated as indicated and reactions were terminated by the addition of 2 x ice-cold lysis buffer: 50mM Tris-HCl (pH 7.4), 150mM sodium chloride, 2% NP-40, 0.25% sodium deoxycholate, 1mM EGTA, 10mM sodium orthovanadate, 0.5mM phenylmethylsulfonylfluoride (PMSF), 10µg/ml chymostatin, 10µg/ml leupeptin, 10µg/ml antipain, and 10µg/ml pepstatin A. Lysates were solubilised for 30min on ice before centrifugation at 19,800g for 15min. The resulting supernatants were stored at -20°C until they were used.

2.3.8 Immunoprecipitation

Whole cell lysates were pre-cleared with 10µl of protein G bead slurry and incubated for 1h at 4°C on an orbital rotator. Samples were centrifuged to remove beads (19,800g, 30min, 4°C) and the supernatant was decanted. Samples were diluted to 1mg/ml with lysis buffer (without protease inhibitors) and incubated with antibody (1.5µg per 10^6 cells) overnight at 4°C, on a orbital rotator. Protein G slurry (25µl) was added and incubated for 4h at 4°C, on an orbital rotator. Samples were centrifuged at 19,800g for 30min at 4°C. The bead pellet contains the immune complexes. The beads were washed four times at 19,800g for 30min at 4°C, with 1ml of ice-cold lysis buffer (with protease inhibitors) and 2xloading buffer (60µl) was added. Before use, the samples were boiled for 5min to separate the immune complexes from the beads. The samples were then centifuged for 2min at 13,000g and the supernatant was used for SDS-PAGE and western blotting.

2.3.9 SDS-PAGE

Protein lysates (100µg/well as determined by MicroBCA protein assay) or immune complexes were resolved by SDS-PAGE. A running gel (7.5-12% acrylamide, 0.38M TRIS-HCl pH8.8, 0.15% ammonium persulphate, 0.15% SDS, 0.07% TEMED) was set between glass plates within a purpose built Bio-Rad kit. On top of the running gel, a stacking gel (5% acrylamide, 0.062M TRIS pH6.8, 0.1% ammonium persulphate, 0.1% SDS, 0.07% TEMED) was layered and a comb was used to create wells for sample loading. The samples were loaded and electro-separated under constant current (100-200mA) using the following electrophoresis buffer: 41mM TRIS, 19mM Glycine, 3.5mM SDS. Electro-transfer onto PVDF membrane preformed with transfer buffer (48mM TRIS, 1.3mM SDS, 20% methanol) in a purpose built Bio-Rad kit, under constant electric potential (~30mV for at least 2h).

2.3.10 Western blotting

SDS-PAGE blots were blocked for non-specific protein binding at room temperature for 1h with 10% non-fat dried milk in PBS/Tween 20 (0.1%) under constant agitation. The milk solution was washed with PBS/Tween 20 and the primary antibody was then incubated with the blot for 1-2h at room temperature. The blots were washed 6 times for 15min with PBS/Tween 20 before addition of the appropriate HRP conjugated secondary antibody (1:3000) in 5% non-fat dried milk for 1h with constant agitation. The blots were washed again 6 times for 15min with PBS/Tween 20 and then were developed with ECL reagent and exposed to film. Prestained molecular weight markers were used to elucidate the molecular weights of unknown proteins. Even protein loading/sample recovery of gels was determined by Ponceau Red staining. For stripping of the gel blot in order to re-expose to a different antibody, the blots were incubated in stripping buffer (10mM Glycine, 10mM NaCl, pH2.6) for 1h at room temperature.

2.3.11 Antibody purification

Purified monoclonal anti-IgM antibodies (anti-mouse mu-chain) and anti-CD40 antibodies were produced from the B7.6 and FGK45 hybridomas, respectively.

For purification of anti-IgM, B7.6 hybridoma supernatant was filtered through 0.2μm filters, to avoid cell debris. The filtered supernatant was loaded overnight onto a purification column (Protein G-agarose). After a wash with 50ml PBS, the antibody was eluted with 15ml 0.2M Acetic acid. The eluted antibody was mixed immediately with 1.5M TRIS-HCl pH8.8 solution (10% of total volume). The mixure was dialysed overnight against PBS and the antibody concentration was determined at A_{280nm} using a spectrophotometer (Becton DU640; A=1.43 is equivalent to 1mg/ml protein).

For purification of anti-CD40, FGK45 hybridoma supernatant was mixed overnight at 4^{0}C with equivalent volume of saturated ammonium sulphate solution. The mixture was centrifuged at 10,000g for 15min at 4^{0}C. The pellet was resuspended in 200ml Malonate buffer (44mM

Malonic acid disodium, 12mM Malonic acid, 8.5 mM betaine) and loaded overnight on a SP Sepharose FastFlow column. After a wash with 50ml Malonate buffer, the antibody was eluted with 15ml 0.5M NaCl/Malonate buffer. The eluted antibody was dialysed overnight against PBS and the antibody concentration was determined at A_{280nm} using a spectrophotometer (A=1.43 is equivalent to 1mg/ml protein).

2.3.12 Flow cytometry

Cells (10^6 per sample) were stained with the appropiate antibodies for 15min at 4°C and washed with PBS/2mM EDTA (EDTA is added to prevent cells from clumping). For non-conjugated antibodies, secondary antibodies were used repeating the same procedure. For example, for detection of Ig kappa chain, cells were incubated first with anti-kappa-biotin conjugated antibody, washed, incubated with streptavidin-APC, and washed again. Cells then were acquired on a Becton Dickinson FACScalibur flow cytometer and analysed using CellQuest software.

2.3.12.1 Assesment of mitochondrial potential

Incorporation of the cationic lipophilic dye $DiOC_6$ (3) into the mitochondria is propotional to the mitochondrial transmembrane potential, $\Delta\psi_m$. Cells were first stained if required, for either Ig kappa chain or PNA (for bone marrow cells and Germinal Centre cells, respectively). Cells were washed with PBS/2mM EDTA, incubated for 30min with 50nM $DiOC_6$ (3) at room temperature and then washed again in PBS/2mM EDTA. An example of mitochondrial potential profile is given in fig. 8.

2.3.12.2 Analysis of Annexin V binding to phosphatidylserine on the cell surface

Cells to be examined for annexin-V binding were washed in PBS and incubated for 30min at 4°C with annexin V-biotin conjugate, at a defined calcium concentration (9mM HEPES, 140mM NaCl, 5mM $CaCl_2$, pH 7.4), according to the manufacturer's instructions. The cells were washed and

then incubated with streptavidin-FITC for 15min and washed in the calcium buffer.

2.3.12.3 Cell cycle analysis

For primary cells, cell staining was performed as described above and then cells were fixed with 70% ethanol, for 15min at 4°C. Cells were washed in PBS/2mM EDTA and incubated for 30min in 250µg/ml propidium iodide (PI; in PBS/2mM EDTA) and analysed for PI incorporation as a measure of DNA content.

WEHI-231 cells become autofluorescent when using the above method. Therefore, such cells were incubated in a non-fixing solution (0.1% Sodium Citrate, 0.1% Triton X-100, 50µg/ml PI) for 15min at 4°C and then analysed.

An example of how DNA content was determined is given in fig. 9.

2.3.13 Intracellular staining and immunohistochemistry

Cells (10^6 per sample) were washed in PBS and fixed in fixation buffer (4% w/v formaldehyde in PBS, pH=7.4). Cells were then washed and permeabilised for 5min in Permeabilisation buffer (2% FCS, 2mM EDTA, 0.1% w/v saponin in PBS) and incubated with 1µg of the relevant primary antibody (30min, 4°C). Bone marrow cells were stained for Ig kappa chain prior to fixation.

For detection of intracellular staining by flow cytometry WEHI-231 cells were further washed and similarly stained with an appropriate FITC-conjugated secondary antibody.

For immunohistochemistry, the cells were further washed and stained with the appropriate biotinylated antibody. Cells were then simultaneously stained with streptavidin-Texas Red and 50nM Rhodamine 123 or 200nM MitoTracker Green (for mitochondria detection). In some experiments, anti-ANT (adenine nucleotide transferase) antibody (and anti-rabbit-FITC secondary) was used to detect mitochondria. Fluorescence microscopy was performed using an Axioskop microscope (Zeiss), CCD camera and digital capture programme (IPlab, Signalanalytics, Vienna, VA, USA).

2.3.14 Qualitative analysis of internucleosomal DNA fragmentation by agarose gel electrophoresis

WEHI-231 cells were centrifuged at 430g for 5min at 20°C. Cell pellets were mixed with 0.5ml TTE buffer (10mM TRIS, 1mM EDTA, 0.2% Triton X-100) and centrifuged at 19,800g for 10min at 4°C. The supernatants were mixed with 0.1ml ice-cold 5M NaCl and 0.7ml ice-cold iso-propanol and kept overnight at -20°C before centrifuged at 19,800g for 10min at 4°C. The DNA pellet was left to dry and washed with 70% ethanol and centrifuged again. The pellet was air dried for 3h at room temperature, and then incubated overnight with 20-50µl TE buffer (10mM TRIS, 1mM EDTA). The samples (10µl) were mixed with 10xloading buffer and then resolved on a 1% agarose gel. Fragmented DNA released from the nuclei of cells undergoing apoptosis was analysed by ethidium bromide staining of DNA ladders (visible under UV light).

2.3.15 Preparation of mitochondria-free extracts

Cells (10^7 per sample) were washed in PBS and resuspended in extraction buffer (50mM Pipes-KOH (pH 7.4), 50mM KCl, 5mM EGTA, 2mM $MgCl_2$, 220mM mannitol, 68mM sucrose, 1mM DTT, 10µM cytochalasin B and protease inhibitors). Cells were left at 4°C for 30min and then lysed with a glass homogeniser, with 40 strokes of the glass dounce. Finally, cells were centrifuged at 14,000g for 15min and the mitochondria-free supernatant and mitochondrial pellets were taken for Western blot analysis of cytochrome C release. The purity was determined by western blotting for the mitochondrial protein ANT.

2.3.16 Isolation of mitochondria

Cells (10^7 per sample) were washed in PBS and then resuspended in 1ml of MI buffer (200mM mannitol, 70mM sucrose, 1mM EGTA, 10mM HEPES (pH 7.5)) and left for 5min on ice. Cells were lysed with a glass Dounce homogeniser, with 20 strokes of the glass dounce. Samples were centrifuged at 700g for 5min at 4°C, and the supernatant was retained (the pellet contains the nucleus and non-lysed cells). The supernatant

was centrifuged at 10,000g, for 5min at 4°C, and resuspended in 0.5ml of MI buffer (non-functional, for size determination or staining) or Mitochondrial Physiological buffer (250mM sucrose, 1mM EGTA, 20mM HEPES, 5mM succinate, 3mM KH_2PO_4, 1.5mM $MgCl_2$, 10mM KCl, 3µM Rotenone; for functional assays such as $cPLA_2$ assay).

2.3.17 ATP determinations

ATP levels were measured using a commercial luciferase kit, ViaLight HS, according to the manufacturer's instructions and using a Turner TD-20e luminometer. The kit determines the ATP concentration using its reaction with luciferin in the presence of luciferase (both included in the kit buffer) which produces luminescence at 590nm.

2.3.18 Cytosolic Phospholipase A_2 assay

Cytosolic phospholipase A_2 ($cPLA_2$) activity in whole cell lysates or mitochondrial fractions was determined using a commercial $cPLA_2$ assay kit based on spectrophotometric detection (A_{414nm}) of free thiol by Ellman's reagent (5,5'-dithiobis(2-nitrobenzoic acid); DTNB) following hydrolysis of the arachidonyl thioester bond at the *sn*-2 position of the $cPLA_2$ substrate, arachidonyl thio-phosphatidylcholine.

2.3.19 Protease activity assays

Cell lysates were prepared as described in section 2.3.6 ($5x10^6$ cells per sample). However, only the serine protease inhibitor PMSF and phosphatase inhibitor sodium orthovanadate were used. Each sample (100µl) was incubated for 30min at RT with 100µM of either Cathepsin B substrate, zRR-*p*NA or Caspase 3 substrate Ac-DEVD-*p*Na. The cleaved substrate was measured at 405nm on a Dynex MRXII plate reader using Revelation software.

2.4 Company and distributor addresses

BioMol
c/o Affinity
Mamhead Castle
Mamhead, Exeter EX6 8HD

Alexis/Cayman
3 Moorbridge Court
Moorbridge Road East
Bingham, Nottingham NG13 8QG

Amersham
Amersham Place
Little Chalfont HP7 9NA

Aventis Pasteur MSD (formely Rhône Mérieux)
Clivemont House
Maidenhead SL6 7BU

PharMingen/Transduction Laboratories
c/o Beckton Dickinson
Between Towns Road
Cowley, Oxford OX4 3LY

Bio-Rad
Maylands Avenue
Hemel Hempstead HP2 7TD

The Binding Site
POB 4073
Birmingham B29 6AT

Calbiochem/Oncogene
c/o Calbiochem Novabiochem
Boulevard Industrial Park
Padge Road
Beeston, Nottingham NG9 2JR

Molecular Probes
c/o Cambridge Bioscience
24-25 Signet Court
Newmarket Road
Cambridge CB5 8LA

Alza
c/o Charles River
Manston Road
Margate CT9 4LT

DAKO
Angel Drove
Ely CB7 4ET

Diagnostics Scotland (formely SAPU)
Law Hospital
Carluke ML8 5ES

ECACC
Centre for Applied Microbiology & Reaserch
Salisbury SP4 0JG

GibcoBRL
c/o Life Technologies
3 Fountain Drive
Paisley PA4 9RF

Santa Cruz/Zymed Laboratories
c/o Insight Biotechonology
POB 520
Wembley HA9 7YN

Lumitech
Nottingham Business Park
City Link
Nottingham NG2 4LA

Miltenyi Biotech
Church Lane
Bisley GU24 9DR

New England BioLabs
Knowl Place
Wilbury Road
Hitchin SG4 0TY

Pierce & Warriner
44 Upper Northgate Street
Chester CH1 4EF

Roche Diagnostics
Bell Lane
Lewes BN7 1LG

Serotec
Station Approach
Kidlington, Oxford OX5 1JE

Sigma-Aldrich
The Old Brickyard
New Road
Gillingham SP8 4BR

Jackson ImmunoReaserch Laboratories
c/o Stratech Scientific
61-63 Dudley Street
Luton LU2 0NP

Caltag Laboratories
c/o TCS Biologicals
Botolph Claydon
Buckingham MK18 2LR

Vector Laboratories
3 Accent Park
Bakewell Road
Orton Southgate, Peterborough PE2 6XS

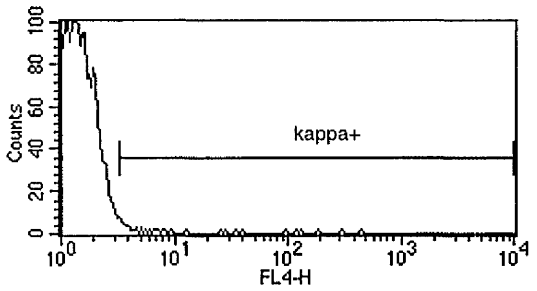

Sample ID: stp-APC alone

Marker	Left, Right	% Total	Mean	Median
All	1, 9910	100.00	1.58	1.30
kappa+	3, 9910	0.86	19.63	3.73

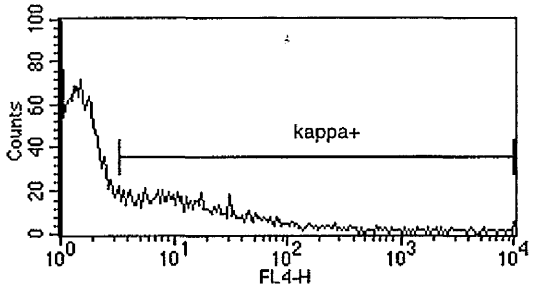

Sample ID: 1/10

Marker	Left, Right	% Total	Mean	Median
All	1, 9910	100.00	36.78	1.84
kappa+	3, 9910	34.11	104.89	11.65

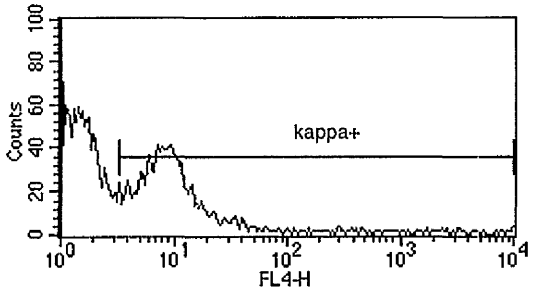

Sample ID: 1/20

Marker	Left, Right	% Total	Mean	Median
All	1, 9910	100.00	28.72	2.53
kappa+	3, 9910	46.18	60.41	8.43

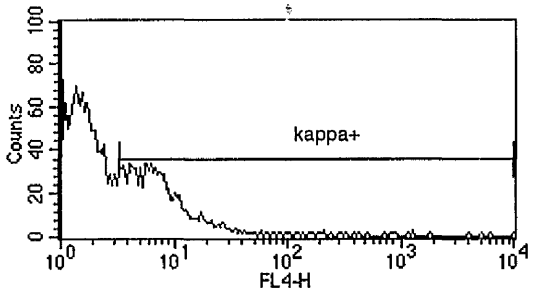

Sample ID: 1/40

Marker	Left, Right	% Total	Mean	Median
All	1, 9910	100.00	8.28	2.02
kappa+	3, 9910	35.88	20.21	6.38

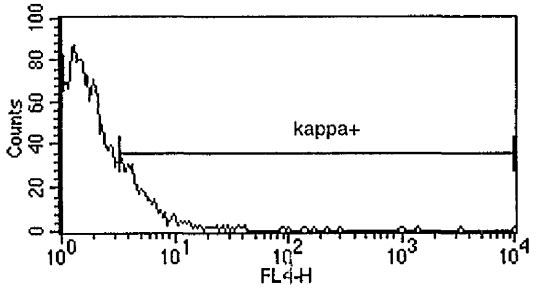

Sample ID: 1/100

Marker	Left, Right	% Total	Mean	Median
All	1, 9910	100.00	3.94	1.58
kappa+	3, 9910	16.71	15.69	4.61

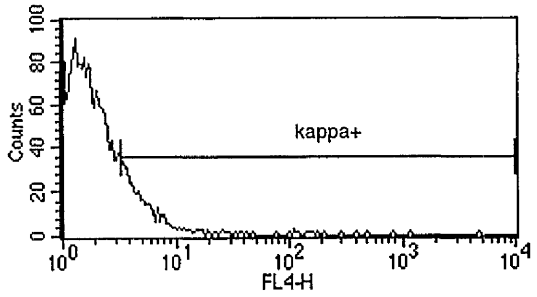

Sample ID: 1/200

Marker	Left, Right	% Total	Mean	Median
All	1, 9910	100.00	3.12	1.64
kappa+	3, 9910	14.74	11.69	4.45

Fig. 7

Figure 7: Antibody titrations. Whole spleen cells (10^6 cells/concentration) were stained for surface expression with anti-kappa chain (0 to 1:200)-biotin and streptavidin-APC (1:100). As control, streptavidin-APC was used alone. As demonstrated in the upper panel, in this control the positive population was <1%. The optimal dilution in this case was 1:20 as demontrated by the clear peak and maximal staining (46%). This method was employed for titrating all other antibodies used for immunofluorescence.

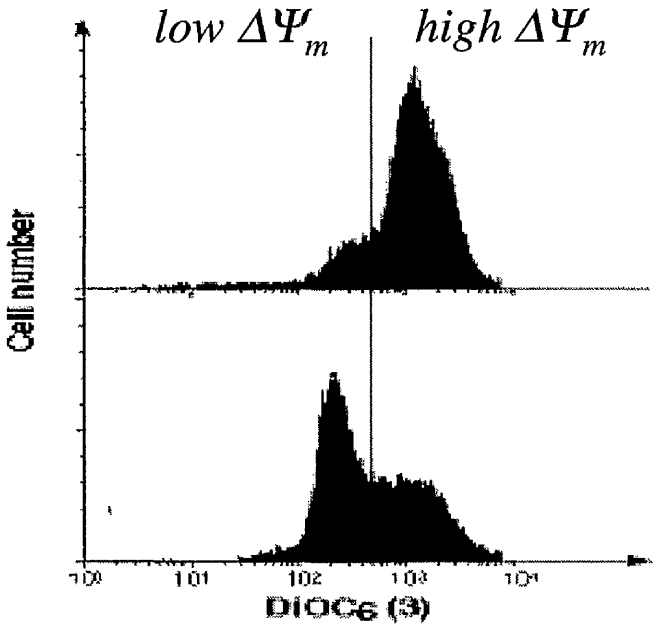
low $\Delta\Psi_m$
high $\Delta\Psi_m$
Cell number
10⁰
10¹
10²
10³
10⁴
DiOC6 (3)

Fig. 8

Figure 8: Determination of mitochondrial potential. WEHI-231 immature B cells (10^6 cells) were treated with 0-10μg/ml anti-IgM. Measurement of mitochondrial potential ($\Delta\psi_m$) by the fluorescent dye, $DiOC_6$ (3) is shown for control (upper histogram) and anti-Ig-treated WEHI-231 cells (lower histogram) 24h post stimulation. As a result of treatment the percentage of cells with low mitochondrial potential has increased from 16% to 60%.

untreated

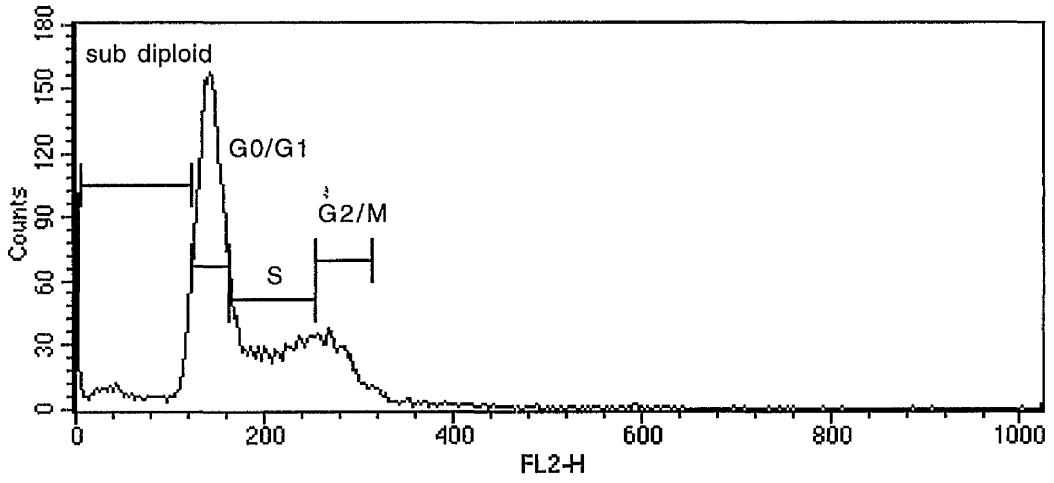

anti-Ig 10µg/ml

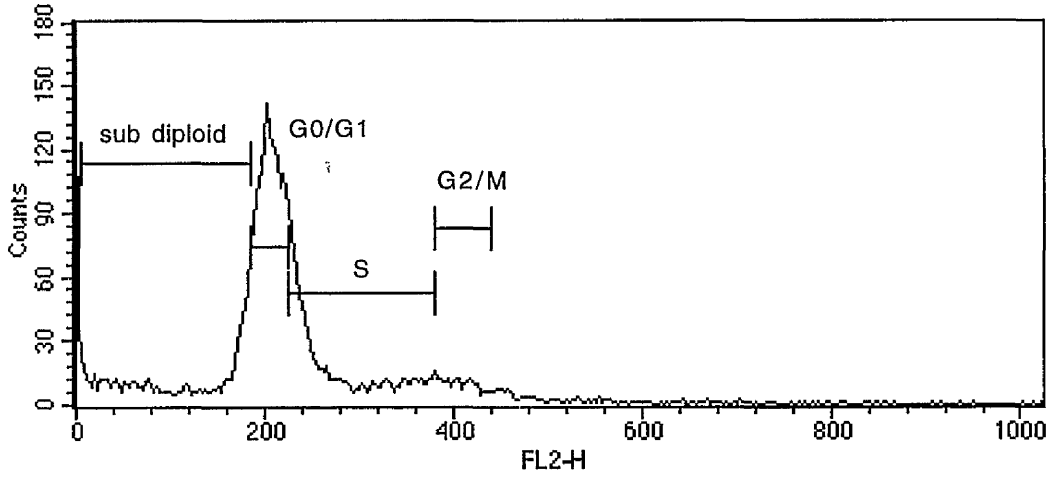

DNA content →

Fig. 9

Figure 9: Propidium iodide incorporation as a measure of DNA content. WEHI-231 cells ($5x10^6$ per sample) were treated with 0-10μg/ml anti-IgM for 2d and subjected to PI incorporation. DNA content was determined for individual samples as follows: (i) the G_0/G_1 was identified and the 2N gate determined at 40 fluorescence units width (peak±20 units, which allow an approximate 20% margin); (ii) the G_2/M gate was determined as G_0/G_1 peak±30 units; (iii); S gate was determined as the gap bewteen G_0/G_1 and G_2/M; (iv) Sub-diploid gate (<2N) was determined as the gap between 5 units (non-stained cells normally have fluorescence between 0 and 5 units) and G_0/G_1 gate.

Chapter 3. MITOCHONDRIAL AND CELL CYCLE RELATED EVENTS DURING BCR-INDUCED APOPTOSIS IN WEHI-231 IMMATURE B CELLS

3.1 Introduction

Apoptosis plays a key role in the regulation of the immune system. For example, the immune system has evolved selection processes which result in clonal deletion, by apoptosis, of autoreactive B and T lymphocytes during their development in the bone marrow and thymus respectively. Moreover, apoptosis provides a major molecular mechanism not only for the induction of peripheral tolerance and cytotoxic T cell killing but also for the termination of normal immune responses [224-226]. Whereas cells which die from damage typically swell and burst (necrosis), apoptosis is a rigorously controlled and highly ordered process which is characterised by dramatic morphological changes in the cell including shrinkage, chromatin condensation and cleavage and disassembly into membrane-enclosed vesicles called apoptotic bodies that are rapidly phagocytosed by neighbouring cells to prevent induction of inflammation and autoimmune responses [39, 227]. This systematic disassembly of the apoptotic cell appears generally to be executed by Caspases, cysteinyl aspartate-specific proteases, which have recently been identified as mammalian homologues of the cell death protein, CED-3 from the nematode *C. elegans* [228, 229]. Indeed, molecular studies have shown that over-expression of Caspases is sufficient to cause apoptosis and Caspase-deficient mice have reduced levels of apoptosis [230, 231]. However, examples of Caspase-independent commitment to cell death can be found in several of the classic models of apoptosis, including glucocorticoid-induced death of thymocytes and lymphoid cells, death of haematopoietic cell lines induced by growth factor withdrawal and Bax-mediated cell death [232-234].

It has recently emerged that mitochondrial function plays a pivotal role in determining cellular commitment to survival or apoptosis [234-236].

Thus, during apoptotic signalling, mitochondrial changes result in enhanced production of reactive oxygen species, calcium cycling and disruption of the inner mitochondrial potential [43]. Collapse of the mitochondrial potential has been thought to represent a "point of no return" in commiting the cell to apoptosis as the resulting increase in the permeability of the outer mitochondrial membrane leads to the release of Caspases and factors which promote activation of effector Caspases (cytochrome C) and/or induce apoptosis (apoptosis-inducing factor (AIF) and a Caspase-independent endonuclease) [237-242]. Mitochondrial integrity has been proposed to be regulated by pro- and anti-apoptotic members of the Bcl-2 family [239, 243] as these regulators of cell survival or apoptosis appear to target a number of aspects of mitochondrial function including mitochondrial permeability and homeostasis of reactive oxygen species status and calcium cycling.

Cell death receptors such as Tumour Necrosis Factor Receptor (TNF-R) and Fas (CD95) mediate much of the rapid apoptotic cell death required by the immune system [244]. They initiate apoptosis by directly recruiting pro-Caspases belonging to the ICE-like family, such as Caspase 1 or 8 to their accessory "death domain" transducing molecules, FADD, TRADD, RIP and RAIDD to induce proteolytic activation of effector Caspases (Caspase-3 (CPP32)-like subfamily) which have proved to be important for the execution of the later stages of apoptosis [244]. However, repertoire selection during lymphocyte development is mediated via the antigen receptors [224-226, 244].

The B cell line WEHI-231 was used in this part of the work as a model for clonal deletion of immature B cells. The aims of studies described in this chapter were:

(i) To observe the mitochondrial events downstream of the BCR signal in WEHI-231 cells, including changes in the mitochondrial potential, expression and distribution of Bcl-2 family proteins and protease activity.

(ii) To determine the role of $cPLA_2$ and its product, arachidonic acid, in BCR-induced apoptosis.

(iii) To examine the possible relationship between mitochondrial events and the cell cycle machinery.

3.2 Ligation of the antigen receptors on the immature B cell line, WEHI-231 induces growth arrest and apoptosis

Crosslinking of the antigen receptors with anti-Ig leads to a concentration-dependent induction of growth arrest and apoptosis in the B cell lymphoma, WEHI-231 (fig. 10). This is a widely used model system for investigating the signalling mechanisms underlying clonal selection of normal IgM^+ IgD^- immature B cells. Growth arrest was assessed by the anti-Ig-mediated suppression of DNA synthesis in WEHI-231 B cells (fig. 10a) which showed that maximal growth inhibition was essentially achieved at concentrations of anti-Ig between 0.1-1 μg/ml. This growth arrest was confirmed by cell cycle analysis which showed the anti-Ig-driven accumulation of WEHI-231 cells in the G_0/G_1 phase of the cell cycle (70±7% of stimulated live cells versus 47±10% for control live WEHI-231 cells 24h post-stimulation with anti-Ig (1μg/ml), *n=4* independent experiments).

Commitment to apoptosis was also assessed by examining the expression of phosphatidylserine (Annexin V binding, fig. 10b) at the cell surface, DNA laddering (fig. 10c) and propidium iodide-staining of subdiploid DNA content during cell cycle analysis (fig. 10b) . These studies showed that commitment to apoptosis required higher concentrations of anti-Ig (1-10μg/ml; fig. 10b and results not shown) than those needed for induction of growth arrest following crosslinking of the antigen receptors.

Importantly, rescue of WEHI-231 cells, via CD40, specifically overcomes the transition from growth arrest to apoptosis. The internal division of living cells between the different phases of cell cycle shows that anti-Ig treatment blocks cells from entering S phase, in addition to the induction of apoptosis. The co-stimulatory signal transduced from CD40 overcomes this phenomena in the time window of 16-24h post-stimulation (fig. 11). This move beyond the Start restriction point is facilitated by an increase in the G_1-cyclin cdk4 ([212] and not shown).

3.3 Disruption of the mitochondrial potential ($\Delta\psi_m$) plays a key role in antigen receptor-driven apoptosis: signals which rescue from apoptosis stabilise $\Delta\psi_m$

Disruption of mitochondrial function and integrity has been shown to play a central role not only in the commitment to apoptosis but also in the initiation of the execution of the later stages of apoptosis in many cell systems [234, 235, 245]. Therefore, the role of mitochondrial disruption in antigen receptor-driven apoptosis was investigated by characterising the effects of anti-Ig on the inner mitochondrial transmembrane potential, $\Delta\psi_m$. To do this quantitatively, the incorporation of the cationic lipophilic dye $DiOC_6(3)$ into WEHI-231 B cells was analysed, as the uptake of this dye into mitochondria is directly propotional to $\Delta\psi_m$ [246]. Crosslinking of the antigen receptors on WEHI-231 immature B cells induced an early (within 5h) substantial decrease in $\Delta\psi_m$ followed by a profound dissipation of $\Delta\psi_m$ which was maximal by 20-24h (fig. 12). In contrast, mature splenic B cells, which proliferate rather than apoptose following crosslinking of their antigen receptors (see section 5.4), do not exhibit this decrease in $\Delta\psi_m$ at either 3 or 24h (see fig. 79 and not shown). Thus, the mitochondrial depolarisation observed in WEHI-231 cells following crosslinking of the antigen receptors correlates with the commitment and induction of apoptosis.

The importance of $\Delta\psi_m$ stabilisation to the survival of WEHI-231 immature B cells is further supported by the finding that costimulation via CD40, which has been widely shown to rescue antigen receptor-driven apoptosis (nuclear DNA loss; fig. 13) and growth arrest in G_0/G_1 (fig. 11), acts to stabilise $\Delta\psi_m$ (albeit at an intermediate $\Delta\psi_m$) and prevent the profound dissipation of $\Delta\psi_m$ observed in anti-Ig-treated cells (fig. 12). Furthermore, the mitochondrial inhibitors, antimycin (an inhibitor of respiratory chain complex III which blocks the transfer of electrons to

inhibits proton transport back into the mitochondria by blocking the proton channel, F_0 protein) which can be used to stabilise the mitochondrial potential [247], maintain ATP levels [248] and protect against apoptosis [249], are not only capable of maintaining almost normal $\Delta\psi_m$ levels even in the presence of anti-Ig (fig. 14) but are also able to protect against the sIg-driven commitment of WEHI-231 immature B cells to apoptosis (nuclear DNA loss; fig. 13a). Like CD40-signalling, the mitochondrial inhibitor antimycin, and oligomycin to a very much lesser extent, is also able to prevent anti-Ig-mediated arrest in G0/G1 as indicated by its ability to protect entry into S phase (fig. 13a). However, unlike the CD40 rescue signals they are unable to allow cell cycle progression through G2/M (fig. 13b). Together, these data suggest that mitochondrial function not only plays a central role in the commitment to death signalling in B cells but also in the reversible induction of growth arrest by anti-IgM [154].

The immunosupressant cyclosporin A (CsA) has been shown to act on the cyclophilins coupled to channels on membranes of both mitochondria and ER [250]. Interestingly, nanomolar concentrations of CsA, which were suggested to block the mitochondrial permeability transition pore as a result of $\Delta\psi_m$ depolarisation, did not block apoptosis in WEHI-231 cells, although more cells entered into the cell cycle (fig. 15). Micromolar concentrations, which block the Ca^{+2} channels on the ER [43] were efficient, as reported elsewhere [162] in relieving BCR-induced growth arrest. This observation may indicate that the effect of CsA on apoptosis in WEHI-231 cells is mediated through modulation of Ca^{+2} influx from the ER and is not a result of direct manipulation of the mitochondrial PTP.

3.4 BCR-mediated disruption of $\Delta\psi_m$ results in cellular ATP depletion and is associated with induction of mitochondrial PLA_2 activity

Loss of mitochondrial function and integrity has been shown to contribute to the effector stages of apoptosis via production of reactive oxygen species, ATP depletion, calcium cycling and release of cytochrome C, Caspases and apoptosis-inducing factors. Since disruption of mitochondrial function was detected downstream of the BCR signal, the potential downstream effector mechanisms involved in the execution of antigen receptor-driven apoptosis of WEHI-231 immature B cells were investigated.

Nitric oxide (NO) is a source for a range of reactive oxygen species influencing many cellular functions. It is synthesised by three distinct NO synthases (NOSs) [251], one of them being the inducible (iNOS), which has been implicated in regulating lymphocyte cell fate [252]. NO is thought to act downstream of mitochondrial reactive oxygen species (ROS) [43], but other functions have been well documented (reviewed in [253]), including an essential role for NO in macrophage activation, where it assists cell killing [254, 255]. It has also been suggested that apoptosis of splenic B cells can be prevented by NO through a Bcl-2-dependent mechanism [256], although a role for NO was ruled out in the case of thymocyte apoptosis [42]. In this sytem, inhibition of nitric oxide production, has been found to exacerbate BCR-induced growth arrest of WEHI-231 cells, as demonstrated by using L-NMMA, a pan-NOS inhibitor (fig. 16a). L-NIL, a specific inhibitor of iNOS, did not block or exacerbate either sIg-induced growth arrest or apoptosis (fig. 16b and not shown). In fact, iNOS protein was could not be detected in these cells (not shown). These observations suggest that during BCR-induced apoptosis involves blockage of NO production by a NOS enzyme different than iNOS. If this enzyme is one of the known constitutive enzymes, eNOS or nNOS, it is possible that its regulation is carried out by other means than protein expression levels.

The role of ATP depletion in antigen-driven apoptosis of WEHI-231 cells was elucidated: crosslinking of the antigen receptors induces a profound depletion of cellular ATP (fig. 17a). The kinetics of ATP depletion, which showed a lag before onset (5-10h), are consistent with ATP depletion resulting from mitochondrial disruption. Moreover, as ATP depletion was apparent before the appearance of DNA ladders (≥16h), this depletion did not simply reflect cell necrosis resulting from apoptosis. Importantly, such ATP depletion and apoptosis could be blocked not only by the CD40 rescue signal but also by the mitochondrial inhibitors, antimycin and oligomycin (fig. 17). Taken together, these results suggest that ATP depletion resulting from mitochondrial disruption plays a key role in antigen receptor-driven apoptosis of WEHI-231 immature B cells.

Generation of unsaturated fatty acids, such as arachidonic acid, by a mitochondrial phospholipase A_2 activity has been reported to alter the permeability of the mitochondrial inner membrane resulting in the collapse of $\Delta\psi_m$ [43, 257-259]. Interestingly, it was recently shown [171] that cytosolic phospholipase A_2 ($cPLA_2$) is only expressed and coupled to the antigen receptors on B cells under conditions of apoptotic signalling. Moreover, consistent with a role for $cPLA_2$ in sIg-mediated apoptosis, addition of exogeneous arachidonic acid induces a dose-dependent state of profound growth arrest [171] and apoptosis as indicated by DNA laddering (fig. 18a) and induction of loss of nuclear DNA content (fig. 18b) in WEHI-231 immature B cells. Therefore, it was investigated whether $cPLA_2$ played a role in the sIg-mediated collapse of $\Delta\psi_m$ and ATP depletion by determining whether signalling via sIg induced mitochondria-associated $cPLA_2$ activity under conditions which correlated with the collapse of $\Delta\psi_m$, ATP depletion and commitment to apoptosis: anti-Ig not only stimulated total cellular PLA_2 activity under apoptotic conditions but some 20-25% of this activity was found in purified isolated mitochondrial preparations (fig. 19a). The sIg-coupled PLA_2 activity is (i) calcium-dependent [260], (ii) blocked by the $cPLA_2/iPLA_2$-selective inhibitor, arachidonyl trifluoromethyl ketone [260] and (iii) not inhibited by the $iPLA_2$-selective inhibitor, bromoenol lactone (not shown) ruling out a rule for either $iPLA_2$ or $sPLA_2$ in such arachidonic acid generation. In

addition, *in situ* immunofluorescence analysis of permeabilised cells indicates that $cPLA_2$ translocates to the mitochondria and the nucleus within 3h of stimulation of WEHI-231 B cells via the BCR and this is at least partially reversed/prevented by costimulation via CD40 (fig. 20). Moreover, addition of exogeneous arachidonic acid elicited $\Delta\psi_m$ collapse in a manner analogous to that observed with anti-Ig (fig. 18b). Furthermore, whilst anti-Ig treatment was found to upregulate $cPLA_2$ mRNA (not shown) and protein (fig. 19b; 2.25-fold basal levels at 48h) levels, costimulation with anti-CD40 was found to prevent/reverse this upregulation (0.65-fold basal levels of $cPLA_2$ protein at 48h). Taken together, these results suggest that sIg-mediated induction of mitochondrial $cPLA_2$ activation may play a key role in the collapse of $\Delta\psi_m$ and commitment to apoptosis in WEHI-231 immature B cells.

3.5 Arachidonic acid, rather than its metabolites, participates in BCR-induced death

A wide range of inhibitors were employed to examine the possibility that arachidonic acid, produced by $cPLA_2$ during apoptosis of WEHI-231 cells, is metabolised further to induce cell death via the COX or the LOX pathways.

COX-2 is the the inducible form of the COX enzymes and it has been shown to take part in various intracellular signalling cascades. For example, a possible link between COX-2 and apoptosis regulation was elucidated by a study which showed that over-expression of COX-2 indirectly induces the expression of Bcl-2 [261]. Moreover, exposure to dexamethasone, a known inducer of apoptosis [262], can lead to a bias in the post-transcriptional balance of COX-2, in favour of a short instable isoform ($COX\text{-}2_{2.8}$) instead of the long stable isoform ($COX\text{-}2_{4.6}$) [263]. Two inhibitors of COX-2 activity, Niflumic Acid and NS-398, were found not to block BCR-induced growth arrest of WEHI-231 cells (as measured by thymidine incorporation; fig. 21). Rather, NS-398 was found to augment BCR-induced apoptosis (as determined by nuclear DNA loss; not shown).

These observations support other evidence for the involvement of PGE_2 in rescue signalling by CD40 in WEHI-231 cells[10].

Arachidonic acid can be also processed into leukotrienes by the LOX enzymes [172]. High concentrations of 5-LOX have been found to be present in B cells, but not in T cells and several mechanisms have been suggested for the activation of such 5-LOX enzymes: (i) signal transduction via tyrosine kinases [264]; (ii) stimulation by calcium ions or ATP (neither calcium ions nor ATP have been reported to be required for purified 12- and 15-LOXs although activation of these by calcium ions or other divalent ions has been reported in crude preparations); (iii) 5-LOX, the 5-LOX activating protein (FLAP), and COX-2 are also associated with nuclear membrane suggesting that these enzymes form a functional complex for the production of eicosanoids [172]. Murine 12-LOX is in fact more related to human leukocyte 15-LOX than to human 12-LOX [265] and 15-LOX needs to translocate to membranes in order to be activated [266]. Interestingly, oxidative modifications of membrane phospholipid and low-density lipoprotein by 15-LOX have been noted in relation to breakdown of mitochondria during reticulocyte maturation and development of atherosclerosis respectively [172]. Thus, key inhibitiors were used to examine to role of LOX in BCR-induced apoptosis in WEHI-231 cells. The pan-LOX inhibitor, ethyl 3,4-dihydroxy-benzylidene-cyano-acetate, was found to enhance BCR-induced growth arrest, in a range of concentrations which will inhibit all known LOX enzymes (fig. 22a). The more specific 12-LOX inhibitor, Baicalein had no effect on BCR-induced growth arrest or apoptosis (fig. 22b and not shown). Therefore, it is likely that either 5-LOX or 15-LOX play a similar role to that of COX-2 in rescue signalling. A lack of inhibitors specific for these forms of LOX prevented further investigation in this direction.

Many studies have demonstrated that diverse stresses (oxidative, UV, ionizing radiation and others) activate the sphingomyelin pathway during signalling of the death response in eukaryotic systems. Ceramide production has been linked to arachidonic acid production by $cPLA_2$ [267] and its metabolism by COX enzymes [201]. Ceramide production is also

[10] Gauld, S. B., and M. M. Harnett, personal communication.

one of the well documented processes in BCR signalling, and it was suggested that resistance to BCR-induced apoptosis in a WEHI-231 subline is due to insufficient production of ceramide [193]. Although the source of ceramide production in WEHI-231 cells is still in doubt, more recently it was suggested to be *de novo* synthesis [195]. *De novo* synthesis of ceramide occurs via the enzyme ceramide synthase, which in mammalian cells catalyses the condensation of the sphingoid base sphinganine and fatty acyl-CoA to form dihydroceramide. Dihydroceramide is rapidly oxidised to ceramide. Ceramide synthase has not been characterised at the molecular level and its activity has been detected only in the ER and mitochondria. Fumonisin B_1, an inhibitor of ceramide synthase, was used to examine whether *de novo* synthesis is the source for ceramide production in WEHI-231 cells and whether it was responsible for growth arrest or apoptosis [195]. However, this inhibitor did not reverse the effects of IgM cross-linking (fig. 23), during a wide range of incubations: -2 to +8 hours of anti-IgM stimulation (not shown).

3.6 The role of Bcl-2 family proteins in regulating BCR signalling

Three methods were employed to dissect the regulatory role of Bcl-2 family members in apoptosis and rescue in WEHI-231 cells. First, western blotting of whole cell lysates were used to determine overall changes in protein levels of Bcl-2 family members. Anti-IgM treatment was found to cause a sustained decrease in the protein levels of the anti-apototic protein Bcl-x_L, Bcl-2 and Mcl-1 levels (fig. 24). This effect was reversed by the addition of anti-CD40, but only in the case of Bcl-x_L and Mcl-1.

Figure 25 shows the effect of the different treatments on levels of pro-apoptotic protein expression. In contrast to what have been predicted, an increase in Bad, Bak and Bax expression were all induced by CD40 signalling, with a maximal induction achieved after 8h. In addition, anti-IgM treatment alone appeared to produce a decrease in the protein levels of Bad, Bak and Bax. Interestingly, none of the treatments appeared

capable of inducing phosphorylation of Bad (not shown), which could potentially inactivate this pro-apoptotic protein [268]. This evidence has suggested that the role of Bcl-2 family members in determining cell fate in WEHI-231 could not be defined solely in terms of whole cell protein levels.

A second approach has been taken in order to link the expression and distribution of Bcl-2 family members to mitochondrial events. An earlier time point of 3h was chosen, preceeding growth arrest and mitochondrial potential disruption, and correlating with the peak in $cPLA_2$ activity (not shown). In agreement with the results from western blotting of whole cell lysates, many Bcl-2 family members, anti- and pro-apoptotic, were induced by anti-Ig treatment (figs. 26-27). Using mitochondrial staining, it was possible to determine whether rescue signal via CD40 could change the distribution of these proteins in a way which potentially favours survival. Two events were observed as result of the combined treatment: (i) further induction of Bcl-x_L presumably biasing the balance between all Bcl-2 proteins into an anti-apoptotic favour (fig. 26); (ii) prevention of Bad and Bid entry to the mitochondria (fig. 27).

Finally, WEHI-231 cells stably transfected with Bcl-x_L, were used to examine more directly the influence of Bcl-x_L on BCR signalling. As reported previously, WEHI-231-Bcl-x_L do not undergo apoptosis in response to BCR cross-linking, although their growth arrest resulting from this stimulation is not relieved ([269] and fig. 28a). Interstingly, Bcl-x_L over-expression was sufficient to block apoptosis induced by exogeneous arachidonic acid (fig. 28b). This novel evidence indicates a link between the apoptotic activity of $cPLA_2$ and its prevention by Bcl-x_L.

3.7 BCR-mediated disruption of $\Delta\Psi_m$ is not associated with cytochrome C release from the mitochondria or activation of Caspase 3

To determine whether the observed antigen receptor-driven mitochondrial disruption also results in Caspase-dependent execution of apoptosis of WEHI-231 immature B cells, we investigated whether the

loss of mitochondrial potential correlated with activation of effector Caspases as evidenced by release of cytochrome C from the mitochondria and cleavage of the Caspase-3 substrates, PARP and Bcl-x_L [270, 271]. Examination of mitochondria-free extracts showed that antigen receptor-mediated stimulation of WEHI-231 immature B cells failed to induce any release of cytochrome C into the cytosol over the 48h time course of apoptosis measurements (fig. 29a), results consistent with a recent report that BCR-mediated apoptosis in WEHI-231 cells is independent of cytochrome C translocation from the mitochondria [78]. In contrast, cytochrome C release to such cytosolic fractions was easily detectable within 4h following treatment of Jurkat cells with anti-Fas antibodies (not shown). Moreover, *in situ* immunofluorescence analysis of intact cells showed that whilst cytochrome C remained localised to the mitochondria following stimulation of WEHI-231 cells with anti-Ig, cytochrome C release to the cytosol could be strongly detected (fig. 30) following stimulation with the cell permeant sphingolipid, C_2-ceramide (25 μM) which can induce apoptosis of WEHI-231 B cells via the classical Caspase-dependent route [194].

Similarly, although there appears to be a very low level of constitutive Caspase activity in untreated WEHI-231 cells, resulting in the generation of low levels of the cleaved form of PARP, no stimulation of Caspase 3 activity, as evidenced by the lack of stimulated cleavage of PARP (fig. 29) or Bcl-x_L (not shown) was observed following stimulation (for up to 48h) of these immature B cells via the antigen receptors. In contrast, PARP cleavage was easily detectable within 24h following culture with C_2-ceramide (25μM; fig. 29c). These results were again confirmed by *in situ* immunofluorescence analysis which showed the presence of cleaved PARP fragments in intact cells stimulated with C_2-ceramide but not anti-Ig (fig. 30). Interestingly, and consistent with sIg-mediated induction of mitochondrial PLA_2 activation playing a key role in anti-Ig-stimulated apoptosis of WEHI-231 immature B cells, we find that whilst addition of exogeneous arachidonic acid (25μM) induces apoptosis (fig. 18), it does not stimulate activation of Caspase-3 and resultant PARP cleavage in these cells (fig. 29c).

3.8 Caspase inhibitors do not relieve BCR-mediated growth arrest or apoptosis

The failure of anti-Ig to induce a PARP-cleaving Caspase activity or the release of cytochrome C from the mitochondria of WEHI-231 immature B cells suggested that antigen receptor-driven apoptosis of these cells may occur in a Caspase-independent manner. To investigate this possibility further, the effect of Caspase inhibitors on the antigen receptor-driven growth arrest and apoptosis of WEHI-231 immature B cells was examined. In order to control for the efficacy of these reagents parallel experiments were conducted demonstrating their ability to protect against the Caspase-dependent growth arrest and programmed cell death of Jurkat T cells resulting from stimulation via the antigen receptors (anti-CD3 or PHA), TNF-α or Fas death receptors (not shown) in order to determine whether the antigen receptors on WEHI-231 immature B cells (BCR) and Jurkat T cells (TCR/CD3 complex) utilised different apoptosis pathways.

The role of individual Caspase subtypes in these models of lymphocyte apoptosis was assessed by the use of selective Caspase inhibitors: (i) zVAD-fmk is considered to be a pan-Caspase inhibitor [272] with a high affinity for the Caspase-1-like subfamily and a lower affinity for the Caspase-3-like subfamily [273]; (ii) Ac-DEVD-CHO shows greater affinity for Caspase-3 than for the Caspases-1, -4 and -7; (iii) zVEID-fmk is a potent Caspase-6 inhibitor which has little effect on Caspase-3, -4, -7 and -8 [73]. zVAD-fmk was able to completely reverse Fas-mediated growth arrest and partially overcome anti-CD3 and, to a lesser extent, TNF-α-induced growth arrest (fig. 31 and results not shown), findings consistent with previously published studies [270]. However, Ac-DEVD-CHO and zVEID-fmk were unable to rescue either Fas- or TNF-α-mediated growth arrest (fig. 31 and results not shown). Nevertheless, and in agreement with previous studies [238, 274], all three inhibitors, albeit to a lesser extent, zVEID-fmk, were able to prevent Fas-mediated apoptosis of Jurkat T cells (fig. 31).

In contrast, none of these inhibitors had any effect on anti-Ig-mediated growth arrest, Annexin V binding, cell cycle progression or nuclear DNA loss (subdiploid cells) of WEHI-231 immature B cells (figs. 32-33 and not shown). However, zVAD-fmk (1nM-10 μM, maximal 1 nM), Ac-DEVD-CHO (maximal >100 pM) and z-VEID-fmk (≥10 μM) were able to partially block C_2-ceramide induction of nuclear DNA loss (but not growth arrest, fig. 32) in WEHI-231 B cells (fig. 33 and results not shown) and both z-VAD-fmk and Ac-DEVD-CHO were able to inhibit apoptosis of Germinal Centre (PNA^+) B cells (see section 5.4), results demonstrating the efficacy of these inhibitors in B cell systems. In addition, whilst treatment of WEHI-231 cells with C_2-ceramide can induce activation of a Caspase 3-like activity, which can be blocked by the Caspase 3 inhibitor, Ac-DEVD-CHO, crosslinking of the BCR for up to 24h (2, 5, 8 and 24h) does not induce activation of this Caspase (fig. 33 and not shown).

3.9 Non-Caspase proteases involved in the execution phase of BCR-induced apoptosis

A wide range of protease inhibitors were employed in a search for the specific protease involved in the proteolytic activities which are part of any proliferative and apoptotic responses. While high concentrations of zVAD-fmk, TLCK and chymostatin had some effect on growth arrest and/or DNA degradation, their lack of specificity at these levels prevents a conclusive explanation about the nature of these proteases. Table 2 summarises the effects of most protease inhibitors tested. Surprisingly, in most cases, the inhibitors were effective in relieving growth arrest. This evidence supports relatively early involvement of protease activity in BCR-signalling of WEHI-231 cells, as suggested by others [78].

The cathepsin B inhibitor, EST [275] was capable of inhibiting sIg-mediated apoptosis, but not growth arrest, of WEHI-231 cells (as indicated by loss of nuclear DNA content, fig. 34a). In addition, whilst crosslinking of the BCR does not induce activation of Caspase-3 activity, it does stimulate the cleavage of the Cathepsin B substrate, zRR-*p*NA (z-Arg-Arg-*p*NA; fig. 34b). Moreover, although inhibition of sIg-mediated

apoptosis by EST was maximal by 1nM, the percentage of subdiploid cells resulting from stimulation with C_2-ceramide was not reduced by this reagent at concentrations of EST ≤10μM (fig. 34a), providing further evidence that anti-Ig and C_2-ceramide stimulate apoptosis of WEHI-231 cells by distinct mechanisms. Despite preventing BCR-driven apoptosis, EST did not block anti-Ig-stimulated growth arrest (fig. 35a) nor did it prevent anti-Ig driven collapse of $\Delta\psi_m$ (fig. 35b). In contrast, zVAD-fmk (1nM-100μM) was able to block C_2-ceramide, but not anti-Ig-mediated disruption of $\Delta\psi_m$ in WEHI-231 cells. Taken together, these results suggest that the execution phase of BCR-driven apoptosis is mediated by Cathepsin B (or similar proteases) rather than by effector Caspases.

3.10 The nature of the involvement of p53 and related proteins in proliferation and apoptosis of WEHI-231 cells

Exogenous p53 can be recruited within hours during BCR-induced cell death of WEHI-231 cells [114]. Only very low levels of endogenous p53 are detectable in WEHI-231 cells [213]. An increase above basal levels in p53 has been observed for both proliferative and apoptotic stimuli, without substantial alteration of phosphorylation levels (fig. 36a). However, a substantial increase in Mdm2 levels was observed in response to anti-Ig treatment, suggesting that the BCR signal is regulating p53 levels, at least in part, by targeting it for degradation (fig. 36b). Although direct interaction of p53 and Mdm2 is hard to investigate by co-immunopercipitation, because of blockage of most epitopes by the antibody interaction itself, in some cases cleaved p53 or Mdm2:p53 complexes are detectable even following resolution by SDS-PAGE (fig. 36b: upper band). One of most important mediator of p53 activity at the Start restriction point appears to be p16 [89]. This protein is barely detectable in WEHI-231 cells, although it may slightly induced by anti-Ig treatment and abolished by anti-CD40 and IL-4 treatments (fig. 36c), suggesting that it may be involved in BCR-induced apoptosis.

An important factor of p53 signalling in growth arrest and apoptosis pathways, appears to be the involvement of the protein Rb. This protein, however, appears to be hardly affected by any of the stimuli in this system. It displays a cyclic behaviour in which levels peak at 24 hours regardless of treatment (*n=3*). In examining this time point, Rb is dephosphorylated in response to anti-Ig treatment and co-incubation with anti-CD40 induced a middle band, which may reflect sufficient phosphorylation of Rb to enable entry to the cell cycle (fig. 36d). No association of Rb with one of its main downstream mediators, the histone deacetylase HDAC-1 [103], which is expressed in low levels in WEHI-231 cells, could be detected, under any of the conditions tested. Interestingly, p130, a Rb family member [276], was induced at 24h by the rescue signal and it may be that this is more important than Rb in the return of WEHI-231 into the cell cycle (fig. 36e). Similarly, p130 was induced by AA plus anti-CD40, in comparison to AA treatment.

3.11 Discussion

Commitment to antigen receptor-driven apoptosis of the B cell lymphoma, WEHI-231 correlates with mitochondrial phospholipase A_2 activation leading to disruption of mitochondrial function and ATP depletion. Rather surprisingly, however, such apoptosis is executed independently of Caspase activation and instead, the executioner phase appears to involve the BCR-driven, post-mitochondrial activation of the protease cathepsin B. This novel mechanism of B cell apoptosis is supported by several lines of evidence: firstly, it was demonstrated a pivotal role for mitochondrial function in determining commitment to B cell survival or apoptosis by showing that $cPLA_2$ expression and mitochondrial activity is upregulated under conditions of sIg-driven apoptosis and downregulated during CD40-mediated rescue (figs. 18-19 and 29). Secondly, the $\Delta\psi_m$ is disrupted resulting in depletion of cellular ATP under conditions of apoptotic, but not proliferative, signalling via the BCR (fig. 17). Importantly, such collapse of $\Delta\psi_m$ can be mimicked by addition of exogeneous arachidonic acid whilst disruption of $\Delta\psi_m$, ATP-depletion and

apoptosis can be blocked by rescue signals via CD40 or by $\Delta\psi_m$ stabilisers such as antimycin or oligomycin (figs. 13-14). Thirdly, it was shown that activation of Caspases is not essential for commitment and post-mitochondrial execution of BCR-mediated apoptosis by demonstrating that apoptotic signalling via the BCR or following addition of exogeneous arachidonic acid does not induce either the release of cytochrome C from mitochondria which is required for the activation of the Caspase-3 cascade [72, 277] nor does it cause cleavage of PARP (figs. 19 and 29) or Bcl-x_L (results not shown) which have been reported to be suitable markers of Caspase-3-like effector activity in various cell types [270, 271]. Indeed, apoptotic signalling via the BCR in WEHI-231 B cells does not appear to stimulate the activation of Caspase-3 (fig. 33). Consistent with this, BCR-mediated disruption of $\Delta\psi_m$ and commitment to apoptosis takes place in the presence of Caspase inhibitors (figs. 32-33) indicating that none of the known initiator or effector Caspases are essential for the commitment or execution of BCR-induced apoptosis of WEHI-231 immature B cells. Rather, apoptotic signalling via the BCR stimulates the post-mitochondrial activation of the protease, cathespin B (figs. 34-35) which has previously been shown to be a key executioner protease in alternative mechanisms of apoptosis which have recently been described [74]. That this PLA_2-dependent mechanism of mitochondrial function is likely to be a key checkpoint of antigen-driven cell fate is evidenced by the downregulation of PLA_2 activation and expression, and protection of mitochondrial function, resulting from signalling via CD40 which effects rescue from BCR-mediated apoptosis in these WEHI-231 immature B cells.

ATP depletion resulting from oxidant-induced calcium release from mitochondria followed by excessive calcium cycling and collapse of $\Delta\psi_m$ has been proposed to be a hallmark of apoptosis [43]. Interestingly, production of ROS been previously been shown to increase following apoptotic signalling via sIg on WEHI-231 immature B cells [269]. Moreover, CD40 signalling, which rescues these cells from apoptosis, leads to an increase in the expression of Bcl-x_L ([158] and figs. 24 and 26) which prevents accumulation of intracellular oxidants [158, 269], blocks

thapsigargin-induced intracellular mobilisation of calcium from the endoplasmic reticulum [278] and stabilises $\Delta\psi_m$ and mitochondrial homeostasis [243]. However, observations that the mitochondrial inhibitors, antimycin and oligomycin, which will induce the production of ROS [42], protect against sIg-mediated ATP depletion and apotosis (fig. 13), argue against a role for ROS in BCR-driven collapse of $\Delta\psi_m$ in WEHI-231 B cells. Consistent with this, it has recently been shown that rather than induce apoptosis, low levels of ROS appear to exert mitogenic or anti-apoptotic effects [279, 280].

An alternative candidate apoptotic pathway for the collapse of $\Delta\psi_m$ and ATP depletion involves the stimulation of mitochondrial phospholipase A_2 activity resulting in the accumulation of unsaturated fatty acids (arachidonic acid) which have been reported to alter the permeability of the mitochondrial inner membrane resulting in the collapse of $\Delta\psi_m$ [43, 257-259]. Indeed, whereas apoptotic signalling via sIg upregulates $cPLA_2$ expression, induces its translocation to the mitochondria and strongly stimulates $cPLA_2$ activity (figs. 18, 19, 29 and results not shown), rescue from BCR-mediated apotosis by co-stimulation via CD40 downregulates $cPLA_2$ expression and uncouples sIg from $cPLA_2$ translocation and signalling in WEHI-231 immature B cells (figs. 18, 19, 29 and results not shown). In addition, and consistent with a role for $cPLA_2$ in this sIg-mediated, mitochondrial-dependent mechanism of apoptosis, addition of exogeneous arachidonic acid induces a profound collapse of $\Delta\psi_m$ and resultant induction of growth arrest [171] and apoptosis (fig. 18) in WEHI-231 immature B cells. Taken together, these results suggest that sIg-mediated induction of mitochondrial PLA_2 and generation of arachidonic acid may play a key role in the collapse of $\Delta\psi_m$ and commitment to apoptosis in WEHI-231 immature B cells.

The Bcl-2 family proteins are differentially expressed during B cell development [281, 282]. Whereas Bcl-x_L is expressed in immature and transitional B cells, Bcl-2 appears to be the predominant family member expressed in mature cells [8]. Recently, other anti-apoptotic members, such as Mcl-1, have been suggested to play an important role in survival

at different stages of B cell development [282]. Many members of the Bcl-2 family have been shown to target calcium and/or mitochondrial responses [65, 76, 283]. However, the lack of evidence for a different mode of action between anti-apoptotic Bcl-2 proteins [284], for example, makes it hard to assess what role plays induction of Bcl-x_L and A1 by anti-CD40 treatment of B cells [269, 278, 285, 286]. Nonetheless, over-expression of either Bcl-2 or Bcl-x_L were shown to alter B cell development considerably. Perhaps most importantly, whilst over-expression of Bcl-x_L is sufficient to enable self-reactive B cells to escape negative selection in the bone marrow [287], no such correlation has been found with Bcl-2 expression [288], which, by contrast can rescue GC B cells from apoptosis [289, 290].

The Bcl-2 family, which has been proposed control the effector Caspase cascade (i.e. the members of Caspase-3-like subfamily), appears to act in a non-conventional manner in WEHI-231 cells. For example, anti-IgM treatment causes a decrease in the expression of most of the Bcl-2 family members, regardless of their known function. Moreover, anti-CD40 treatment alone appears to provoke a transient increase in pro-apoptotic protein levels. Therefore, long-term induction of Bcl-x_L expression in the mitochondria is essential for the rescue of WEHI-231 cells (fig. 26) and probably blocks BCR-induced Bid and Bad pro-apoptotic activities there (fig. 27). Further experiments in WEHI-231 cells overexpressing Bcl-x_L can elucidate more about the modes of action of Bcl-x_L in relation to other parts of the apoptotic pathway described here, especially $cPLA_2$ activation and ATP depletion. Preliminary results in this direction already show that Bcl-x_L over-expression can override BCR-induced mitochondrial $cPLA_2$ activation[11].

Caspases are usually regarded as essential to the induction of cell death in the immune system (for review see [50, 69]). Nevertheless, there is increasing evidence that apoptotic stimuli which differ from the TNF/Fas cascades may not necessarily utilise effector (Caspase-3-like) Caspase cascade [291]. The mechanisms downstream of mitochondrial membrane depolarisation and ATP depletion have not, as yet, been delineated.

However, the failure of anti-Ig to induce a PARP-cleaving Caspase activity or the release of cytochrome C from the mitochondria of WEHI-231 immature B cells (figs. 19-20 and 29-30) suggested that BCR-driven apoptosis of these cells is not dependent on Caspase activation. This suggestion is supported by findings here that signalling via sIg does not induce Caspase-3 activation and that Caspase inhibitors did not prevent BCR-mediated growth arrest and apoptosis in such cells (fig. 33). At first sight therefore, these results appear to conflict with previously published reports which showed that sIg was coupled to the activation of Caspases and that such Caspase activation played a role in sIg-mediated apoptosis of WEHI-231 [194, 292]. However, by using z-VAD-fmk at high concentrations (≥100μM) we have been able to reproduce some of the effects of Caspase inhibitors on sIg-mediated apoptosis presented in the earlier papers: these apparent differences may therefore simply reflect the use of high concentrations (≥20μM) of Caspase inhibitors in the earlier studies as it is now widely recognised that at concentrations >10μM, z-VAD-fmk will inhibit other cysteine proteases such as Calpain [78] and Cathepsin B [74]. Consistent with this, apoptotic signalling via the BCR stimulates cathepsin B activity (fig. 34) and the post-mitochondrial stages of antigen receptor-driven apoptosis in WEHI-231 immature B cells are blocked by the cathepsin B inhibitor EST (fig. 34). Similarly, BCR-mediated apoptosis can also be prevented by the serine and cysteine protease-selective, Caspase-independent inhibitor, TLCK [73, 293] and partially by the calpain and/or cathepsin-selective inhibitors, leupeptin, antipain and pepstatin (table 2) [293-295]. Interestingly, recent evidence now suggests that ATP depletion can lead to the induction of DNA fragmentation and consequent apoptosis in a Caspase-independent, but TLCK or TPCK-sensitive, protease-dependent manner [296]. Taken together, these findings suggest that, in addition to an inability to drive the energetically unfavourable reactions involved in the metabolic, biosynthetic and signal transduction processes required for cell survival and cell cycle progression [234, 236, 279, 297, 298], ATP depletion can trigger the post-mitochondrial activation of a cathepsin-B-

[11] Lord, C. And M. M. Harnett, personal communication.

like protease-dependent mechanism of DNA fragmentation and apoptosis in WEHI-231 B cells stimulated via the BCR.

Finally, Caspase inhibitors were found to block sIg-mediated apoptosis of Germinal Centre (PNA^+) B cells suggesting that B cells may employ distinct maturation stage-specific mechanisms of apoptosis. However, this rescue by Caspase inhibitors is only partial and may reflect the results of a recent study which show that apoptosis of human Germinal Centre B cells requires the activation of both Caspase and Cathepsin activities, the Cathepsin activity being downstream of Caspase 3 and responsible for exonuclease activity and execution of apoptosis [275]. Taken together with Caspase-dependent processes of apoptosis observed in Jurkat T cells therefore, these results may suggest that there is a fundamental difference in the way that the antigen receptors on B and T cells signal commitment to growth arrest and apoptosis and this proposal could reflect recent reports that whilst Caspase-deficient mice exhibited aberrant T cell development, they did not appear to have significant defects in B cell selection and development [230, 231, 299].

3.12 Summary

Crosslinking of the antigen receptors on the immature B cell lymphoma,WEHI-231, leads to growth arrest and apoptosis. Commitment to such BCR-mediated apoptosis has been found here to include two important cellular aspects:

- Induction of specific mitochondrial-associated activities: mitochondrial phospholipase A_2 activation, arachidonic acid-mediated collapse of $\Delta\psi_m$, and ATP depletion.
- Cathepsins, and not Caspases, are the active killer proteases. This apoptotic signal also does not induce release of cytochrome C.

Disruption of $\Delta\psi_m$, ATP-depletion and apoptosis can be prevented by rescue signals via CD40 or by $\Delta\psi_m$ stabilisers. CD40 also causes an increase in of Bcl-x_L protein levels and prevents the pro-apoptotic proteins from the Bcl-2 family, Bad and Bid from entering the mitochondria.

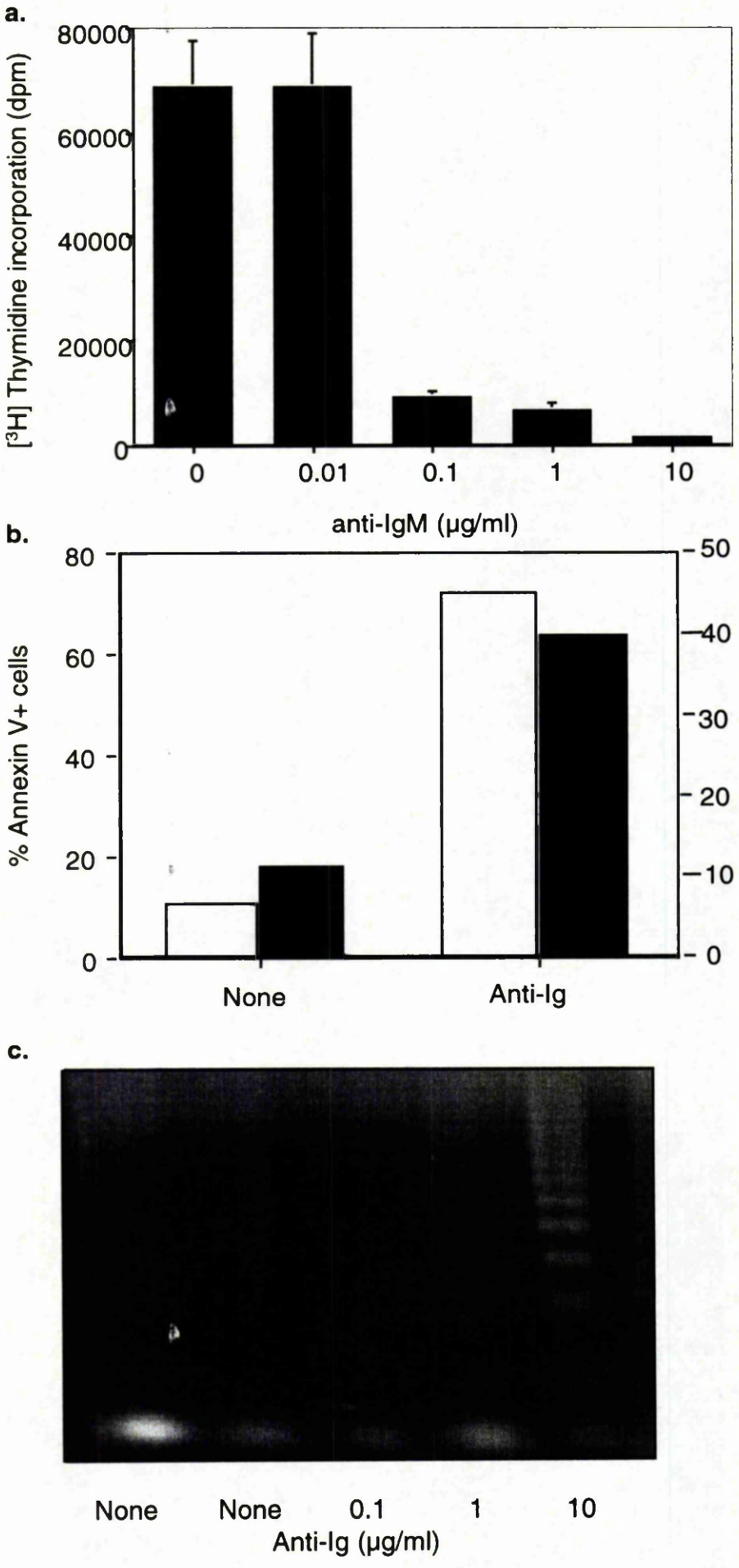
a.
80000
60000
40000
20000
0
[3H] Thymidine incorporation (dpm)
0
0.01
0.1
1
10
anti-IgM (µg/ml)
b.
80
60
40
20
0
% Annexin V+ cells
50
40
30
20
10
0
None
Anti-Ig
c.
None
None
0.1
1
10
Anti-Ig (µg/ml)

Fig. 10

Figure 10: Ligation of the BCR induces growth arrest and apoptosis of WEHI-231 immature B cells. Growth arrest was assessed by measurement of anti-Ig-mediated suppression of DNA synthesis by WEHI-231 B cells (a). WEHI-231 B cells were treated for 48 hours with 0-10mg/ml of anti-IgM and levels of [^{3}H]-Thymidine incorporation into DNA measured. Data are expressed as means ± SD (*n=3*) from a single experiment. Apoptosis was also analysed by Annexin V (open bars, y-axis) binding to cell surface phosphatidylserine, propidium iodide staining (panel b, filled bars). of subdiploid DNA (panel b, open bars; 10µg/ml anti-Ig), and DNA laddering (c) at 48h post-stimulation with the indicated concentration of anti-Ig. All data are from single experiments representative of at least two other independent experiments.

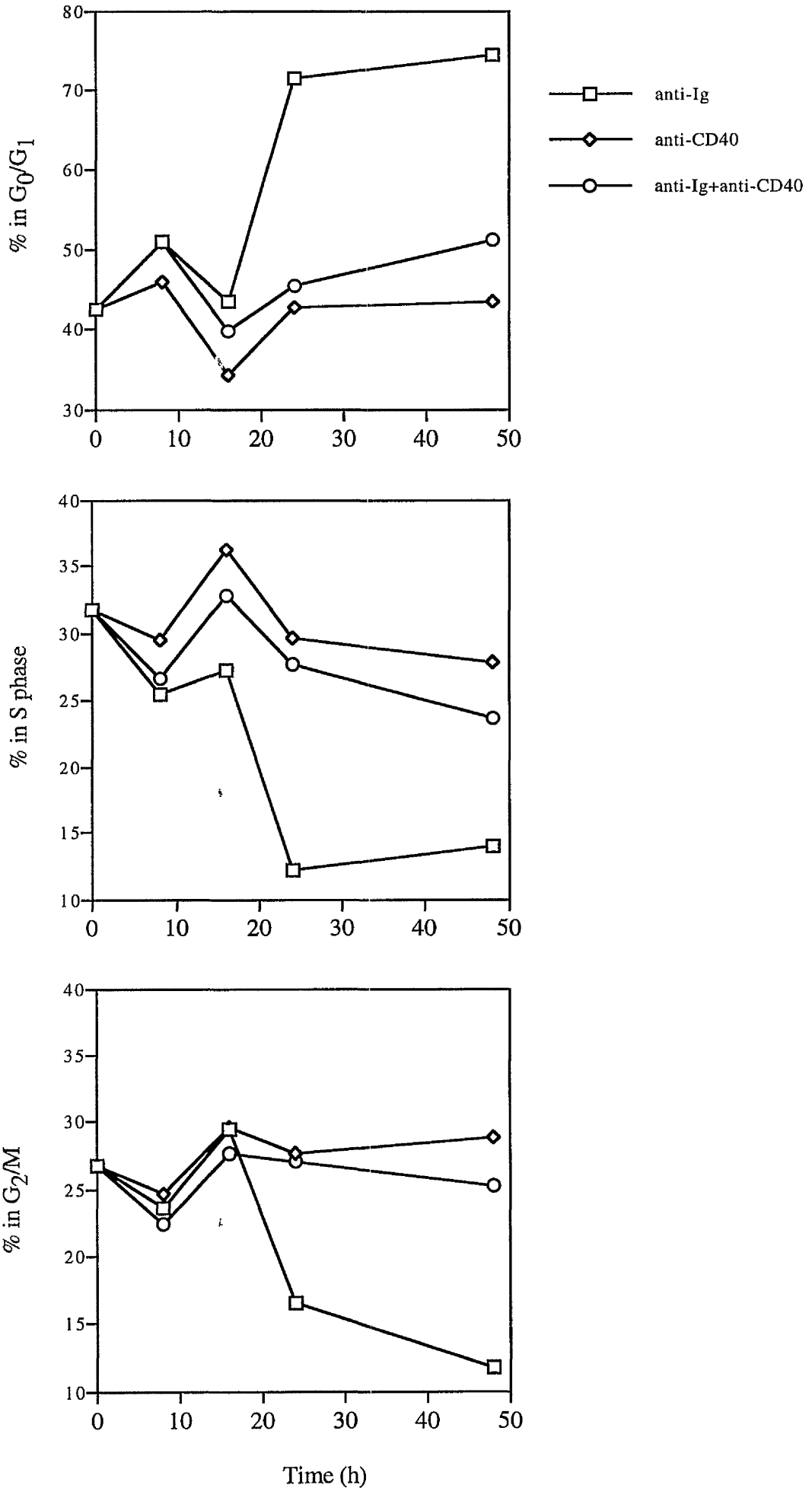
% in G_0/G_1
% in S phase
% in G_2/M
Time (h)
anti-Ig
anti-CD40
anti-Ig+anti-CD40

Fig. 11

Figure 11: The timing of CD40 mediated rescue from BCR-induced apoptosis. WEHI-231 cells were treated with anti-IgM (10μg/ml) and/or anti-CD40 (10μg/ml) for 48h. DNA content was measured by PI incorporation. Subpopulations were determined as described in *Materials and Methods* and % of cells calculated from the total ≥2N DNA population.

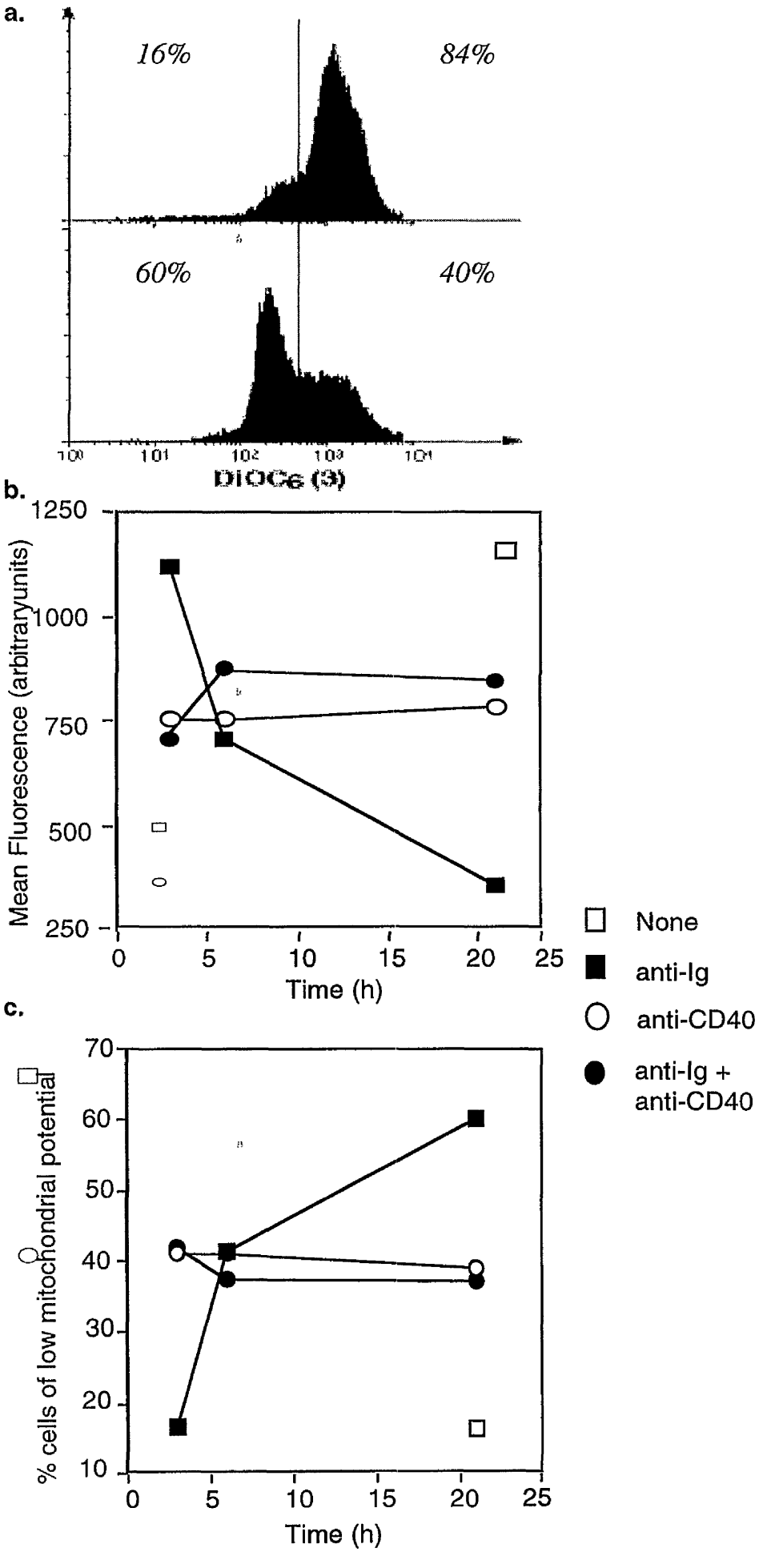
a.
16%
84%
60%
40%
DiOCe (3)
b.
Mean Fluorescence (arbitraryunits)
1250
1000
750
500
250
0
5
10
15
20
25
Time (h)
None
anti-Ig
anti-CD40
anti-Ig +
anti-CD40
c.
% cells of low mitochondrial potential
70
60
50
40
30
20
10
0
5
10
15
20
25
Time (h)

Fig. 12

Figure 12: Anti-Ig-induces a decrease in the $\Delta\psi_m$ of WEHI-231 immature B cells. WEHI-231 immature B cells (10^6 cells) were treated with 0-10μg/ml anti-IgM and/or anti-CD40. In panel a, commitment to apoptosis was assessed by measurement of mitochondrial potential ($\Delta\psi_m$) by the fluorescent dye, $DiOC_6$ (3) in control (upper histogram) and anti-Ig-treated WEHI-231 cells (lower histogram) 24h post stimulation. A decrease in $\Delta\psi_m$ is indicated by decrease in mean fluroescence intensity (MFI) of $DiOC_6$ (3) staining. In panel b, the data are represented as the mean fluorescence intensity of $DiOC_6$ (3) staining to demonstrate the extent of depolarisation whereas in panel c this data is presented as % cells of low mitochondrial potential. All data are from single experiments representative of at least two other independent experiments.

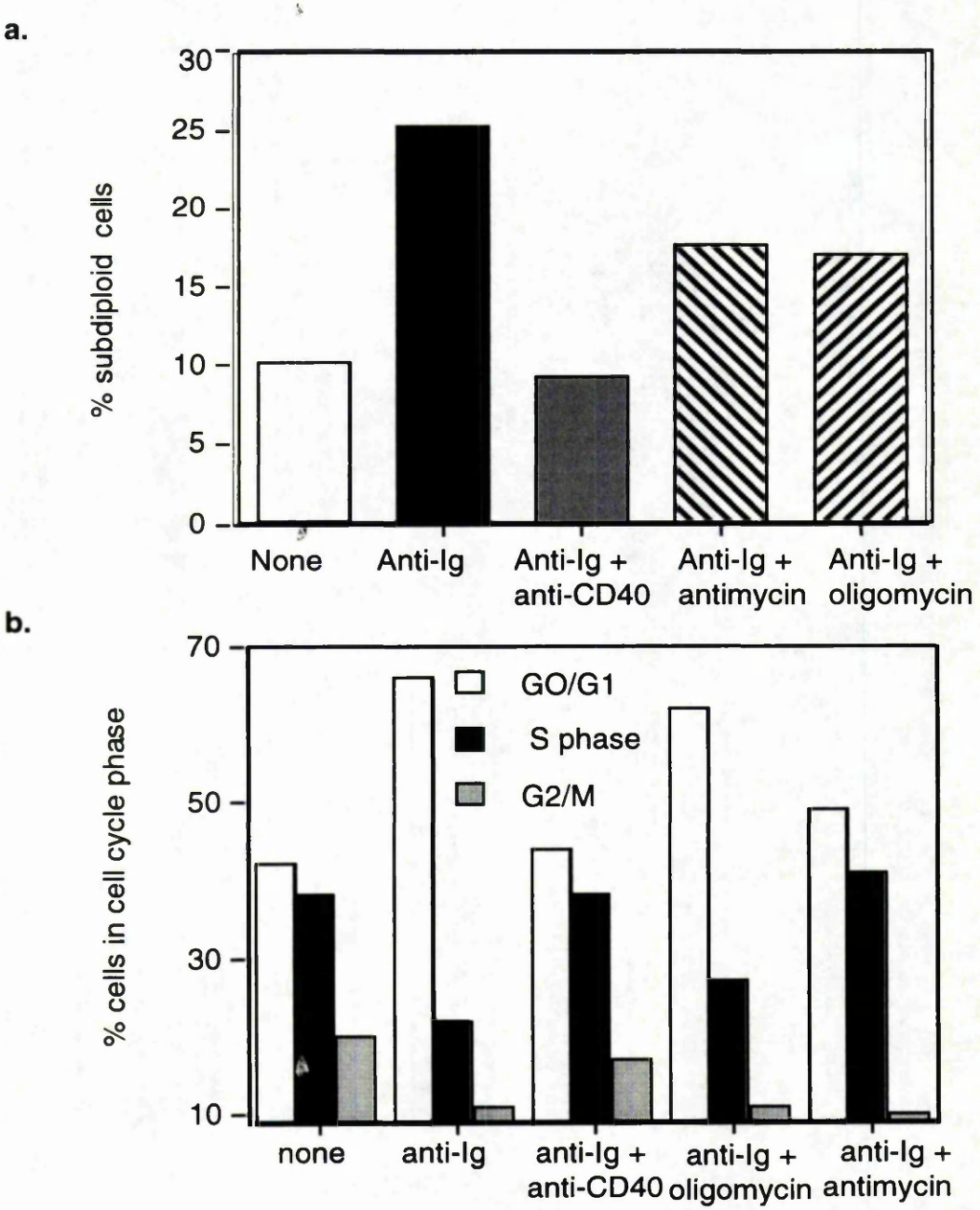
a.
% subdiploid cells
30
25
20
15
10
5
0
None
Anti-Ig
Anti-Ig + anti-CD40
Anti-Ig + antimycin
Anti-Ig + oligomycin
b.
% cells in cell cycle phase
70
50
30
10
GO/G1
S phase
G2/M
none
anti-Ig
anti-Ig + anti-CD40
anti-Ig + oligomycin
anti-Ig + antimycin

Fig. 13

Figure 13: Anti-CD40 and mitochondrial inhibitors prevent BCR-driven apoptosis and cell cycle arrest in G_0/G_1. In panel a, anti-Ig (10μg/ml)-mediated apoptosis of WEHI-231 cells was blocked by costimulation with anti-CD40 (10μg/ml) or the mitochondrial inhibitors, antimycin (50ng/ml) or oligomycin (8ng/ml). In panel b, anti-Ig (10μg/ml)-mediated growth arrest of WEHI-231 cells was blocked by costimulation with anti-CD40 (10μg/ml) or the mitochondrial inhibitors, antimycin (50ng/ml) or oligomycin (8ng/ml). Apoptosis and cell cycle progression was measured by PI staining of DNA content as decribed in *Materials and Methods*.

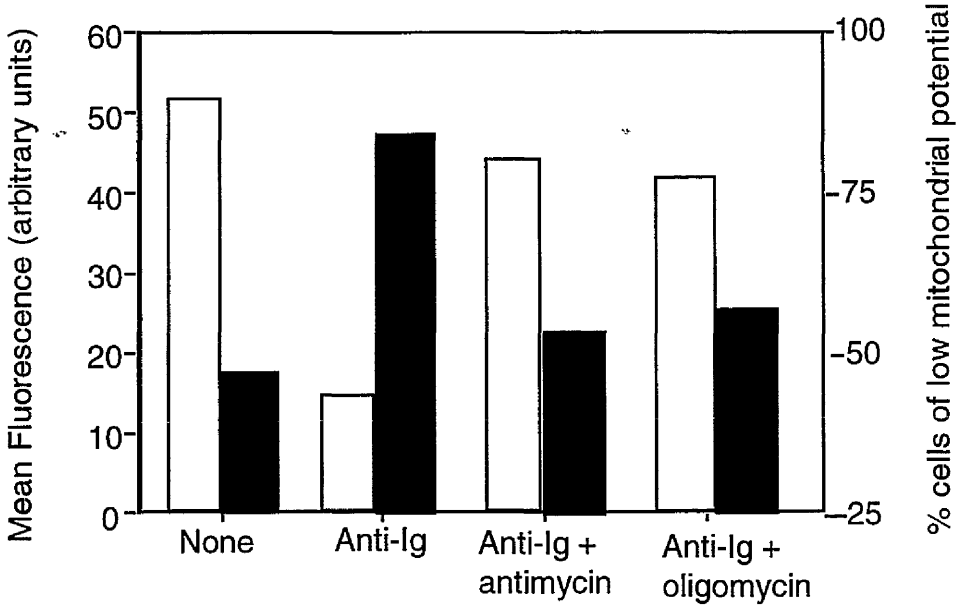
Mean Fluorescence (arbitrary units)
60
50
40
30
20
10
0
100
75
50
25
% cells of low mitochondrial potential
None
Anti-Ig
Anti-Ig + antimycin
Anti-Ig + oligomycin

Fig. 14

Figure 14: Mitochondrial inhibitors block mitochondrial potential depolarisation. WEHI-231 immature B cells were treated with 0-10μg/ml anti-IgM with or without antimycin (50ng/ml) or oligomycin (8ng/ml). Mitochondrial potential ($\Delta\psi_m$) was assessed by the fluorescent dye, $DiOC_6$ (3). A decrease in $\Delta\psi_m$ is indicated by decrease in mean fluorescence intensity (MFI) of $DiOC_6$ (3) staining (open bars) or the percentage of cells with low mitochondrial potential (close bars). All data are from single experiments representative of at least two other independent experiments.

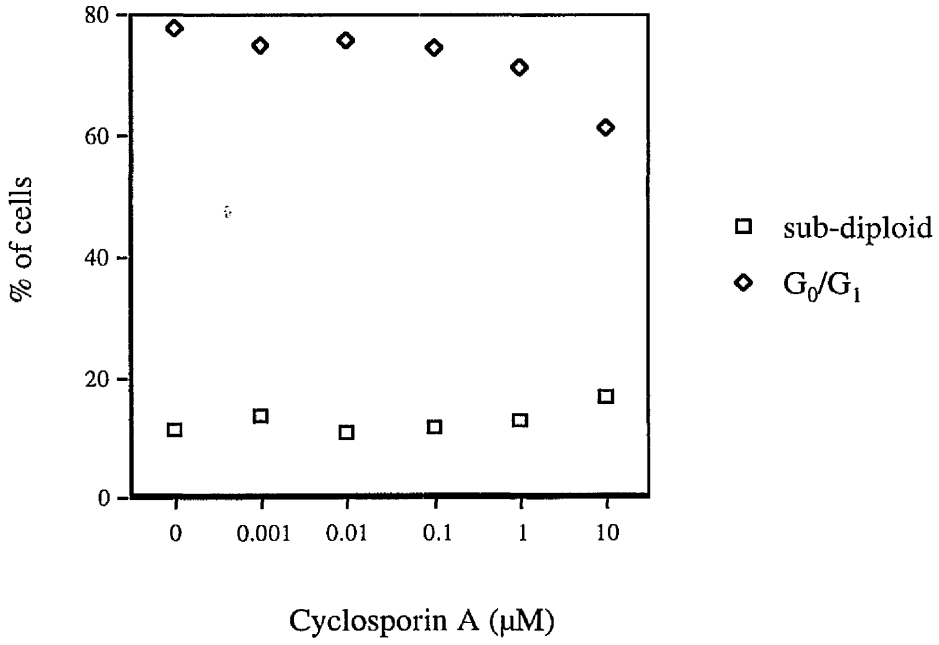
80
60
40
20
0
% of cells
0
0.001
0.01
0.1
1
10
Cyclosporin A (μM)
sub-diploid
G_0/G_1

Fig. 15

Figure 15: The effect of cyclosporin A on apoptosis and growth arrest. WEHI-231 cells were treated with anti-IgM (10µg/ml) and cyclosporin A (0-10µM) for 48h. DNA content was measured by PI incorporation. % of sub-diploid cells was determined as the <2N DNA population. % of cells in G_0/G_1 are shown as calculated from the ≥2N ("living") DNA population.

a.

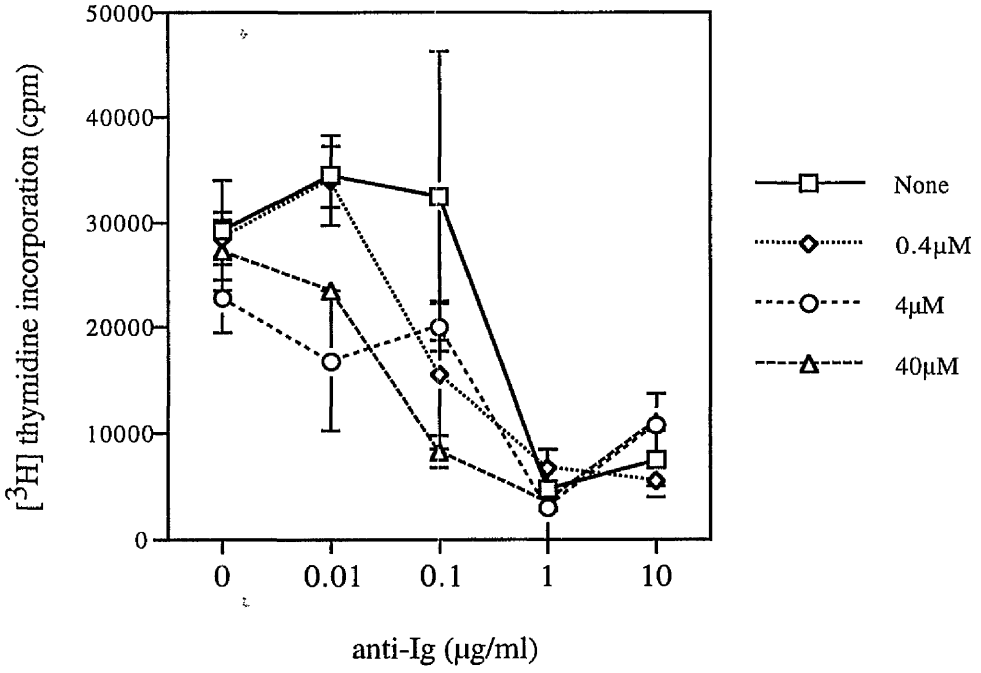
50000
40000
30000
20000
10000
0
[3H] thymidine incorporation (cpm)
0
0.01
0.1
1
10
anti-Ig (µg/ml)
None
0.4µM
4µM
40µM

b.

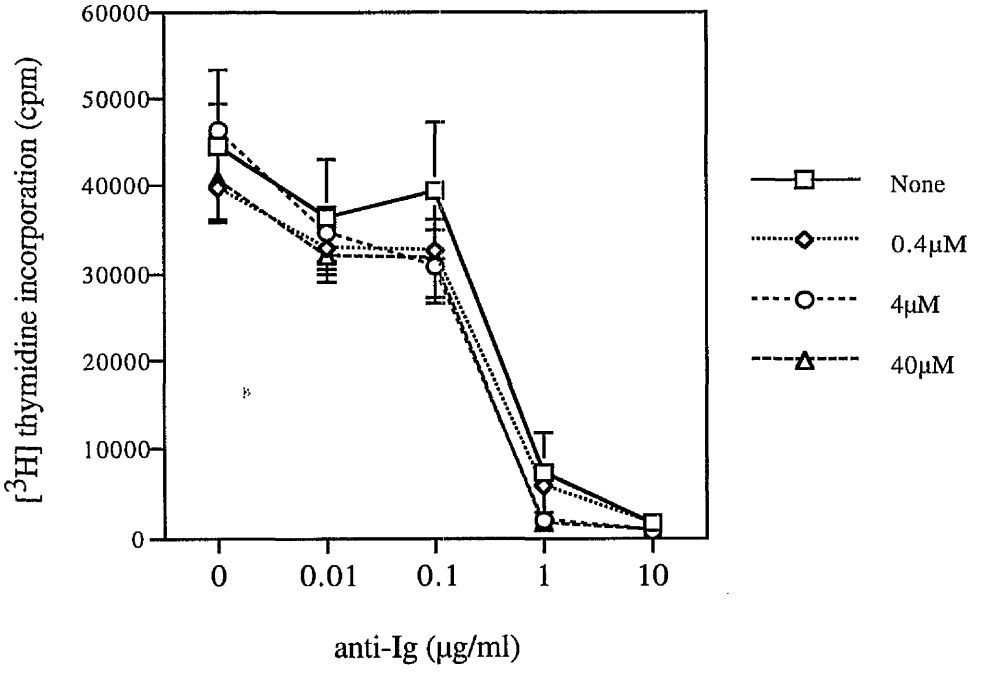
60000
50000
40000
30000
20000
10000
0
[3H] thymidine incorporation (cpm)
0
0.01
0.1
1
10
anti-Ig (µg/ml)
None
0.4µM
4µM
40µM

Fig. 16

Figure 16: Effect of Nitric Oxide Synthase inhibitors on BCR-induced growth arrest. Growth arrest was assessed by measurement of anti-Ig-mediated suppression of DNA synthesis by WEHI-231 B cells. WEHI-231 B cells ($5x10^4$ per well) were treated for 48h with 0-10mg/ml of anti-IgM and (a) 0-40μM L-NMMA or (b) 0-40μM L-NIL. Levels of [^{3}H] thymidine incorporation into DNA were measured after further 4h. Data are expressed as means ± SD (*n=3*) from a single experiment, representative of at least two other independent experiments.

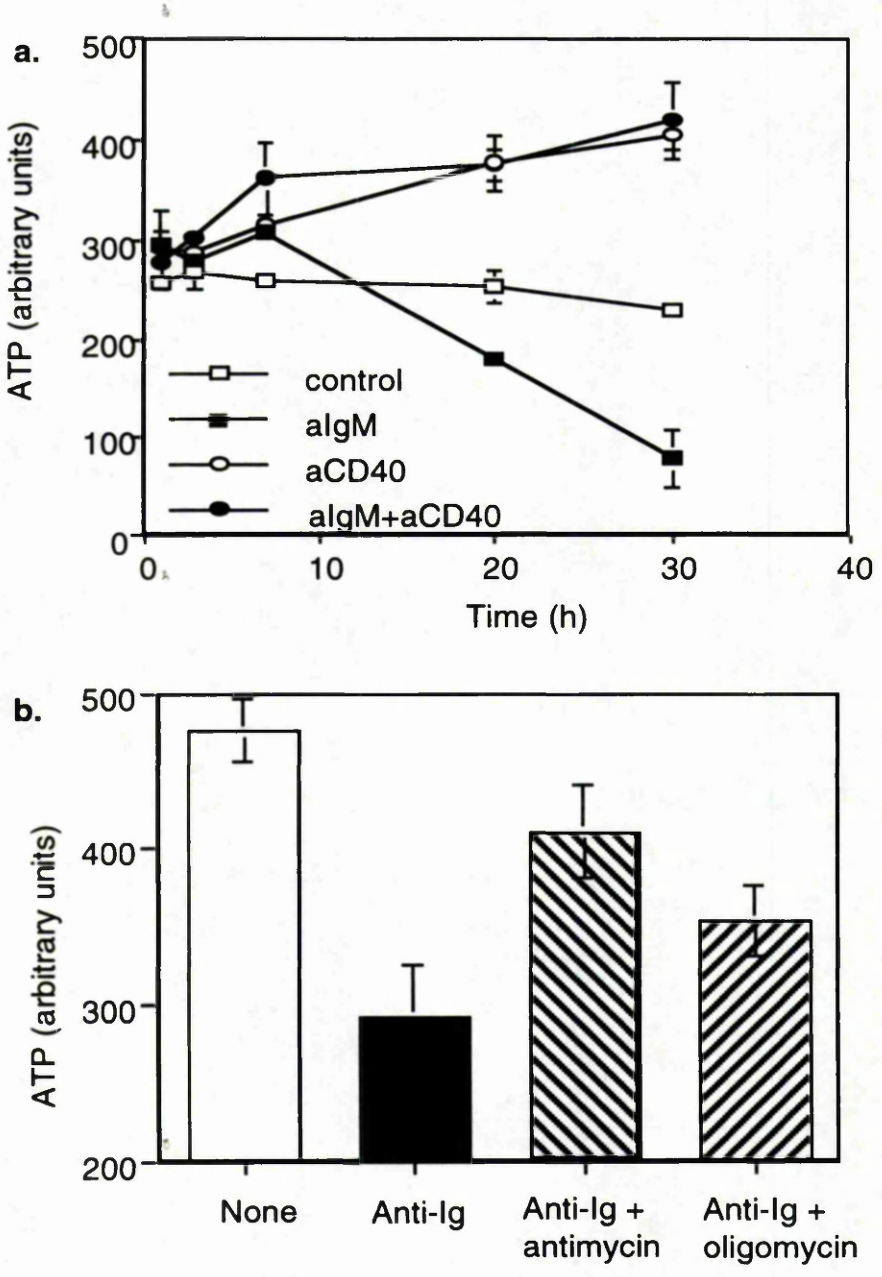
a.
ATP (arbitrary units)
500
400
300
200
100
0
0
10
20
30
40
Time (h)
control
aIgM
aCD40
aIgM+aCD40
b.
ATP (arbitrary units)
500
400
300
200
None
Anti-Ig
Anti-Ig + antimycin
Anti-Ig + oligomycin

Fig. 17

Figure 17: Anti-Ig induces ATP depletion in WEHI-231 B cells which can be rescued by anti-CD40 or mitochondrial inhibitors. WEHI-231 cells were treated with anti-IgM (10µg/ml) and/or anti-CD40 (10µg/ml) for up to 30h and ATP content assessed as indicated in *Materials and Methods* (panel a). Anti-Ig-stimulated depletion of ATP in WEHI-231 B cells was blocked (panel b) by costimulation with the mitochondrial inhibitors, antimycin (50ng/ml) or oligomycin (8ng/ml). Data are presented as means ± SD (n=3) from single experiments. All data are from single experiments representative of at least two other independent experiments.

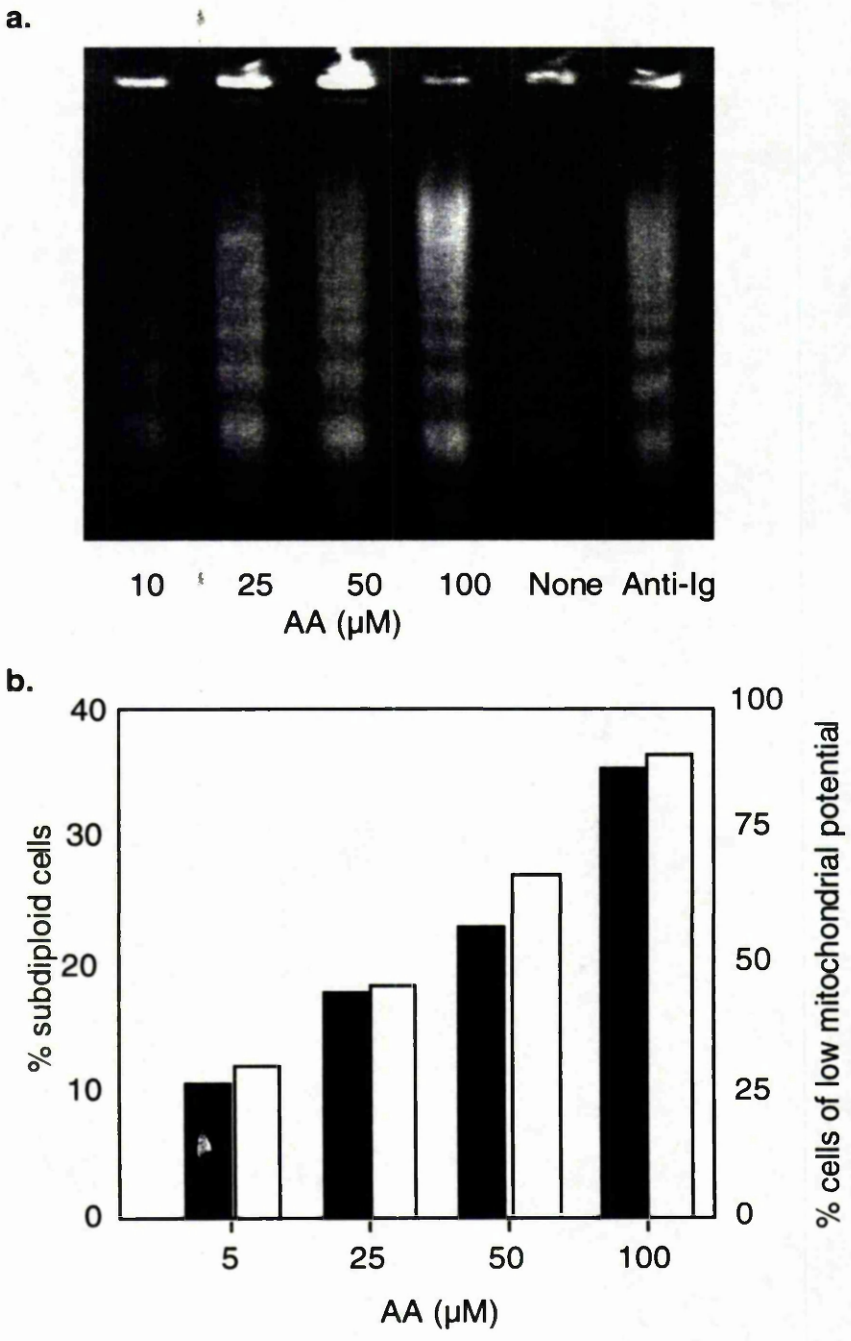
a.
10
25
50
100
None
Anti-Ig
AA (μM)
b.
40
30
20
10
0
% subdiploid cells
100
75
50
25
0
% cells of low mitochondrial potential
5
25
50
100
AA (μM)

Fig. 18

Figure 18: Anti-Ig induces mitochondrial translocation and activation of cytosolic phospholipase A_2 resulting in arachidonic acid generation, disruption of mitochondrial potential and apoptosis. Anti-Ig (10 μg/ml) and arachidonic acid (10-100μM) induce apoptosis of WEHI-231 cells as indicated by DNA laddering 48h post-stimulation (panel a). Exogeneous arachidonic acid (5-100μM) induces collapse of mitochondrial potential (as assessed using the dye $DiOC_6$ (3); panel b: open bars) and induction of subdiploid DNA content (panel b: filled bars). All experiments are single experiments representative of at least two other independent experiments.

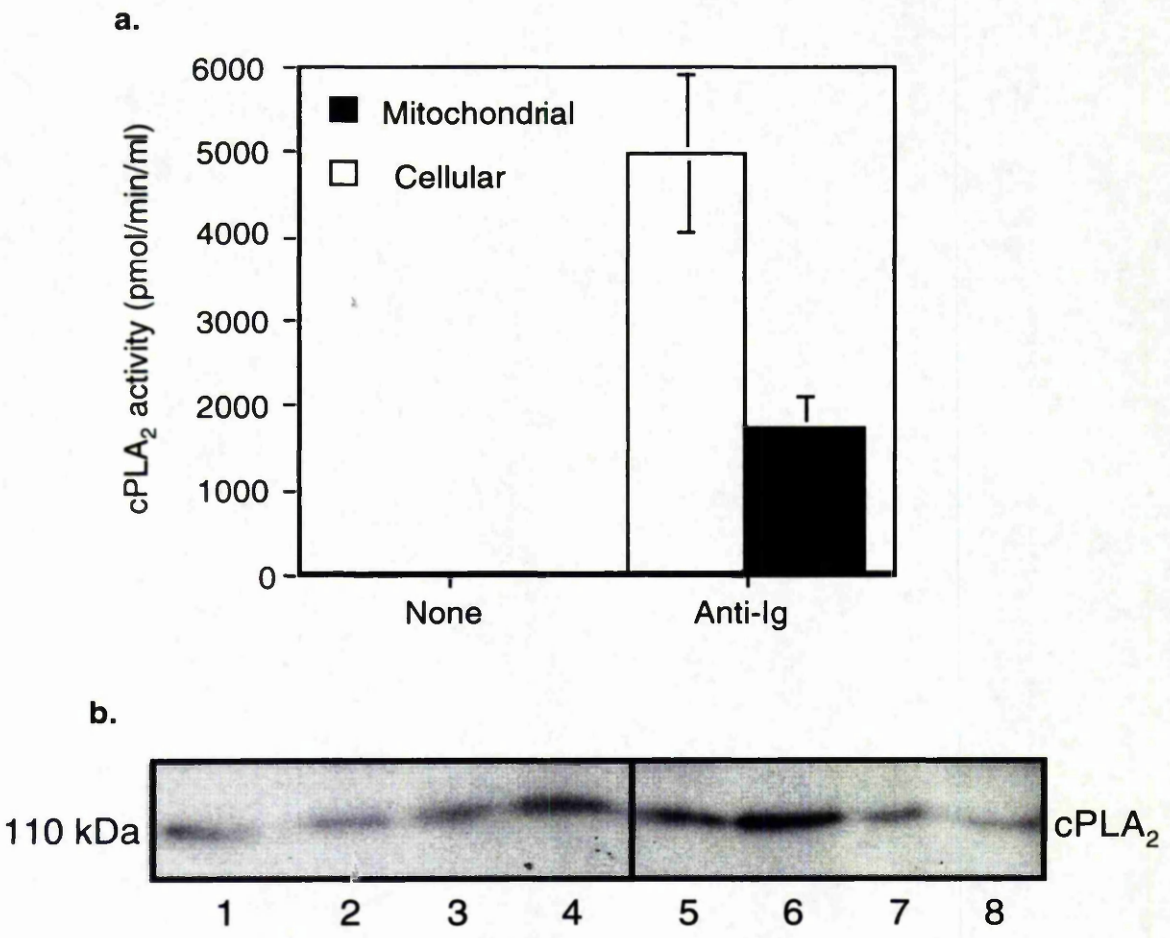
a.
6000
5000
4000
3000
2000
1000
0
cPLA2 activity (pmol/min/ml)
Mitochondrial
Cellular
T
None
Anti-Ig
b.
110 kDa
cPLA2
1
2
3
4
5
6
7
8

Fig. 19

Figure 19: Anti-Ig modulates phospholipase A_2 expression and activity.

Mitochondrial and cellular phospholipase A_2 activity is induced by anti-Ig (10µg/ml) 24h post-stimulation (a). Expression of $cPLA_2$ protein (Western Blot; panel b) is modulated during apoptotic sinalling in WEHI-231 immature B cells: WEHI 231 cells were incubated with media (lanes 1 and 5), 10µg/ml anti-IgM (lanes 2 and 6), 10µg/ml anti-CD40 (lanes 3 and 7) or a combination of these stimuli (lanes 4 and 8) for 1 hour (lanes 1-4) or 24 hours (lanes 5-8).

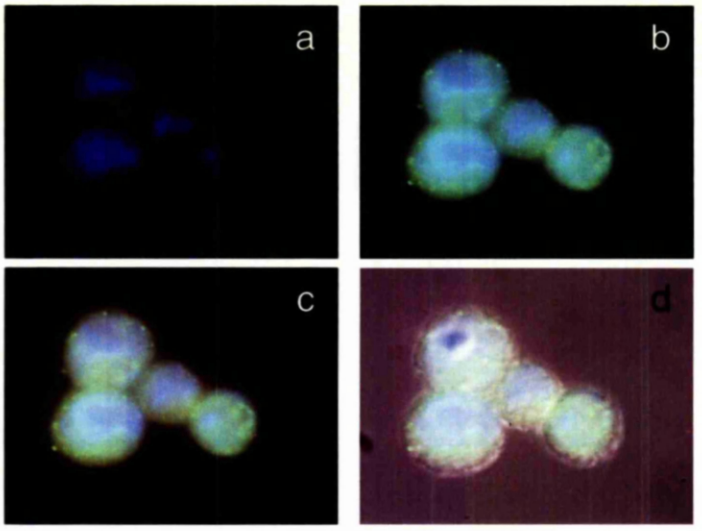

none

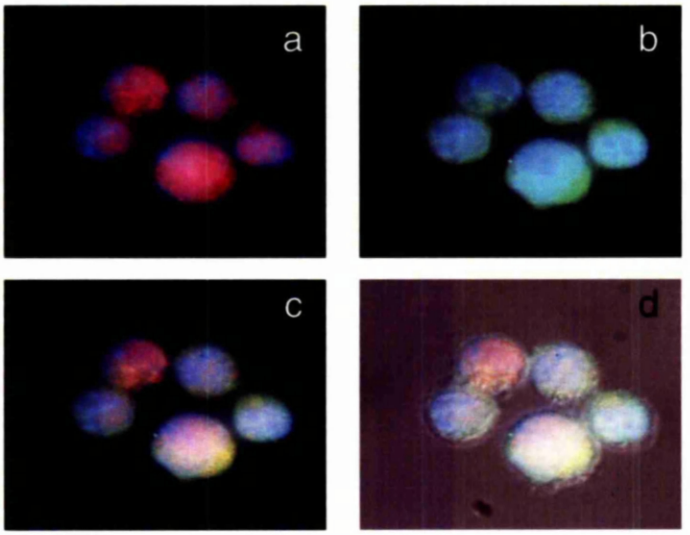

anti-Ig

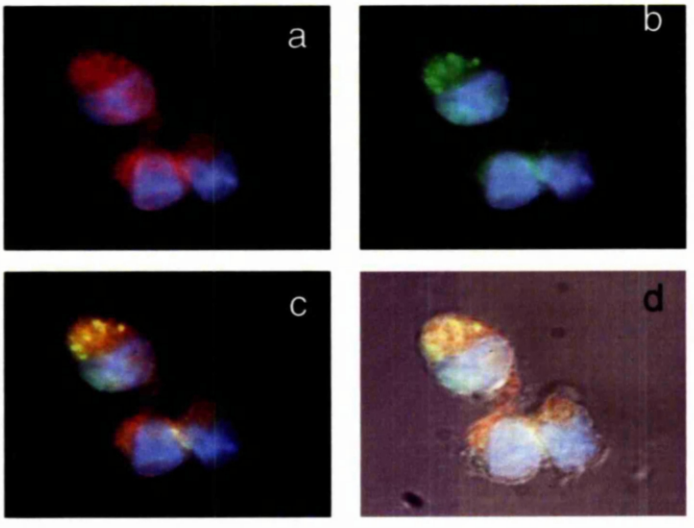

anti-Ig+anti-CD40

Figure 20: $cPLA_2$ expression and mitochondrial translocation. The cell nucleus is stained blue (DAPI), $cPLA_2$ (Texas red) and mitochondria (green). In unstimulated WEHI-231 cells, there is little or no $cPLA_2$ expression (red) in either the nucleus, cytoplasm (panel a; underestimated here due to the loss of soluble $cPLA_2$ during staining (as reported in [300]) or mitochondria (panel c). In contrast in anti-Ig-cells there is indication of upregulation of cPLA2 expression (panel a) and strong and diffuse nuclear (purple, panels a, c & d) and mitochondrial (yellow, panels c & d) translocation by 3h. Although in cells costimulated with anti-CD40 there is still evidence of mitochondrial and to a lesser extent, nuclear $cPLA_2$ localisation, this is more discrete (panels a, c & d) and there is strong red cytoplasmic staining (panels a, c & d). Downregulation of $cPLA_2$ by anti-CD40 is not seen at 3 h. panel a: staining of nucleus (DAPI; blue) and $cPLA_2$ (Texas red); panel b: nucleus (blue) and mitochondria (anti-ANT+anti-rabbit-FITC); panel c: nucleus, $cPLA_2$ and mitochondria & panel d: as panel c+ bright field.

a.

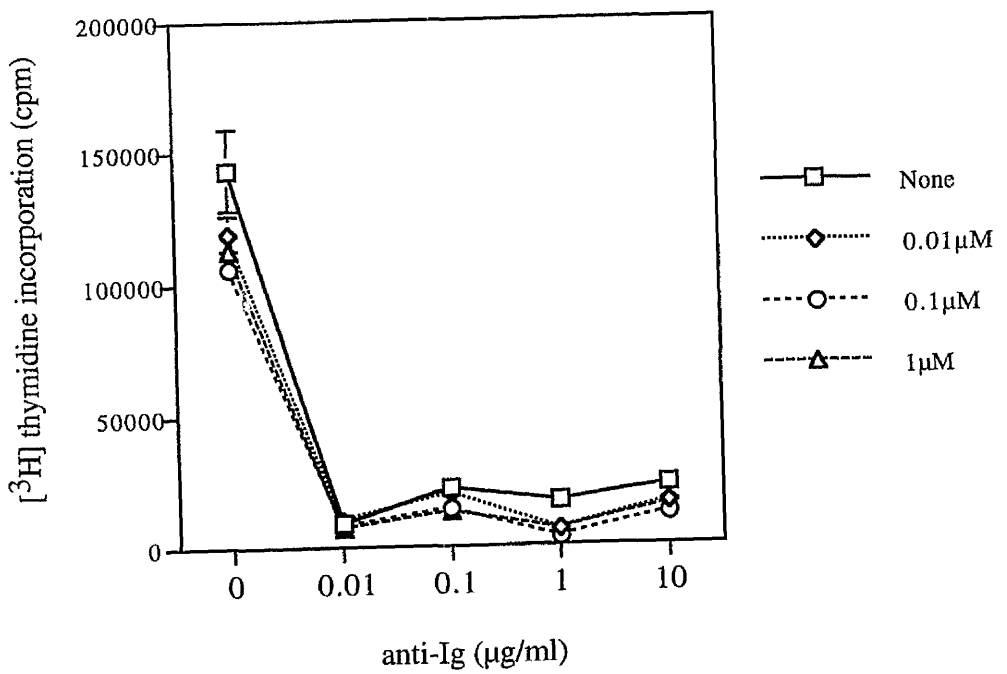
200000
150000
100000
50000
0
[3H] thymidine incorporation (cpm)
0
0.01
0.1
1
10
anti-Ig (µg/ml)
None
0.01µM
0.1µM
1µM

b.

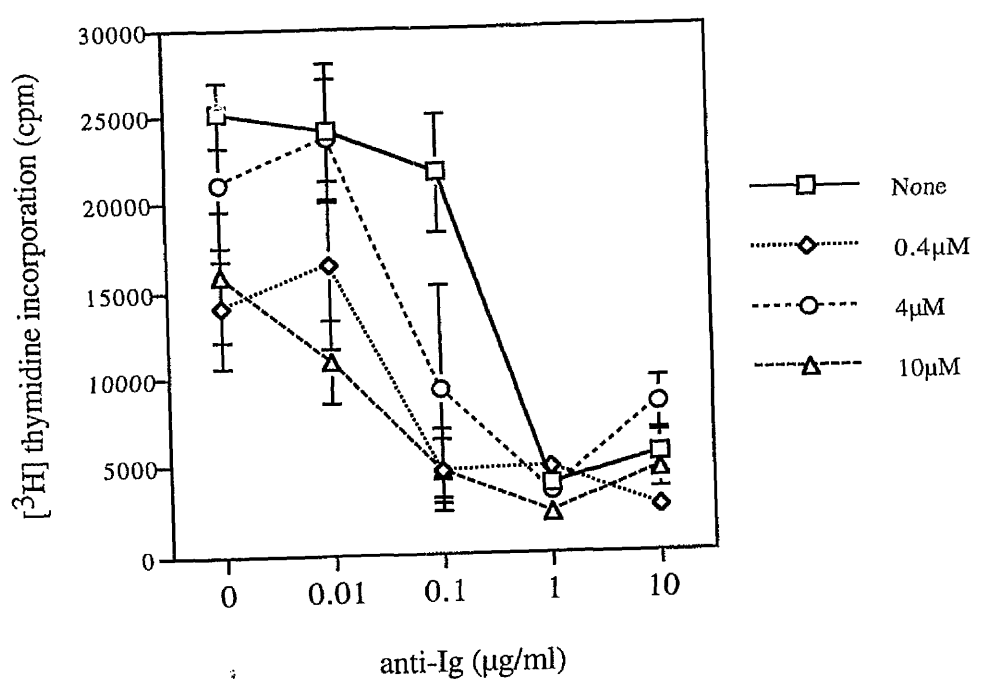
30000
25000
20000
15000
10000
5000
0
[3H] thymidine incorporation (cpm)
0
0.01
0.1
1
10
anti-Ig (µg/ml)
None
0.4µM
4µM
10µM

Fig. 21

Figure 21: Effect of COX-2 inhibitors on BCR-induced growth arrest. Growth arrest was assessed by measurement of anti-Ig-mediated suppression of DNA synthesis by WEHI-231 B cells. WEHI-231 B cells ($5x10^4$ per well) were treated for 48h with 0-10μg/ml of anti-IgM and (a) 0-1μM niflumic acid or (b) 0-10μM NS-398. Levels of [^{3}H] thymidine incorporation into DNA were measured after further 4h. Data are expressed as means ± SD (*n=3*) from a single experiment, representative of at least two other independent experiments.

a.

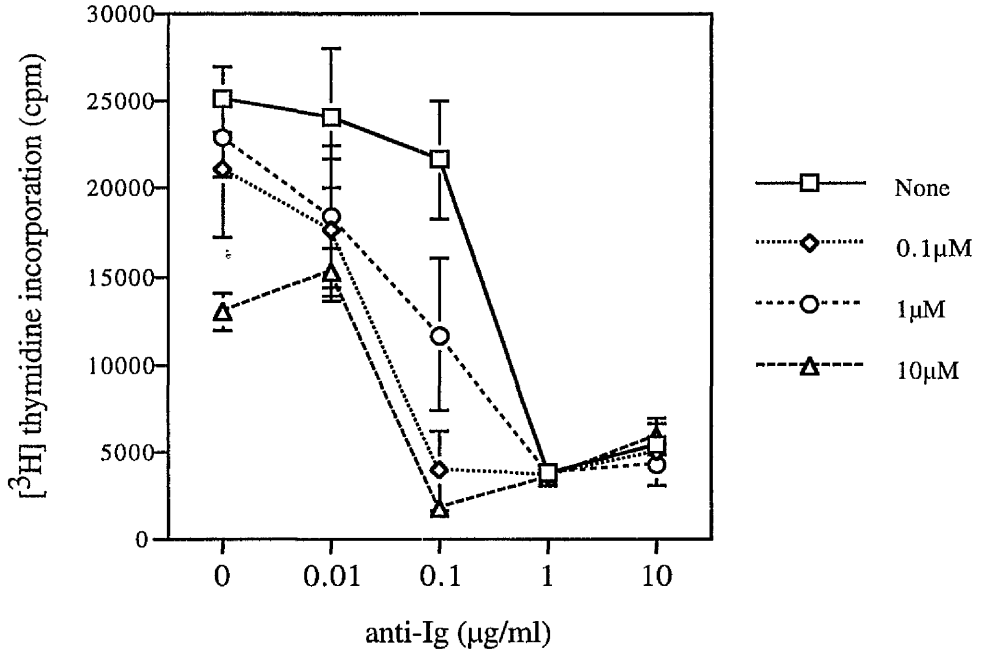
30000
25000
20000
15000
10000
5000
0
[3H] thymidine incorporation (cpm)
0
0.01
0.1
1
10
anti-Ig (µg/ml)
None
0.1µM
1µM
10µM

b.

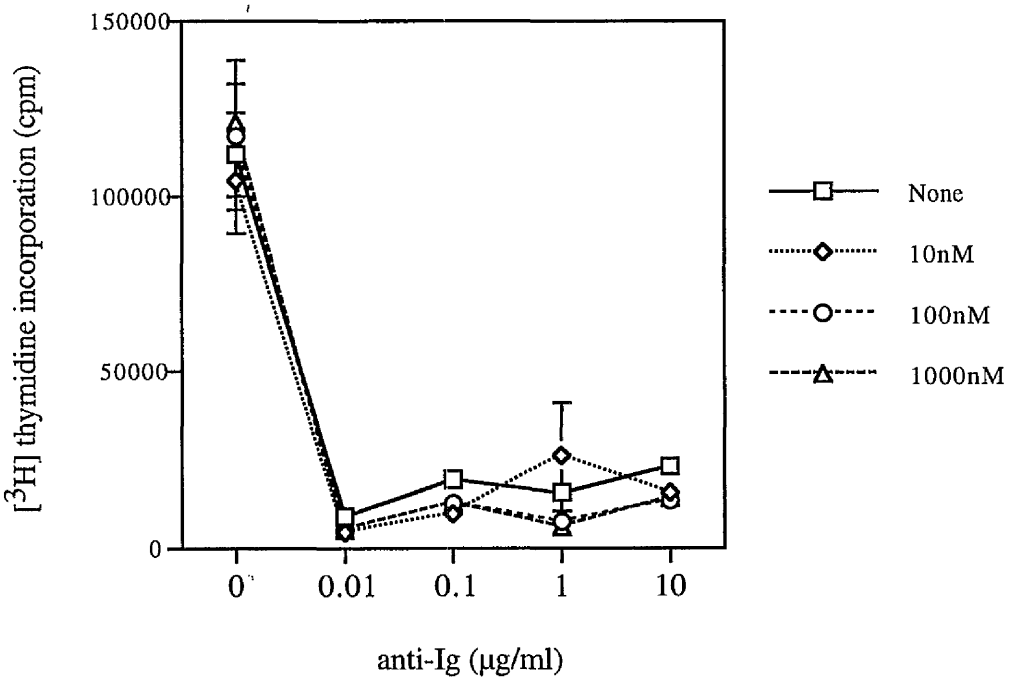
150000
100000
50000
0
[3H] thymidine incorporation (cpm)
0
0.01
0.1
1
10
anti-Ig (µg/ml)
None
10nM
100nM
1000nM

Fig. 22

Figure 22: Effect of LOX inhibitors on BCR-induced growth arrest. Growth arrest was assessed by measurement of anti-Ig-mediated suppression of DNA synthesis by WEHI-231 B cells. WEHI-231 B cells ($5x10^4$ per well) were treated for 48h with 0-10μg/ml of anti-IgM and (a) 0-10μM pan-LOX inhibitor or (b) 0-1μM Baicalein. Levels of [^{3}H] thymidine incorporation into DNA were measured after further 4h. Data are expressed as means ± SD (*n=3*) from a single experiment, representative of at least two other independent experiments.

The pan-LOX inhibitor IC_{50} values, according to the manufacturer, are estimated as follows: 12-LOX ~ 0.1μM, 15-LOX ~ 1μM, 5-LOX ~ 10μM.

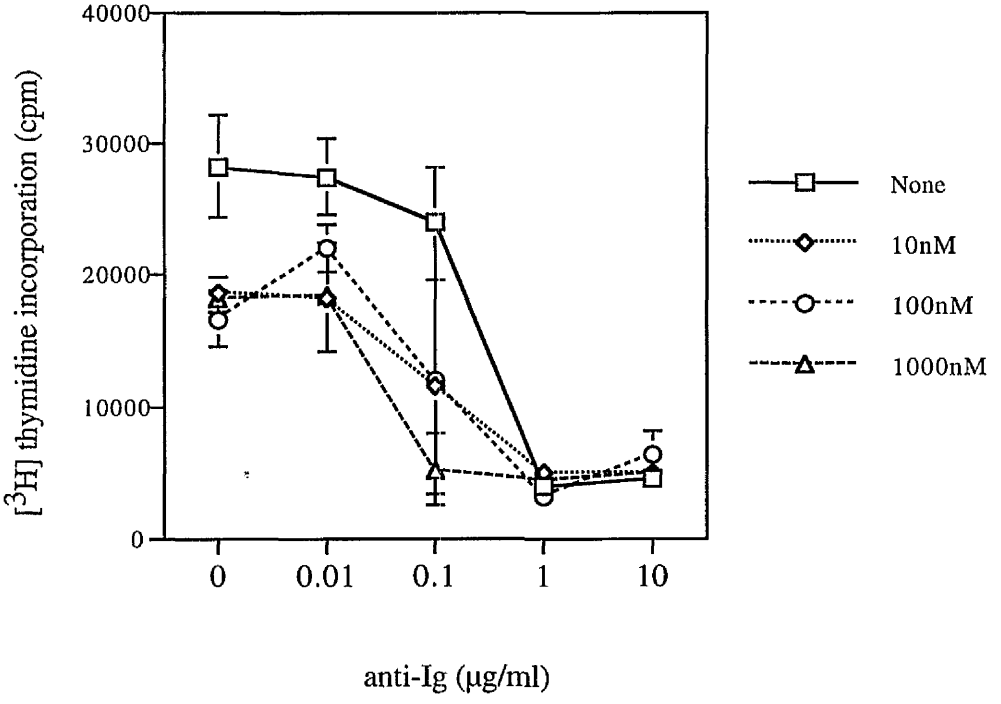
40000
30000
20000
10000
0
[3H] thymidine incorporation (cpm)
0
0.01
0.1
1
10
anti-Ig (µg/ml)
None
10nM
100nM
1000nM

Fig. 23

Figure 23: Effects of ceramide synthase inhibitor on BCR-induced growth arrest. Growth arrest was assessed by measurement of anti-Ig-mediated suppression of DNA synthesis by WEHI-231 B cells. WEHI-231 B cells ($5x10^4$ per well) were treated for 48h with 0-10μg/ml of anti-IgM and 0-1μM Fumonisin B_1. Levels of [^{3}H] thymidine incorporation into DNA were measured after further 4h. Data are expressed as means ± SD (*n=3*) from a single experiment, representative of at least two other independent experiments.

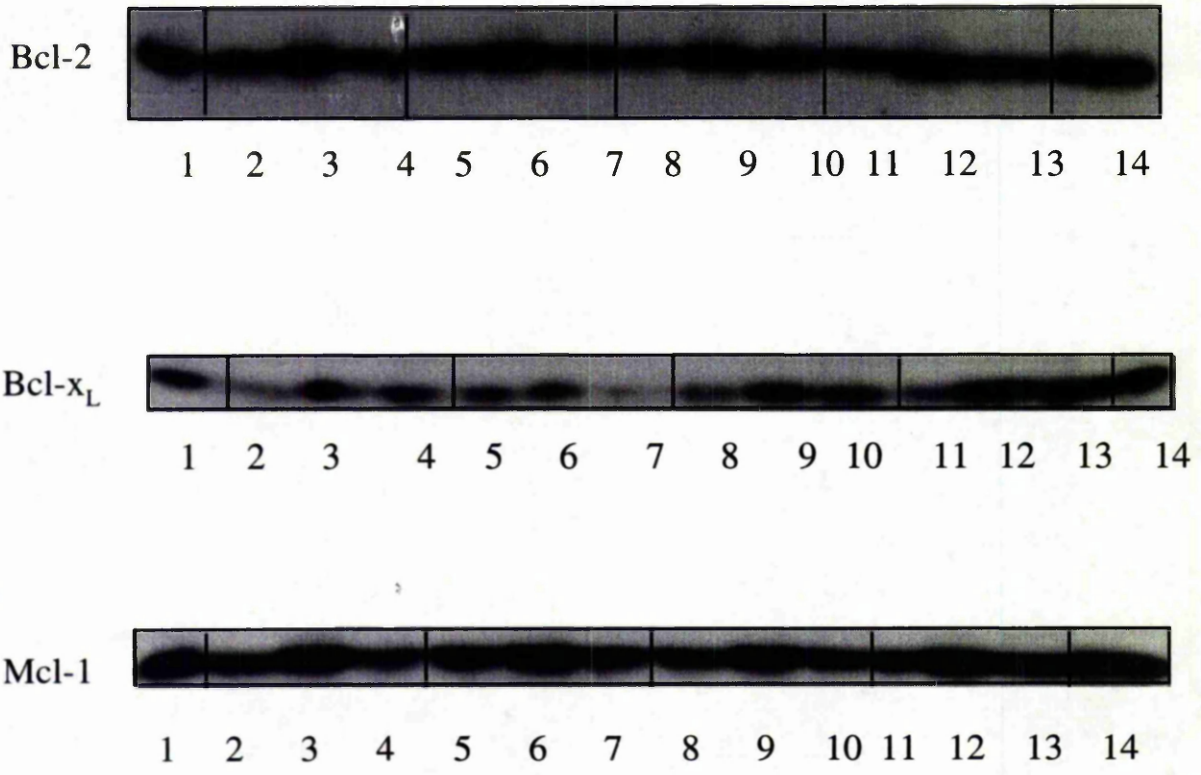
Bcl-2
1 2 3 4 5 6 7 8 9 10 11 12 13 14
Bcl-x_L
1 2 3 4 5 6 7 8 9 10 11 12 13 14
Mcl-1
1 2 3 4 5 6 7 8 9 10 11 12 13 14

Fig. 24

Figure 24: Expression of anti-apoptotic Bcl-2 proteins in apoptosis and survival of WEHI-231 cells. WEHI-231 cells (10^7 per sample) were stimulated as follows - 1: none 0; 2: anti-Ig (5μg/ml) 8h; 3: anti-CD40 (10μg/ml) 8h; 4: anti-Ig+anti-CD40 8h; 5: anti-Ig 16h; 6: anti-CD40 16h; 7: anti-Ig+anti-CD40 16h; 8: anti-Ig 24h; 9: anti-CD40 24h; 10: anti-Ig+anti-CD40 24h; 11: anti-Ig 48h; 12: anti-CD40 48h; 13: anti-Ig+anti-CD40 48h; 14: none 48h. At the end of the stimulation cells were lysed and Western blotting was preformed with the appropriate antibodies as descibed in *Materials and Methods*.

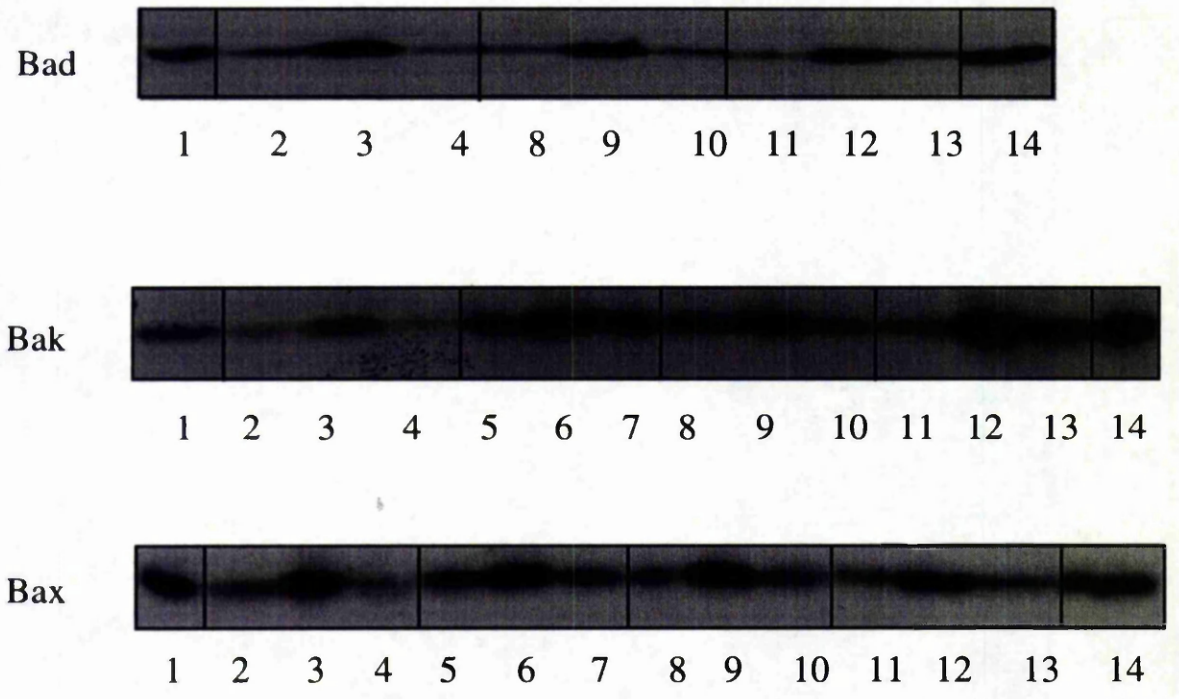
Bad
1 2 3 4 8 9 10 11 12 13 14
Bak
1 2 3 4 5 6 7 8 9 10 11 12 13 14
Bax
1 2 3 4 5 6 7 8 9 10 11 12 13 14

Fig. 25

Figure 25: Expression of pro-apoptotic Bcl-2 proteins in apoptosis and survival of WEHI-231 cells. WEHI-231 cells (10^7 per sample) were stimulated as follows - 1: none 0; 2: anti-Ig (5µg/ml) 8h; 3: anti-CD40 (10µg/ml) 8h; 4: anti-Ig+anti-CD40 8h; 5: anti-Ig 16h; 6: anti-CD40 16h; 7: anti-Ig+anti-CD40 16h; 8: anti-Ig 24h; 9: anti-CD40 24h; 10: anti-Ig+anti-CD40 24h; 11: anti-Ig 48h; 12: anti-CD40 48h; 13: anti-Ig+anti-CD40 48h; 14: none 48h. At the end of the stimulation cells were lysed and Western blotting was preformed with the appropriate antibodies as descibed in *Materials and Methods*.

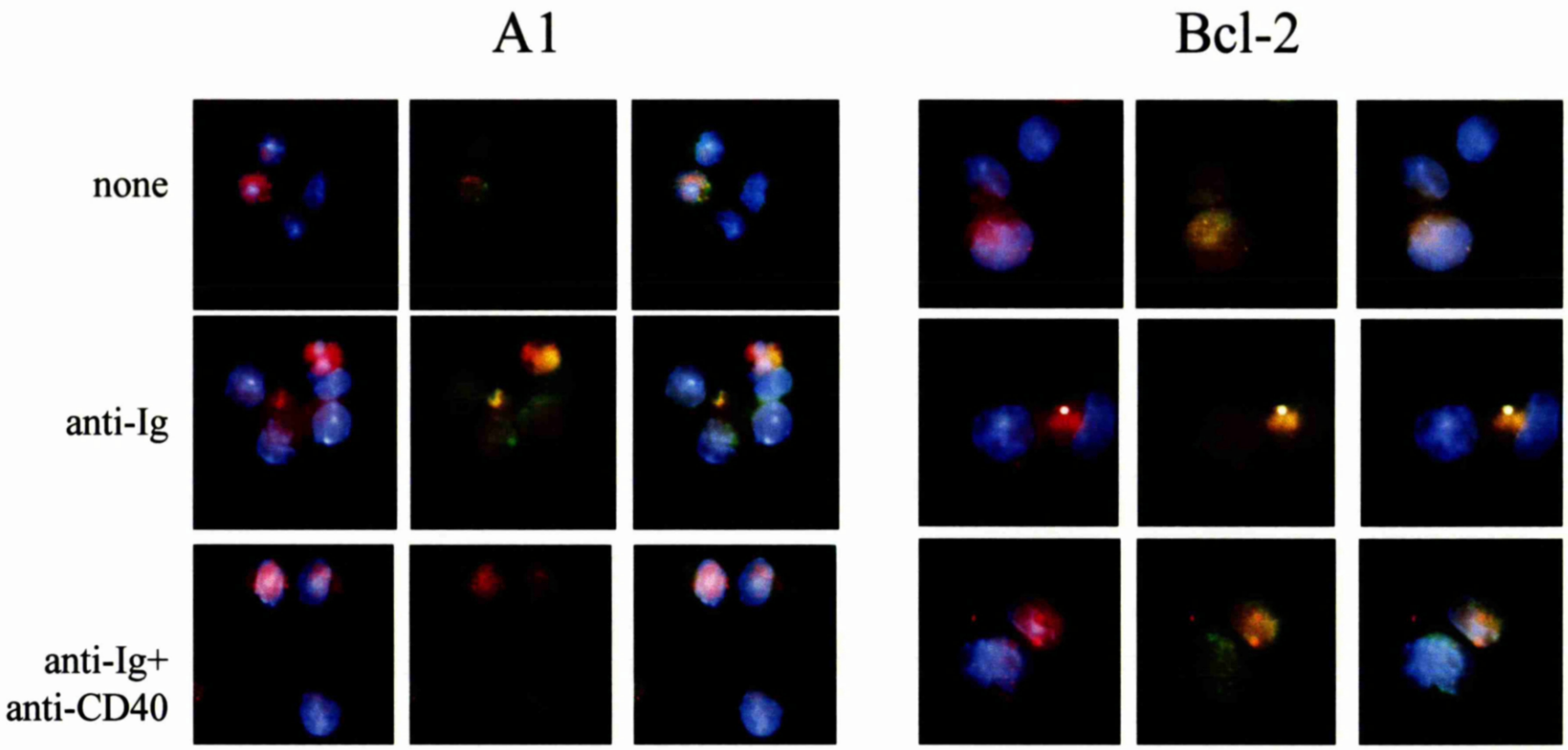
A1
Bcl-2
none
anti-Ig
anti-Ig+
anti-CD40

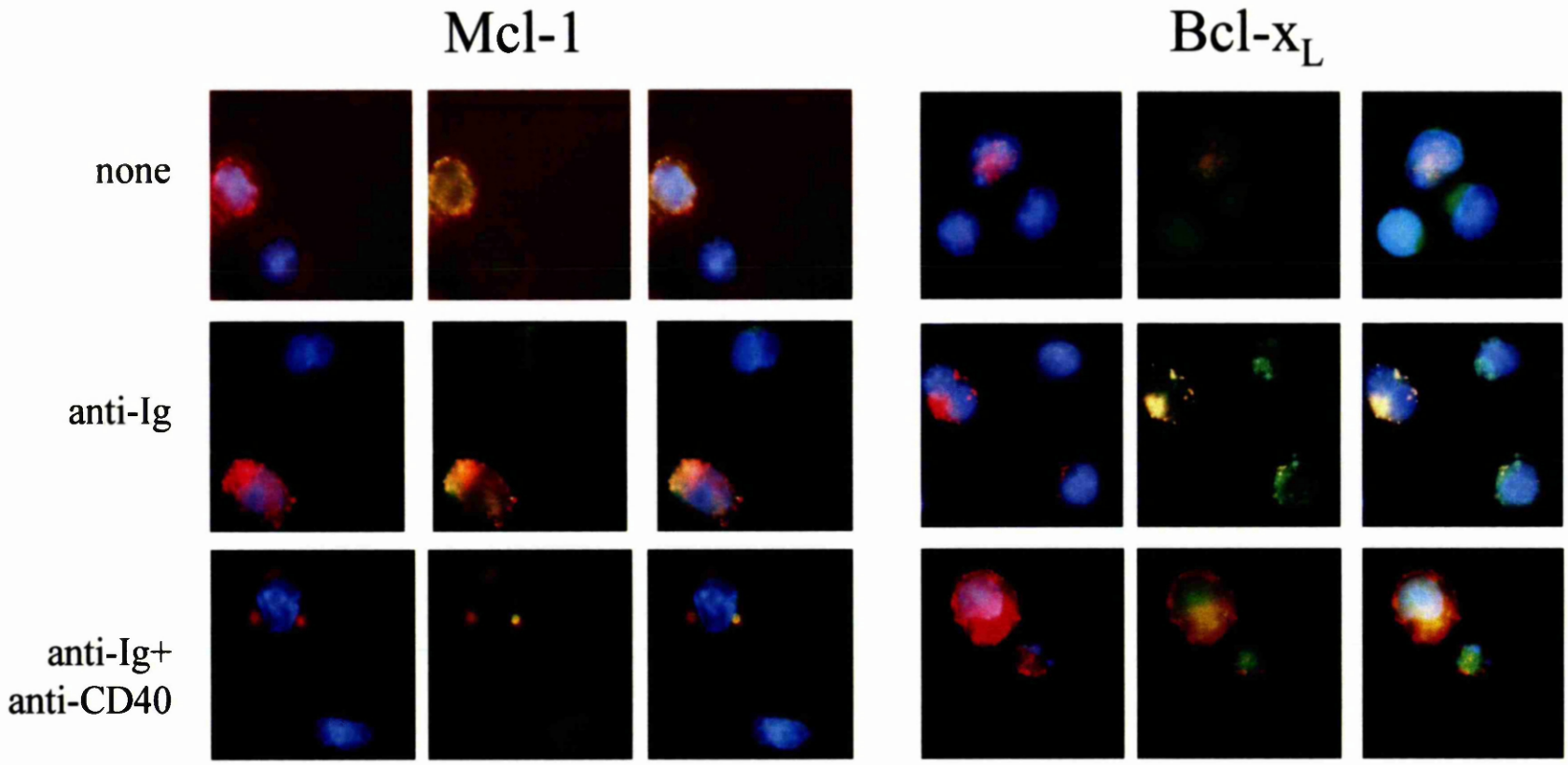
Mcl-1
Bcl-x$_L$
none
anti-Ig
anti-Ig+
anti-CD40

Figure 26: Expression and mitochondrial translocation of anti-apoptotic Bcl-2 proteins. WEHI-231 cells (10^6 per sample) were stimulated with media, anti-Ig (10μg/ml) or anti-Ig+anti-CD40 (10μg/ml) for 3h and then were subjected to intracellular staining as described in *Materials and Methods*. For the detection of A1, anti-goat-biotin and streptavidin-Texas Red were used. For the detection of Bcl-2, Mcl-1 or Bcl-x_L, anti-mouse-gamma-chain-biotin and streptavidin-Texas Red were used. For mitochondria staining in A1, Bcl-2 and Mcl-1 samples MitoTracker Green was used. For Bcl-x_L samples, Rhodamine 123 was used for mitochondria staining.

In each set of panels, the cell nucleus is stained blue (DAPI), the protein (A1, Bcl-2, Mcl-1 or Bcl-x_L) in red and mitochondria is green. The left panel shows nucleus plus protein, the middle panel mitochondria plus protein and the right panel all colours superimposed.

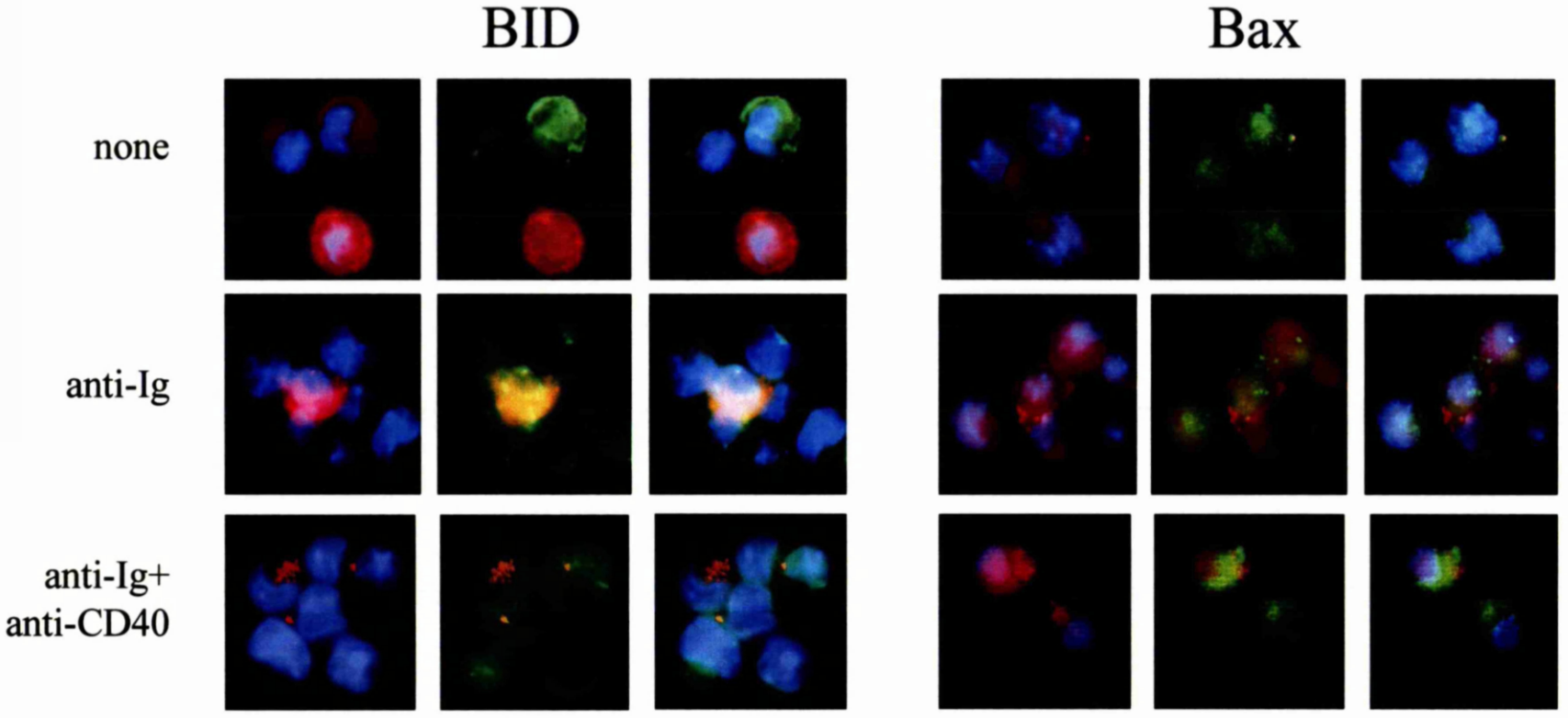
BID
Bax
none
anti-Ig
anti-Ig+
anti-CD40

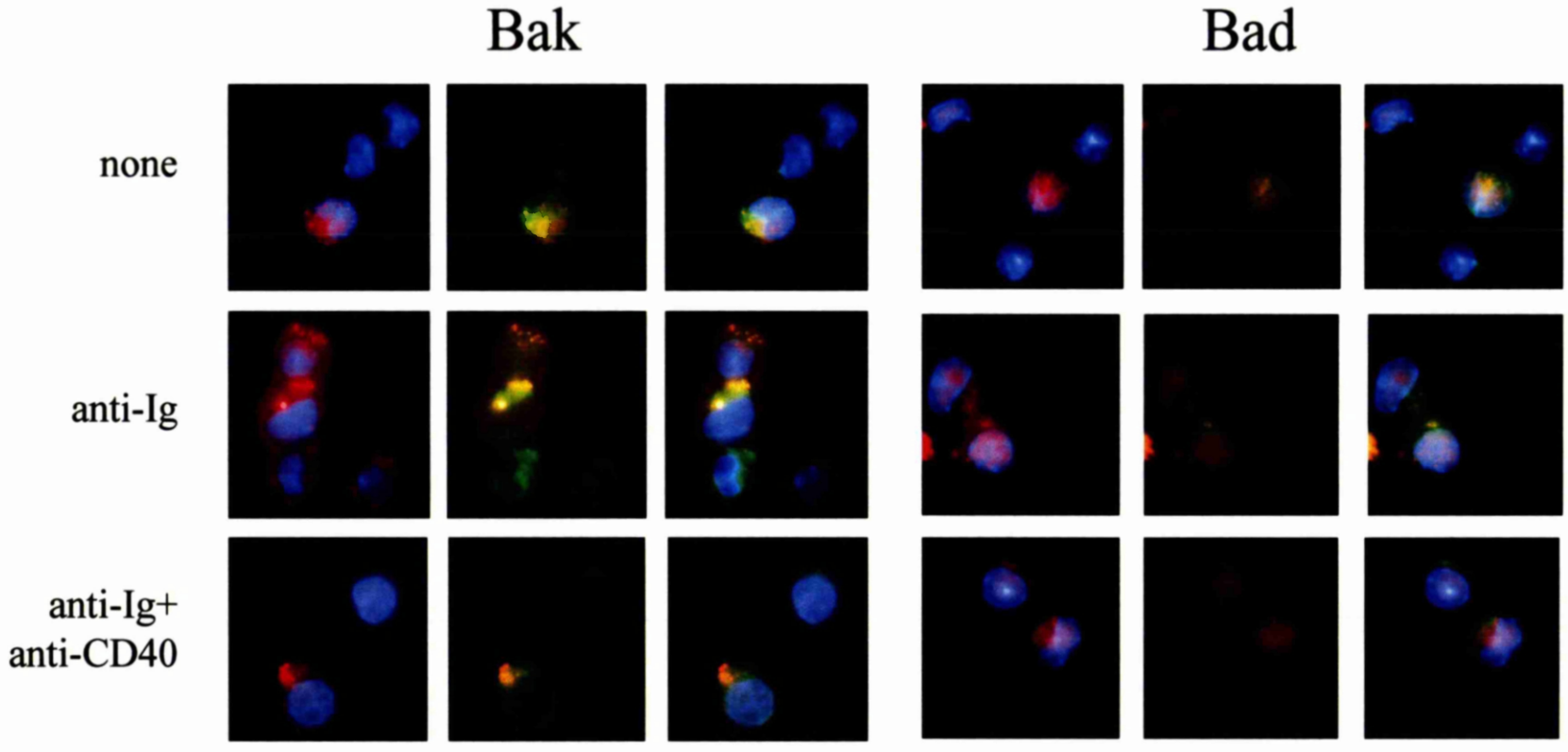
Bak
Bad
none
anti-Ig
anti-Ig+
anti-CD40

Figure 27: Expression and mitochondrial translocation of pro-apoptotic Bcl-2 proteins. WEHI-231 cells (10^6 per sample) were stimulated with media, anti-Ig (10μg/ml) or anti-Ig+anti-CD40 (10μg/ml) for 3h and then were subjected to intracellular staining as described in *Materials and Methods*. For the detection of Bid or Bad, anti-goat-biotin and streptavidin-Texas Red were used. For the detection of Bax or Bak, anti-mouse-gamma-chain-biotin and streptavidin-Texas Red were used. For mitochondria staining in Bad and Bak samples MitoTracker Green was used. For Bid and Bax samples, anti-ANT and anti-rabbit-FITC were used for mitochondria staining.
In each set of panels, the cell nucleus is stained blue (DAPI), the protein (Bad, Bak, Bax or Bid) in red and mitochondria is green. The left panel shows nucleus plus protein, the middle panel mitochondria plus protein and the right panel all colours superimposed.

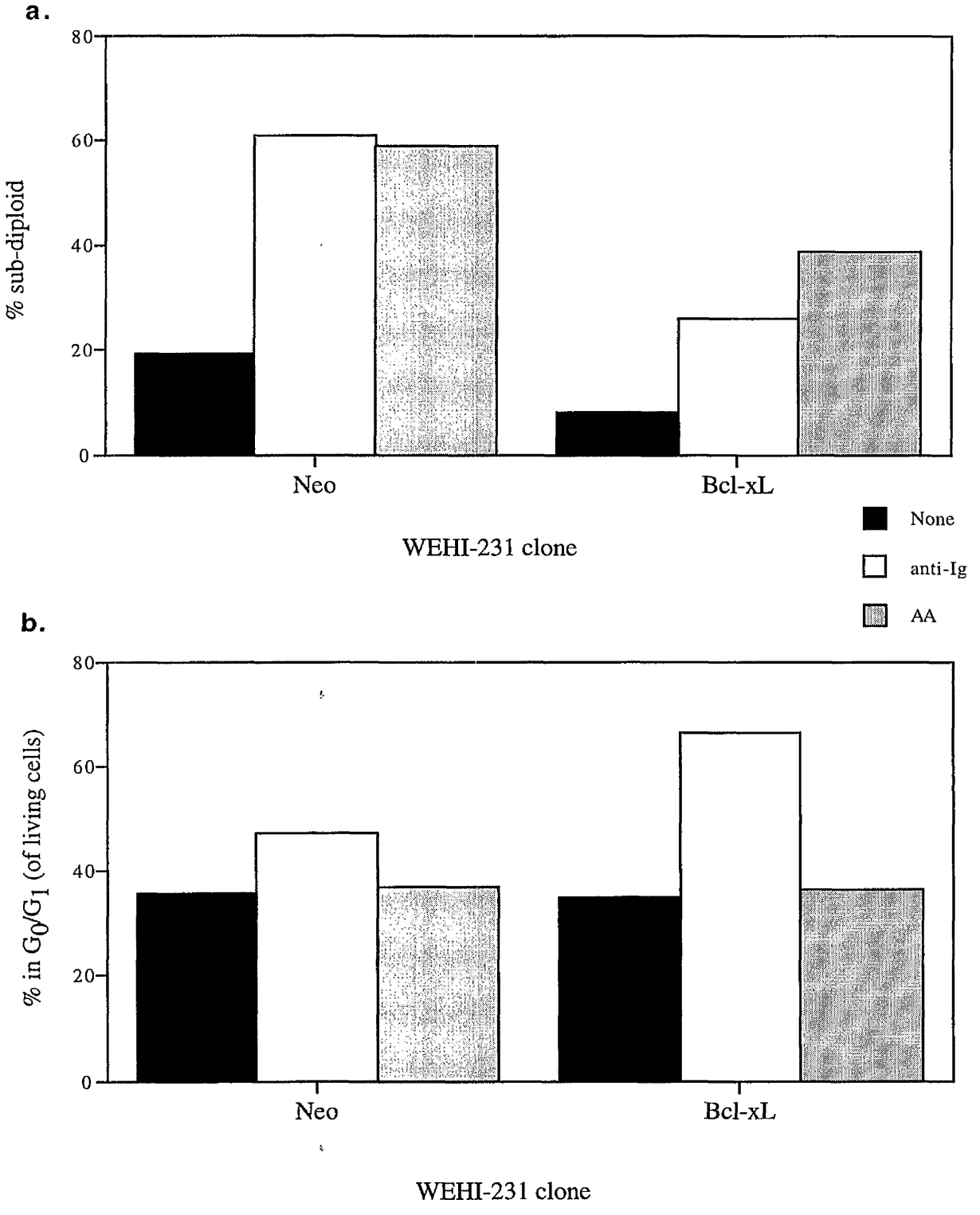
a.
80
60
40
20
0
% sub-diploid
Neo
Bcl-xL
WEHI-231 clone
None
anti-Ig
AA
b.
80
60
40
20
0
% in G0/G1 (of living cells)
Neo
Bcl-xL
WEHI-231 clone

Fig. 28

Figure 28: Bcl-x_L over-expression blocks BCR- and AA-induced apoptosis in WEHI-231 cells. WEHI-231-neo and WEHI-231-Bcl-x_L cells were treated with media, anti-IgM (10µg/ml) or AA (100µM) for 48h. DNA content was measured by PI incorporation. (a) % of sub-diploid cells was determined as the <2N DNA population. (b) % of cells in G_0/G_1 are shown as calculated from the ≥2N DNA population.

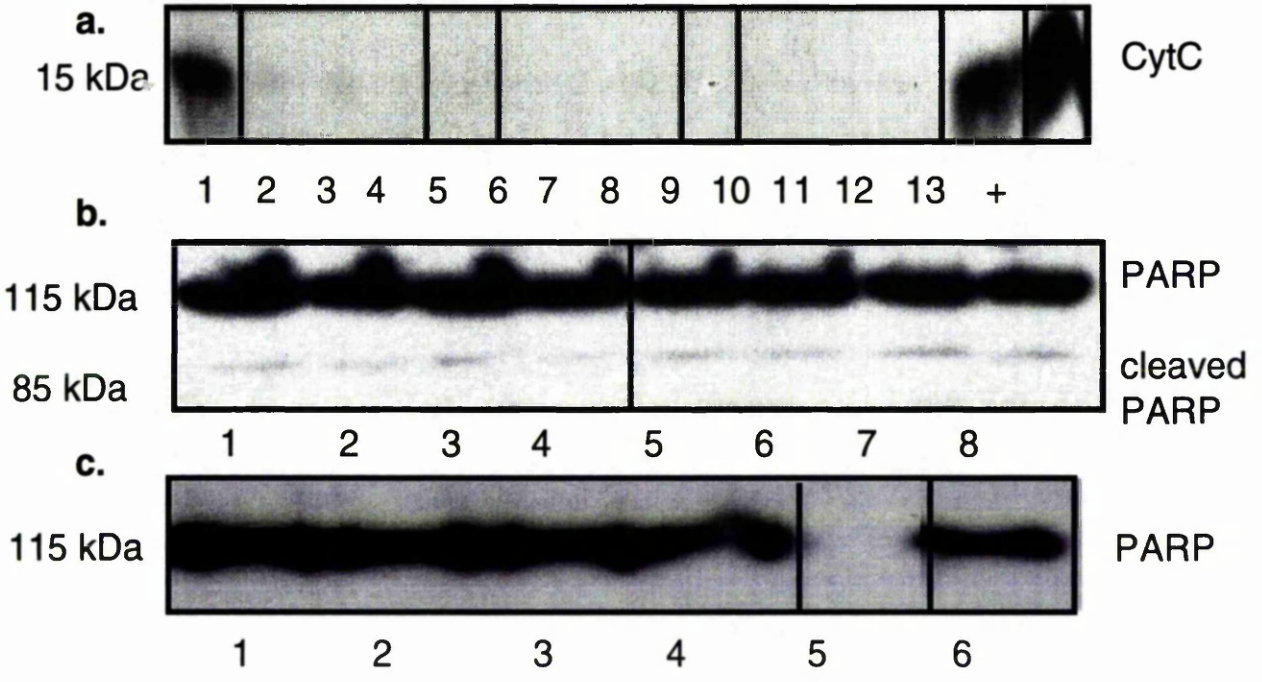
a.
15 kDa
CytC
1 2 3 4 5 6 7 8 9 10 11 12 13 +
b.
115 kDa
85 kDa
PARP
cleaved PARP
1 2 3 4 5 6 7 8
c.
115 kDa
PARP
1 2 3 4 5 6

Fig. 29

Figure 29: Anti-Ig does not induce mitochondrial release of cytochrome C nor PARP cleavage in WEHI-231 B cells. Mitochondrial release of cytochrome C was assessed by Western Blot analysis of whole cell lysate and mitochondria-free fractions of WEHI-231 B cells (panel a). WEHI 231 cells were incubated with media (lanes 5 and 9), 10μg/ml anti-IgM (lanes 2, 6 and 10), 10μg/ml anti-CD40 (lanes 3, 7 and 11) or a combination of these stimuli (lanes 4, 8 and 12) for 8 hours (lanes 2-4), 24 hours (lanes 5-8) or 48 hours (lanes 9-12). Lanes 1 and 13 are whole cell lysates of untreated WEHI 231 cells at 0 and 48 hours, respectively. Lanes 2-12 are mitochondria-free extracts prepared as described in *Materials and Methods*. (lane +) represents purified cytochrome C (from chicken). Effector Caspase activation as assessed by PARP cleavage was determined WEHI 231 cells (b and c). In panel b, WEHI-231 B cells were incubated with 10μg/ml anti-IgM (lanes 2 and 5), 10μg/ml anti-CD40 (lanes 3 and 6) or a combination of these stimuli (lanes 4 and 7) for 24 hours (lanes 2-4) or 48 hours (lanes 5-7). Lanes 1 and 8 are untreated WEHI 231 cells at 0 and 48 hours, respectively. In panel c, WEHI-231 cells were treated for 48 h with media (lane 1), anti-Ig (10μg/ml; lane 2), anti-CD40 (10μg/ml; lane 3), anti-Ig plus anti-CD40 (lane 4), C_2-ceramide (25μM; lane 5) and arachidonic acid (25μM; lane 6). All experiments are single experiments representative of at least two other independent experiments.

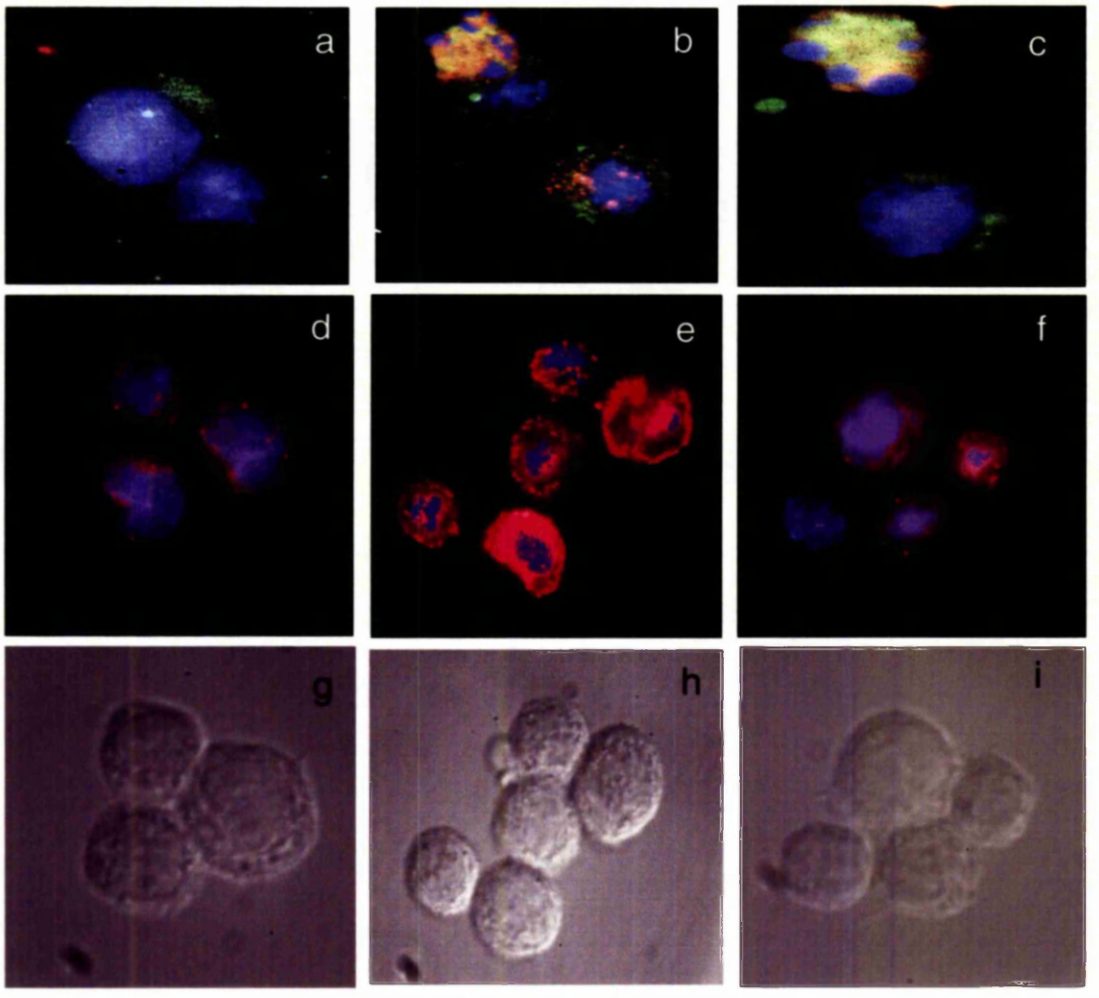
a
b
c
d
e
f
g
h
i
None 24 h
Ceramide 24 h
anti-Ig 24 h
j
k
l
Ceramide 5 h
Ceramide 24 h
anti-Ig 24 h

Figure 30: *In situ* analysis of mitochondrial release of cytochrome C and consequent PARP cleavage. The cell nucleus is stained blue (DAPI), cytochrome C is red (panels a-c), cleaved PARP is red (panels d-f & j-l) and mitochondria are green (rhodamine 123). Cytochrome C: In unstimulated (panel a) or anti-Ig (panel c)-treated WEHI-231 cells, there is little or no release of cytochrome C from the mitochondria (yellow) even when commitment to apoptosis has progressed sufficiently to generate apoptotic nuclei (panel c). In contrast, treatment with ceramide induces strong release (red) of cytochrome C. Cleaved PARP: In unstimulated (panel d) or anti-Ig (panel f) WEHI-231 cells, there is little or no cleaved PARP (red) present. In contrast, treatment with ceramide induces strong cleavage (red; panel e) of PARP. Bright field visualisation of these cells is given in panels g-i. A time course (panels j-l) shows that there is no PARP cleavage induced by ceramide within 5 h (panel j) and no PARP cleavage can be seen in anti-Ig-treated cells even when commitment to apotosis has progressed as far as the generation of apoptotic nuclei (panel l). In contrast, in ceramide-treated cells cleaved PARP (red) is easily detected in such cells (panel k).
panels a-c: staining of nucleus (DAPI; blue), cytochrome C (texas red) and mitochondria (rhodamine 123, green); panel d-f: nucleus (blue) and cleaved PARP (Texas red) ; panels g-h: bright field; panels j-l: staining of nucleus (DAPI; blue), cleaved PARP (Texas red) and mitochondria (rhodamine 123, green).

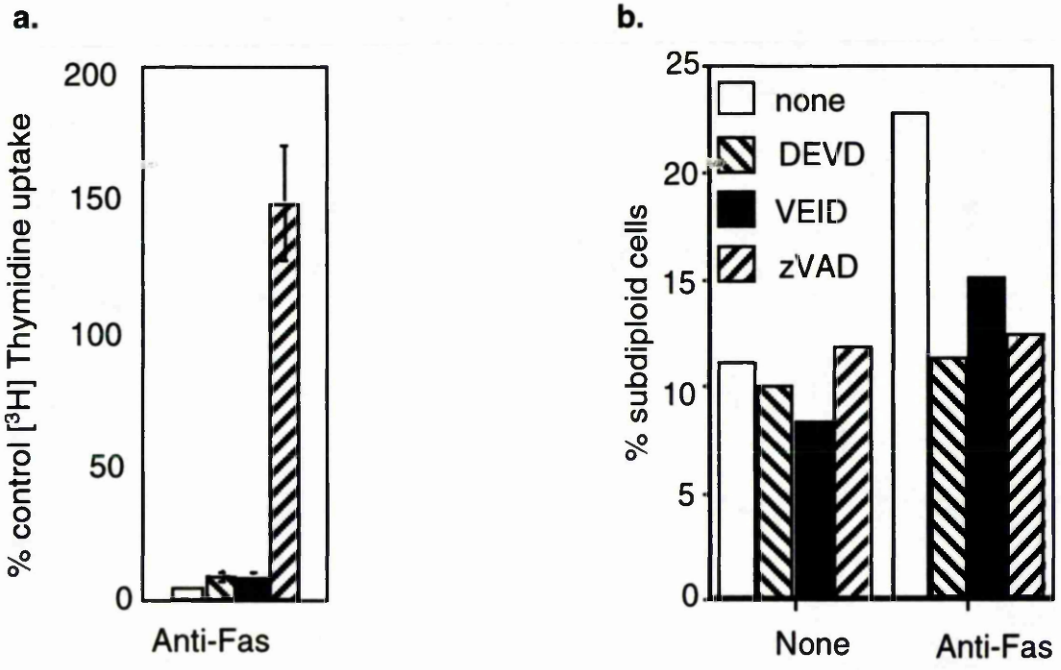
a.
% control [3H] Thymidine uptake
200
150
100
50
0
Anti-Fas
b.
% subdiploid cells
25
20
15
10
5
0
none
DEVD
VEID
zVAD
None
Anti-Fas

Fig. 31

Figure 31: Caspase inhibitors relieve anti-Fas-induced growth arrest and apoptosis in Jurkat T cells. Jurkat T cells were induced to undergo growth arrest by the anti-Fas (62.5 ng/ml) in the presence or absence of Caspase inhibitors and levels of [^{3}H]-Thymidine incorporation measured. The data (means ± SD, *n=3*) in panel a have been normalised with control unstimulated cells expressed as 100%. In panel b, Jurkat cells were treated with Caspase inhibitors with or without anti-Fas and apoptosis (subdiploid DNA content) assessed by propidium iodide staining. All data are from single experiments representative of at least two other independent experiments.

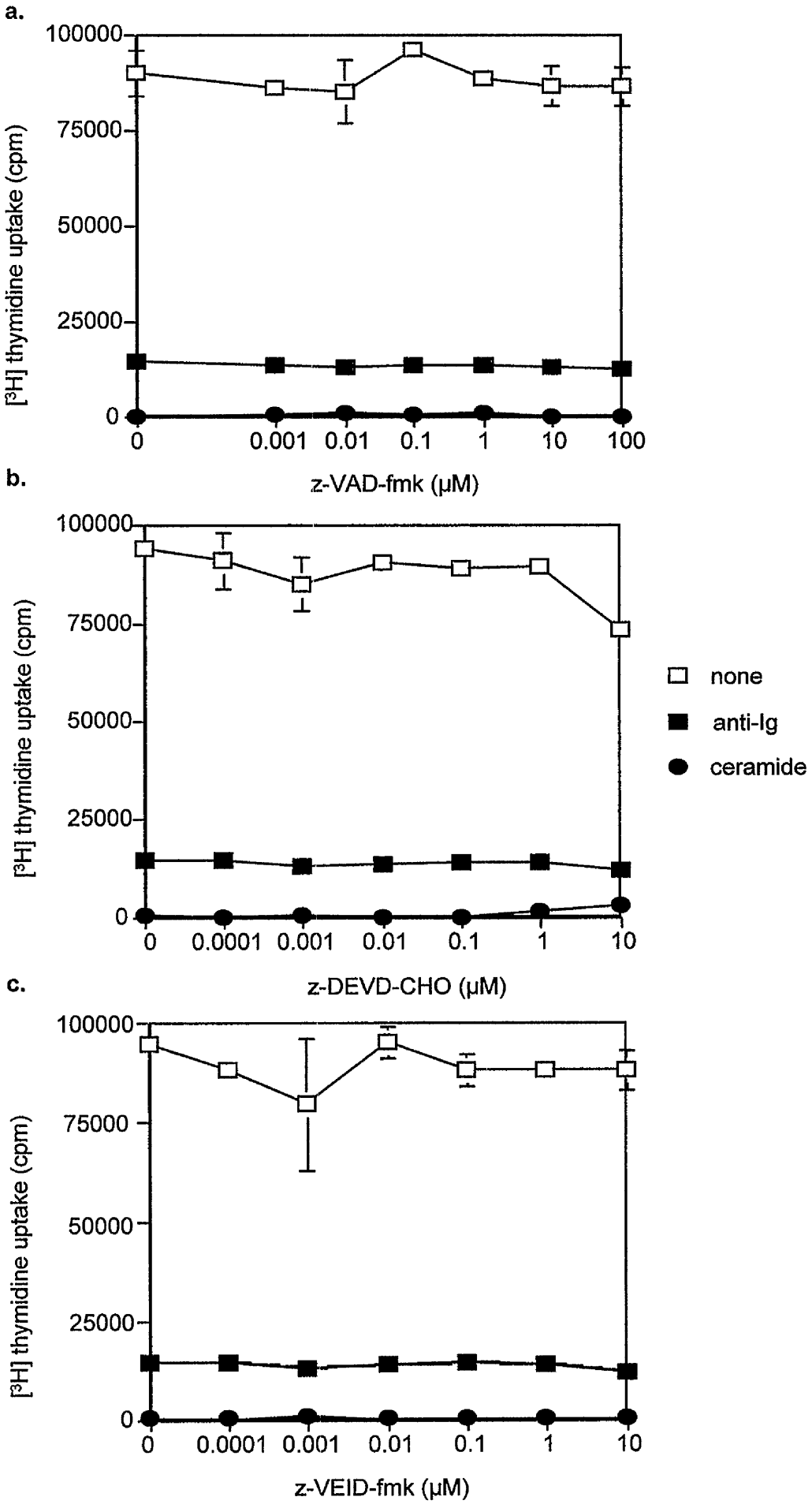
a.
100000
75000
50000
25000
0
[³H] thymidine uptake (cpm)
0
0.001
0.01
0.1
1
10
100
z-VAD-fmk (μM)
b.
100000
75000
50000
25000
0
[³H] thymidine uptake (cpm)
0
0.0001
0.001
0.01
0.1
1
10
z-DEVD-CHO (μM)
none
anti-Ig
ceramide
c.
100000
75000
50000
25000
0
[³H] thymidine uptake (cpm)
0
0.0001
0.001
0.01
0.1
1
10
z-VEID-fmk (μM)

Fig. 32

Figure 32: Caspase inhibitors do not block anti-Ig-mediated growth arrest in WEHI-231 cells. WEHI-231 immature B cells were induced to undergo growth arrest by anti-Ig (10μg/ml) or C_2-ceramide (25μM) in the presence or absence of Caspase inhibitors and levels of [^{3}H]-Thymidine incorporation measured (means ± SD, *n=3*) ng/ml).

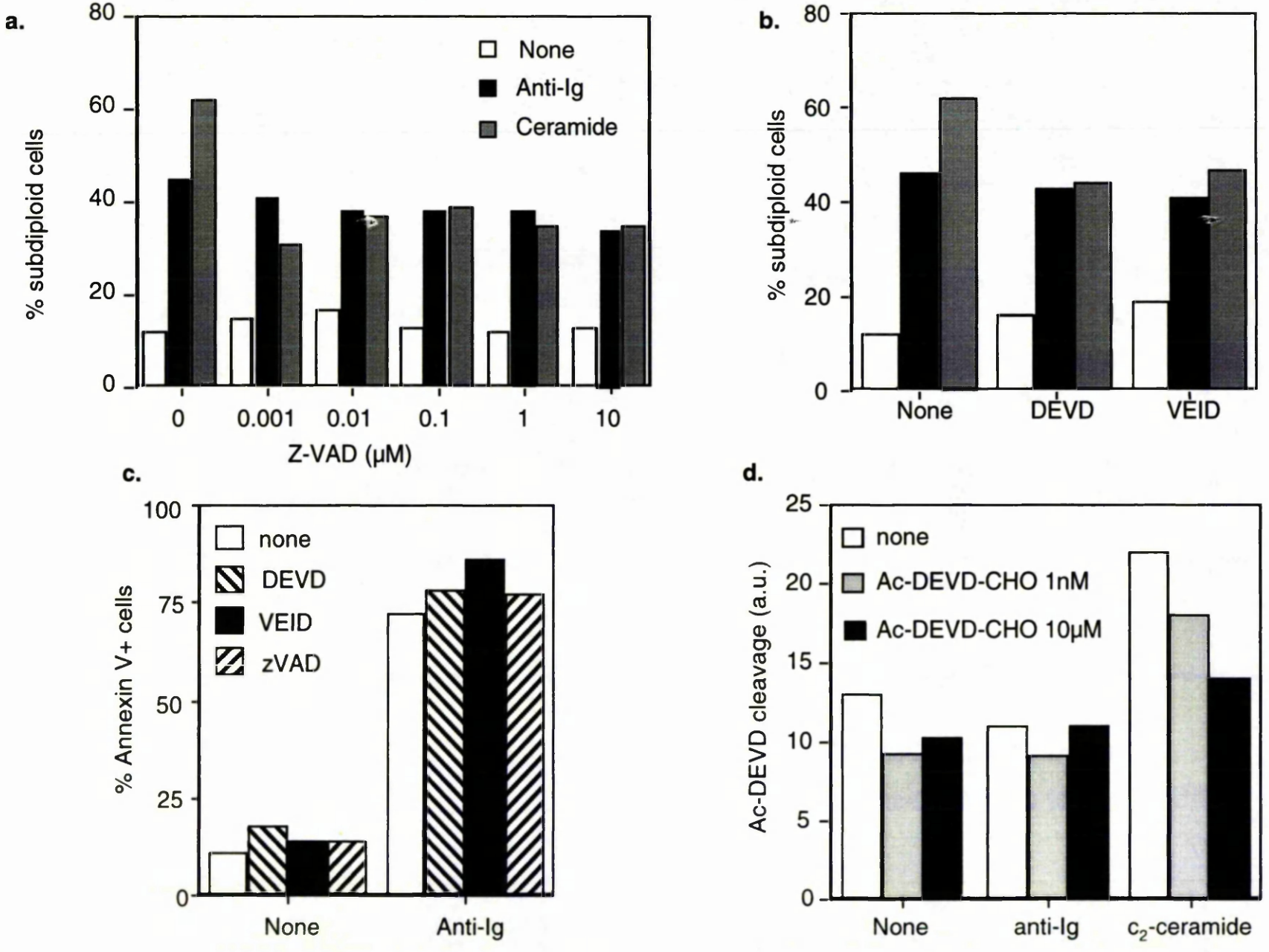
a.
% subdiploid cells
80
60
40
20
0
None
Anti-Ig
Ceramide
0
0.001
0.01
0.1
1
10
Z-VAD (μM)
b.
% subdiploid cells
80
60
40
20
0
None
DEVD
VEID
c.
% Annexin V+ cells
100
75
50
25
0
none
DEVD
VEID
zVAD
None
Anti-Ig
d.
Ac-DEVD cleavage (a.u.)
25
20
15
10
5
0
none
Ac-DEVD-CHO 1nM
Ac-DEVD-CHO 10μM
None
anti-Ig
c2-ceramide

Fig. 33

Figure 33: Caspase inhibitors do not block anti-Ig-mediated apoptosis but do relieve ceramide-induced apoptosis in WEHI-231 B cells. In panels a & b, WEHI-231 B cells were cultured with media or anti-Ig (10μg/ml) or ceramide (25μM) for 48h in the presence and absence of the indicated concentration of z-VAD-fmk (panel a) or 100pM Ac-DEVD-CHO or 10μM z-VEID-fmk (panel b) before assessing DNA content (PI staining, panels a & b). In panel c, WEHI-231 B cells were cultured with media or anti-Ig (10μg/ml) for 48h in the presence and absence of of 10μM z-VAD-fmk or 2nM Ac-DEVD-CHO or 100nM z-VEID-fmk (panel b) before staining with Annexin V. In panel d, WEHI-231 B cells were incubated with media, anti-Ig (10μg/ml) or ceramide (25μM) in the presence or absence of the Caspase 3 inhibitor, Ac-DEVD-CHO (1nM or 10μM) for 24h and cell lysates prepared. Caspase 3 activity as evidenced by the cleavage of the Caspase-3 substrate, Ac-DEVD-*p*Na (N-Acetyl-Asp-Glu-Val-Asp-*p*NA) was then assayed as described in *Materials and Methods*. All data are from single experiments representative of at least two other independent experiments.

Inhibitor (concentration)	**Target Proteases**	**Sub-diploidity**	**Growth arrest**	$\Delta\psi_m$
Chymostatin (100ng/ml)	Serine/Cysteine	⇓	⇔	ND
E64d (10μM)	Cathepsins (Cysteine)	⇓	⇔	⇔
TLCK (100μM)	Serine (Trypsin-like)	⇓	⇓	⇑
TPCK (100μM)	Serine (Chymotrypsin-like)	⇑	⇓	ND
zVAD-fmk (100μM)	Caspases (Cysteine)	⇓	⇑	⇑

Table 2: Summary of the effects of different protease inhibitors on the progress of apoptosis in WEHI-231 cells. ⇔ - incdicates no change observed; ⇑ - a reduction; ⇓ - an increase; and ND - not done. In $\Delta\Psi_m$ values, an increase means proportionaly less cells in low mitochondrial potential.

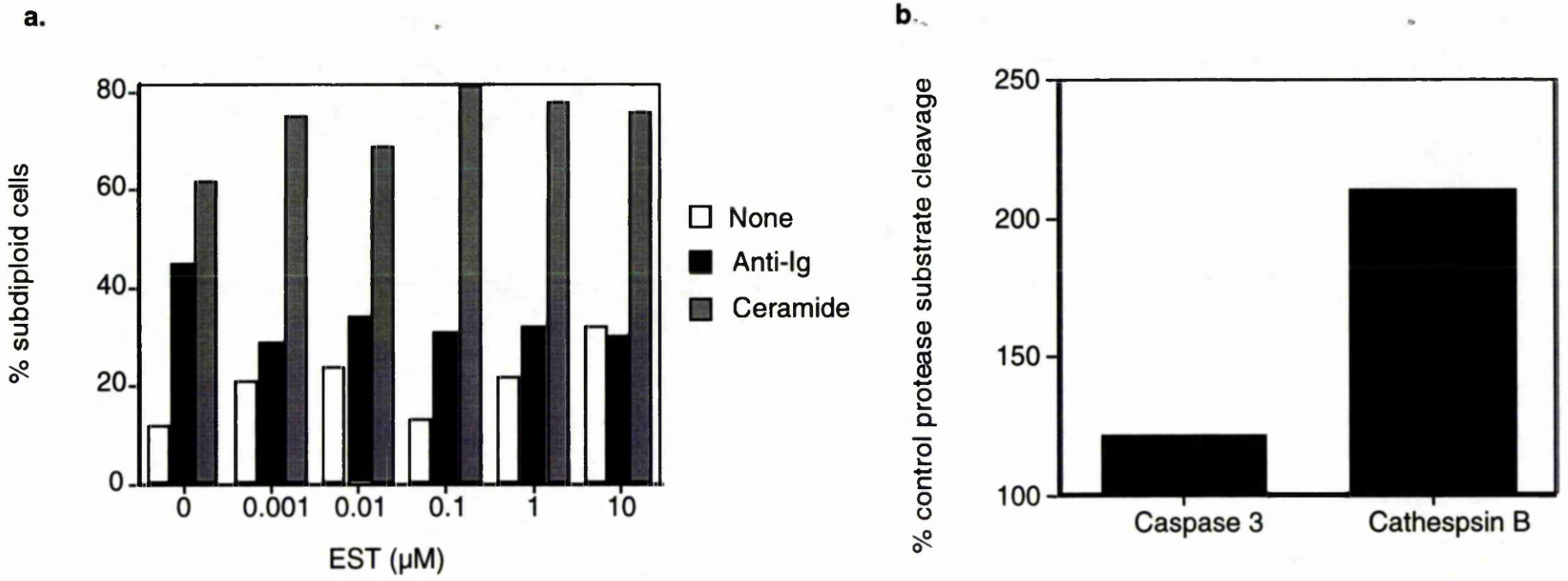
a.
% subdiploid cells
80
60
40
20
0
0
0.001
0.01
0.1
1
10
EST (μM)
None
Anti-Ig
Ceramide
b.
% control protease substrate cleavage
250
200
150
100
Caspase 3
Cathespsin B

Fig. 34

Figure 34: Anti-Ig-stimulates the post-mitochondrial activation of cathepsin B and the cathepsin B inhibitor, EST blocks BCR-driven apoptosis in WEHI-231 B cells. WEHI-231 immature B cells were induced to undergo apoptosis by anti-Ig (10μg/ml) or C_2-ceramide (25μM) in the presence or absence of the indicated concentrations of EST and the levels of subdiploid DNA content measured (panel a). In panel b, WEHI-231 B cells were incubated with anti-Ig (10μg/ml) for 24h and cell lysates prepared. Caspase-3 and Cathepsin B activity as evidenced by cleavage of the Caspase-3 substrate, Ac-DEVD-*p*Na (N-Acetyl-Asp-Glu-Val-Asp- *p*NA) or the cathepsin B substrate, zRR-*p*NA (z-Arg-Arg- *p*NA) was then assayed as described in *Materials and Methods*.

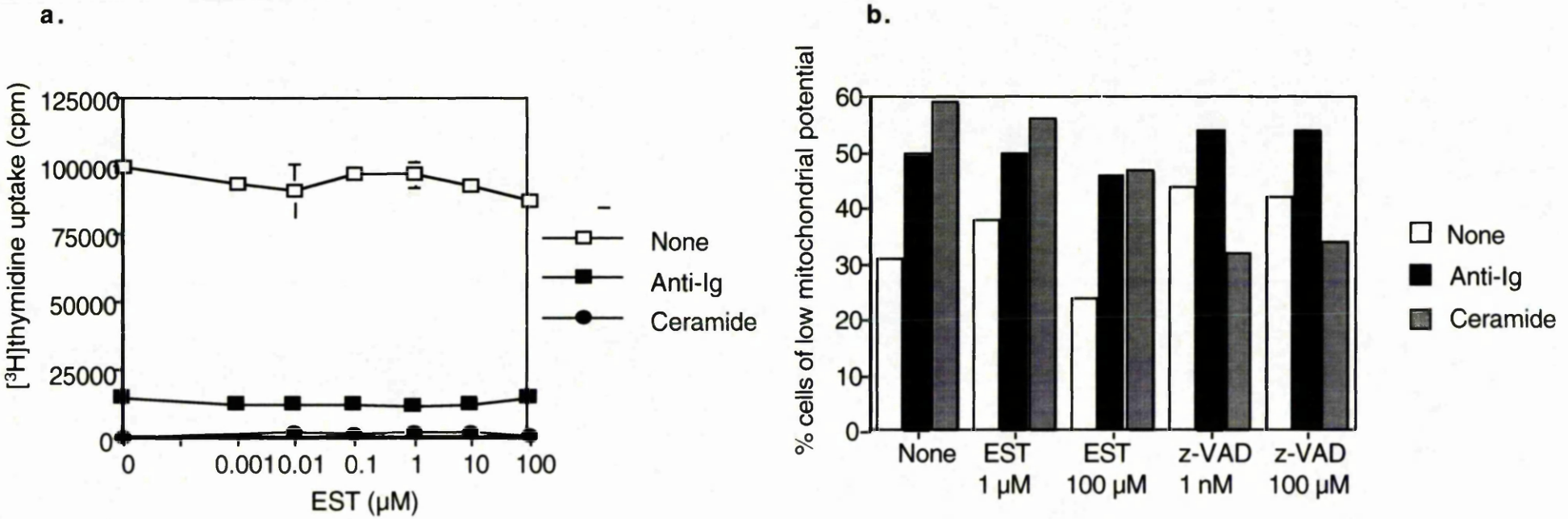
a.
[3H]thymidine uptake (cpm)
125000
100000
75000
50000
25000
0
0
0.001
0.01
0.1
1
10
100
EST (μM)
None
Anti-Ig
Ceramide
b.
% cells of low mitochondrial potential
60
50
40
30
20
10
0
None
EST 1 μM
EST 100 μM
z-VAD 1 nM
z-VAD 100 μM
None
Anti-Ig
Ceramide

Fig. 35

Figure 35: The cathepsin B inhibitor, EST does not BCR-driven growth arrest or mitochondrial potential depolarisation in WEHI-231 B cells. In panel a, WEHI-231 B cells were cultured with media or anti-Ig (10 μg/ml) or C_2-ceramide (25μM) for 48h in the presence and absence of the indicated concentrations of EST before assessing growth arrest as indicated by the level of [^{3}H]thymidine uptake. In panel b, WEHI-231 B cells were cultured with media, anti-Ig (10μg/ml) or C_2-ceramide (25μM) for 48h in the presence and absence of the indicated concentrations of EST or z-VAD-fmk before assessing the resulting level of mitochondrial potential by $DiOC_6$ staining as described in *Methods*.

a.
none
anti-CD40
IL-4
anti-Ig
anti-Ig+ anti-CD40
anti-Ig+ IL-4
b.
none
anti-Ig
IL-4
anti-CD40
anti-Ig+ anti-CD40
c.
none
anti-Ig
IL-4
anti-CD40
anti-Ig+ anti-CD40
+
d.
none
anti-CD40
IL-4
anti-Ig
anti-Ig+ anti-CD40
AA+ anti-CD40
e.
none
anti-Ig
anti-CD40
AA
anti-Ig+ anti-CD40
AA+ anti-CD40

Fig. 36

Figure 36: The p53 network in apoptosis and rescue of WEHI-231 cells. WEHI-231 cells (10^7 per sample) were stimulated as follows for 24h with the following treatments: none; anti-CD40 (10µg/ml); IL-4 (10U/ml); anti-Ig (5µg/ml); anti-Ig+anti-CD40; anti-Ig+IL-4; AA (25µM); AA+anti-CD40; +: positive (macrophage lysate). At the end of the stimulation cells were lysed and Western blotting was preformed as descibed in *Material and Methods*with the appropriate antibodies: (a) anti-p53; (b) anti-Mdm2; (c) anti-p16; (d) anti-Rb; (e) anti-p130. Arrows in panels a and d indicate the multiple phosphorylation states of p53 and Rb. Lower arrow in panel b indicate Mdm2 and upper arrow indicate possible Mdm2:p53 complexes.

Chapter 4. *EX VIVO* DEVELOPMENT OF WHOLE BONE MARROW CULTURES

4.1 Introduction

The question of how immature B cells are selected in the bone marrow has been addressed in many different ways, using both cell line models [286, 301] and by observing what happens *in vivo* [8, 12]. To date, there is no agreement how this selection proceeds and what are the limiting factors of the selection process (reviewed in [6, 11, 135]). The discovery of a transitional state between immature and mature B cells [8] has suggested that these are in fact the cells in which selection occurs. Again, this aspect of B cell development is unclear and there is some evidence that the majority of transitional B cells migrate to the periphery before their selection [12].

Previous studies have employed several biochemical and genetic approaches in order to investigate different features of the crucial selection steps of B cell development.

Biochemical approaches have been taken mainly where it has been possible to employ model systems. The most commonly used models are:

(i) Cell lines, such as WEHI-231 cells, which are of an immature (IgM^+ IgD^-) B cell phenotype. This approach has achieved many insights into the signals involved in the deletion and rescue of immature B cells, as discussed in chapter 1. Cell line models are unsatisfactory, though, in some ways. For example, there is difficulty interpreting the role of cell cycle related events as these may be different from the situation *in vivo*, due to the constant cell proliferation of the cell lines. Moreover, these cell lines are usually fixed at a particular stage of maturation with no ability to develop further.

(ii) Repopulation studies where spleens of sub-lethally irradiated mice were used to examine relatively immature transitional B cells in large numbers. This is essentially an artificial process to gain access to transitional B cells, through the gradual repopulation of the periphery with newly produced B cells, a process which occurs naturally in the

neonatal animal. This technique has been very sucessful in identifying different types of transitional cells and their susceptability to cell death (see for example: [12]).

Completing these model systems, two genetic approaches have been widely used to identify the key molecules involved in B cell selection:

(i) Construction of transgenic mice which bear a relatively higher proportion of B cells specific to a known antigen. Studies in specific BCR transgenic mice have contributed to the understanding of the balance between deletion, anergy and receptor editing of immature/transitional B cells in the bone marrow [3].

(ii) A variety of knock-out mice and naturally occuring immunodeficient mice. These mice have enabled genetic analysis of B cell receptor signalling during development and have established role for tyrosine kinases (Btk, Syk) and other factors such as Igα, in transitional B cell selection (reviewed in [37]).

There were two main reasons to devise an alternative *in vitro/ex vivo* model system for B cell development in the bone marrow: (i) to find a way to investigate the signals required for B cell development in an environment closely resembling the bone marrow *in vivo*; (ii) to gain insight into the nature of BCR signals involved in bone marrow derived cells, without the compromises involved in working with cell lines.

In the system devised, the stimulated cultures included all the haemopoietic and stromal cells in the bone marrow, allowing the normal micro-environment to be kept as close as possible to the situation *in vivo*. Subsequent observations showed that although many cells die within a few hours of culture, the remaining population is stable for at least 3 days. Even after 48h in culture about 75% of these cells survive, a percentage which exceeds the rate of survival of other primary B cell populations cultured *in vitro*. This stability is presumably achieved by cell-cell interactions and continuing secretion of IL-7 by different cell types, such as stromal cells [302, 303]. Importantly, in this *ex vivo* experimental system, immature B cells do not seem to die of neglect. In fact, a small proportion (~5%) of these cells spontaneously develop into transitional cells. Using *ex vivo* whole bone marrow cultures it is shown

here that polyclonal stimulation of the BCR using anti-Ig is sufficient to drive positive selection of immature B cell into phenotypically mature (kappa^{hi} delta^{hi}) B cells.

4.2 Polyclonal activation of immature B cells leads to positive selection and development of mature B cells

The bone marrow population of mice contains few kappa chain positive B cells. However, the most abundant kappa^{+} B cell population, which consists typically of around 5-15% of the whole bone marrow cell population, is that of immature B cells (kappa^{lo} delta^{-}). In some mouse strains, the transitional B cell population (kappa^{lo} delta^{lo}) is also apparent. In Balb/c mice, which were used in most of the experiments described below, this population usually comprises not more than 5% of the whole bone marrow. In some cases, a small population (<1%) of mature cells (kappa^{hi} delta^{hi}) could be also detected. Some plasma B cells are also present in the bone marrow [304]. Due to their very low percentage and obscure role in B cell development, it was decided not to investigate these cells.

Two concentrations of anti-Ig were chosen to stimulate the BCR of immature and transitional cells *ex vivo*. In peripheral B cells, a concentration of 5µg/ml functions as a survival signal, whilst high dose of 50µg/ml stimulates mature B cells to proliferate (see section 5.4). Furthermore, it was previously suggested that the strength of BCR signal can determine which cell fate decision will be taken [138].

As B220 expression was reported to be upregulated gradually in the progression of B cells from immature to transitional to mature cells, in initial experiments B220 expression was used to identify B cell phenotype. Previous reports differentiated between these populations according to B220 expression and cell size [8]. In practice, though, only B220^{lo} and B220^{hi} populations could be clearly discriminated (fig. 37a). This preliminary experiment showed, that as reported elsewhere [8], that the B220^{lo} population (which contains pre-B, pro-B and immature B

cells) can undergo apoptosis in response to BCR stimulation (fig. 37b). The $B220^{hi}$ population, in contrast, appears to expand through enhanced proliferation (cf. 17% of untreated cells in S, G_2 and M phases, 29% with 5µg/ml anti-Ig and 21% with 50µg/ml anti-Ig). This detection method could not distinguish between transitional B cells and other sub-populations. Hence, it was hard to resolve which B cell population was being selected and allowed to proliferate. Therefore, a different approach for distinction of the B cell populations had to be established.

In order to discriminate better between the immature, transitional and mature B cells, double staining for kappa (for both IgM and IgD) and delta (for IgD) chains was employed. Kappa chain was chosen because its expression is restricted to B cell populations from the immature B cell stage onwards, while the mu chain is already expressed as part of the pre-BCR [305].

Using this staining method it was observed that high concentration (50µg/ml) of anti-Ig clearly drives cells from the immature state ($kappa^+$ $delta^-$) to mature cells ($kappa^{hi}$ $delta^{hi}$; fig. 38) [6]. The lower dose of anti-Ig (5µg/ml) was sufficient to drive development to transitional B cells, but not to mature cells, suggesting that this process is dose dependent. Using flow cytometry staining together with cell counting at the end of the stimulation, it was possible to estimate how many cells survive the BCR stimulation and develop and/or proliferate (fig. 39). With both doses of anti-Ig, the $kappa^+$ B cell population was reduced almost to the same extent: ~40% of control at 5µg/ml and about 30% at 50µg/ml. Furthermore, the number of immature B cells was reduced substantially as well: they were about 25% of control in 5µg/ml anti-Ig and ~15% of control in 50µg/ml anti-Ig. In both cases, the expansion of transitional cells was similar in response to both doses of anti-Ig: 2.5- to 3-fold. Taken together, these data suggest that even a low dose of anti-Ig is sufficient to drive immature B cells into transitional state. This might be most easily explained by the change in the ratio of immature to transitional cells: in a typical experiment this ratio stands at approximately 17:1 in cells which have simply been cultured with media. A low dose of anti-Ig improves this ratio ten-fold (to about 2:1) and a high dose almost equalises the numbers of immature and transitional B cells in the

culture. The identification of kappa^{lo} delta^{lo} cells as transitional cells was supported by parallel experiments where the induction of transitional B cells alone (i.e., 5µg/ml anti-Ig treatment) produced the highest numbers of kappa^{+} CD44^{hi} (fig. 40) and kappa^{+} Fas^{+} cells (see below). These data correlate with earlier observations which documented the transitional B cells as uniquely expressing these markers, within the kappa^{+} B cell population [8]. Furthermore, an increase in RAG-1 expression in kappa+ B cells was detectable within 4h of anti-Ig (50µg/ml) treatment, indicating, that *ex vivo* stimualtion can also induce receptor editing (fig. 41).

Negative selection of B cells is proposed to occur during the development of transitional B cells to mature cells [8]. Consistent with this, a massive increase in the number of apoptotic cells was observed following treatment with 50µg/ml anti-Ig, as measured by DNA content (fig. 42). Nonetheless, the surviving cells developed into mature B cells, to comprise about 15% of the kappa^{+} population (*n=5*), in comparison to less than 5% in control and 5µg/ml anti-Ig treated bone marrow cultures. Depletion of IgD^{hi} cells (mature B cells) on a magnetic column did not affect the phenomena described here (not shown). Hence, this IgD depletion excluded the formal possibility of emergence of mature B cell population solely due to its proliferation in culture in response to anti-Ig stimulation.

T cell help in the periphery, as demonstrated here by CD40 ligation, can not overcome the checkpoint barrier in the development of transitional B cells. At all stages checked, 5µg/ml anti-Ig plus 10µg/ml anti-CD40 treatment, which is co-mitogenic in mature B cells, did not enhance B cell development further than 5µg/ml anti-Ig alone, which caused progression into transitional B cells. Moreover, anti-CD40 treatment alone has no positive effect on these bone marrow cultures and for unknown reasons causes wide-spread death in all populations (not shown). The observation that mature B cells, which developed in the *ex-vivo* bone marrow set-up, undergo apoptosis (fig. 43), may suggest that T cell help is needed at this stage for mature B cell survival. Gain of IgD is widely acknowledged to enable B cells to migrate to the periphery [17] and therefore it may not be surprising that mature B cells were not able

to proliferate in an *ex vivo* bone marrow to the same extent as in the periphery *in vivo* (fig. 44). This may indicate a limitation of tissue-restricted cultures, although the precise reason for this is unknown.

4.3 Fas participates in transitional but not immature B cell deletion

Previous observations suggested that Fas-induced death was important for the regulation of maturation of B cells in the bone marrow [8, 302], although direct deletion by FasL was not reported. In order to verify the role of Fas using the *ex vivo* system, two approaches were used.

Firstly, cells were stained for both kappa chain and Fas simultaneously. The numbers of Fas^+ $kappa^+$ cells were reduced considerably with anti-Ig treatment, in a dose dependent manner. Nonetheless, the prevalence of Fas expression within the $kappa^+$ B cell population correlated with the induction of transitional B cells, by 5µg/ml anti-Ig treatment (fig. 45). Susceptibility to Fas was suggested as a unique feature of transitional B cells [8], but it is only in this model system that it has been shown, for the first time, that they can be deleted *in vitro* by anti-Fas treatment (fig. 46). Moreover, the numbers of $kappa^{hi}$ Fas^+ cells were reduced with 50µg/ml anti-Ig treatment to a lesser extent than 5µg/ml anti-Ig (cf. 73% and 26% of control, respectively). The preferential deletion of $kappa^{lo}$ cells suggests that BCR stimulation causes indirect Fas-induced cell death of these cells.

Secondly, the significance of Fas during B cell development was examined by utilising *lpr* transgenic mice. These mice are $Fas^{-/-}$ and have widely reported defects in their immune system, including B cell development, resulting in the production of autoantibodies [306, 307]. However, in the *ex vivo* bone marrow cultures, at first sight, anti-Ig treatment induced a similar profile of maturation to that observed in WT strains (fig. 47). The overall survival rate of kappa chain positive B cells after treatment with anti-Ig was similar to the WT average (73% of $kappa^+$ cells in control) and a similar proportion of $kappa^+$ cells was found to mature (14% of $kappa^+$ B cells). Nonetheless, a closer examination

revealed some important differences. When comparing this anti-Ig driven development to observations in normal cells, it was apparent that Fas deficient kappa$^+$ B cells have a higher rate of development to mature cells (fig. 48). This enhanced selection process in the absence of Fas is not apparent overall because in parallel to accumulation of cells at the transitional stage, apoptosis in immature B cells is augmented (fig. 49). This enhancement in the apoptosis of immature B cells did not occur until the second day of stimulation and may reflect competition on an unidentified resource (such as IL-7). Combined treatment of anti-Ig plus anti-CD40 had different effects on *lpr* mice-drived bone marrow culture from normal cultures. In WT cultures this treatment leads to an increase in apoptosis rate of all cells, and especially transitional B cells (cf. 17% in treated cells and 9% in unstimulated transitional cells) and to a substantial increase in Fas expression on kappa$^+$ B cells (not shown). Surprisingly, in *lpr* cultures, the combined treatment results in the recovery of more immature and mature cells whilst the number of transitional B cells is kept as in control (fig. 50). This suggests that a Fas deficiency enables more cells to mature with anti-Ig plus anti-CD40. Although this treatment is still not as effective as high doses of anti-Ig, this may reflect a rescue scenario in which absence/blockage of Fas is needed for successful CD40 co-stimulation.

4.4 Deletion of immature and transitional B cells by self-antigen

In the bone marrow *ex vivo* model, a high dose of anti-Ig can drive immature B cells to develop into mature B cells. HEL-BCR transgenic mice were used to observe the response of immature B cells to a specific antigen. A large proportion of the B cells (50-70%) in these mice are specific for the chicken egg lysosyme (HEL) and they have been widely employed as a model system for investigating B cell tolerance in the periphery [15]. Here, these transgenic mice were used to test how exposure to soluble self antigen influences maturation of immature B cells in a *ex vivo* bone marrow cultures. The extent of response to self

antigen was suggested to determine whether B cell selection is essentially positive or negative. Exposure to polyclonal anti-Ig was effective in driving immature B cells into maturation in this system and the number of HEL^+ B cells was increased following this treatment, particularly with low dose of anti-Ig (fig. 51). Polyclonal anti-Ig stimulation simulation may, therefore, represent positive selection of B cells via a weak or low affinity signal, as suggested in other models [138]. In accordance with this theory, exposure to high concentrations of high affinity self-antigen (i.e. HEL) caused deletion and maturation of B cells. The low affinity self-antigen, the duck egg lysosyme (DEL) was even more effective than anti-Ig in driving B cells into maturation, similarly to low anti-Ig (fig. 52). It is important to note that this is not necessarily due to receptor editing, because absolute numbers of HEL^+ cells did not decrease due to DEL treatment (fig. 53). Fas expression correlated well with the extent of BCR stimulation, although numbers of apoptotic transitional B cells for high doses of either HEL or DEL were similar (fig. 54), possibly suggesting induction of anergy.

This evidence suggests that the crucial selection step may be in the transitional B cell stage, when a very strong BCR signal (such as the signal induced by HEL here) will lead to deletion. In order to verify this possibility, further experiments of two kinds are needed: first, determination of the number of cells in each $kappa^+$ B cell population after treatment with anti-Ig, HEL and DEL in a wide range of antigen concentrations. Second, determination of the number and nature (immature or transitional) of cells under these treatments which undergo receptor editing or apoptosis. This evidence can help in understanding to what extent B cell selection is dependent on antigen affinity and concentration.

4.5 Role for Btk in B cell selection

The tyrosine kinase Btk is an important mediator of BCR signalling. It is well documented that the *Xid* phenotype, which is deficient in Btk, has reduced numbers of B cells in the periphery and poor responses to BCR

stimulation [147]. Bone marrow cultures were used to examine the role of Btk in the maturation of B cells *ex vivo*. The Btk deficient phenotype is exclusive to the male population of these mice and therefore a direct comparison to wildtype (female) mice is possible.

The kappa$^+$ B cell population from Xid cultures showed surprisingly better rates of survival, relative to WT cultures, either when untreated or treated with 50µg/ml anti-Ig (~25% more kappa$^+$ cells in Xid cultures with either stimulus, than in wildtype cultures). Therefore the data is presented as fold change after 50µg/ml anti-Ig treatment, in comparison to the appropriate control (fig. 55). The absolute number of Btk$^{-/-}$ transitional B cells, as induced by anti-Ig, was also approximately 2 times the number in WT cells. This pattern in induction of the transitional stage, correlates with accumulation of Fas$^+$ cells (cf. 16% kappa$^+$ Fas$^+$ in Xid and 12% in littermates after 50µg/ml anti-Ig treatment), although without any significant increase in the apoptosis of these cells. In contrast and as expected, the number of mature cells was reduced by 3-fold in comparison to wild-type culture.

In conclusion, it seems that immature B cells are able to develop normally into transitional cells in the absence of Btk. Nonetheless, Btk appears to be essential for the development of transitional B cells into full maturity, as previously reported [308].

4.6 Involvement of the mitochondria in the selection of immature and transitional B cells

One of the most important events in the apoptotic cascade is the depolarisation of the mitochondrial potential. As discussed above in the WEHI-231 cell line model (section 3.3), this event is likely to be crucial for the generation of BCR apoptotic signal in immature B cells. Indeed, measurement of the mitochondrial potential has shown that it is reduced substantially by anti-Ig treatment (fig. 56). Furthermore, this reduction was specific for the kappa^{lo} population which reflects the immature and transitional B cells.

Changes in the mitochondrial potential are closely linked in many cases to initiation of the effector Caspase cascade. Therefore, it was of interest to determine the role of Caspases in BCR-induced apoptosis of immature B cells in the bone marrow, using the broad inhibitor Ac-DEVD-CHO, which blocks the activation of effector Caspases such as Caspase-3, -6 and -9. Although the addition of Ac-DEVD-CHO alone improved the overall survival of kappa$^+$ B cells in culture (not shown), inhibition of Caspase activity did not improve the ability of immature B cells to develop to mature cells (fig. 57a). Moreover, there was no reduction in the rates of cell death when cells treated with both anti-Ig and the inhibitor (fig. 57b). These results are in agreement with the observations in the WEHI-231 model, which suggest that other proteases such as Cathepsins may substitute for Caspases in immature B cell death (sections 3.8-9). In addition, Caspase inhibition alone did not cause a specific increase in the number of transitional B cells and this observation may suggest that Caspase activation in these cells is linked to their Fas susceptibility after BCR stimulation.

Other mitochondria-related events were described by others to be important for the selection of B cells *in vivo*. The anti-apoptotic protein Bcl-x_L is regarded as necessary for the rescue of immature B cells from cell death [309] and its close homologue, Bcl-2, appears to be important for the maintainance of mature B cells [310]. Both proteins were found to be upregulated within 4h of anti-Ig (50µg/ml) treatment as measured by intracellular staining of all kappa$^+$ cells. The pro-apoptotic protein p53 was, in contrast, downregulated (fig. 58). Taken together, these findings suggest that the surviving cells after anti-Ig treatment exhibit a protective profile of proteins.

4.7 A specific role for IgM in the selection of transitional B cells

Deletion of the transmembrane domain of the mu chain (µm(TM)) leads to a full blockage in B cell development and to absolute loss of peripheral B cells [4]. In an alternative knock-out system, a deletion of the Cµ region

and the μ-δ intron caused a replacement of the mu chain region by delta chain, a change that has been reported to allow normal B cell development [5]. This report of apparently normal selection and distribution is surprising regarding the well documented differences between surface IgM and IgD signalling [14]. Therefore, it was of interest to examine whether normal B cell development occurs in these mice *ex vivo*.

Upon sacrifice the percentage of IgD^{lo} ($delta^{lo}$) cells in $IgM^{-/-}$ mice is comparable to the $kappa^{lo}$ cells in WT littermates (21% vs. 22%), although the absolute number of these cells was significantly higher (cf. $2.3x10^6$ and $1.5x10^6$ cells, respectively). However, bone marrow from knock-out mice contained more apoptotic B cells (about 2.5-fold the percentage in littermate). As a whole, the cell cycle profile of IgD^+ $IgM^{-/-}$ B cells compromised an appearance slightly closer to $IgM^{+/+}$ transitional B cells than to immature cells (fig. 59). The profile of mitochondrial potential was different in $IgM^{-/-}$ bone marrow, where more cells had a higher potential (fig. 60). Taken together, this is the first evidence that $IgM^{-/-}$ bone marrow consists of $delta^+$ B cells, which are not entirely identical to immature B cells in the wild-type mice, due to the different BCR they carry.

Responses to *ex vivo* stimuli were in most cases similar. Notably, however, the expansion of bone marrow IgD^{lo} B cells in response to 50μg/ml anti-Ig was less apparent (fig. 61). In normal bone marrow, the Caspase inhibitor Ac-DEVD-CHO is able to synergise with a high dose of anti-Ig in pushing more IgD^{lo} cells into the IgD^{hi} stage (on background of more death in the IgD^{lo} population). This was not observed in KO cells and therefore points to dependency of normal transitional B cells upon signalling from IgM (fig. 62). This unique IgM signal may be Caspase-regulated and cannot be substituted by delta chain usage.

4.8 ES-62 can enhance maturation of B cells *in vitro* and *in vivo*

ES-62 is a phosphorylcholine-containing parasite-derived glycoprotein which is capable of inducing Th2-type responses *in vivo*, and desensitising BCR-induced proliferation of peripheral B cells [311]. ES-62 has a significant effect on BCR signalling, predominantly via manipulation of the MAPK cascade [311]. Therefore, It was of interest to examine whether this molecule is able to subvert BCR signalling in earlier stages of B cell development, which rely heavily on signals transduced via the BCR.

ES-62 was found to be capable of substantially decreasing the death of kappa$^+$ B cells in bone marrow cultures (from 29% in untreated cells to 20% in ES-62 treated). Increased survival is evident across all sub-populations of B cells, but is especially significant in transitional B cells, where their numbers increase by 138% (fig. 63). Moreover, when treated simultaneously with ES-62 and 50µg/ml anti-Ig, numbers of immature and mature cells are considerably higher than with anti-Ig alone (fig. 64). These data probably reflect an increase in the maturation rate since the ratio of transitional cells to mature is 1.6:1 (cf. 3:1 in anti-Ig alone). Indeed, a possible explanation for the increase in the number of mature cells arises from examination of changes in mitochondrial potential due to addition of ES-62. Using $DiOC_6(3)$ staining, it is apparent that ES-62 is inducing an almost 6-fold increase in the mitochondrial potential of kappa$^+$ B cells (fig. 65a). Together with anti-Ig treatment it is increasing the potential of kappa^{hi} cells, hence giving them a better chance of survival against apoptosis (fig. 65b).

Fas-induced cell death is a known pathway utilising mitochondrial pore transition (as reflected by a decrease in mitochondrial potential). Therefore Fas/kappa chain double staining was preformed to check the possibility that protection of kappa^{hi} cells by ES-62 is achieved by blocking the Fas pathway. ES-62 alone did not change the overall number of kappa$^+$ Fas$^+$ cells, although it appears to preferentially support survival of the kappa^{lo} Fas$^+$ population. Together with 50µg/ml anti-Ig, ES-62 continues to protect them and their numbers are increased by 22% in comparison to anti-Ig alone (fig. 66). Nevertheless, this is only a minor phenomenon - most kappa$^+$ Fas$^+$ cells disappear with anti-Ig treatment with or without ES-62 (22% of kappa$^+$ Fas$^+$ cells in control at 50µg/ml

anti-Ig, 25% at 50μg/ml anti-Ig+ES-62). In conclusion, it seems unlikely that blocking Fas-induced cell death is a mechanism utilised by this parasite product.

To examine whether the effects of ES-62 could be reproduced *in vivo*, cultures from mice which were continously exposed to ES-62 by osmotic mini-pumps for two weeks were used (see *Materials and Methods* for further details). The observation that ES-62 is capable of increasing the number of B cells which mature with anti-Ig treatment *ex vivo* could be reproduced in mice exposed to ES-62 *in vivo* (fig. 67). The rise in the number of transitional B cells did not entirely correlate with the rise in mature cells, indicating that ES-62 has a limited ability to help transitional B cells. The molecular basis to this observation is still obscure. However, at the first 24h of anti-Ig stimulation it is clear that ES-62 reduces substantially the number of transitional B cells which undergo apoptosis and induces proliferation (fig. 68), similarly to what is observed *in vitro* (not shown).

4.9 Discussion

The development of B cells from their progenitors in the bone marrow into mature B cells entering the naive pool in the periphery has been a centre of attention for many years in the field of B cell biology. Using many approaches, numerous studies have tried to address the issue of selection of non-self-reactive B cells (reviewed in [3, 9, 11]). In the past few years, some key observations have altered the classical model of B cell development. Now it is well established that some intermediate stages exist between immature (IgM^+ IgD^-) and mature B cells (IgM^+ IgD^+), although the precise number of "transitional" states is still unclear [9]. It has also became apparent that the selection process is not absolutely restricted to the bone marrow and a secondary selection process must exist in the periphery. This secondary selection in the periphery seems to contrast with the concept of maturation of B cells as an instructive process. The classical model has predicted that immature B cells will be negatively selected based on their affinity. According to this model, a self-

reactive B cell will be deleted [7], anergised [312] or undergo receptor editing [11], according to the strength of signal transduced from its BCR. If, indeed, some transitional B cells leave the bone marrow to the periphery, they will encounter non-self antigens and therefore it is not feasible that all of them will be deleted this way. This scenario predicts some level of positive selection in the periphery. Therefore B cell selection in the bone marrow would not be necessarily dependent on BCR specificity and may be stochastic, i.e. based on parameters such as cell density.

This study has tried to address the questions underlying B cell selection by utilising a different approach for tracking the signals required for this process. The usage of *ex vivo* bone marrow cultures enabled investigation of what happens to immature and transitional B cells upon stimulation via their surface Ig. About 4% of immature cells upon sacrifice were lead to mature after 2d stimulation with anti-Ig, a number similar to estimates derived from other systems [6]. Stimulation of immature B cells under conditions which mimic signalling at a low threshold induces the development of transitional B cells (kappa^{lo} delta^{lo}). Strong stimulation of the BCR of transitional B cells leads to their negative selection - deletion of most cells together with development of a small number into mature cells (kappa^{hi} delta^{hi}) (fig. 38).

Strong stimulation of the BCR, as observed by others, enhanced cell death [11, 12]: while untreated kappa^{+} B cells have around 75% survival rate after 48h, only 30% of them survive with 5µg/ml anti-Ig and 25% with 50µg/ml. Nonetheless, only transitional B cells were found to undergo substantial growth arrest in G_0/G_1. This may be consistent with the studies of Nemazee *et al.* which suggested that weak stimulation of the BCR would causes growth arrest and allow receptor editing [7]. Therefore, it is feasible that receptor editing happens, in fact, during the transitional state.

This *ex vivo* model enabled examination of the role of Fas in selection processes during B cell maturation. It was shown that Fas is being upregulated in correlation to the induction of transitional B cells and downregulated with their development to mature cells, in agreement with previous reports [8]. Anti-Fas treatment also selectively deleted

transitional B cells which developed following BCR stimulation (fig. 46). Furthermore, development in cultures derived from the Fas deficient *lpr* mice, showed a considerable increase in the number of transitional B cells (fig. 48), providing further evidence that these cells are deleted in Fas-dependent manner. Nevertheless, the ability to count and compare precentage of surviving cells enhances our knowledge of Fas function during this developmental process. It is clear from the data presented here that the main role of Fas is to limit the number of transitional B cells. When Fas is absent, more transitional cells survive and mature and this defective selection may be linked to the autoimmunity prevailing in *lpr* mice [306]. Although the proportions of transitional to mature B cells are kept, *de facto* more B cells reach the naive pool and some of them may be self-reactive due to inappropriate selection. This implies again that the selection of B cells in the bone marrow is, to a certain extent, stochastic and not necessarily dependent on the BCR specifity of the cell. If the selection of B cells is purely instructive - i.e, dependent only on deletion by self-antigen - then the number of mature B cells should not increase when Fas is omitted. In this type of selection, B cells will selected only on the basis of their BCR specificity. An alternative view is that Fas^+ transitional B cells represent a population which failed to rearrange their BCR after its ligation and therefore is designated to die. In this scenario, Fas deficiency will enable self-reactive B cell to avoid positive selection in the transitional stage and to become mature B cells.

In agreement with the stochastic model, it was shown using HEL-BCR mice, that there is no complete deletion by self-reactive antigens and, in fact, weak stimulation via the BCR using the partial agonist DEL, promotes B cell maturation (figs. 52-53). Furthermore, in wild-type mice, changes that favour survival could be detected in some cells shortly after BCR stimulation (fig. 58), suggesting that a proportion of immature B cells may be genetically predisposed to have the right combination of protein expression to develop further.

Interestingly, this *ex vivo* model has not identified the maturation context of CD40-mediated rescue signal. As discussed by Monroe [9], this signal can lead potentially to autoimmunity and therefore its physiological context is ambiguous. In *ex vivo* bone marrow cultures described here, no

role but maintaining higher numbers of immature B cells can be attributed for CD40. This is in agreement with Monroe's suggestion that CD40 ligation *in vivo* leads only to immature B cell activation, but does not support their maturation. The results presented here for $Fas^{-/-}$ bone marrow culture may assist in resolving this issue (fig. Fas.5). In contast to the full rescue by CD40 in WEHI-231 cells, a third signal, which blocks Fas-induced apoptosis, may be required in transitional B cells in order to ensure their development. Such a signal may be transduced by MHC class II or B7.2 [313].

The strengths of this *ex vivo* model were demonstrated in a few more ways. For example, it was possible to examine how different surface Ig isotypes determine B cell maturation. Replacement of IgM by IgD was sufficient for transitional B cell formation but not for their full potential of maturation (fig. 61).

Other examples included establishing an unique role for Btk in different signalling situations (fig. 55). Firstly, the dysfunctional B cell development observed in $Btk^{-/-}$ Xid mice was reproduced in this *ex vivo* model, as reported previously, transitional B cells accumulated with little further maturation [314]. Interestingly, cells from $Btk^{-/-}$ bone marrow cultures maintained their mitochondrial potential responses (not shown). Therefore, it is possible that the Btk-sensitive pathway is segregated from the mitochondrial branch of BCR signalling. This segregation may explain how transitional B cells reduce their mitochondrial potential in response to BCR crosslinking, but at the same time are unable to mature.

Manipulation of B cell maturation by naturally occuring pathogens was demonstrated by utilising the parasite-derived molecule, ES-62 (figs. 64 and 67). These effects were evident not only by direct addition of exogenous ES-62 to the bone marrow cultures, but also by using mice that were pre-treated in advance with ES-62 *in vivo*. It is unknown how the ES-62 molecule is brought into the bone marrow. ES-62 affects a wide variety of cells ranging from mature lymphocytes to macrophages. It is therefore possible that it is transported to the bone marrow by any of the recirculating cells who pass there. Importantly, there are reports of mature B cells returning to the bone marrow and influencing B cell maturation [315]. Again, the mechanism of this influence is not clear.

In summary, the *ex vivo* system described here offers an unique opportunity to observe changes in different B cell populations in the bone marrow. Cultures derived from different knock out mice or those manipulated *in vitro* give a powerful tool to examine the importance of distinct components of signalling pathways. Studies using cells isolated after stimulation could prove even more potent in enhancing our understanding of the signals underlying B cell development in the bone marrow.

4.10 Summary

In this chapter a physiologically relevant model of bone marrow B cell development is described. In this model, polyclonal stimulation of the BCR leads to both selection and maturation of immature B cells. The main observations in this model were:

- Transitional B cells depend on Fas, IgM and Btk for progression into the mature B cell pool.
- During the anti-Ig response, kappa$^+$ B cells reduce also their mitochondrial membrane potential, similarly to WEHI-231 cells.
- It was investigated how antigen specificity/affinity influences the selection of B cells in the bone marrow, using a soluble antigen (HEL and DEL).
- B cell maturation is manipulated by external factors, such as the pathogen product ES-62, even in the bone marrow.

a.

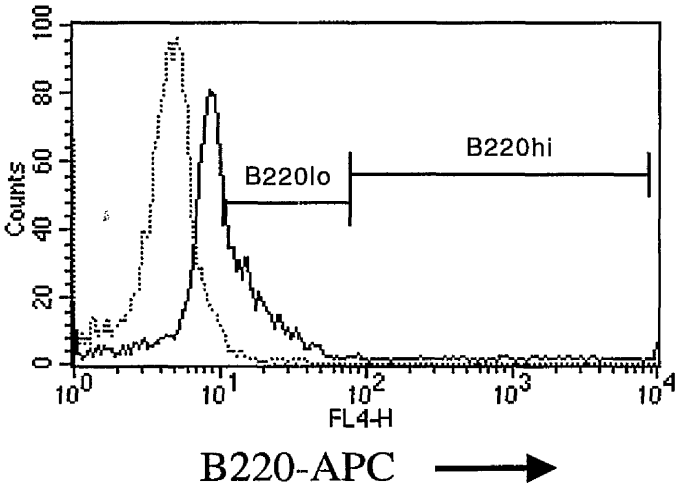
Counts
B220lo
B220hi
FL4-H
B220-APC

b.

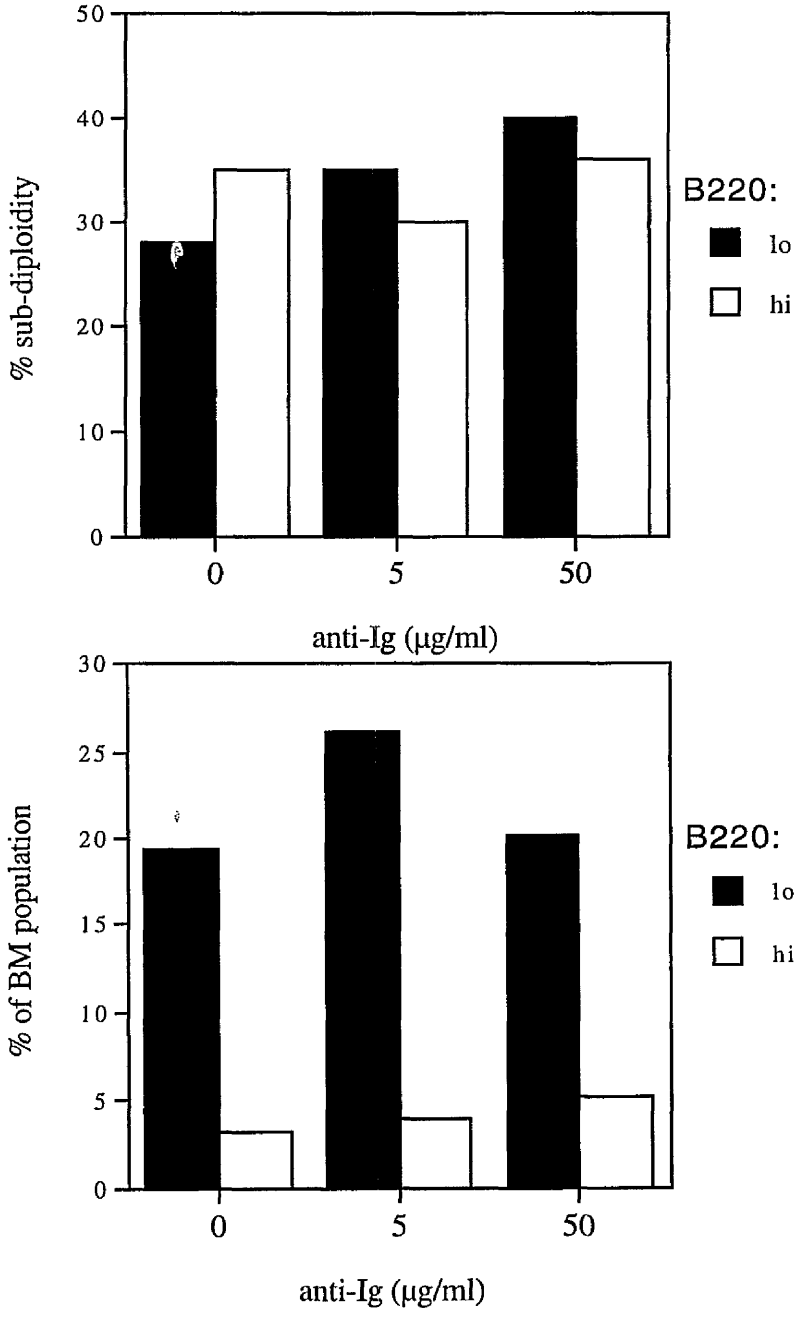
% sub-diploidity
anti-Ig (µg/ml)
B220:
lo
hi
% of BM population
anti-Ig (µg/ml)
B220:
lo
hi

Fig. 37

Figure 37: $B220^{lo}$ B cells undergo apoptosis in response to anti-Ig whilst the $B220^{hi}$ population expands. (a) B220 expression in whole bone marrow cultures. The cells were incubated with B220-APC (1:50) and analysed by flow cytometry. The background fluorescence (using streptavidin-APC, 1:100) is shown in the dotted line. The $B220^{+}$ population was of <1% with the background staining (a shift in the overall fluorescence is also apparent due to unspecific binding of the B220 antibody). (b) Whole bone marrow cultured with 0-50µg/ml anti-Ig for 1d. Cells then were stained with B220-APC as in *(a)* and were subjected to PI incorporation to determine DNA content.

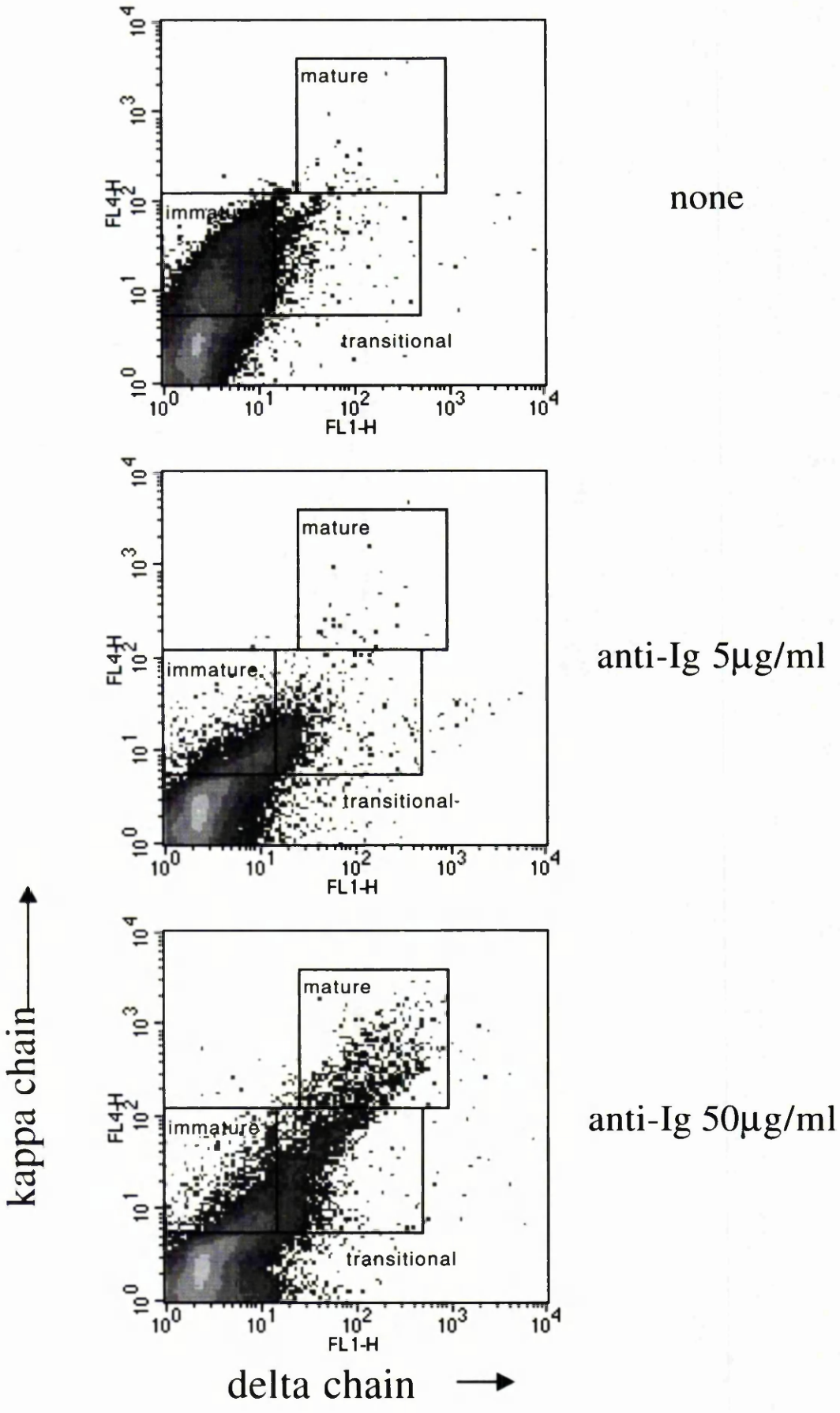
mature
immature
transitional
FL4-H
FL1-H
none
anti-Ig 5µg/ml
anti-Ig 50µg/ml
kappa chain
delta chain

Fig. 38

Figure 38: B cell development in the bone marrow *ex vivo*. Whole bone marrow cultures (10^6 cells/sample) were stimulated with 0-50µg/ml anti-Ig for 2d and stained for surface expression with anti-delta chain (1:50)+anti-rat-IgG-FITC (1:100) and anti-kappa chain (1:50)-biotin +streptavidin-APC (1:100). For negative staining control, only the secondary antibodies were used and all gates consisted of <1% of the cell population.

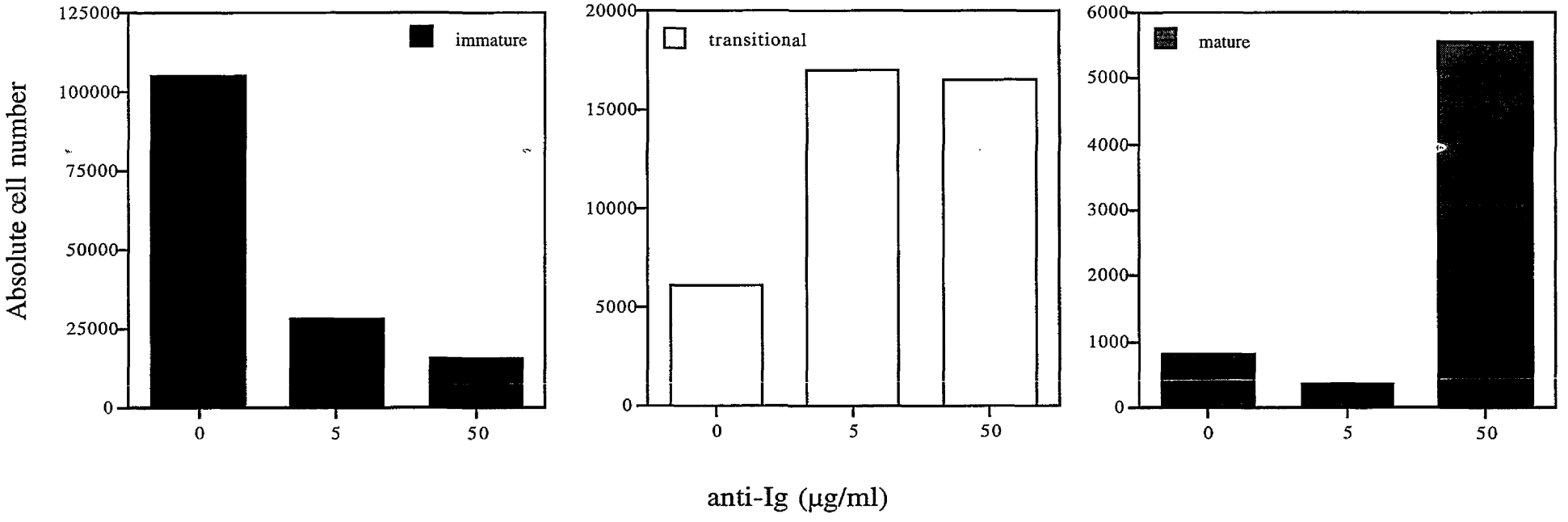
Absolute cell number
125000
100000
75000
50000
25000
0
immature
0
5
50
20000
15000
10000
5000
0
transitional
0
5
50
6000
5000
4000
3000
2000
1000
0
mature
0
5
50
anti-Ig (μg/ml)

Fig. 39

Figure 39: Immature B cells are selected by BCR stimulation *ex vivo*. Whole bone marrow cultures (10^6 cells/sample) were stimulated with 0-50µg/ml anti-Ig for 2d. The total cell number of bone marrow cultures was determined by counting after stimulation. Cells were stained for surface expression with anti-delta chain (1:50)+anti-rat-IgG-FITC (1:100) and anti-kappa chain (1:50)-biotin+streptavidin-APC (1:100). Immature B cells were kappa$^+$ delta$^-$, transitional cells: kappa^{lo} delta^{lo}, mature cells: kappa^{hi} delta^{hi}. For negative staining control, only the secondary antibodies were used and all gates consisted of <1% of the cell population.

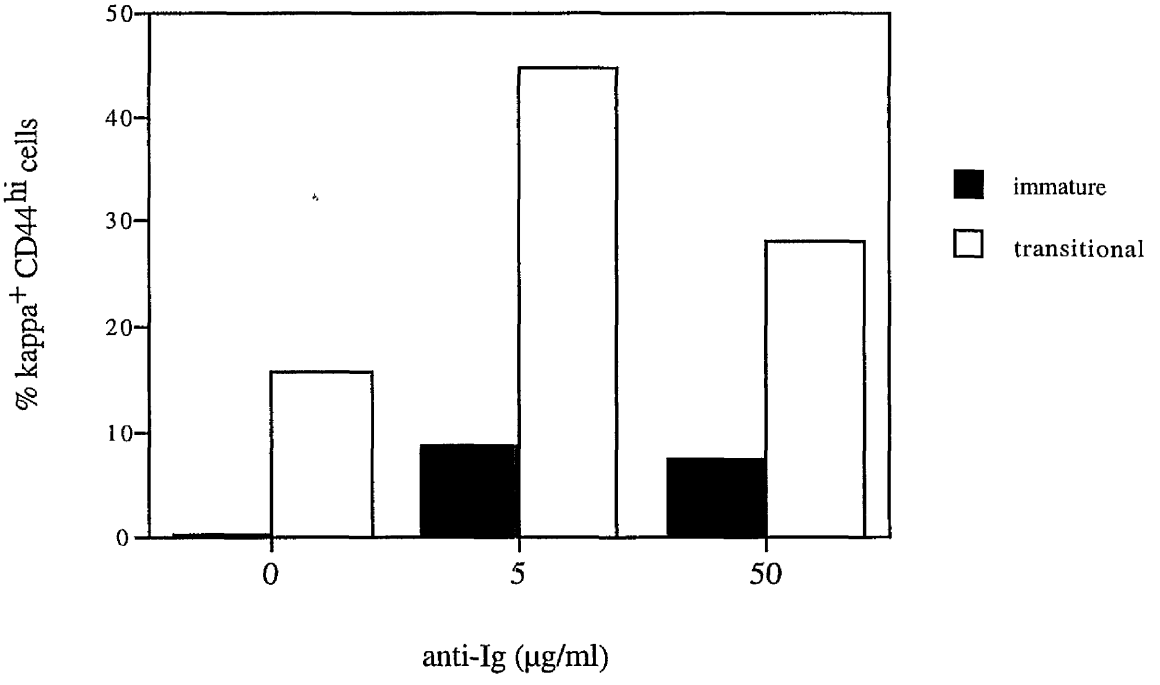
50
40
30
20
10
0
% kappa+ CD44hi cells
0
5
50
anti-Ig (µg/ml)
immature
transitional

Fig. 40

Figure 40: Induction of CD44 expression correlates with induction of transitional B cells. Whole bone marrow cultures (10^6 cells/sample) were stimulated with 0-50μg/ml anti-Ig for 2d. The total cell number of bone marrow cultures was determined by counting after stimulation. Cells were stained for surface expression with anti-CD44-FITC (1:200), anti-kappa chain (1:50)-biotin+streptavidin-PerCP (1:100) and anti-delta (1:50)+anti-rat-APC (1:20). Immature B cells were kappa$^+$ delta$^-$ and transitional cells were kappa^{lo} delta^{lo}. For negative staining control, only the secondary antibodies were used and all gates consisted of <1% of the cell population.

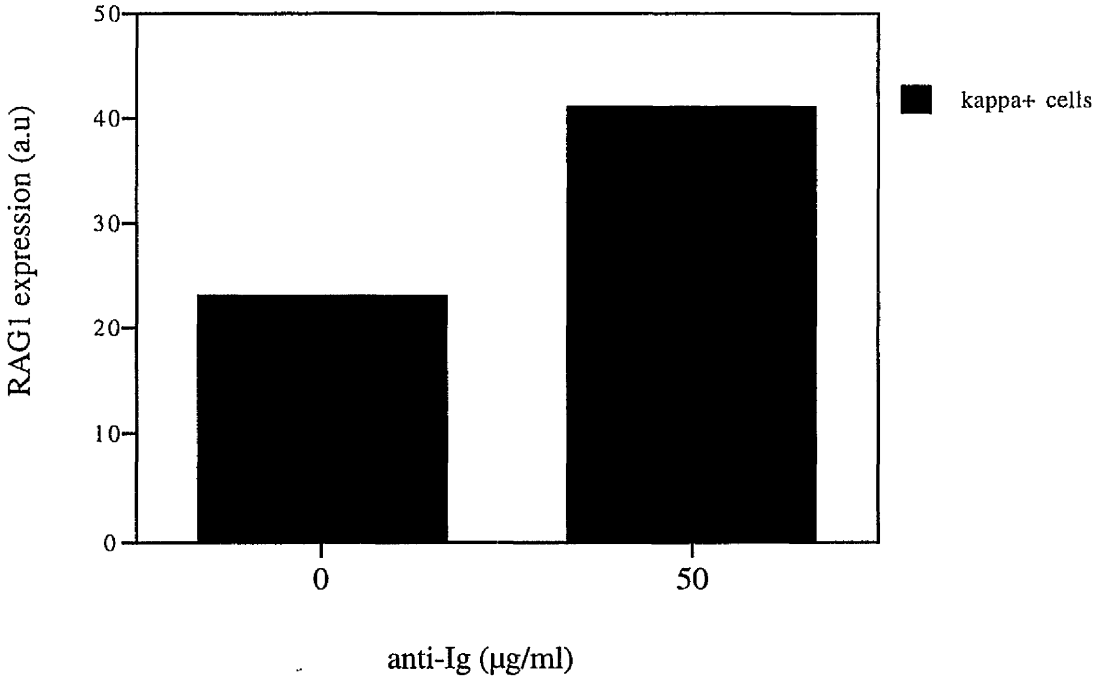
50
40
30
20
10
0
RAG1 expression (a.u)
0
50
anti-Ig (µg/ml)
kappa+ cells

Fig. 41

Figure 41: Induction of RAG-1 protein expression in kappa$^+$ B cells after stimulation of bone marrow cultures. Whole bone marrow cultures (10^6 cells/sample) were stimulated with 0-50μg/ml anti-Ig for 4h. Cells were stained for surface expression with anti-kappa chain (1:50)-biotin+streptavidin-PerCP (1:100). Cell surface staining was followed by intracellular staining for RAG-1 of the whole population (see *Materials and Methods* for full details). For negative staining control, only the secondary antibodies were used and all gates consisted of <1% of the cell population. Results are shown for kappa$^+$ cells only.

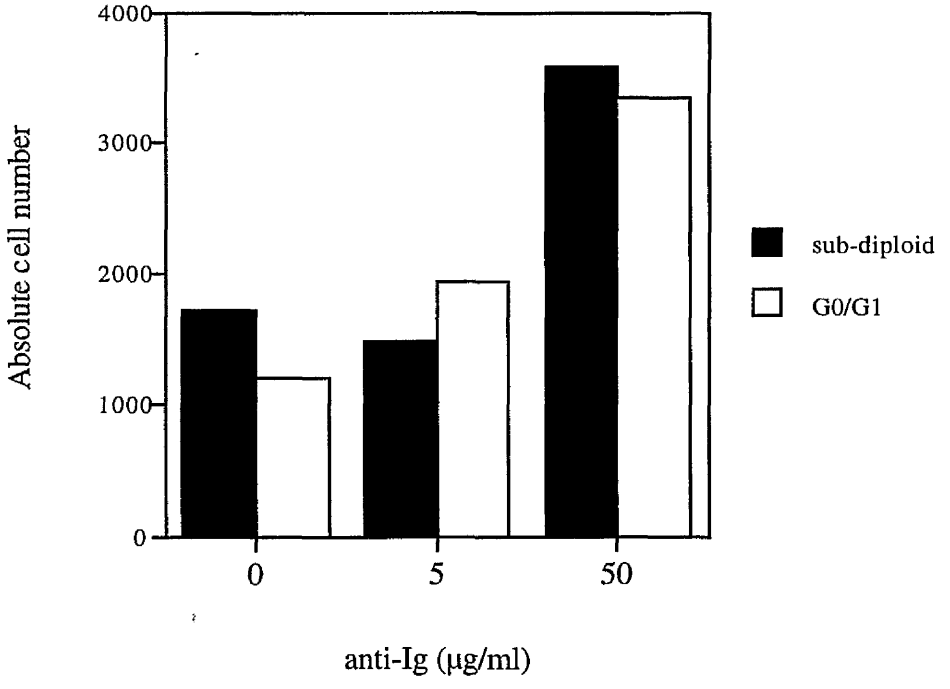
4000
3000
2000
1000
0
Absolute cell number
0
5
50
anti-Ig (µg/ml)
sub-diploid
G0/G1

Fig. 42

Figure 42: Transitional B cells undergo growth arrest and apoptosis in response to strong anti-Ig stimulation ex vivo. Whole bone marrow cultures (10^6 cells/sample) were stimulated with 0-50μg/ml anti-Ig for 2d. The total cell number of bone marrow cultures was determined by counting after stimulation. Cells were stained for surface expression with anti-delta chain (1:50)+anti-rat-IgG-FITC (1:100) and anti-kappa chain (1:50)-biotin+streptavidin-APC (1:100). Staining was followed by PI incorporation to determine DNA content. Transitional B cells were kappa^{lo} delta^{lo}. For negative staining control, only the secondary antibodies were used and all gates consisted of <1% of the cell population.

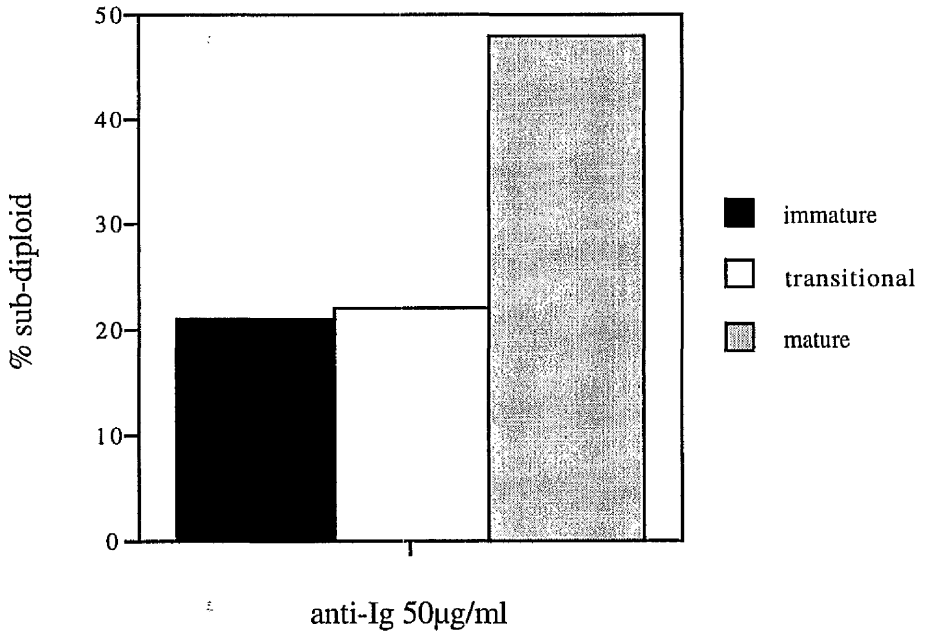
50
40
30
20
10
0
% sub-diploid
immature
transitional
mature
anti-Ig 50µg/ml

Fig. 43

Figure 43: Chronic anti-Ig stimulation leads to apoptosis of mature B cells in the bone marrow. Whole bone marrow cultures (10^6 cells/sample) were stimulated with 0-50µg/ml anti-Ig for 2d. The total cell number of bone marrow cultures was determined by counting after stimulation. Cells were stained for surface expression with anti-delta chain (1:50)+anti-rat-IgG-FITC (1:100) and anti-kappa chain (1:50)-biotin+streptavidin-APC (1:100). Immature B cells were kappa$^+$ delta$^-$, transitional cells: kappa^{lo} delta^{lo}, mature cells: kappa^{hi} delta^{hi}. Staining was followed by PI incorporation to determine DNA content.
For negative staining control, only the secondary antibodies were used and all gates consisted of <1% of the cell population. Sub-diploid cells were the <2N DNA population.

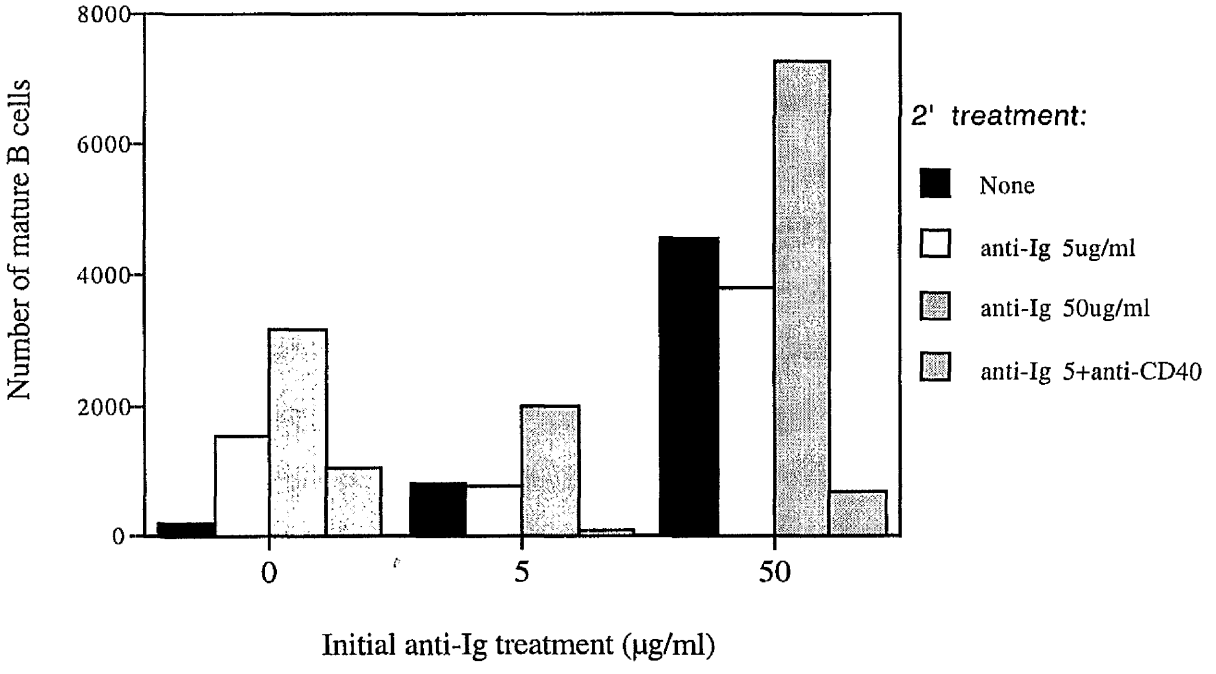
8000
6000
4000
2000
0
Number of mature B cells
0
5
50
Initial anti-Ig treatment (µg/ml)
2' treatment:
None
anti-Ig 5ug/ml
anti-Ig 50ug/ml
anti-Ig 5+anti-CD40

Fig. 44

Figure 44: Restimulation of cells from bone marrow cultures. Whole bone marrow cultures (10^6 cells/sample) were stimulated with 0-50µg/ml anti-Ig for 2d and then for a further 2d with 0-50µg/ml anti-Ig with or without 10µg/ml anti-CD40. The total cell number of bone marrow cultures was determined by counting after stimulation. Cells were stained for surface expression with anti-delta chain (1:50)+anti-rat-IgG-FITC (1:100) and anti-kappa chain (1:50)-biotin+streptavidin-APC (1:100). Mature B cells were kappa^{hi} delta^{hi}. For negative staining control, only the secondary antibodies were used and all gates consisted of <1% of the cell population.

a.

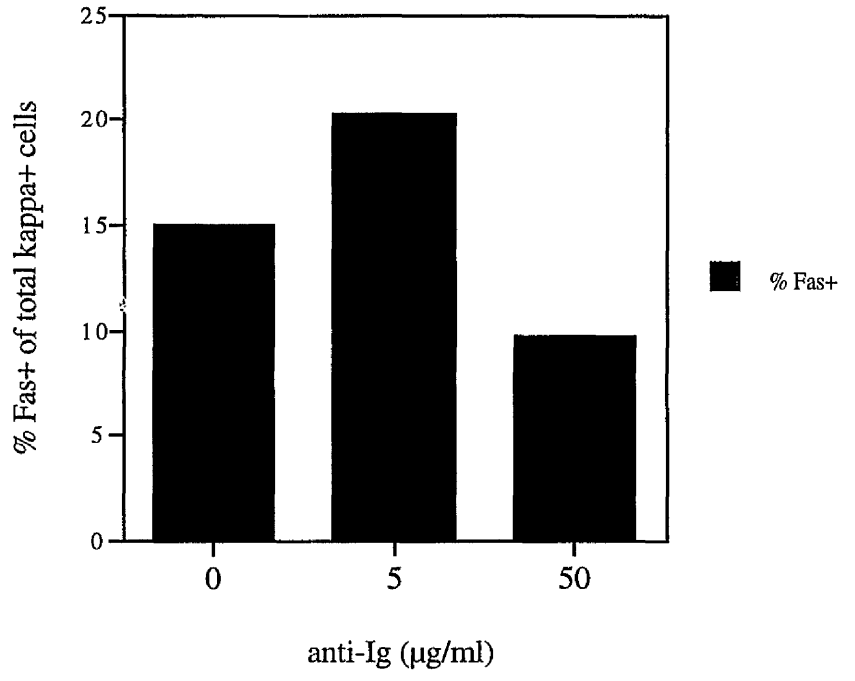
25
20
15
10
5
0
% Fas+ of total kappa+ cells
0
5
50
anti-Ig (µg/ml)
% Fas+

b.

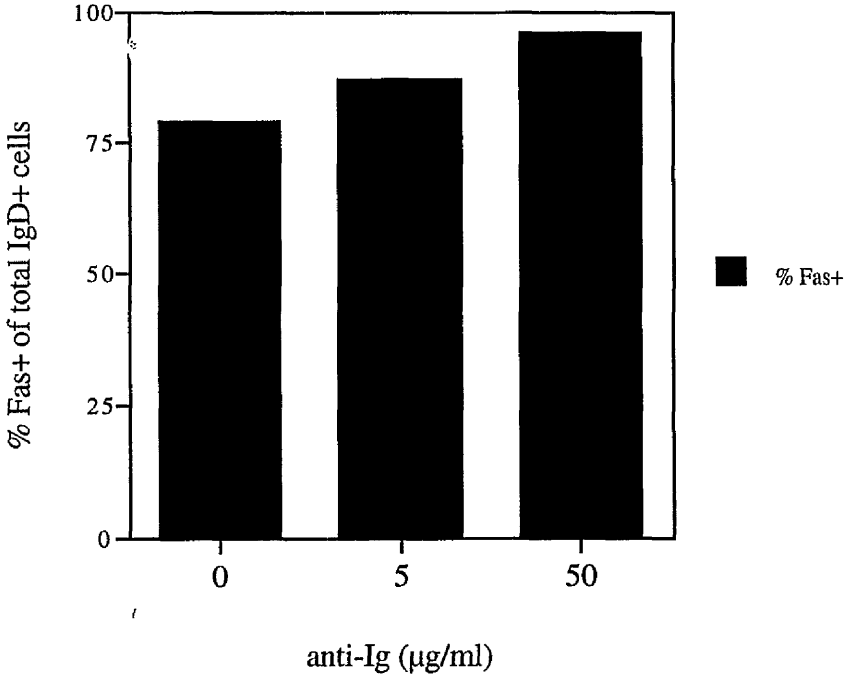
100
75
50
25
0
% Fas+ of total IgD+ cells
0
5
50
anti-Ig (µg/ml)
% Fas+

Fig. 45

Figure 45: Strong BCR stimulation supports the development of Fas$^+$ IgD$^+$, not kappa$^+$, B cells. Whole bone marrow cultures (10^6 cells/sample) were stimulated with 0-50μg/ml anti-Ig for 2d and detected for co-expression of Fas with either kappa chain (a) or delta chain (b). The total cell number of bone marrow cultures was determined by counting after stimulation. Cells were stained for surface expression with (a) anti-kappa chain (1:50)-biotin+streptavidin-APC (1:100) and anti-Fas (1:100)+anti-mouse Ig-FITC (1:100); or (b) anti-delta chain (1:50)+anti-rat-IgG-FITC (1:100) and anti-Fas-biotin (1:100)+streptavidin-APC (1:100). For negative staining control, only the secondary antibodies were used and all gates consisted of <1% of the cell population.

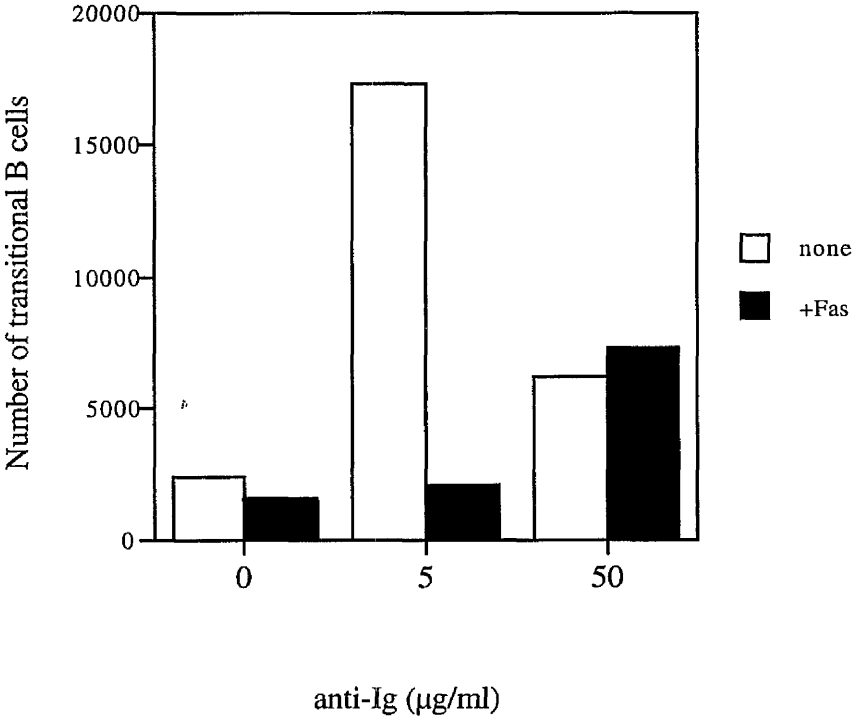
20000
15000
10000
5000
0
Number of transitional B cells
0
5
50
anti-Ig (µg/ml)
none
+Fas

Fig. 46

Figure 46: Deletion via Fas is specific to transitional B cells. Whole bone marrow cultures (10^6 cells/sample) were stimulated with 0-50µg/ml anti-Ig for 2d and then for a further 4h with 0-0.1µg/ml anti-Fas. The total cell number of bone marrow cultures was determined by counting after stimulation. Cells were stained for surface expression with anti-delta chain (1:50)+anti-rat-IgG-FITC (1:100) and anti-kappa chain (1:50)-biotin+streptavidin-APC (1:100). Immature B cells were kappa$^+$ delta$^-$ and transitional cells: kappa^{lo} delta^{lo}. For negative staining control, only the secondary antibodies were used and all gates consisted of <1% of the cell population.

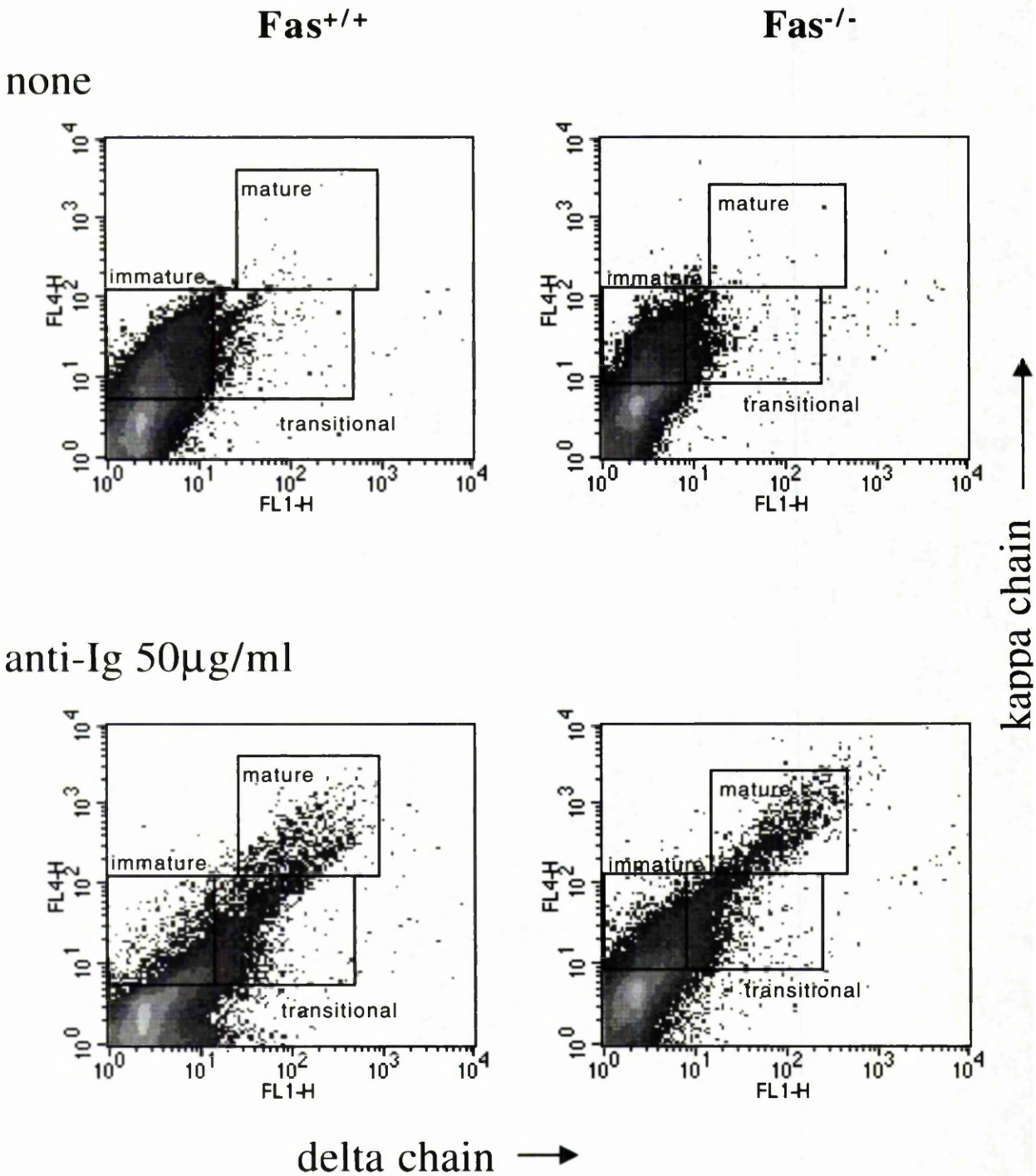
Fas+/+
Fas-/-
none
anti-Ig 50µg/ml
mature
immature
transitional
FL4-H
FL1-H
kappa chain
delta chain

Fig. 47

Figure 47: B cell development in lpr ($Fas^{-/-}$) mice *ex vivo*. Whole bone marrow cultures (10^6 cells/sample) from either WT BALB/c or *lpr* mice were stimulated with 0-50μg/ml anti-Ig for 2d and stained for surface expression with anti-delta chain (1:50)+anti-rat-IgG-FITC (1:100) and anti-kappa chain (1:50)-biotin+streptavidin-APC (1:100). For negative staining control, only the secondary antibodies were used and all gates consisted of <1% of the cell population.


40
30
20
10
0
% recovery
immature
transitional
mature
Fas +/+
Fas -/-
Bone marrow origin

Fig. 48

Figure 48: Enhanced expansion of mature B cells in Fas$^{-/-}$ bone marrow cultures. Whole bone marrow cultures (10^6 cells/sample) from either WT BALB/c or *lpr* mice were stimulated with 0-50µg/ml anti-Ig for 2d. The total cell number of bone marrow cultures was determined by counting after stimulation. Cells were stained for surface expression with anti-delta chain (1:50)+anti-rat-IgG-FITC (1:100) and anti-kappa chain (1:50)-biotin+streptavidin-APC (1:100). Immature B cells were kappa$^+$ delta$^-$, transitional cells: kappa^{lo} delta^{lo}, mature cells: kappa^{hi} delta^{hi}. For negative staining control, only the secondary antibodies were used and all gates consisted of <1% of the cell population. Percentages calculated from total kappa$^+$ cells in untreated cultures of each cell type.

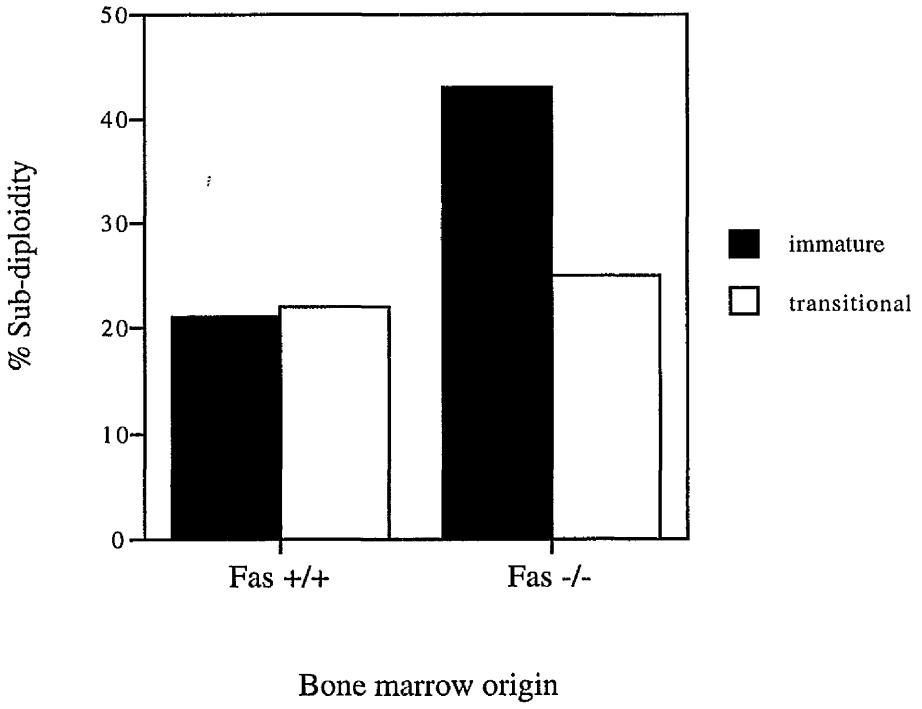
50
40
30
20
10
0
% Sub-diploidity
Fas +/+
Fas -/-
Bone marrow origin
immature
transitional

Fig. 49

Figure 49: Enhanced anti-Ig induced expansion and apoptosis of transitional B cells in *lpr* mice. Whole bone marrow cultures (10^6 cells/sample) from either WT BALB/c or *lpr* mice were stimulated with 0-50μg/ml anti-Ig for 2d. The total cell number of bone marrow cultures was determined by counting after stimulation. Cells were stained for surface expression with anti-delta chain (1:50)+anti-rat-IgG-FITC (1:100) and anti-kappa chain (1:50)-biotin+streptavidin-APC (1:100). Staining was followed by PI incorporation.

Immature B cells were kappa$^+$ delta$^-$, transitional cells: kappa^{lo} delta^{lo}, mature cells: kappa^{hi} delta^{hi}. For negative staining control, only the secondary antibodies were used and all gates consisted of <1% of the cell population. Sub-diploidity was determined by DNA content (<2N) of the immature and transitional B cells.

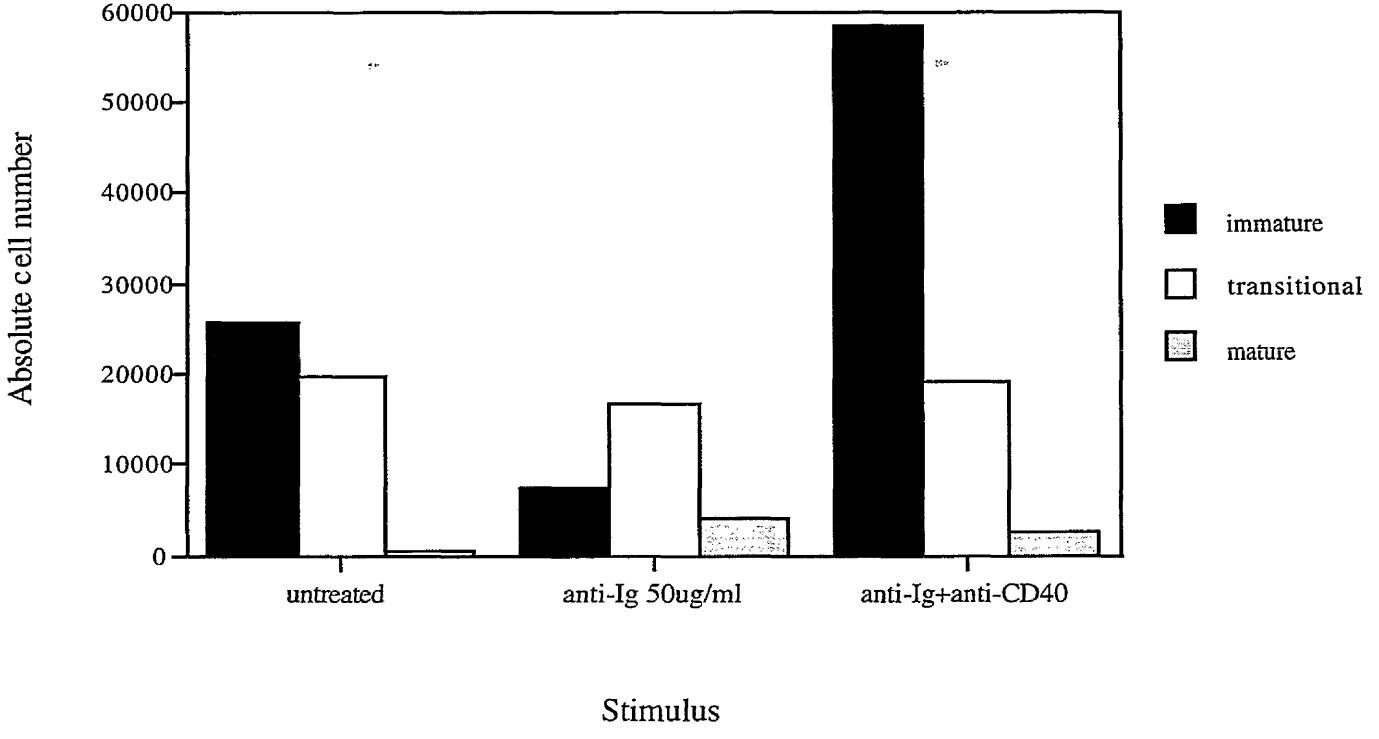
60000
50000
40000
30000
20000
10000
0
Absolute cell number
immature
transitional
mature
untreated
anti-Ig 50ug/ml
anti-Ig+anti-CD40
Stimulus

Fig. 50

Figure 50: Co-stimulation with anti-CD40 is more effective in *lpr* mice. Whole bone marrow cultures (10^6 cells/sample) from either WT BALB/c or *lpr* mice were stimulated with 0-50µg/ml anti-Ig with or without 10µg/ml anti-CD40 for 2d. The total cell number of bone marrow cultures was determined by counting after stimulation. Cells were stained for surface expression with anti-delta chain (1:50)+anti-rat-IgG-FITC (1:100) and anti-kappa chain (1:50)-biotin+streptavidin-APC (1:100). Immature B cells were kappa$^+$ delta$^-$, transitional cells: kappa^{lo} delta^{lo}, mature cells: kappa^{hi} delta^{hi}. For negative staining control, only the secondary antibodies were used and all gates consisted of <1% of the cell population.

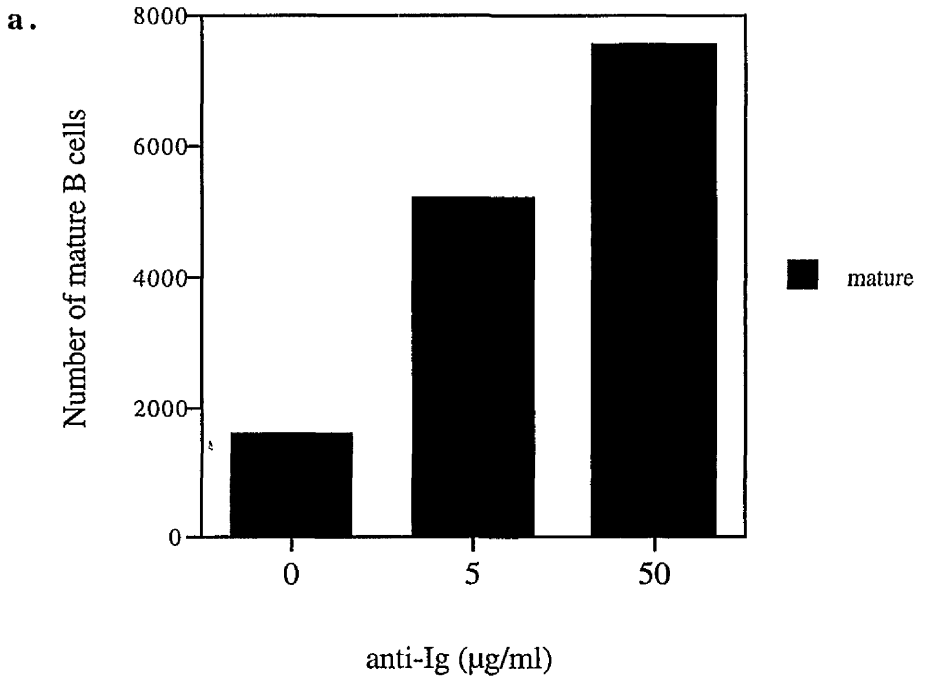
a.
8000
6000
4000
2000
0
Number of mature B cells
0
5
50
anti-Ig (µg/ml)
mature

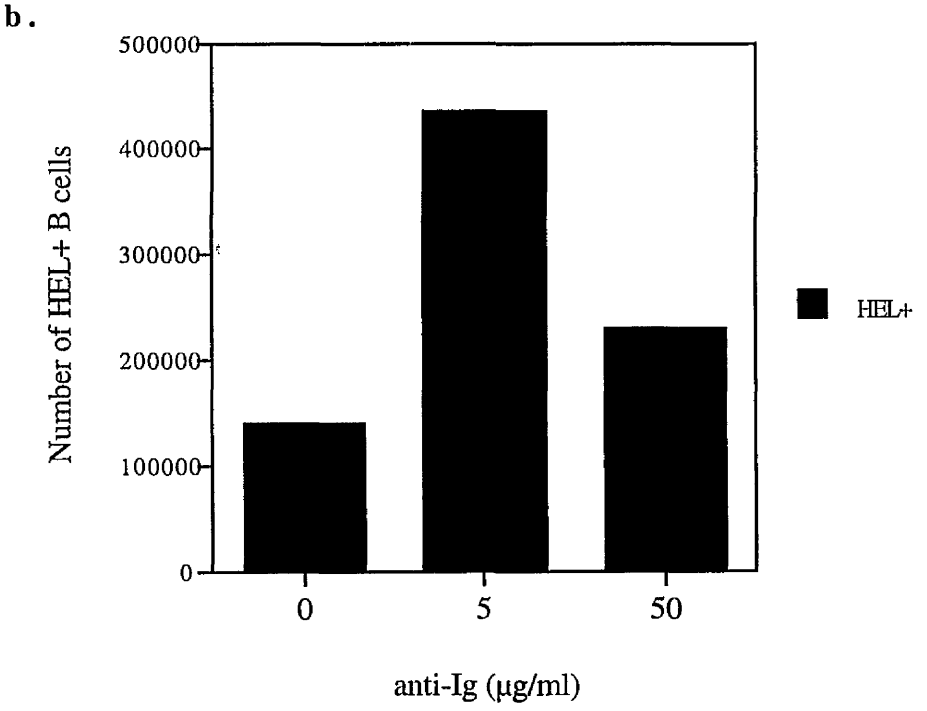
b.
500000
400000
300000
200000
100000
0
Number of HEL+ B cells
0
5
50
anti-Ig (µg/ml)
HEL+

Fig. 51

Figure 51: B cell maturation in HEL-BCR mice. Whole bone marrow cultures (10^6 cells/sample) from MD4 mice were stimulated with 0-50µg/ml anti-Ig for 2d. The total cell number of bone marrow cultures was determined by counting after stimulation. Cells were stained for surface expression with anti-kappa chain (1:50)-biotin+streptavidin-APC (1:100) and (a) anti-delta chain (1:50)+anti-rat-IgG-FITC (1:100), or (b) HEL-FITC (1:20). For negative staining control, only the secondary antibodies were used and all gates consisted of <1% of the cell population. In (a) mature B cells were the kappa^{hi} delta^{hi} cells. In (b), kappa^{+} HEL^{+} cells are shown.

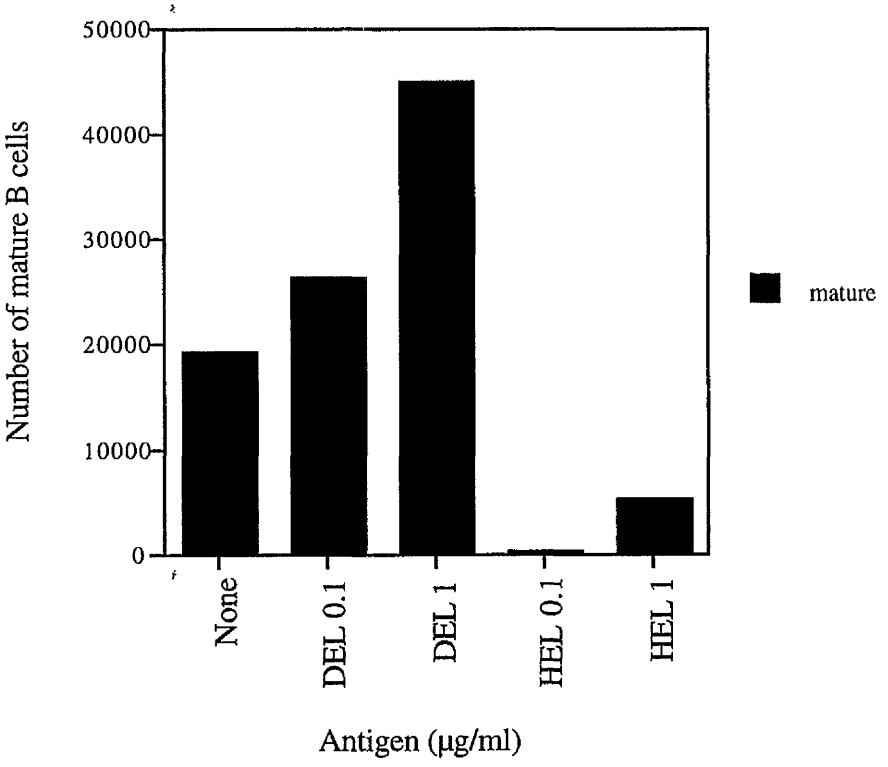
50000
40000
30000
20000
10000
0
Number of mature B cells
None
DEL 0.1
DEL 1
HEL 0.1
HEL 1
Antigen (µg/ml)
mature

Fig. 52

Figure 52: Low affinity self-antigen promotes maturation of B cells. Whole bone marrow cultures (10^6 cells/sample) from MD4 mice were stimulated with 0-1µg/ml HEL or 0-1µg/ml DEL for 2d. The total cell number of bone marrow cultures was determined by counting after stimulation. Cells were stained for surface expression with anti-delta chain (1:50)+anti-rat-IgG-FITC (1:100) and anti-kappa chain (1:50)-biotin+streptavidin-APC (1:100). Mature B cells were the $kappa^{hi}$ $delta^{hi}$ cells. For negative staining control, only the secondary antibodies were used and all gates consisted of <1% of the cell population.

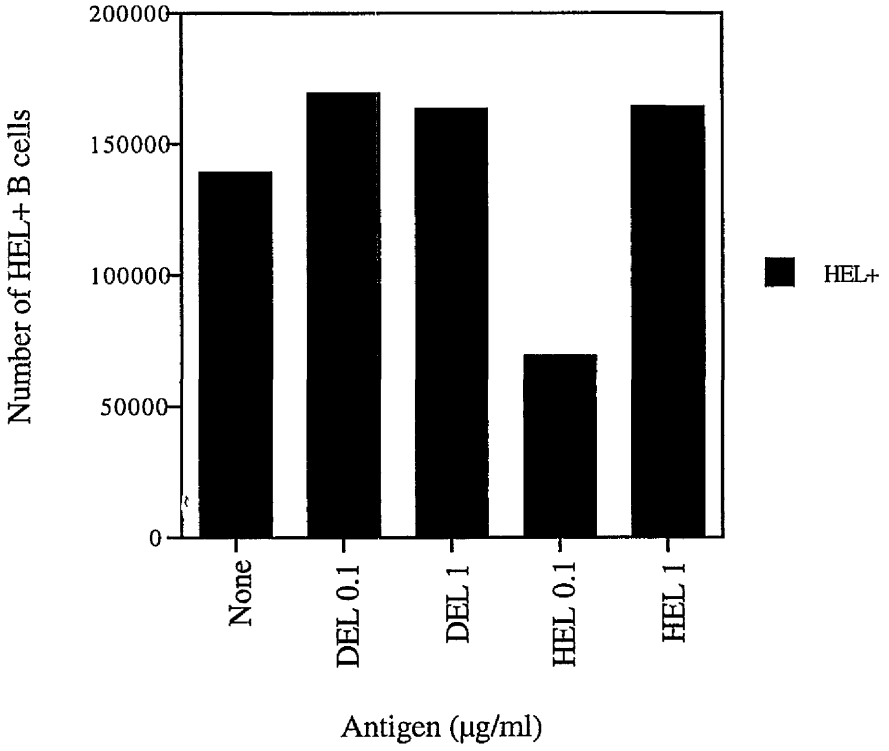
200000
150000
100000
50000
0
Number of HEL+ B cells
None
DEL 0.1
DEL 1
HEL 0.1
HEL 1
Antigen (µg/ml)
HEL+

Fig. 53

Figure 53: Limited deletion of self-reactive B cells by self-antigen. Whole bone marrow cultures (10^6 cells/sample) from MD4 mice were stimulated with 0-1µg/ml HEL or 0-1µg/ml DEL for 2d. The total cell number of bone marrow cultures was determined by counting after stimulation. Cells were stained for surface expression with anti-kappa chain (1:50)-biotin+streptavidin-APC (1:100) and HEL-FITC (1:20). For negative staining control, only the secondary antibodies were used and all gates consisted of <1% of the cell population. Only kappa$^+$ HEL$^+$ cells are shown.

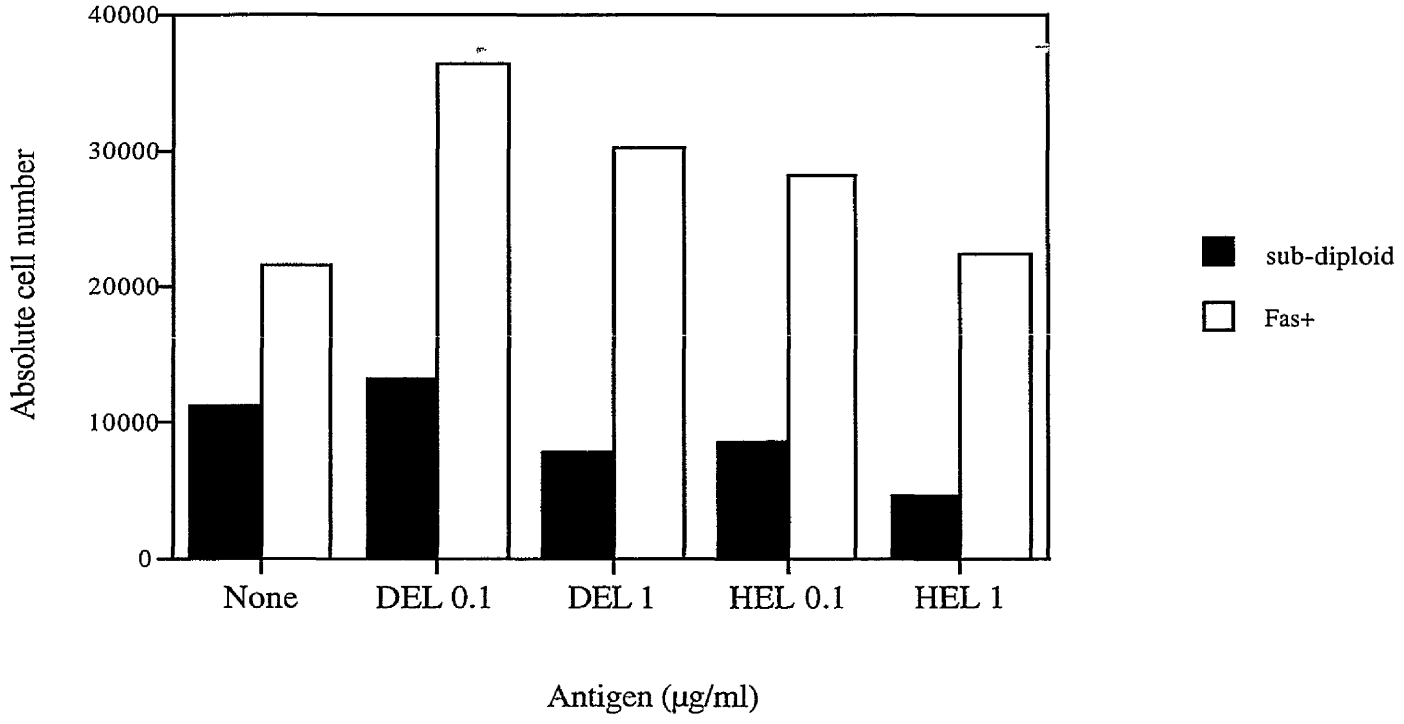
40000
30000
20000
10000
0
Absolute cell number
None
DEL 0.1
DEL 1
HEL 0.1
HEL 1
Antigen (µg/ml)
sub-diploid
Fas+

Fig. 54

Figure 54: Correlation between Fas expression and deletion of transitional B cells. Whole bone marrow cultures (10^6 cells/sample) from MD4 mice were stimulated with 0-1μg/ml HEL or 0-1μg/ml DEL for 2d. The total cell number of bone marrow cultures was determined by counting after stimulation. Cells were stained for surface expression with anti-kappa chain (1:50)-biotin+streptavidin-APC (1:100) and anti-Fas (1:100)+anti-mouse Ig-FITC (1:100). After staining, cells were subjected to PI incorporation. For negative staining control, only the secondary antibodies were used and all gates consisted of <1% of the cell population. Fas^+ B cells were the $kappa^+$ Fas^+ population. Sub-diploidity was determined by DNA content (<2N).

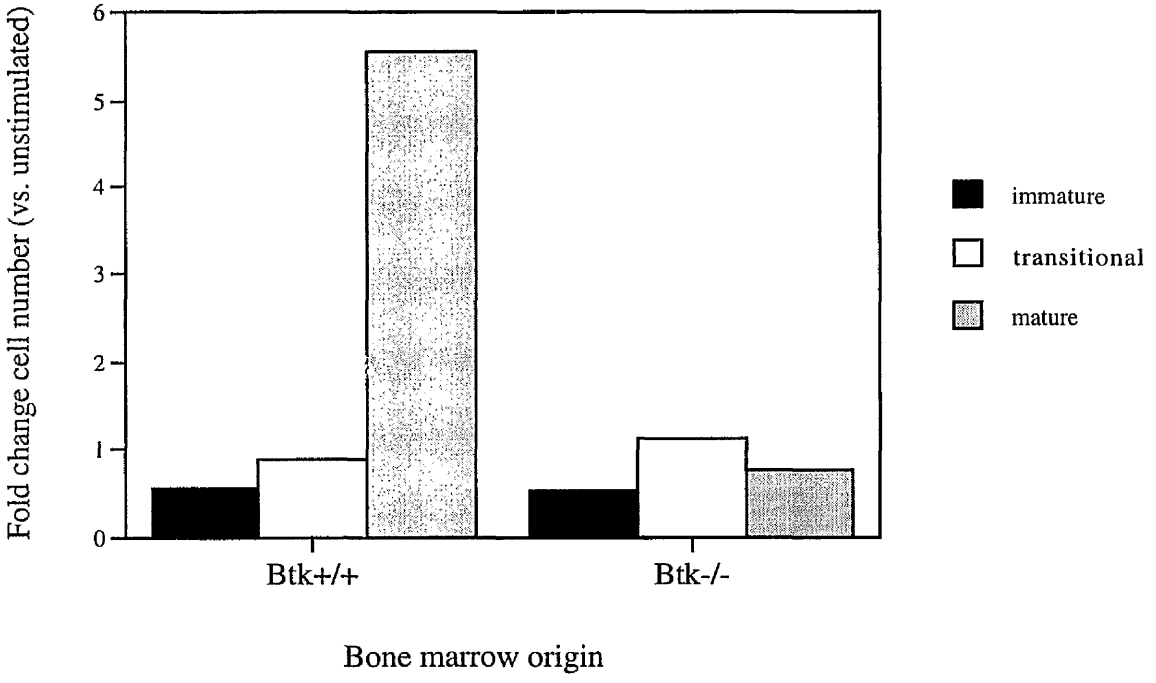
Fold change cell number (vs. unstimulated)
6
5
4
3
2
1
0
Btk+/+
Btk-/-
Bone marrow origin
immature
transitional
mature

Fig. 55

Figure 55: Btk deficiency blocks maturation of transitional B cells in response to anti-Ig treatment. Whole bone marrow cultures (10^6 cells/sample) from either female (WT) or male (*Xid*) CBA/N mice were stimulated with 0-50µg/ml anti-Ig for 2d. The total cell number of bone marrow cultures was determined by counting after stimulation. Cells were stained for surface expression with anti-delta chain (1:50)+anti-rat-IgG-FITC (1:100) and anti-kappa chain (1:50)-biotin+streptavidin-APC (1:100). Immature B cells were kappa$^+$ delta$^-$, transitional cells: kappa^{lo} delta^{lo}, mature cells: kappa^{hi} delta^{hi}. For negative staining control, only the secondary antibodies were used and all gates consisted of <1% of the cell population. Changes in B cell populations were determined as fold change in comparison to untreated cells from the same origin.

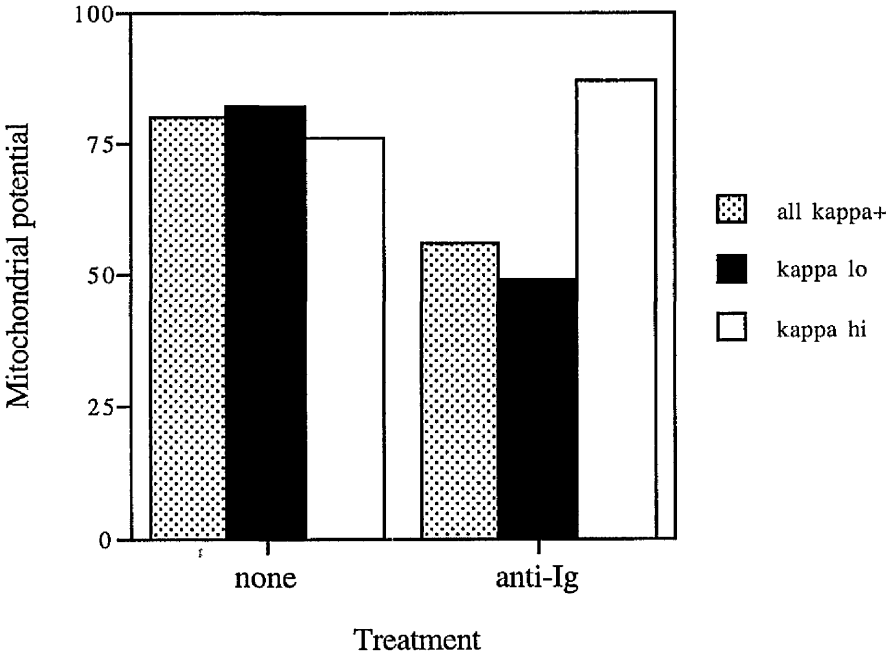
100
75
50
25
0
Mitochondrial potential
none
anti-Ig
Treatment
all kappa+
kappa lo
kappa hi

Fig. 56

Figure 56: anti-Ig treatment leads to a specific reduction in the mitochondrial potential of kappa^{lo} B cells. Whole bone marrow cultures (10^6 cells/sample) were stimulated with 0-50µg/ml anti-Ig for 2d. Cells were stained with anti-kappa-chain-biotin (1:50)+ streptavidin-APC (1:100) and then with 50nM of the mitochondrial dye $DiOC_6(3)$. The mitochondrial potential was determined by the mean fluorescence of the dye of each cell population.

a.

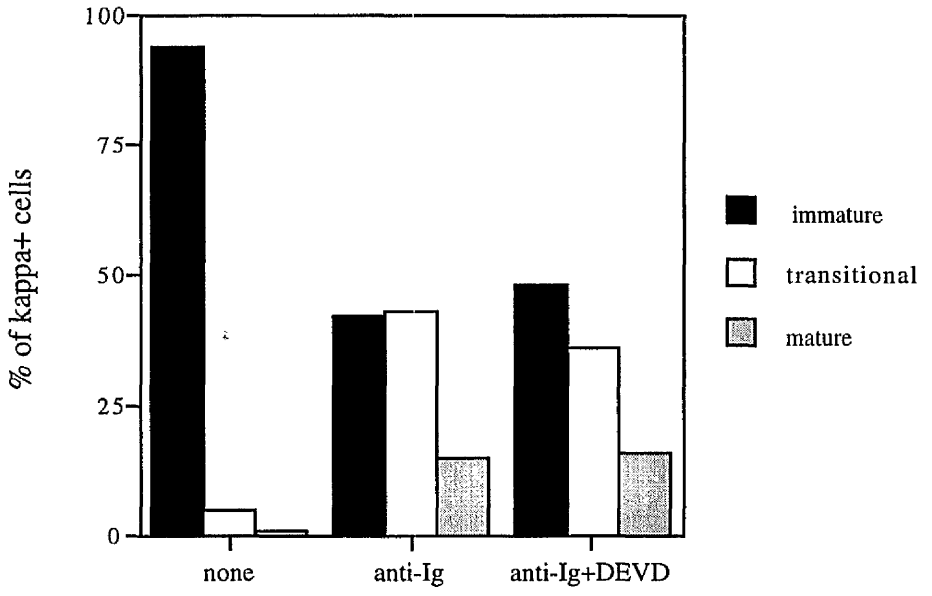
100
75
50
25
0
% of kappa+ cells
none
anti-Ig
anti-Ig+DEVD
immature
transitional
mature

b.

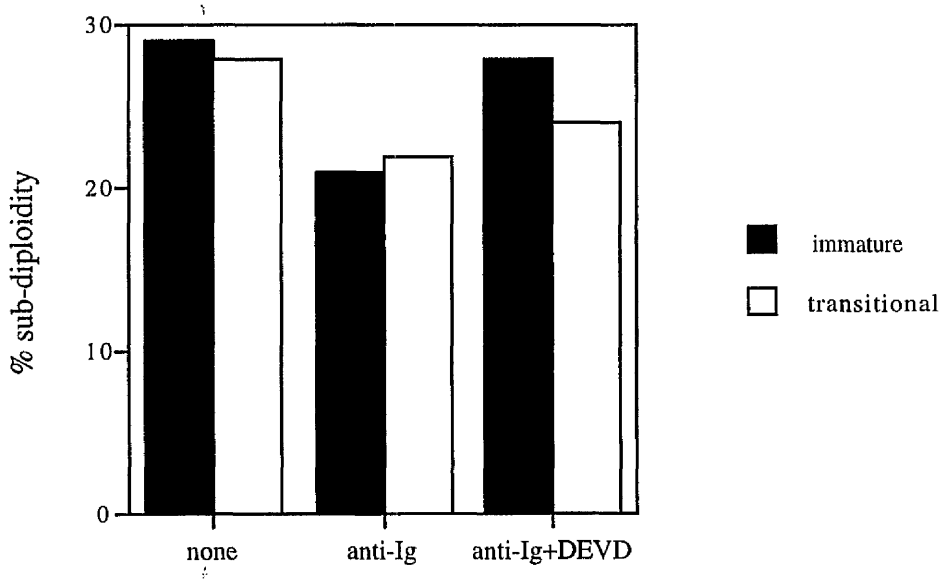
30
20
10
0
% sub-diploidity
none
anti-Ig
anti-Ig+DEVD
immature
transitional

Fig. 57

Figure 57: The effect of Caspase inhibition on B cell maturation. Whole bone marrow cultures (10^6 cells/sample) were stimulated with 0-50μg/ml anti-Ig with or without 10μM Ac-DEVD-CHO for 2d. The total cell number of bone marrow cultures was determined by counting after stimulation. Cells were stained for surface expression with anti-delta chain (1:50)+anti-rat-IgG-FITC (1:100) and anti-kappa chain (1:50)-biotin+streptavidin-APC (1:100). After staining, cells were subjected to PI incorporation. For negative staining control, only the secondary antibodies were used and all gates consisted of <1% of the cell population. (a) Immature B cells were kappa$^+$ delta$^-$, transitional cells: kappa^{lo} delta^{lo}, mature cells: kappa^{hi} delta^{hi}. (b) Sub-diploidity was determined by DNA content (<2N).

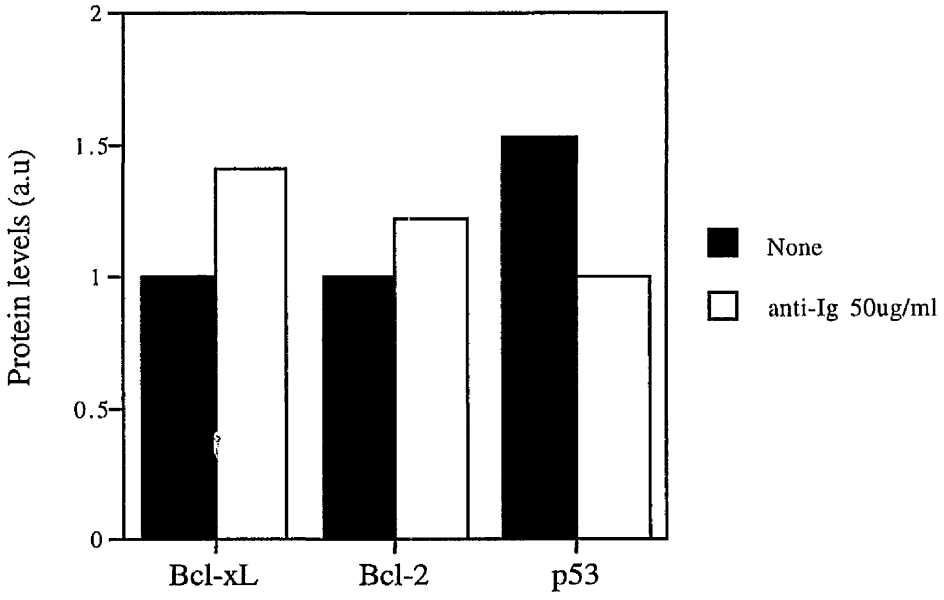
Protein levels (a.u)
2
1.5
1
0.5
0
Bcl-xL
Bcl-2
p53
None
anti-Ig 50ug/ml

Fig. 58

Figure 58: Changes in protein expression of Bcl-x_L, Bcl-2 and p53 in kappa$^+$ B cells after stimulation of bone marrow cultures. Whole bone marrow cultures (10^6 cells/sample) were stimulated with 0-50μg/ml anti-Ig for 4h. Cells were stained for surface expression with anti-kappa chain (1:50)-biotin+streptavidin-APC (1:100). Cell surface staining was followed by intracellular staining of the whole population (see *Materials and Methods* for full details). For negative staining control, only the secondary antibodies were used and all gates consisted of <1% of the cell population. Results are shown for kappa$^+$ cells only.

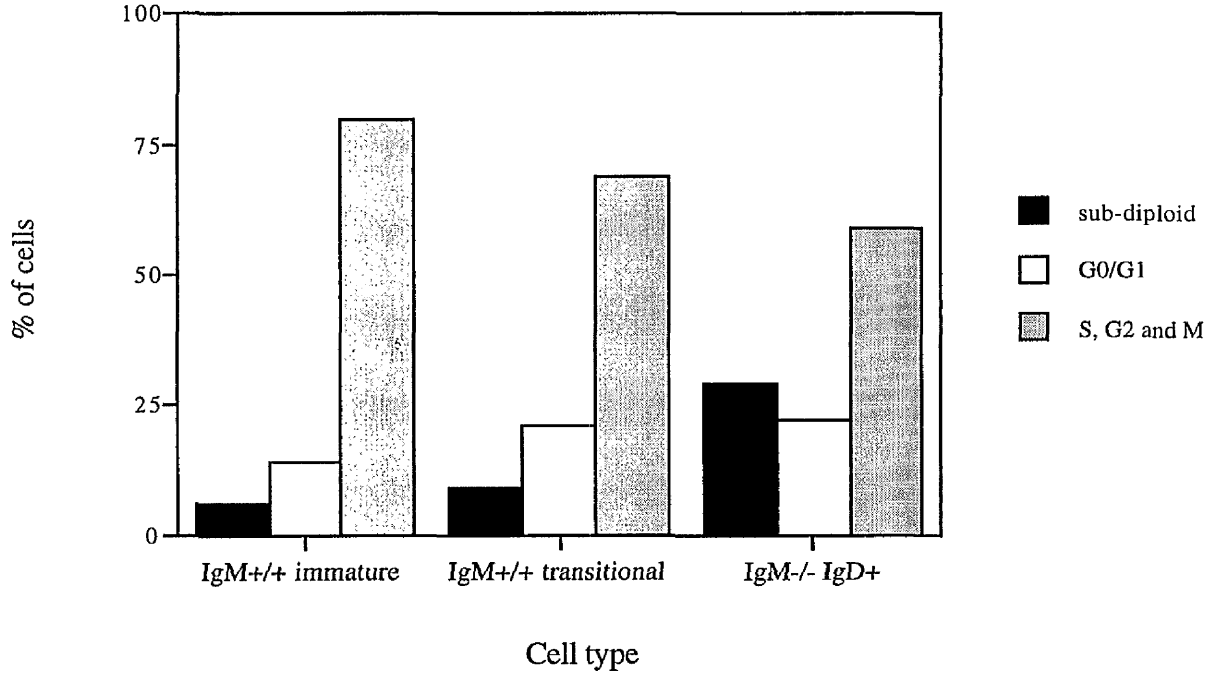
100
75
50
25
0
% of cells
IgM+/+ immature
IgM+/+ transitional
IgM-/- IgD+
Cell type
sub-diploid
G0/G1
S, G2 and M

Fig. 59

Figure 59: Bone marrow of WT and IgM$^{-/-}$ Balb/c mice. B cell populations from either WT or IgM$^{-/-}$ BALB/c mice were determined upon sacrifice by staining for surface expression with anti-delta chain (1:50)+anti-rat-IgG-FITC (1:100) and anti-kappa chain (1:50)-biotin+streptavidin-APC (1:100). After staining, cells were subjected to PI incorporation. For negative staining control, only the secondary antibodies were used and all gates consisted of <1% of the cell population. WT immature B cells were kappa^{+} delta^{-}, WT transitional cells: kappa^{lo} delta^{lo}, IgM$^{-/-}$ IgD^{+} cells: kappa^{+} delta^{+}. Cell cycle phases were determined by DNA content.

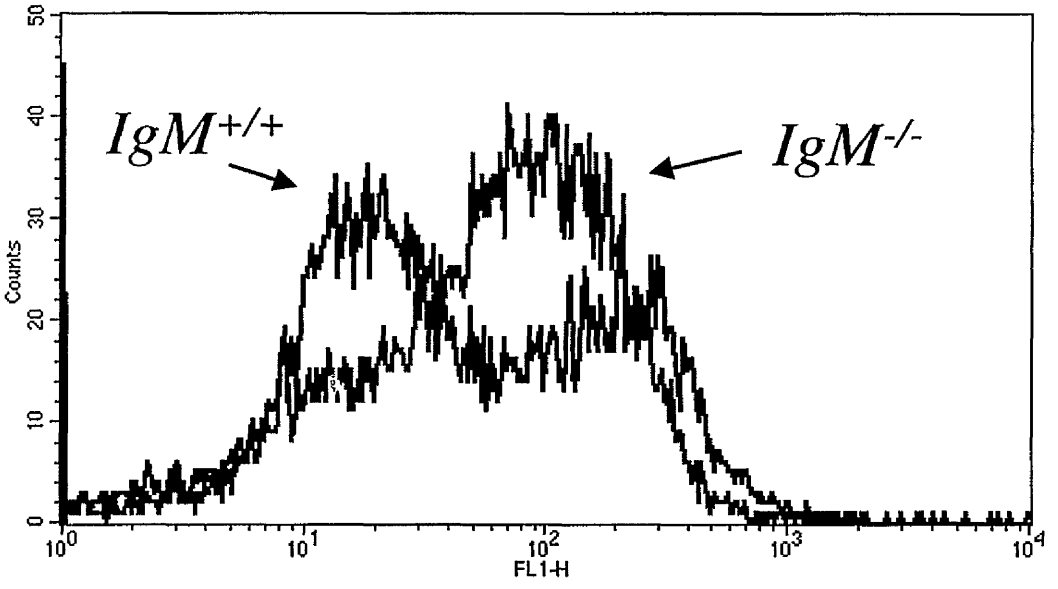

$DiOC_6$ (3) ⟶

Fig. 60

Figure 60: The mitochondrial potential of kappa$^+$ B cells during development in the absence of IgM. Bone marrow cells (10^6 cells/sample) from either WT or IgM$^{-/-}$ BALB/c mice stained upon sacrifice with anti-kappa chain (1:50)-biotin+streptavidin-APC (1:100) and then with 50nM of the mitochondrial dye $DiOC_6(3)$. The mitochondrial potential was determined by the mean fluorescence of the dye.

a.

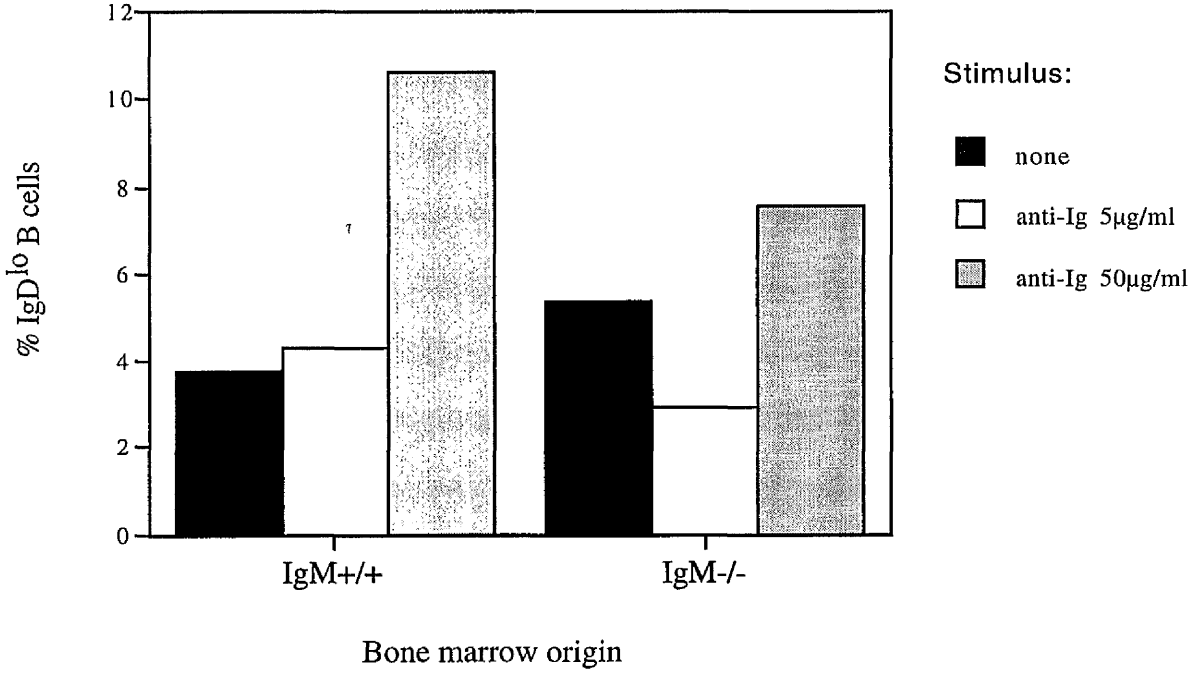
12
10
8
6
4
2
0
% IgD^lo B cells
IgM+/+
IgM-/-
Bone marrow origin
Stimulus:
none
anti-Ig 5µg/ml
anti-Ig 50µg/ml

b.

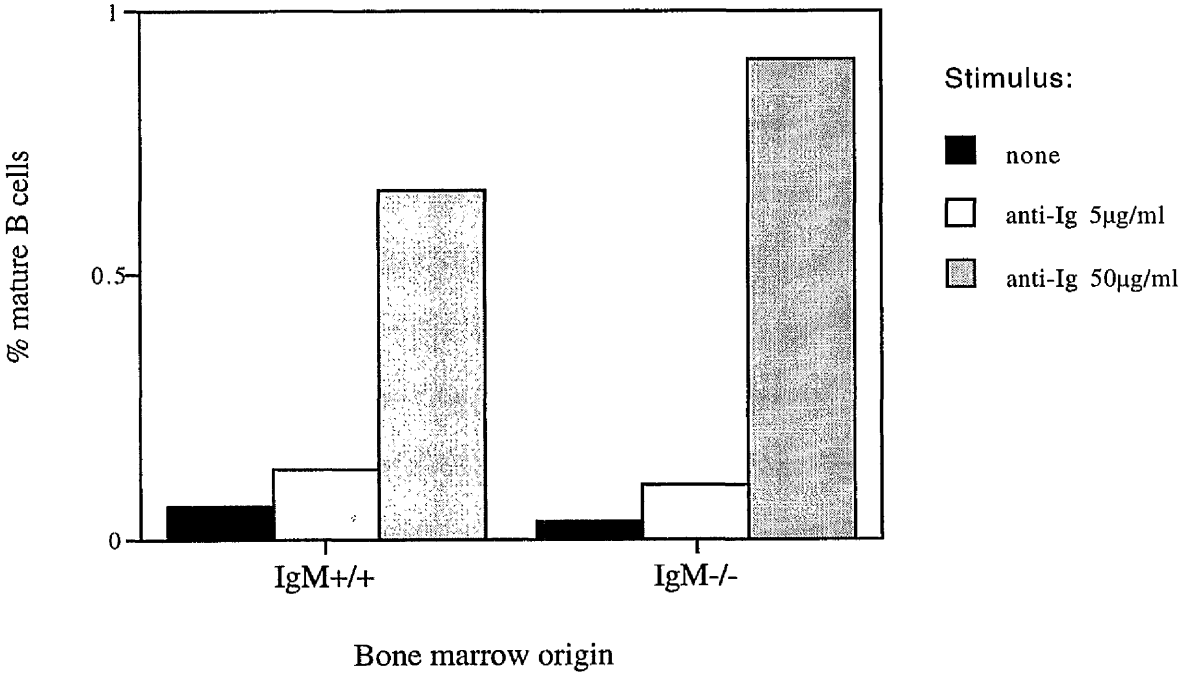
1
0.5
0
% mature B cells
IgM+/+
IgM-/-
Bone marrow origin
Stimulus:
none
anti-Ig 5µg/ml
anti-Ig 50µg/ml

Fig. 61

Figure 62: Effects of Caspase inhibition on recovery from BCR stimulation. Whole bone marrow cultures (10^6 cells/sample) from either WT or IgM $^{-/-}$ BÂLB/c mice were stimulated with 0-50µg/ml anti-Ig with or without 10µM Ac-DEVD-CHO for 2d. Cells were stained for surface expression with anti-delta chain (1:50)+anti-rat-IgG-FITC (1:100) and anti-B220-APC (1:50). Staining was followed by PI incorporation. Percentages are of the total bone marrow population. (a) Mature B cells were $B220^+$ IgD^{hi} cells. (b) Sub-diploidity of mature B cells was determined by DNA content (<2N). For negative staining control, only the secondary antibodies were used and all gates consisted of <1% of the cell population.

a.

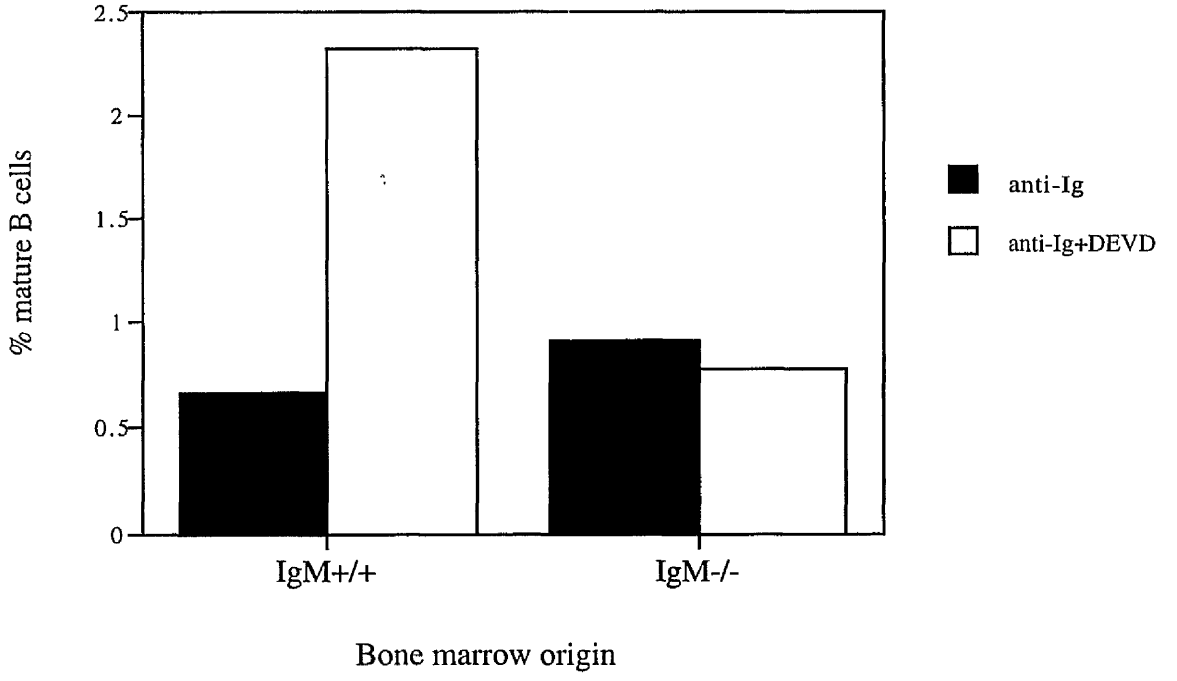
2.5
2
1.5
1
0.5
0
% mature B cells
IgM+/+
IgM-/-
Bone marrow origin
anti-Ig
anti-Ig+DEVD

b.

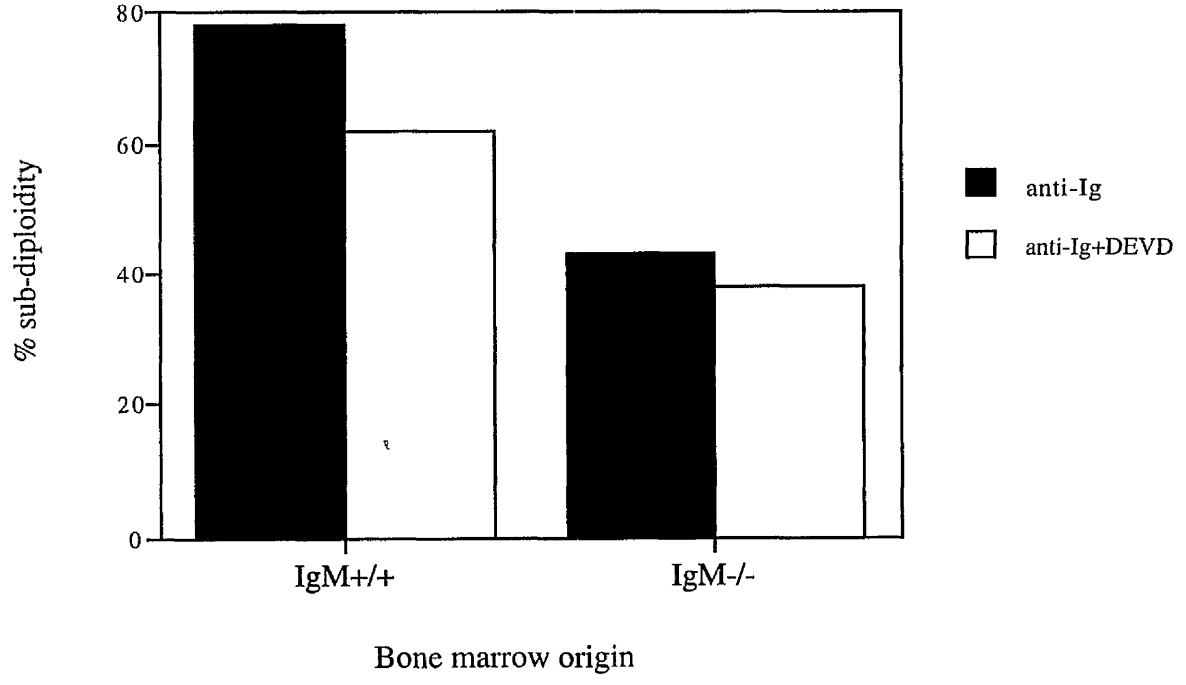
80
60
40
20
0
% sub-diploidity
IgM+/+
IgM-/-
Bone marrow origin
anti-Ig
anti-Ig+DEVD

Fig. 62

Figure 61: B cell development in IgM$^{-/-}$ Balb/c mice *ex vivo*. Whole bone marrow cultures (10^6 cells/sample) from either WT or IgM$^{-/-}$ BALB/c mice were stimulated with 0-50μg/ml anti-Ig for 2d. Cells were stained for surface expression with anti-delta chain (1:50)+anti-rat-IgG-FITC (1:100) and anti-B220-APC (1:50). IgD^{lo} cells were B220^{+} IgD^{lo}; mature B cells were B220^{+} IgD^{hi} cells. Percentages are of the total bone marrow population. For negative staining control, only the secondary antibodies were used and all gates consisted of <1% of the cell population.

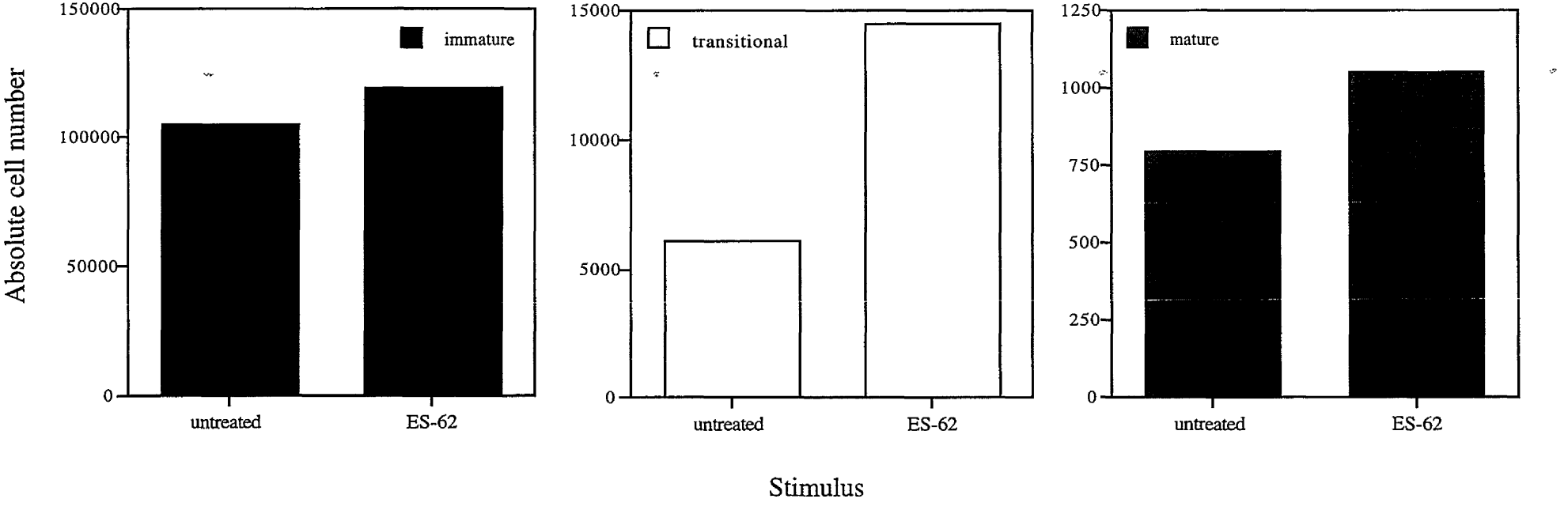
Absolute cell number
150000
100000
50000
0
immature
untreated
ES-62
15000
10000
5000
0
transitional
untreated
ES-62
1250
1000
750
500
250
0
mature
untreated
ES-62
Stimulus

Fig. 63

Figure 63: ES-62 supports the maintenance of all kappa$^+$ B cells in the bone marrow. Whole bone marrow cultures (10^6 cells/sample) were stimulated with 0-2μg/ml ES-62 for 2d. The total cell number of bone marrow cultures was determined by counting after stimulation. Cells were stained for surface expression with anti-delta chain (1:50)+anti-rat-IgG-FITC (1:100) and anti-kappa chain (1:50)-biotin+streptavidin-APC (1:100). For negative staining control, only the secondary antibodies were used and all gates consisted of <1% of the cell population.

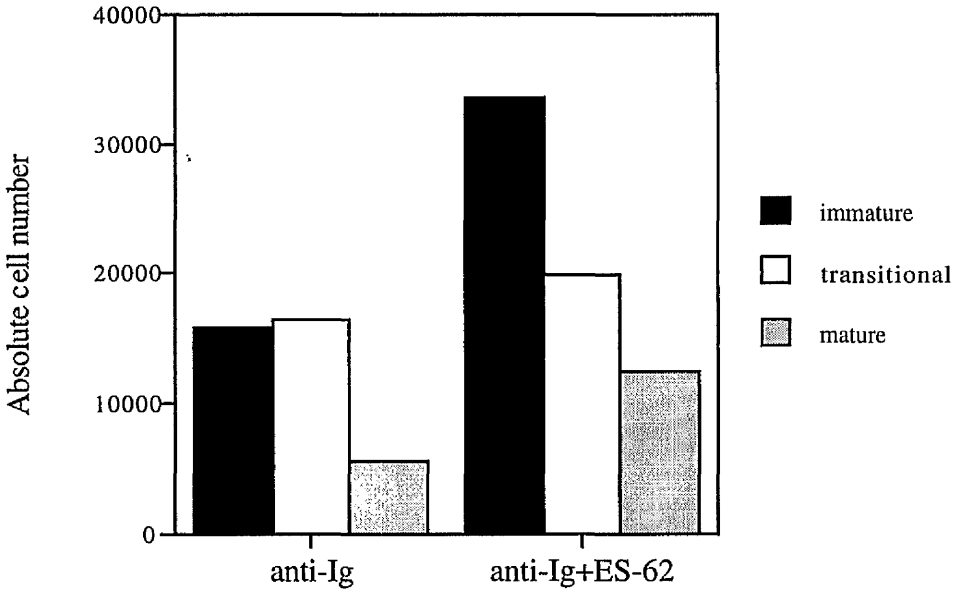
40000
30000
20000
10000
0
Absolute cell number
anti-Ig
anti-Ig+ES-62
immature
transitional
mature

Fig. 64

Figure 64: ES-62 synergises with anti-Ig to drive immature B cells into maturity. Whole bone marrow cultures (10^6 cells/sample) were stimulated with 50μg/ml anti-Ig with or without 2μg/ml ES-62 for 2d. The total cell number of bone marrow cultures was determined by counting after stimulation. Cells were stained for surface expression with anti-delta chain (1:50)+anti-rat-IgG-FITC (1:100) and anti-kappa chain (1:50)-biotin+streptavidin-APC (1:100). For negative staining control, only the secondary antibodies were used and all gates consisted of <1% of the cell population.

a.

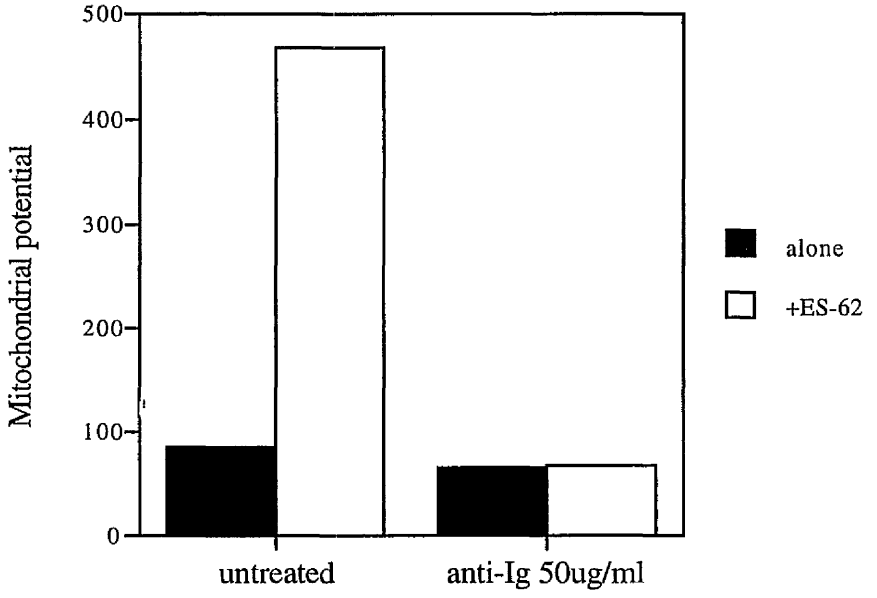
500
400
300
200
100
0
Mitochondrial potential
alone
+ES-62
untreated
anti-Ig 50ug/ml

b.

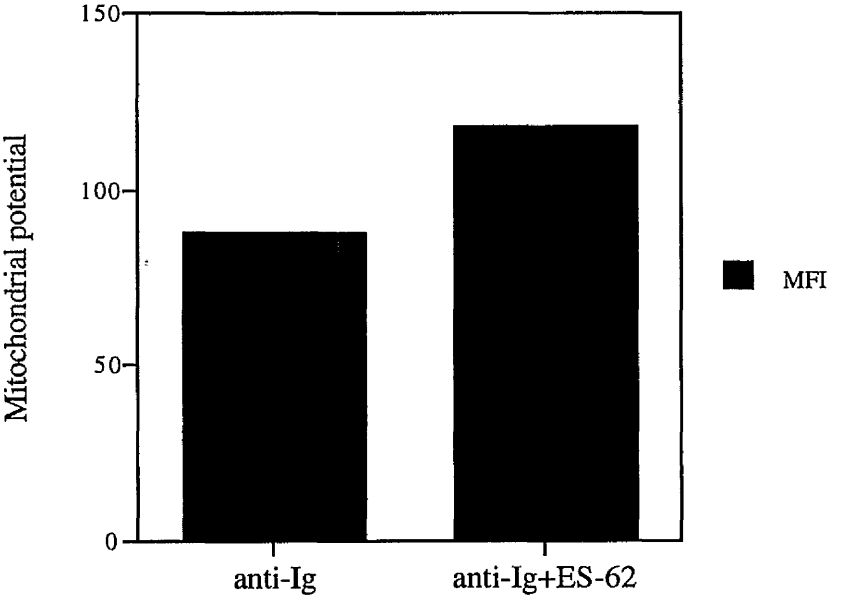
150
100
50
0
Mitochondrial potential
MFI
anti-Ig
anti-Ig+ES-62

Fig. 65

Figure 65: ES-62 increases the mitochondrial potential of kappa$^+$ B cells. Bone marrow cells (10^6 cells/sample) were stimulated with 0-50μg/ml anti-Ig with or without 2μg/ml ES-62 for 2d. Cells were stained with anti-kappa chain (1:50)-biotin+streptavidin-APC (1:100) and then with 50nM of the mitochondrial dye $DiOC_6(3)$. The mitochondrial potential was determined by the mean fluorescence of the dye and it is shown for (a) the whole kappa$^+$ population, or (b) for kappa^{hi} cells.

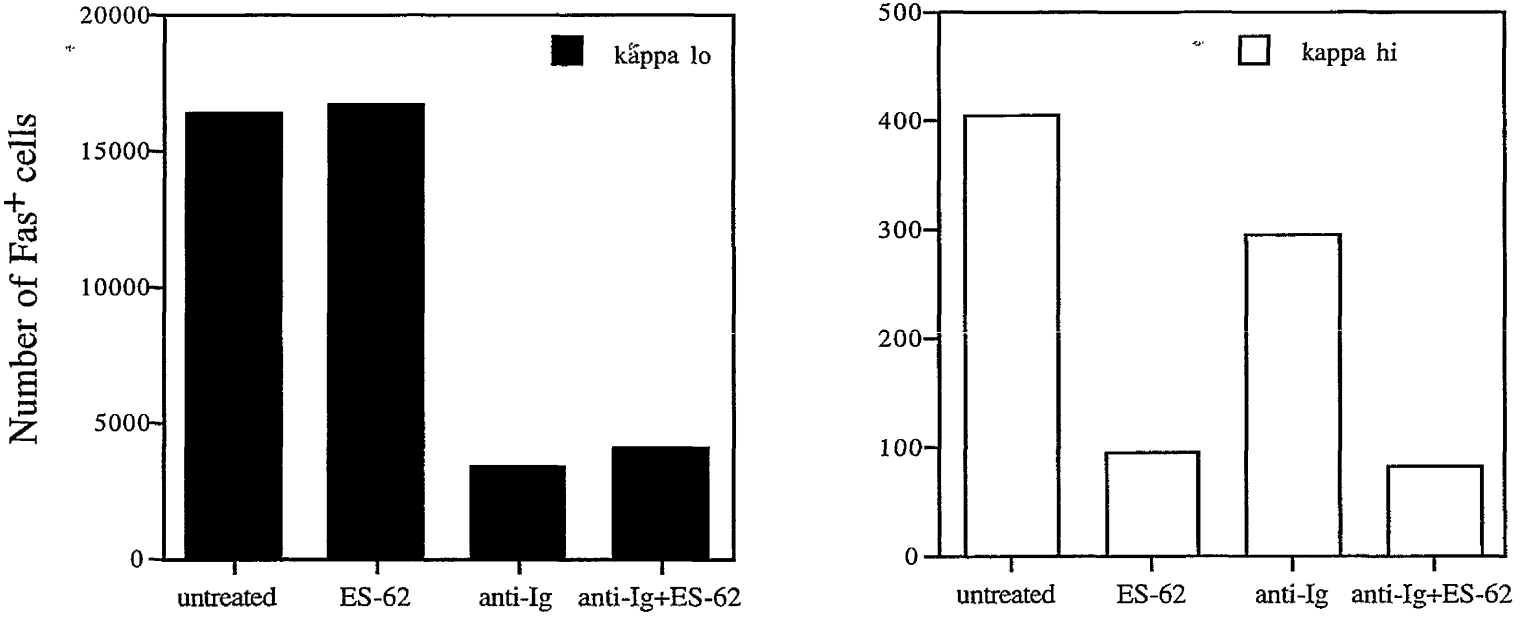
Number of Fas+ cells
20000
15000
10000
5000
0
kappa lo
untreated
ES-62
anti-Ig
anti-Ig+ES-62
500
400
300
200
100
0
kappa hi
untreated
ES-62
anti-Ig
anti-Ig+ES-62

Fig. 66

Figure 66: ES-62 has no effect on Fas expression in kappa$^+$ B cells. Whole bone marrow cultures (10^6 cells/sample) were stimulated with 0-50μg/ml anti-Ig with or without 2μg/ml ES-62 for 2d. The total cell number of bone marrow cultures was determined by counting after stimulation. Cells were stained for surface expression with anti-kappa chain (1:50)-biotin+streptavidin-APC (1:100) and anti-Fas (1:100)+anti-mouse Ig-FITC (1:100). For negative staining control, only the secondary antibodies were used and all gates consisted of <1% of the cell population.

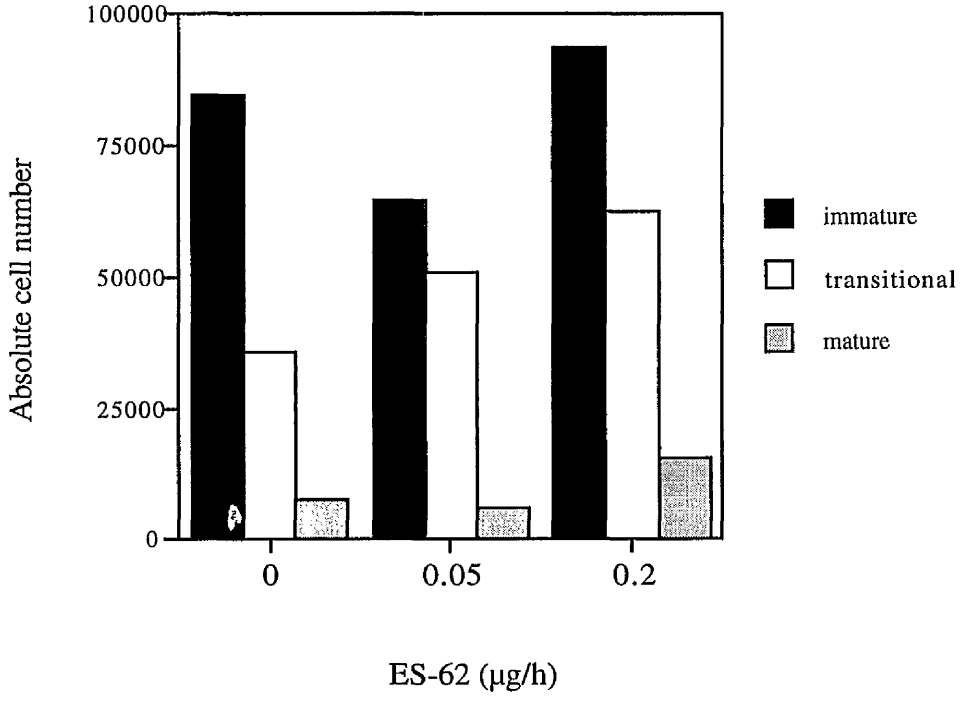
100000
75000
50000
25000
0
Absolute cell number
0
0.05
0.2
ES-62 (μg/h)
immature
transitional
mature

Fig. 67

Figure 67: Recovery from anti-Ig treatment of bone marrow cultures from ES-62 exposed mice. Whole bone marrow cultures (10^6 cells/sample) from mice treated continuously with ES-62 (0-0.2μg/h) were stimulated with 50μg/ml anti-Ig for 2d. The total cell number of bone marrow cultures was determined by counting after stimulation. Cells were stained for surface expression with anti-delta chain (1:50)+anti-rat-IgG-FITC (1:100) and anti-kappa chain (1:50)-biotin+streptavidin-APC (1:100). Immature B cells were kappa$^+$ delta$^-$, transitional cells: kappa^{lo} delta^{lo}, mature cells: kappa^{hi} delta^{hi}. For negative staining control, only the secondary antibodies were used and all gates consisted of <1% of the cell population.

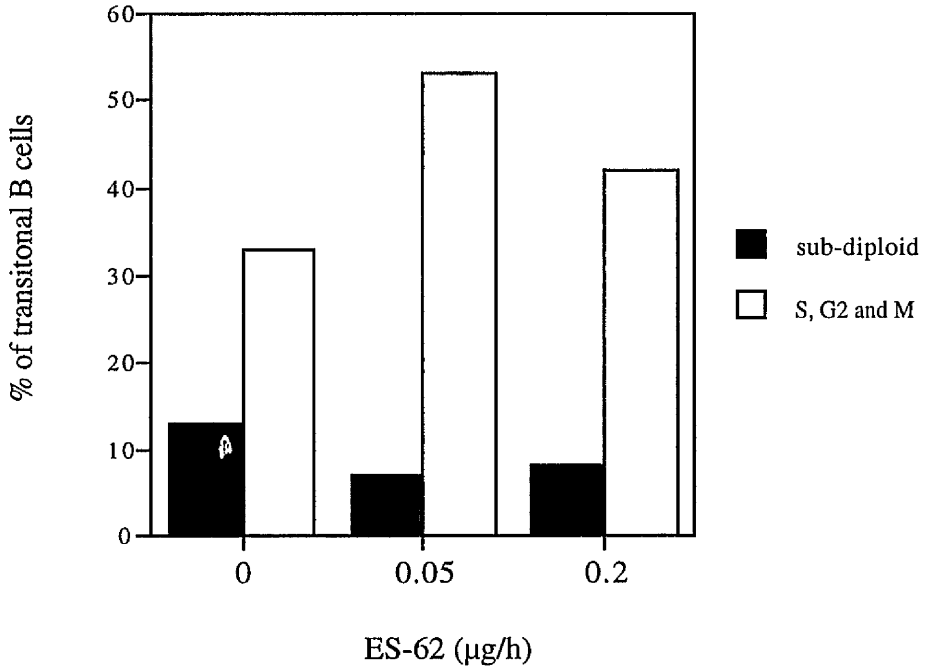
60
50
40
30
20
10
0
% of transitonal B cells
0
0.05
0.2
ES-62 (µg/h)
sub-diploid
S, G2 and M

Fig. 68

Figure 68: Death and proliferation of transitional B cells from ES-62 exposed mice in response to anti-Ig treatment. Whole bone marrow cultures (10^6 cells/sample) from mice exposed continuously with ES-62 (0-0.2µg/h) were stimulated with 50µg/ml anti-Ig for 2d. The total cell number of bone marrow cultures was determined by counting after stimulation. Cells were stained for surface expression with anti-delta chain (1:50)+anti-rat-IgG-FITC (1:100) and anti-kappa chain–biotin (1:50)+streptavidin-APC (1:100). After staining, cells were subjected for PI incorporation. For negative staining control, only the secondary antibodies were used and all gates consisted of <1% of the cell population. Sub-diploidity and hyper-ploidity was determined by DNA content of kappa$^+$ delta^{lo} (transitional B) cells.

Chapter 5. SITE-SPECIFIC EFFECTS OF B CELL STIMULI ON CELL FATE

5.1 Introduction

In peripheral lymphoid tissues (e.g., the spleen and the lymph nodes), the population of B lymphocytes is dynamically maintained. A balance is achieved between the continuous output of B cells from the bone marrow and their proliferation in response to antigen and the terminal differentiation and death of effector B cells. The choices between the alternative fates of proliferation, differentiation and death are largely determined by intracellular signalling cascades triggered by receptor-ligand interactions, with the B cell receptor being a central regulator of B cell fate. BCR signalling is required for survival and recirculation of naive B cells as well as for antigen-specific immune responses [15, 23, 29]. Ligation of the BCR by antigen can have various outcomes in different contexts, including proliferation, differentiation, anergy or apoptosis (reviewed in [11, 17, 302]). There are at least three distinct mechanisms by which BCR ligation can lead to such different consequences:

(i) The affinity and valency of the antigen can affect the response by leading to different degrees of receptor aggregation and consequently differences in signal quantity and perhaps quality.

(ii) The immunological context of antigen encounter can influence the outcome by differential engagement of B cell co-receptors such as CD19 and CD40. These co-receptors can act by directly modifying events in BCR signalling pathways or by activating additional signalling pathways which influence the outcome of BCR signalling. Such a situation is exemplified by T cell help during the Germinal Centre reaction.

(iii) The outcome of BCR ligation may be regulated by activation or differentiation stage-specific changes in the expression or cross-talk of signalling cascades.

The significance of the regulatory mechanisms controlling B cell responses is illustrated by findings that dysregulation of B cell activation

pathways can lead to immunodeficiency, autoimmune and lymphoproliferative disorders, leukemias or lymphomas [146]. The scope of this chapter was to extend the *ex vivo* model of development outlined in chapter 4 and to explore both similarities and differences between the responses of mature B cells in various developmental and immunological contexts.

Traditionally, the measurement of B cell activation is performed by [^{3}H] thymidine incorporation of primary cells in response to *in vitro* stimulation. This method has several limitations: (i) it does not take into account the fact that many B cells are dying immediately upon activation (see below); (2) DNA synthesis of the whole population could not discriminate between a variety of B cells, most notably, those in the Germinal Centre (GC) and those outside of the GCs, which exhibit differential responses to antigen [22]; (3) The widely used time point for incorporation measurements is at its peak (around 48h, including in this study), an obvious restriction in the understanding of activation kinetics. To address these limitations, where possible, different aspects of the B cell response in the periphery were examined. Flow cytometry was used to discriminate between distinct B cell populations, when CD19 is used as a pan-B cell marker in most of the experiments. The other widely used pan-B cell marker, B220 (CD45R), proved in many cases to be unreliable, presumably due to the phenomenon of B220 downregulation in certain types of peripheral B cells, as reported very recently [316].

The aims of the studies described in this chapter were as follows:
(i) To characterise the differences in response to BCR stimulation between different populations of peripheral B cells - in the spleen, the lymph nodes and the peritoneal cavity.
(ii) To establish the nature of the primary and secondary responses to antigen and to compare the behaviour of Germinal Center and non-Germinal Center B cells.
(iii) To define the role of some signalling components (IgM, Btk etc.) in the processes described above.

5.2 Characterisation of peripheral B cell populations

Using flow cytometry it is clear that, post-sacrifice, splenic and lymph node B cells differ in their proliferation rate - more B cells in the lymph nodes are proliferating without any exogenous stimulation (fig. 69). This phenomenon can be explained by the fact that the mice used in this work were not kept in a pathogen-free animal house and the Germinal Centre content of the lymph nodes was rarely below 5% of the B cell population and always higher than that observed in the spleen. It is possible that differences in antigen circulation result in greater exposure of B cells in the lymph nodes to antigen and therefore results in more proliferation and generation of GCs than in the spleen.

Activation of peripheral B cells, either purified B cells or the whole population of splenocytes, can be easily demonstrated *in vitro* following stimulation with $F(ab')_2$ fragments of anti-Ig antibodies, with or without anti-CD40 and recombinant IL-4, using [^{3}H] thymidine incorporation (fig. 70) or cell cycle analysis (fig. 71) after 48h stimulation. These results show the benefit outlined above of using these two methods in parallel - relatively subtle change in the percentage of proliferating cells (i.e. in S, G_2 and M phases) is reflected by a 6-7-fold increase in [^{3}H] thymidine incorporation. The differences between splenic and lymph node B cells are also apparent when examining the cell cycle profile of these cells in response to 24h anti-Ig stimulation *in vitro* (fig. 72).

Moreover, the Germinal Centre B cell population behaves differently in its response to antigen challenge than the rest of follicular B cells, presumably due to the process of affinity maturation [22]. Discrimination between Germinal Centre B cells and non-GC B cells is essential in order to study their unique responses. GC B cells express a marker which can be stained specifically by peanut agglutinin (PNA), a marker widely used to identify them [20]. In fig. 73, it is shown how throughout studies of primary and secondary responses, GC B cells were identified as $CD19^+$

PNA$^+$ and were compared to the non-GC population (CD19$^+$ PNA$^-$) in applications such as determination of cell cycle profiles.

Mature peripheral B cells are IgM$^+$ IgD^{hi} [6] and they lose their surface Ig expression while entering the Germinal Centre to become centroblasts [22]. The expansion of the IgD^{hi} population within isolated B cells is easily detectable within 48h (fig. 74). Interestingly, at first sight, T cell co-stimulation as mimicked by anti-CD40 or IL-4 does not appear as effective as anti-Ig treatment in inducing IgD^{hi} B cells. It is possible, though, that these cells had expanded faster than B cells treated only with anti-Ig and already lost their surface IgD to become Germinal Centre B cells [317]. Although *in vitro* stimulation of Germinal Centre B cells triggers their expansion (fig. 75), this response is accompanied by enhanced cell death (fig. 76).

5.3 The primary response to antigen in the periphery

The transgenic mice model MD4 has been proved useful in investigating a variety of responses of peripheral B cells [318, 319]. In these mice a large percentage of B cells are specific for an epitope from the chicken egg lysozyme (HEL) [320]. Fig. 77 shows how whole spleen and lymph nodes cultures from these mice respond to anti-Ig treatment. Although B cells from both sites have maximum proliferation at 50µg/ml anti-Ig, lymph node B cells can be stimulated even by the lowest concentrations of anti-Ig tested (0.5-5µg/ml). Furthermore, the extent of BCR-induced proliferation of B cells from the lymph nodes is always greater than in splenic B cells ($n=3$; typically ~20-Fold *vs.* Control in the lymph nodes and only up to 10-fold in the spleen).

Responses to specific/partially-specific antigen also vary between the spleen and lymph nodes. In the spleen, specific stimulation with HEL achieves maximal levels of DNA synthesis around 1µg/ml HEL and plateaus over the range of 1-100µg/ml HEL (fig. 77a). An almost as effective stimulation can be achieved using the duck egg lysozyme (DEL) - an antigen with predicted 2000-fold less affinity to the transgenic BCR

in these mice [321]. The peak of the response to DEL in the spleen is around 10μg/ml, surprisingly close to the HEL concentration. Cell cycle analysis allowed to determine which type of B cells were proliferating in response to these different antigens. Almost all treatments induced proliferation in both non-GC and GC B cells, although anti-Ig was best in inducing GC B cell numbers (fig. 78a). Due to this proliferation in both B cell populations, all treatments had a limited success in raising the proportion of GC B cells (cf. 21% GC B cells, out of total B cells, in control and 29-36% in other treatments).

A different dose response to specific antigens was revealed in the lymph nodes (fig. 77b). Here, the response to HEL peaks at 1-10μg/ml and declines at higher concentrations. A similar stimulation by DEL requires at least ten-fold higher concentration (100μg/ml), but it is not as effective as is in the spleen (cf. 70±6% of HEL peak response in lymph nodes and 88±2% of response in the spleen). Cell cycle profiles together with CD19/PNA staining were used to show a distinct response in the lymph nodes, for both non-GC and GC B cells. The expansion of lymph node GC B cells in response to HEL is much more substantial than in the spleen (cf. 3.6-fold of control in lymph nodes and 1.3-fold in the spleen). DEL was, at least, as effective as HEL in inducing total B cell numbers and GC B cell numbers (fig. 78b). Nonetheless, non-GC B cells proliferated less than control by 48h post-stimulation with HEL and DEL (17% of control cells in S, G_2 and M phases, 20-22% of anti-Ig treated cells and 6-11% in HEL or DEL treated cells).

Taken together, these results show that peripheral B cells, non-GC and GC, differ in their responses in the spleen and the lymph nodes. Therefore, the possibility that differences in the responses of peripheral B cells at these sites is solely a function of the GC B cell content in the whole population of the tissue, is excluded.

5.4 Molecular features of Germinal Centre B cells

5.4.1 Changes in the mitochondrial potential in response to BCR stimulation

Resting splenic B cells elevate their mitochondrial potential in response to various stimuli (fig. 79). This elevation, which reflects an increase in ATP production, is necessary for the enlargement in cell size which is part of lymphocyte activation [322]. One of the main features of GC B is that, in contrast to activated naive B cells, these cells have their mitochondrial membrane potential reduced in response to BCR stimulation, similarly to the immature B cell line, WEHI-231 (fig. 80). In addition and in contrast to immature B cells, IL-4 or Caspase inhibition can block in GC B cells the reduction in $\Delta\Psi_m$. It is now well established that BCR-induced apoptosis in Germinal Centre B cells is mitochondria- and Caspase-dependent [275].

5.4.2 CD19 surface expression

Induction of B cell expansion by polyclonal anti-Ig treatment is paralleled by induction of the B cell marker CD19. This co-stimulatory molecule is widely acknowledged as taking part in determining the threshold for BCR signalling, presumably by promoting cell activation [21]. As shown in figure 81, CD19 surface expression is enhanced by anti-Ig treatment of B cells in lymph node and spleen. This increase is surprising because over-expression of CD19 expression has been reported to lead to autoantibody production [318]. The difference in CD19 expression is even more striking when comparing GC and non-GC B cells, where the increase in CD19 surface expression is more profound in GC B cells than in their counterparts in both spleen (fig. 82) and lymph nodes (similar results not shown).

5.4.3 The role of Btk

The tyrosine kinase Btk has been suggested as an important integrator of proliferative signals downstream of both the BCR and CD19 [146]. Xid

mice are therefore a useful model for estimating the role of Btk in BCR stimulation. In these mice, males are Btk deficient whilst females, which carry a dominant normal allele and a defective allele, are healthy. Hence, these mice enable direct comparison of B cell responses on the same genetic background. Upon sacrifice, male Xid mice were found, as expected, to have reduced numbers of B cells ($15.5x10^6$ per spleen of $Btk^{-/-}$ males in comparison to $19.4x10^6$ cells in $Btk^{+/+}$ females) and virtually no GC B cells (1.5% of total splenic B cells in males *vs.* 9% in females). In proliferation assays, as previously published, spleen cultures from Xid mice show a very limited response to BCR stimulation (fig. 83 and not shown). When examining the responses to anti-Ig stimulation, albeit absolute numbers were still about 60% less, it is clear that GC B cell expansion (50µg/ml anti-Ig *vs.* untreated) has increased slightly in Btk deficient mice (cf. 6.2-fold in cells derived from Xid male mice and 5.2-fold increase in cells from female mice; fig. 83). In contrast, non-GC B cells expanded substantially less in cultures from male mice than in female littermates (2.3-fold and 3.7-fold, respectively). Absolute numbers of non-GC $Btk^{-/-}$ B cells after treatment with anti-Ig were ~50% of the number in cultures derived from female mice. Taken together, $Btk^{-/-}$ derived splenic B cells exhibit dysfunctional responses to BCR stimulation when as a whole they expand to a lesser extent than their $Btk^{+/+}$ counterparts. Nonetheless, this overall phenomenon can be carefully dissected into two trends: (i) non-GC $Btk^{-/-}$ B cells respond poorly to antigen; and (ii) the few existing $Btk^{-/-}$ GC cells respond better than wildtype cells. Therefore, it is feasible that the small number of GC cells present in Xid mice is simply due to low cellularity of the follicular compartment as a whole. Hence, Btk may play a restrictive role in GC B cell responses, similar to that observed for immature B cells in section 4.6. In both cases, hyper-responsiveness to BCR cross-linking is observed in the Btk deficient cells. Importantly, this role for Btk may be independent of CD19 surface expression. The expression profiles of CD19, before and after BCR stimulation, for both non-GC and GC B cells of Xid mice were similar to those of wildtype mice (not shown). Therefore, Btk may part of an alternative pathway, CD19-independent, which detemines the threshold for BCR activation.

5.5 Role for Fas in the Germinal Centre reaction

The mechanisms that underly selection of B cells during the Germinal Centre reaction are poorly understood. One suggestion, is that B cells are undergoing activation-induced cell death (AICD) similar to that observed with T cells [25, 323]. Moreover, about half of GC B cells express Fas on their surface (not shown) and therefore are susceptible for induction of apoptosis by FasL expressed on activated T cells [18].

Lymph node cultures from *lpr* ($Fas^{-/-}$) mouse were utilised to examine the possibility of AICR in B cells, in light of the conceivable FasL-Fas interactions between T and B cells. In *lpr* cultures, a higher dose of BCR stimulation (50µg/ml instead of 5µg/ml) was needed in order to effectively increase the relative proportion of GC B cells in the B cell population relative to that seen in WT B cells (fig. 84; see also fig. 75). In addition, for as yet unknown reason, the response to anti-Ig stimulation in non-GC cells from lpr mice is also impaired (fig. 84). However, treatment with anti-Ig plus anti-CD40 induced stronger proliferation of GC B cells in $Fas^{-/-}$ cultures than in wildtype B cells (not shown).

Fas expression may also be linked to the observed mitochondrial events in GC B cells [324]. Fas could thus alter B cell survival in the Germinal Centres, in order to terminate activation. This possiblity was supported by the fact that a long time was needed for reduction in the mitochondrial potential in response to BCR stimulation in GC B cells, enabling changes in Fas expression. If Fas plays a part in such a scenario, then Caspase inhibition may not enhance GC B cell survival.

The Caspase inhibitor Ac-DEVD-CHO, in synergy with anti-Ig treatment, was capable of enhancing GC B cells expantion in reponse to BCR stimulation (fig. 84). Therefore, it is likely that Fas-induced apoptosis of GC B cells does not utilise a mitochondria-dependent pathway, as described in other cells [299].

5.6 The role of IgM in Germinal Centre formation

In certain $IgM^{-/-}$ mice, a deletion of the Cμ region and the μ-δ intron enforces the expression of IgD instead of IgM (see also section 4.7), a change reported to allow normal B cell development [5]. These transgenic mice were used to examine if IgM expression is absolutely essential for B cell activation or whether development driven by IgM can be fully substituted by expression of IgD.

5.6.1 The $IgM^{-/-}$ Spleen

Although the total cellularity of spleens from both $IgM^{+/+}$ and $IgM^{-/-}$ mice has been found to be similar, B cell numbers are reduced by about 40%. The cell cycle profiles of all the B cell sub-populations examined could not provide a full explanation to these differences (fig. 85). However, it clear that there is a greater ratio of apoptosis of both non-GC and GC B cells and more GC B cells are found in G_0/G_1 in $IgM^{-/-}$ mice, compared to B cells derived from WT mice. Moreover, the pattern of expansion of IgD^- B cells, which presumably represent GC B cells, was quite different than that observed with normal B cells. Firstly, it required a higher dose of anti-Ig (50μg/ml) in order to achieve a short-lived 64% expansion of B cells from $IgM^{-/-}$ mice, in comparison to untreated cells, after 24h. Moreover, this exapansion was abolished after 48h. In comparison, $IgM^{+/+}$ cells needed less BCR stimulation (5μg/ml anti-Ig) and after 48h showed 143% expansion in the IgD^- sub-population. Interestingly, in both spleen and lymph nodes, a notable expansion in IgD^+ cells is observed as well (not shown). These data were supported by analysis of DNA synthesis, which was largely reduced, relative to WT cells (fig. 86a). Indeed, in both spleen and lymph nodes preparations, no proliferation was observed in response to anti-Ig. However, proliferation was observed in response to anti-Ig plus anti-CD40, LPS (spleen and lymph nodes) and also to anti-Ig plus IL-4 as anti-CD40 alone (lymph nodes only). These results suggest that $IgM^{-/-}$ peripheral B cells are defective in activation responses via the BCR.

5.6.2 $IgM^{-/-}$ Lymph nodes

The $IgM^{-/-}$ knock-out animals have a higher percentage of B cells in their lymph nodes (cf. 30% in $IgM^{-/-}$ mice and 20% in wildtype), although the difference in total number of B cells (about 2% less in KO) was within the accuracy of counting. This presumably because in the overall B lymphocyte population, less cell death was apparent than in wild-type. Although the proportions of Germinal Centre B cells to total B cells were maintained, $IgM^{-/-}$ non-GC cells were found to be G_0/G_1 arrested but were not as apoptotic as in control littermates (fig. 87). This phenomena was presumably compensated by the fact that non-GC B cells were more prone to proliferate (cf. 84% of KO cells in S, G_2 and M phase and 63% of wildtype cells). Surprisingly, a high dose of anti-Ig, which drives KO cells to expand, seemed to encourage more proliferation in IgD^- cells and more death in IgD^+ cells (fig. 88). This observation can be explained by loss of IgD expression during proliferation of IgD^+ B cells.

In thymidine incorporation assays, as discussed above, the response to anti-Ig was largely impaired with only 5-fold increase in DNA synthesis (Fig. 86b), while the normal response is in the range of 20-100-fold. Responses to co-stimulation with IL-4 and anti-CD40 (with or without anti-Ig) treatments were intact.

5.7 The secondary response to antigen

5.7.1 Changes in antibody specificity

HEL-BCR MD4 mice were used to examine how the secondary response to a specific antigen differs from the primary response. Mice were immunised with either 100μg HEL or DEL, or PBS and after 8d whole spleen and lymph node cultures were examined for *in vitro* proliferative response to antigens. Induction of GC reaction, as observed by flow cytometry upon sacrifice, was evident only with HEL immunisation (fig. 89). Unexpectedly, given the the response to DEL observed *in vivo*, DEL immunisation has increased the number of non-GC B cells but not these of GC B cells.

In the spleen, immunisation with either HEL or DEL improved the response to subsequent HEL stimulation *in vitro*. The proliferative response peaked at 0.1µg/ml HEL, rather than 1µg/ml in PBS control, therefore showing the expected lowering of threshold for activation by antigen (fig. 90). Interestingly, immunisation with DEL or HEL improved the proliferative response *in vitro* to DEL, in comparison to PBS control. Nonetheless, this response has peaked at the same concentration (10µg/ml DEL) as the control. This was also reflected by the distribution of B cells (fig. 91). Interestingly, after 2d culture without further stimulation, the percentage of GC B cells in the B cell population has equalised in cultures from all mice. The basis to this phenomenon is unclear, but may result from apoptosis of GC B cells from the HEL immunised mice.

The lymph node response after immunisation differed from that of the spleen, in a number of aspects. DEL immunisation has reduced dramatically the proliferative response to HEL *in vitro* (maximum HEL-induced proliferation in PBS: 81-fold of untreated, in DEL immunised: 7-fold). In contrast, HEL immunisation increased the proliferative response to HEL by about 3-fold, in comparison to PBS (236-fold increase *vs.* untreated). Taken together, these observations suggest that DEL immunisation has caused tolerance to HEL in the lymph nodes, presumably via affinity maturation to DEL specificity in the Germinal Centres.

HEL immunisation *in vivo* lead to a massive induction of GC reaction - about 50% of B cells were PNA^+ and CD19 expression was elevated (not shown). Similarly to the spleen, immunisation with either HEL or DEL improved the sensitivity to DEL stimulation - the proliferative response peaked in 10µg/ml in comparison to 100µg/ml in PBS, although HEL immunisation performed better than DEL (fig. 92). These finding were also confirmed by CD19/PNA staining (not shown). This evidence suggest again, that induction of affinity maturation is possible here and leads to changes in secondary *in vitro* stimulations.

5.7.2 The secondary response after ES-62 priming

ES-62, a phosphorylcholine containing glyco-protein secreted by the parasite *A. viteae*, is a useful model for the induction of Th2-type responses [311]. Treatment of mice with ES-62 leads to the induction of Germinal Centre reaction *in vivo*, in a dose dependent manner (fig. 93).
The proliferation of B cells from the spleens of ES-62 treated mice, in response to anti-Ig stimulation, is suppressed in comparison to mice treated with PBS (fig. 94). This effect is largely dependent on the dose of ES-62 in the lymph nodes (fig. 95). Since BCR-induced cell death of Germinal Centre B cells can be blocked by Caspase inhibition (see above), the wide-range Caspase inhibitor zVAD-fmk was employed to determine whether it could block the suppression of proliferation by ES-62. Surprisingly, zVAD-fmk has no effect in either the spleen or the lymph nodes (figs. 94-95). These results were corroborated by cell cycle analysis of *in vitro* spleen cultures. In the lower dose of ES-62 treatment (5μg/h) apoptosis was suppressed and proliferation enhanced (fig. 96), although BCR-stimulation had only marginal effects on proliferation as observed in the thymidine incorporation assays (fig. 94). In contrast, at the higher dose of ES-62 (2μg/h), apoptosis was enhanced by anti-Ig treatment (fig. 96). Although zVAD-fmk addition did not improve proliferation (fig. 94), this evidence suggest that Caspase inhibition, although blocking GC B cell apoptosis, is not sufficient to overcome growth arrest.

5.8 B cell responses in the peritoneal cavity

5.8.1 BCR stimulations of B-1 cells

The role of BCR stimulation of B cells in the peritoneal cavity (mostly Mac-1^+ B-1 cells) is unclear [36]. B-1 cells are thought to be self-renewing. B-1 cells are thought to be especially important for the rapid responses to infections in neonatals, by virtue of their specificity to multivalent antigens such as LPS [38]. The broad specificities of B-1 cells may cross-react with selfantigens and are thought to contribute to the development of autoimmunity. Therefore, it was of interest to compare the responses of B-1 cells to B cells present at other lymphoid sites.

Despite the proposal that B cells are self-renewing, whilst untreated B-1 cells appear to proliferate, they do not appear to do so more substantially than any other peripheral B cells (as determined by DNA synthesis; fig. 97). B-1 cell survival in culture, however, is much improved in the presence of the rest of the peritoneal wash (cf. 17% sub-diploid in untreated cells after 24h and 2% in presence of the rest of the wash). This observation may hint at some undocumented support by other cells, most likely to be macrophages which are by far the largest population in this cavity [186]. B-1 cells, however, do proliferate in response to anti-Ig treatment, although DNA synthesis measurement shows clearly that this response is poor in comparison to splenic B cells, for example (5-fold increase in thymidine incorporation of B-1 cells and up to 20-fold in isolated splenic B-2 cells). Stimulation via the BCR does not lead to a vast expansion of these cells, presumably since many of them in fact die in response to this treatment (fig. 98). This death is Caspase-dependent since co-culture with zVAD-fmk prevents BCR-induced apoptosis to B-1 cells (see below).

However, treatment with anti-CD40 and a low dose of anti-Ig was found to be an efficient stimulus of DNA synthesis, similarly to other peripheral B cells (fig. 97). Moreover, in agreement with their supposed role at the front line of anti-bacterial activity [6], LPS also serves as a strong proliferative signal for B-1 cells (not shown).

ES-62, the parasite-derived glycoprotein, contains phosphorylcholine, a natural epitope for B-1 cells [6] and therefore useful in examining *in vivo* responses of B-1 cells. B-1 cell numbers were found to be slightly reduced by *in vivo* exposure to ES-62 (not shown). B-1 cells from ES-62 treated mice were proliferating more profoundly in the absence of any stimuli (up to 50-fold increase in thymidine incorporation). However, responses to anti-Ig stimulations *in vitro* were relatively lower (cf. 12-fold increase in thymidine incorporaion PBS control and 1.6- to 2.8-fold in cells from ES-62 treated mice), presumably because these cells were already fully activated by the parasite product.

Rresponses to BCR stimulation could be enhanced by Caspase inhibition (fig. 99). This evidence suggests antigen exposed B-1 cells have only a restricted ability to respond to secondary BCR stimulation. The

involvement of Caspases in BCR signalling resembles transitional B cells and supports a possible developmental link between them [17].

5.8.2 Molecular factors determining B-1 cell responses

Both Btk and IgM expression and function are thought to be crucial for B-1 cell development. Consistent with this, B-1 cell number in the peritoneal cavity of $IgM^{-/-}$ mice (essentially IgD^{+} B-1 cells [5]) is ~60% of that of WT mice. Interestingly, these cells exhibit remarkably less apoptosis (cf. 10% and 24%, respectively). The cell cycle profile of living cells was mainly unchanged in comparison to wild-type IgM^{+} B-1 cells. Although thymidine incorporation in untreated cells was poor, the response of $IgM^{-/-}$ B-1 cells to anti-Ig treatment alone was normal (about 5-fold increase in comparison to control). Anti-CD40 plus anti-Ig treatment, however, did not lead to a significant induction of proliferation (cf. ~20-Fold increase *vs.* control in WT and 5-fold increase in $IgM^{-/-}$ mice; fig. 100). Moreover, anti-Ig stimulation was not enhanced by the Caspase inhibitor, Ac-DEVD-CHO. This differential response to Caspase inhibition in $IgM^{-/-}$ and WT B-1 cells, resembles that of the loss of Caspase regulation of $IgM^{-/-}$ transitional B cell expansion (section 4.6). Taken together, these results imply that IgD cannot fully subtitute for IgM in B-1 cells, a finding, which may be in agreement with the well known differences in the signalling pathways these different Ig isoforms are known to utilise [14]. Moreover, it provides futher evidence to the similarities between B-1 cells and transitional B cells.

Perhaps as expected, Btk deficient peritoneal cavity B cells (from male Xid mice) had no sustainable proliferative response to BCR simulation and although initially their numbers rose (by about 50% after 24hr) by 48h most of the cells were gone (fig. 101 and not shown).

5.9 Discussion

It has become clearer recently that the various B cell populations in the periphery require different stimuli to move between lymphoid compartments and to respond to immunogenic challenge [18, 146]. Thus, in the spleen and the lymph nodes, naive follicular B cells were compared to Germinal Centre B cells, and results in both population were related to the requirements of B-1 cells.

The GC B cell population differ in its BCR responses in comparison to resting peripheral B cells, undergoing affinity maturation and expansion of specific B cell clones [325]. This process is linked to the GC environment - GC B cell selection utilises additional signals received from T and dendritic cells, such as CD40L and IL-4 receptor ligation [326]. The behaviour of B-1 cells is less understood. These cells have restricted repertoire of receptors specific for multivalent antigens [38]. The extent of their dependency on BCR signalling and which components of it are crucial for the response are largely unknown [32].

5.9.1 Differences between Germinal Centre and non-Germinal Centre B cells

Throughout this chapter, a few novel differences became apparent in the responses of resting B cells and Germinal Centre cells:

First, Germinal Centre and non-Germinal Centre B cells respond very differently to antigen stimulation, the former population undergoing enhanced apoptosis in response to BCR ligation (figs. 71, 75 and 79 and as reported elsewhere). Although after a longer time than that is required for non-GC B cells, GC B cells expand in response to antigen *in vitro* (fig. 75) and *in vivo* (fig. 93). The apoptosis of Germinal Centre B cells is mitochondria-mediated and could be prevented by Caspase inhibition (fig. 80), unlike the death of immature B cells (as detailed in chapter 4). Results concerning the involvement of Caspases (and Cathepsins) in BCR-induced apoptosis of GC B cells have also recently been reported elsewhere [275, 324]. In contrast to previous assumptions, but in agreement with more recent reports [291, 324], the death of GC B cells

was found not to be dependent on Fas expression as demonstrated by using *lpr*-derived cultures (fig. 84).

The increased expression of CD19 found on GC B cells in comparison to non-GC B cells could reflect the possible involvement of Btk, because this protein kinase has been shown to act as an integrator of BCR and CD19 signalling cascades [21, 146]. The Btk deficiency is known to cause the absence of most B cells from the periphery [308] and B cells from Xid mice have a largely impaired proliferative response to the BCR in most B cell populations examined. Surprisingly, it was found $Btk^{-/-}$ Germinal Centre B cells could be induced to expand *in vitro* in response to BCR cross-linking. GC B cells, therefore, resemble in this behaviour immature B cells (fig. 83; see also section 4.5 and [146]) and this similarity could suggest that Btk may be involved in BCR signals which promote receptor editing/affinity maturation, possibly via induction of RAG activity.

Most of differences between $IgM^{-/-}$ and WT mice were relatively minor, although some reduction in total B cell number in the spleen was observed. Notably, $IgM^{-/-}$ spleen GC B cells showed higher apoptotic rate than normal mice upon sacrifice (fig. 85). In contrast, in the $IgM^{-/-}$ lymph nodes, sub-diploidity was reduced in both GC and non-GC B cell populations and growth arrest was enhanced (fig. 87). DNA synthesis was generally reduced in $IgM^{-/-}$ mice in response to anti-Ig stimulation (fig. 86). This evidence suggests that although B cell distribution in the periphery in the $IgM^{-/-}$ mice is similar to WT mice, they are largely dysfunctional.

5.9.2 Site-dependent behaviour of peripheral B cells during the primary and secondary responses

Perhaps one of the most exciting observations in this chapter was that B cells in the spleen and the lymph nodes display different primary and secondary responses to antigen. Nonetheless, the differences described here regarding B cells from the spleen and the lymph nodes are not fully understood.

Data presented here (fig. 77) showed that although the lymph nodes respond to lower antigen threshold, the response is more specific. This was demonstrated by using a partial antigen, DEL which induced a less remarkable proliferation in the lymph nodes than in the spleen. Investigating into the requirement of specific antigen during the secondary response was made using immunisation of MD4 mice with either HEL or DEL. Perhaps not surprisingly, this response has varied between the spleen and the lymph nodes (figs. 90 and 92). During the secondary response in the spleen, stimulation by HEL was enhanced with either DEL or HEL immunisation, while in the lymph nodes that occured only for HEL. The model which seems to emerge from these results is as follows:

(i) In the spleen the secondary response to HEL or DEL antigen could be enhanced by immunisation with either specific (HEL) or partially-specific (DEL) antigen. Moreover, immunisation with DEL enhances the response to DEL or to the original antigen, HEL (fig. 93).

(ii) In the lymph nodes, immunisation with specific antigen, HEL, enhances responses to both HEL and DEL (fig. 92). This seems to be specific to HEL and can not be mimicked by DEL and may suggest that induction of somatic mutation in the lymph nodes requires more specific stimulation of the BCR.

ES-62 is a protein capable of inducing Th2 type response [311]. A more physiological approach to the induction of GC B cells *in vivo* was taken with mice which were chronically exposed to this parasite-derived molecule. This is a useful model for the changes that such prolonged exposure manifest. It was shown here that the number of GC B cells generated was dose dependent (fig. 93). While stimulated by anti-Ig treatment, B cells from mice exposed to ES-62 had reduced proliferative response (fig. 94-95). Interestingly, it was shown that in different doses ES-62 has opposite effects on both apoptosis and proliferation of splenic B cells (fig. 96). However, the molecular basis to this phenomenon is still unclear.

5.9.3 B-1 cell responses

Finally, the responses of B-1 cells from the peritoneal cavity were compared to other peripheral B cells. As reported previously [38], these cells proliferate at a similar rate to other peripheral B cells upon BCR cross-linking. Furthermore, B-1 cells also undergo substantial level of apoptosis during this response (fig. 98). Using a natural epitope, the phosphorylcholine on the ES-62 molecule, it was possible to show that continuously exposed B-1 cells do proliferate at a higher rate than non-exposed cells (fig. 99). Interestingly, a second encounter with antigen (as mimicked by *in vitro* anti-Ig stimulation) has a very limited effect in enhancing further proliferation. This effect can be encouraged, though, by addition of Caspase inhibitors. The basis for this encouragement is unclear and has not previously observed. Together with the dependency of IgM expression (as opposed to its replacement with IgD), this evidence draws previously undescribed parallels between B-1 cells and transitional B cells in the bone marrow. Moreover, both populations are strongly dependent on Btk expression as shown with cells derived from Xid mice. It is possible that adult mice B-1 cells are in fact an unique type of transitional B cells which undergo positive and not negative selection and migrate to the peritoneal cavity [17]. This may happen due to their two specific features: (i) no IgD expression, which is required for migration to other peripheral sites [6]; (ii) restricted usage of mu heavy chains with cross-reactivity to selfantigens which exist in the bone marrow. Such cross-reaction with selfantigens may provide sufficient signal for B-1 cells to survive and migrate to the periphery. It is also possible that because B-1 did not complete the B-2 maturation route they are diverted mainly to a different site, namely the peritoneal cavity. This suggestion is supported by fresh evidence of the similarities between marginal zone B cells and B-1 cells in their positive selection in the bone marrow [21].

5.10 Summary

This chapter has focused on the characteristics of peripheral B cells and their stimulation via the BCR. In addition, the quantitative and qualitative requirements for affinity maturation of GC B cells have differed, dependending on the site of activation. It was show here that B cells in Germinal Centres act differently that those outside the GCs - for example, displaying enhanced apoptosis, involving reduction in their mitochondrial potential and Caspase activation in response to BCR cross-linking. They also have exhibit differential responses in the absence of Btk - thus, $Btk^{-/-}$ GC B cells are hyper-responsive to BCR stimulation, whilst non-GC B cells are hypo-responsive.

B cells in the spleen and the lymph nodes were found to have different proliferation profiles in response to BCR stimulation, when normally the lymph nodes typicaly requiring lower antigen for activation.

B-1 cells have also been shown to undergo BCR-induced apoptosis, which is Caspase-dependent and and were also strongly dependent on IgM and Btk for their responsiveness to BCR stimulation.

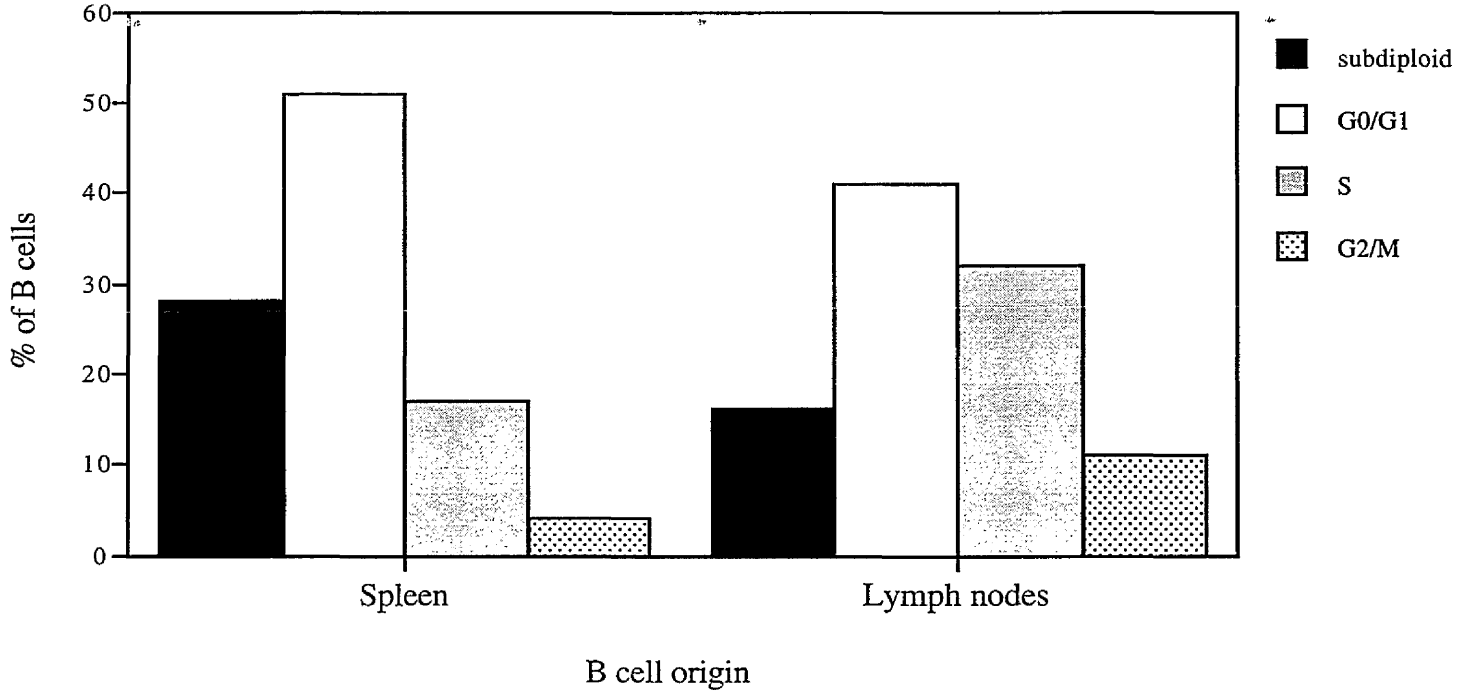
60
50
40
30
20
10
0
% of B cells
Spleen
Lymph nodes
B cell origin
subdiploid
G0/G1
S
G2/M

Fig. 69

Figure 69: Differences between splenic and lymph node B cells. Cells from spleens and lymph nodes of the same mice (*n=5*) were stained upon sacrifice with anti-B220-APC (1:40) subjected to PI incorporation. DNA content of ($B220^+$) B cells was determined as descibed in *Materials and Methods*.

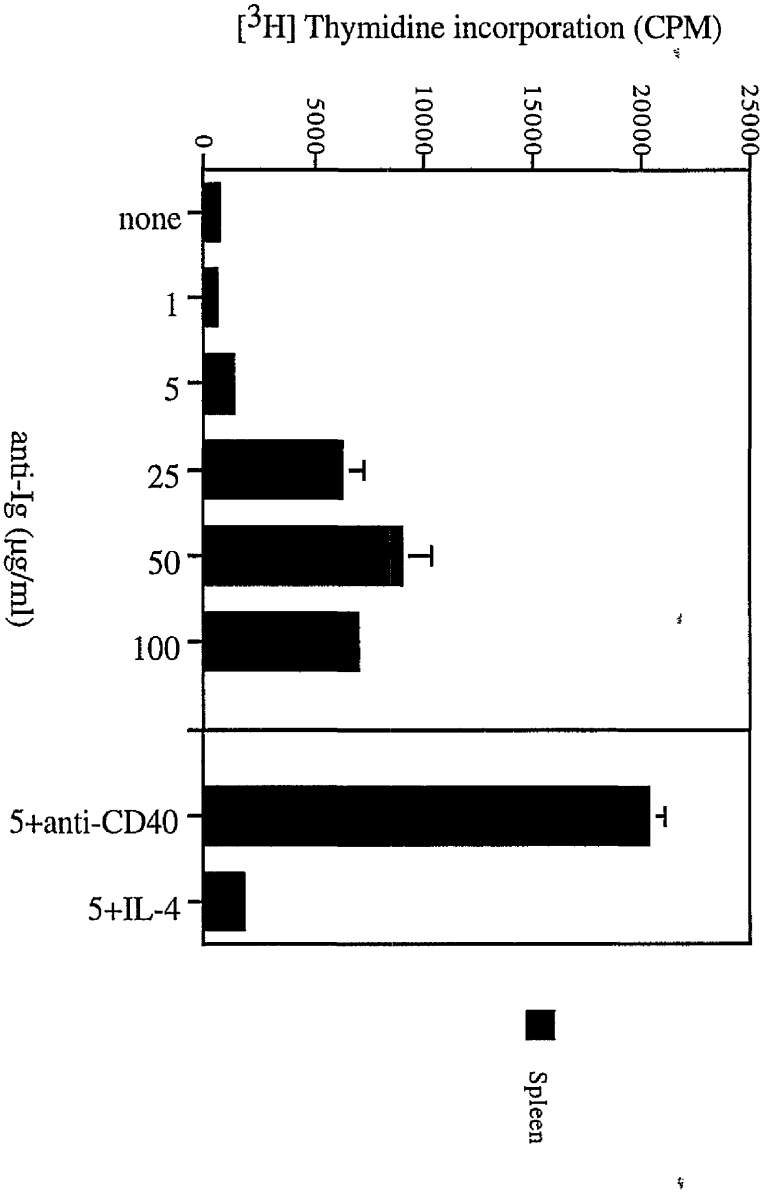
[3H] Thymidine incorporation (CPM)
0
5000
10000
15000
20000
25000
none
1
5
25
50
100
anti-Ig (µg/ml)
5+anti-CD40
5+IL-4
Spleen

Fig. 70

Figure 70: Proliferation of whole spleen cultures. Proliferation was assessed by measurement of DNA synthesis by whole spleen cells. Cells ($5x10^5$ cells/well) were treated for 2d with anti-Ig (0-100µg/ml) with or without anti-CD40 (10µg/ml), IL-4 (10U/ml) or their combinations as indicated. The levels of [^{3}H]-Thymidine incorporation into DNA were measured after further 4h. Data are expressed as means ± SD (*n=3*) from a single experiment.

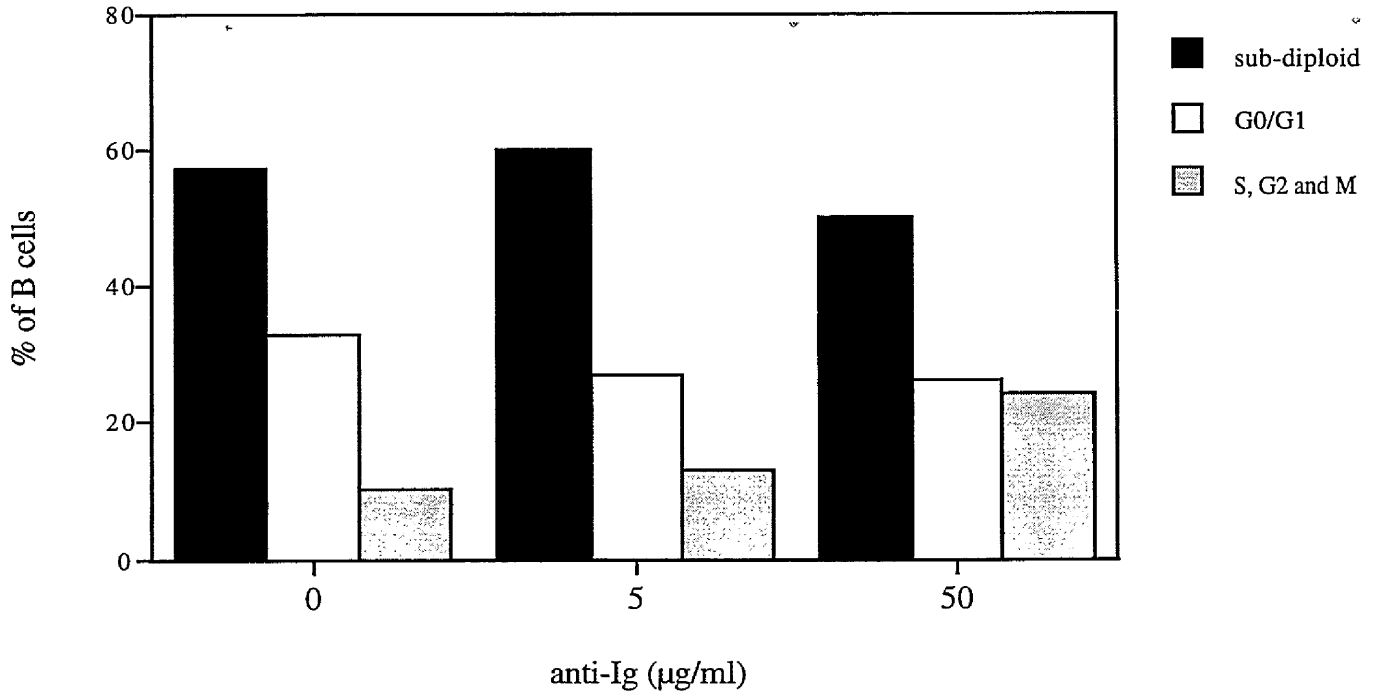
80
60
40
20
0
% of B cells
0
5
50
anti-Ig (µg/ml)
sub-diploid
G0/G1
S, G2 and M

Fig. 71

Figure 71: Proliferation of B cells in spleen cultures in response to BCR stimulation. Whole spleen cells (10^6 cells/sample) were incubated with anti-Ig (0-50µg/ml) for 2d. Cells were stained with anti-B220-APC (1:100) and then subjected for PI incorporation to determine DNA content. Populations are shown for $B220^+$ B cells.

a.

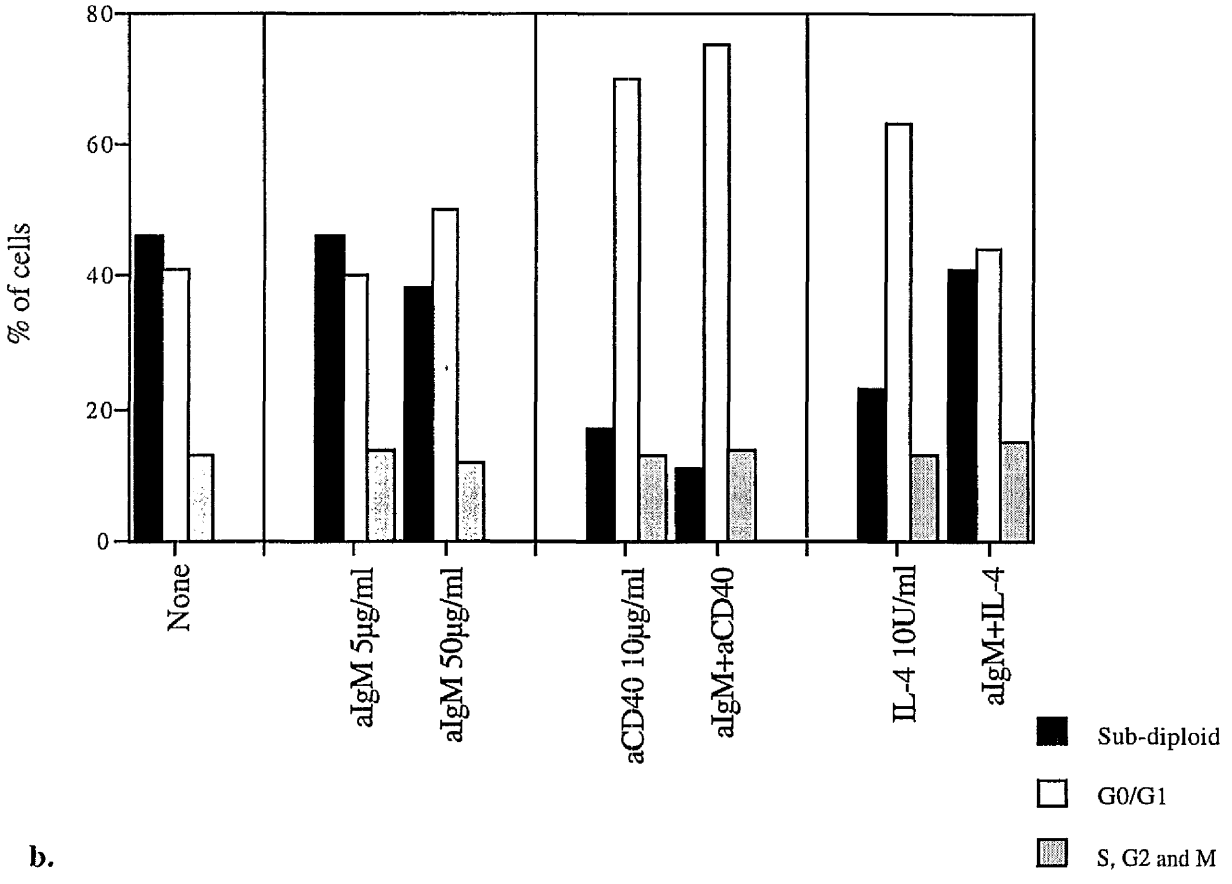
80
60
40
20
0
% of cells
None
aIgM 5µg/ml
aIgM 50µg/ml
aCD40 10µg/ml
aIgM+aCD40
IL-4 10U/ml
aIgM+IL-4
Sub-diploid
G0/G1
S, G2 and M

b.

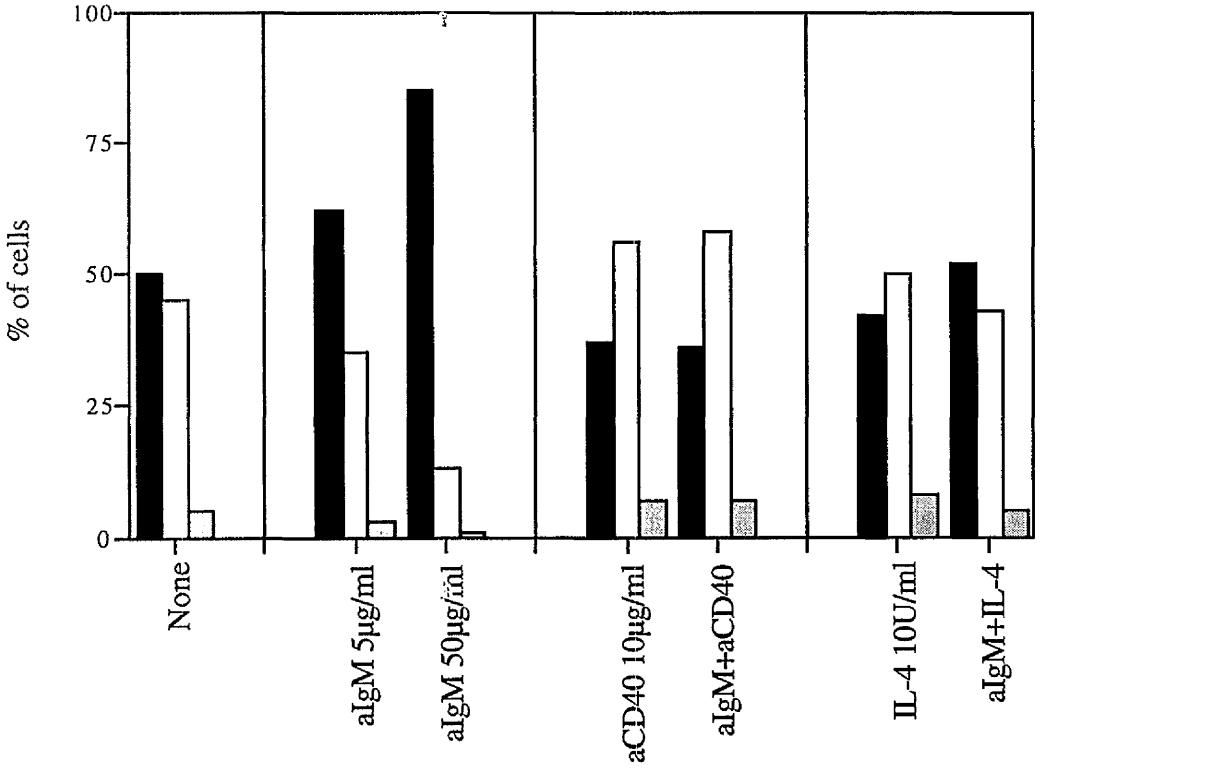
100
75
50
25
0
% of cells
None
aIgM 5µg/ml
aIgM 50µg/ml
aCD40 10µg/ml
aIgM+aCD40
IL-4 10U/ml
aIgM+IL-4

Fig. 72

Figure 72: Changes in cell cycle profile of splenic B cells upon stimulation. Isolated ($CD43^-$) B cells (10^6 cells/sample) from the spleen (a) or the lymph nodes (b) were incubated for 2d with anti-Ig (0-50μg/ml), anti-CD40 (0-10μg/ml), IL-4 (0-10U/ml) or their combinations as indicated. The cells were then subjected for PI incorporation to determine DNA content.

a

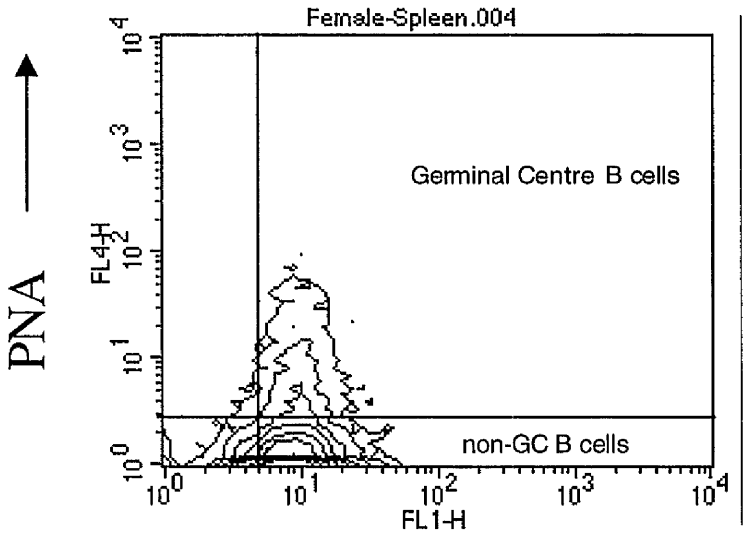

b

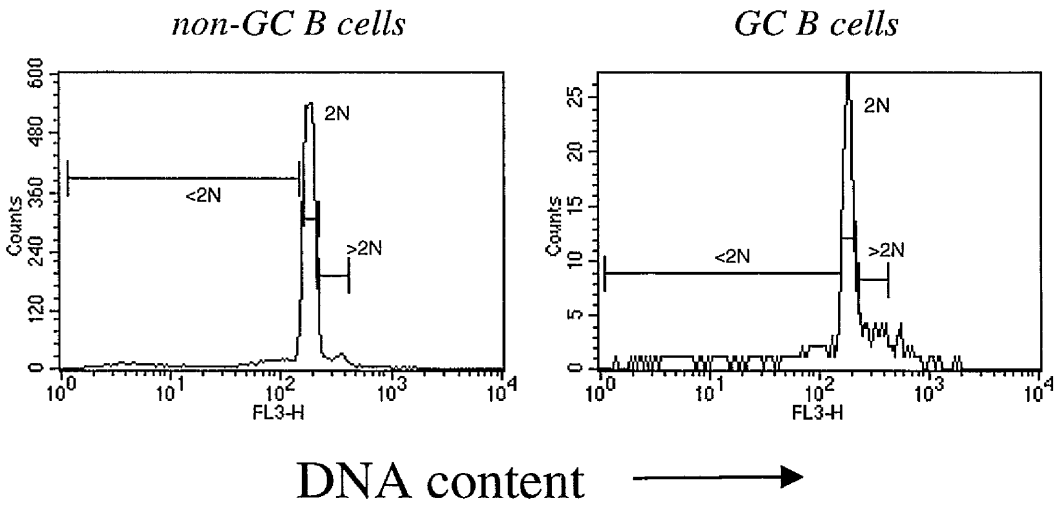

c

	<2N	2N	>2N
non-GC B cells	7%	82%	12%
GC B cells	27%	57%	16%

Fig. 73

Figure 73: Identification of Germinal Centre B cells and their cell cycle profile. Typical data is shown for female CBA/N mice which had upon sacrifice ~9% GC B cells. Cells from 5 spleens were stained with anti-CD19 (1:100)+anti-rat-FITC (1:200) and PNA-biotin (1:500)+ streptavidin-APC (1:100) and then subjected to PI incorporation. In panel a the gating for GC B cells is shown (the $CD19^+$ PNA^+ population). In panels b and c, gating of DNA content is shown for each population. The <2N DNA population is apoptotic cells, the 2N DNA population is cell in G_0/G_1 and the >2N DNA population is cells in S, G_2 and M phases.

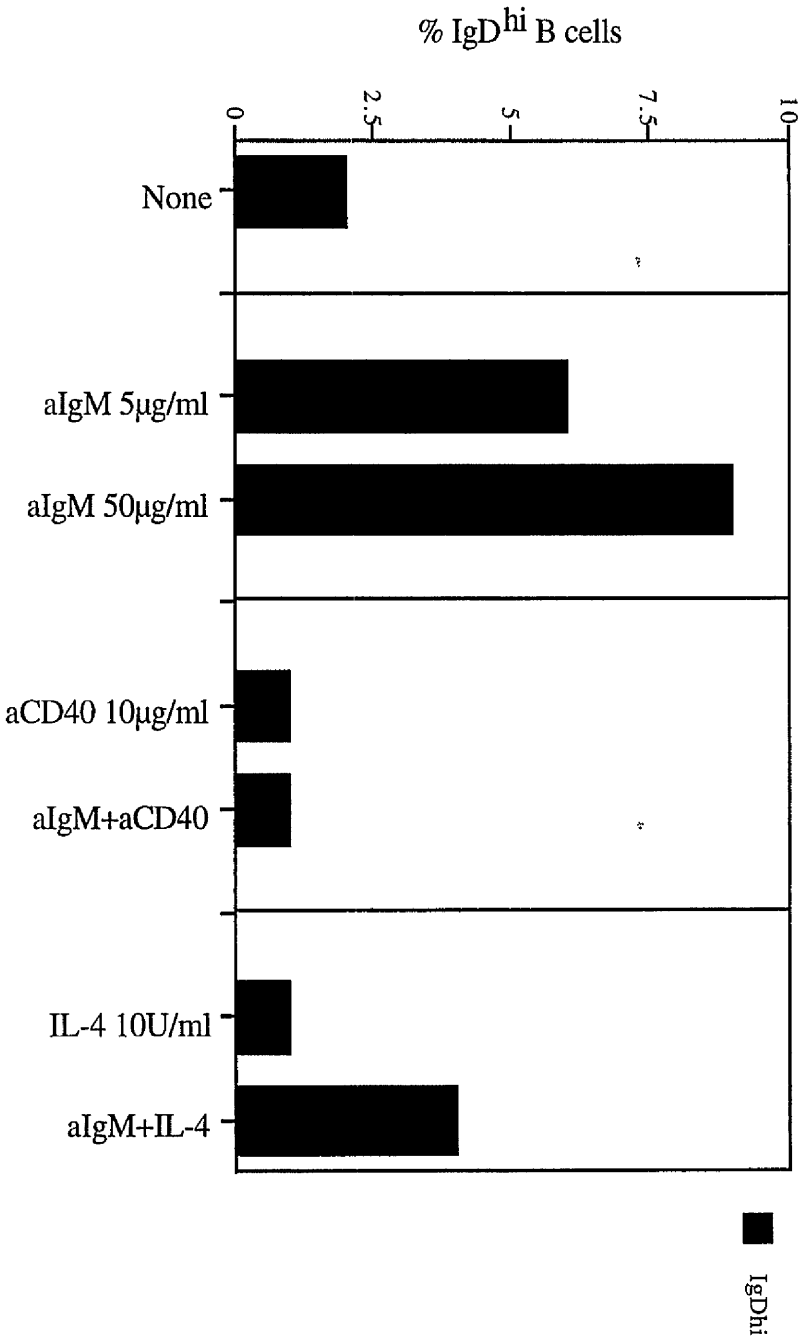
% IgD^hi B cells
0
2.5
5
7.5
10
None
aIgM 5µg/ml
aIgM 50µg/ml
aCD40 10µg/ml
aIgM+aCD40
IL-4 10U/ml
aIgM+IL-4
IgDhi

Fig. 74

Figure 74: Induction of IgD^{hi} B cell expansion *in vitro*. Isolated ($CD43^-$) splenic B cells (10^6 cells/sample) were incubated for 2d with anti-Ig (0-50μg/ml), anti-CD40 (0-15μg/ml), IL-4 (0-10U/ml) or their combinations as indicated. Cells were stained with anti-delta chain+anti-rat-IgG-FITC and their percentage was determined from the whole population.

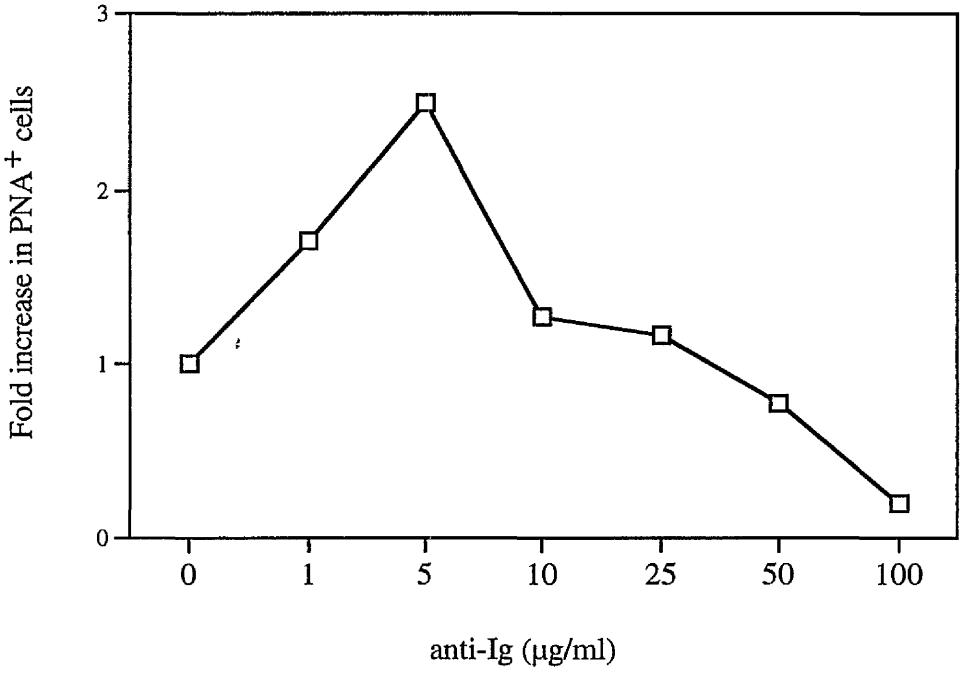

Fig. 75

Figure 75: Induction of Germinal Centre B cell expansion by BCR stimulation. Whole spleen cultures (10^6 cells/sample) were stimulated with 0-100μg/ml anti-Ig for 18h. The cells then stained with PNA-FITC (1:500) and percentage of PNA^+ (GC B) cells was determined by flow cytometry.

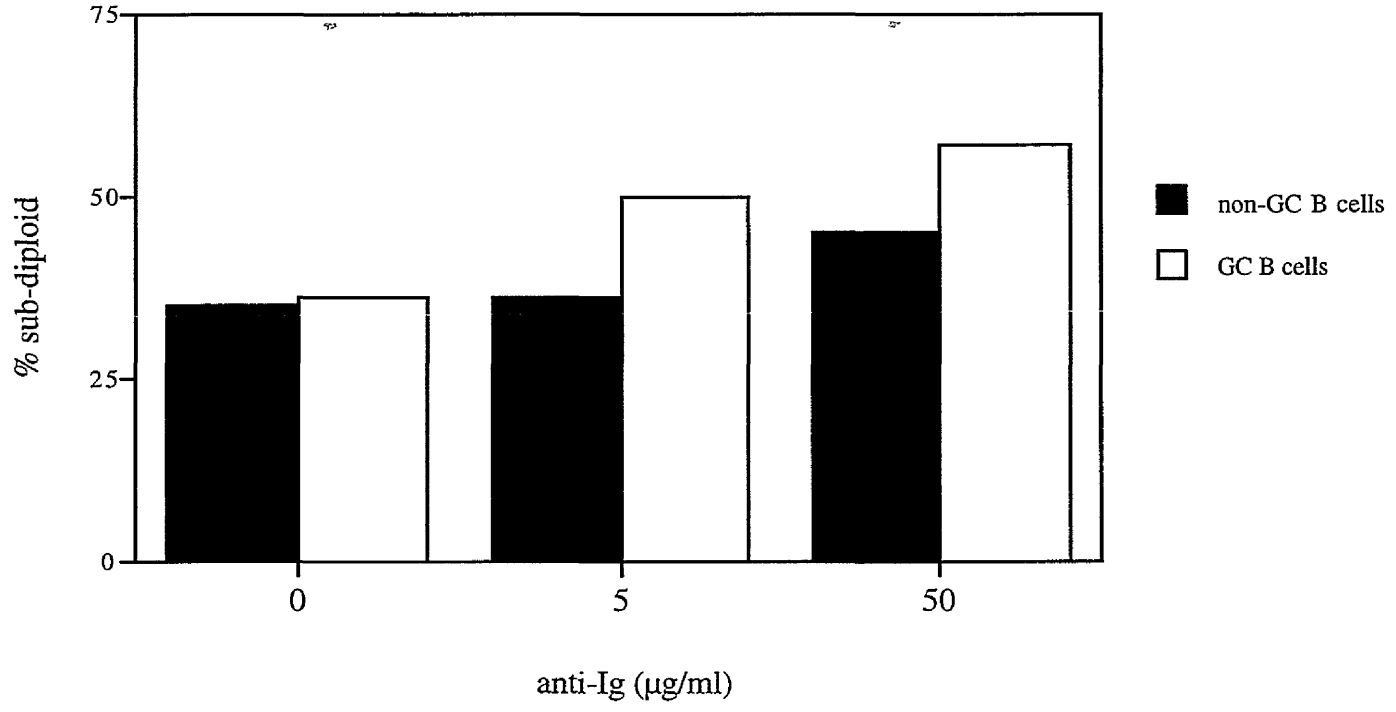
75
50
25
0
% sub-diploid
0
5
50
anti-Ig (µg/ml)
non-GC B cells
GC B cells

Fig. 76

Figure 76: Induction of apoptosis by anti-Ig treatment is enhanced in Germinal Centre B cells. Whole spleen cells (10^6 cells/sample) were stimulated with 0-50μg/ml anti-Ig for 2d. After staining with CD19-FITC (1:20) and PNA-biotin (1:500)+streptavidin-APC (1:100), cells were subjected to PI incorporation. Non-GC B cells are the $CD19^+$ PNA^- population, whereas GC B cells are the $CD19^+$ PNA^+ population. Subdiploidity was determined as the percentage of cells with less than 2N DNA.

a.

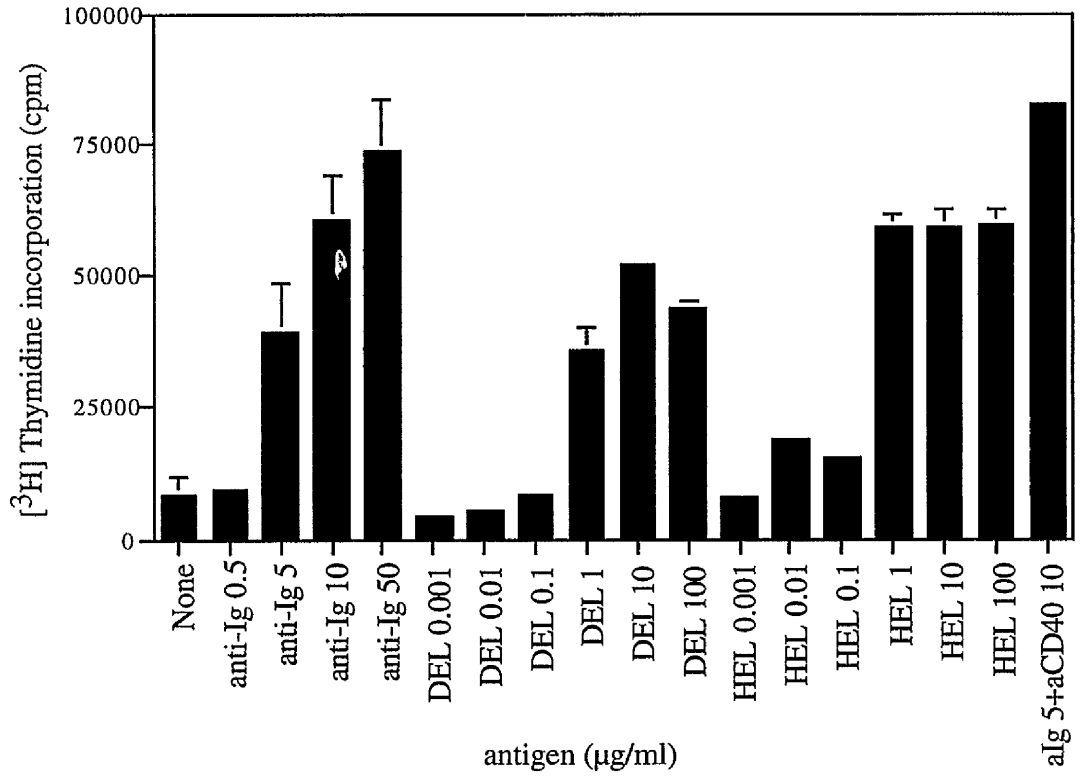
100000
75000
50000
25000
0
[3H] Thymidine incorporation (cpm)
None
anti-Ig 0.5
anti-Ig 5
anti-Ig 10
anti-Ig 50
DEL 0.001
DEL 0.01
DEL 0.1
DEL 1
DEL 10
DEL 100
HEL 0.001
HEL 0.01
HEL 0.1
HEL 1
HEL 10
HEL 100
aIg 5+aCD40 10
antigen (µg/ml)

b.

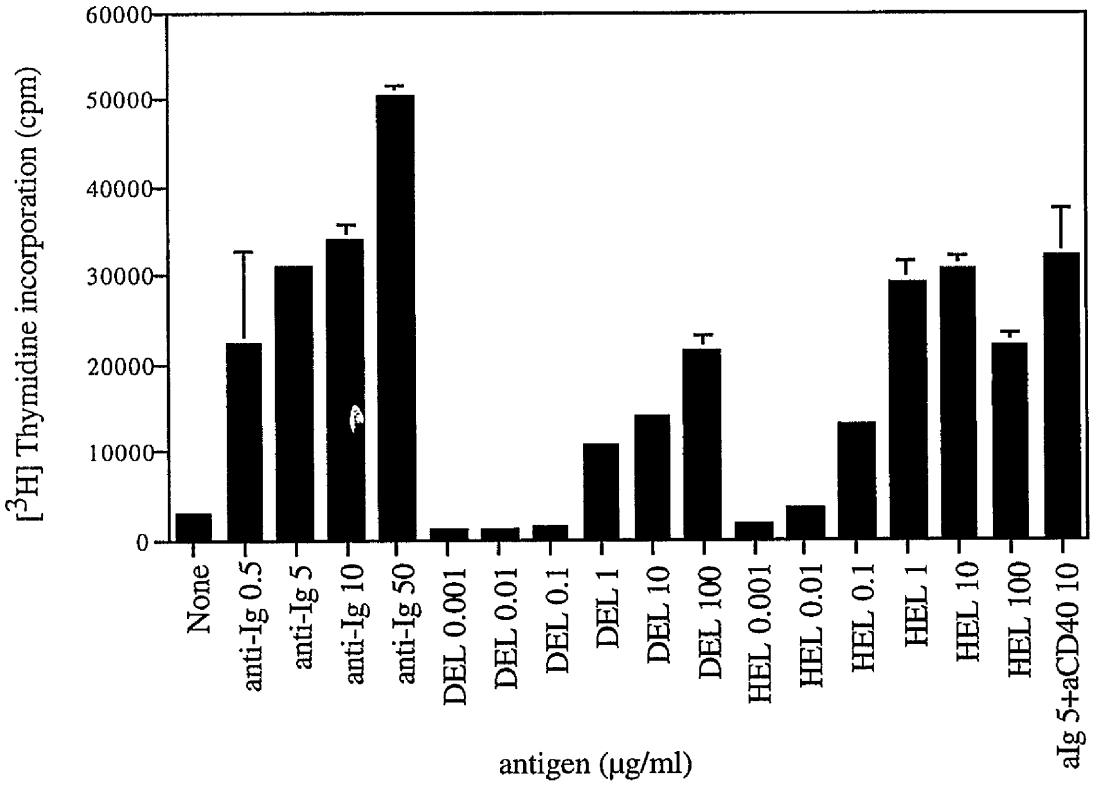
60000
50000
40000
30000
20000
10000
0
[3H] Thymidine incorporation (cpm)
None
anti-Ig 0.5
anti-Ig 5
anti-Ig 10
anti-Ig 50
DEL 0.001
DEL 0.01
DEL 0.1
DEL 1
DEL 10
DEL 100
HEL 0.001
HEL 0.01
HEL 0.1
HEL 1
HEL 10
HEL 100
aIg 5+aCD40 10
antigen (µg/ml)

Fig. 77

Figure 77: The primary response to antigen of HEL-BCR mice. Proliferation in whole spleen (a) or lymph node (b) cells from MD4 mice ($5x10^5$ cells/well) were was assessed by measurement of DNA synthesis. Cells ($5x10^5$ cells/well) were treated for 2d with anti-Ig (0-100μg/ml), DEL (0-100μg/ml), HEL (0-100μg/ml) or anti-Ig (5μg/ml)+anti-CD40 (10μg/ml). The levels of [^{3}H]-Thymidine incorporation into DNA were measured after further 4h. Data are expressed as means ± SD (*n=3*) from a single experiment.

a.

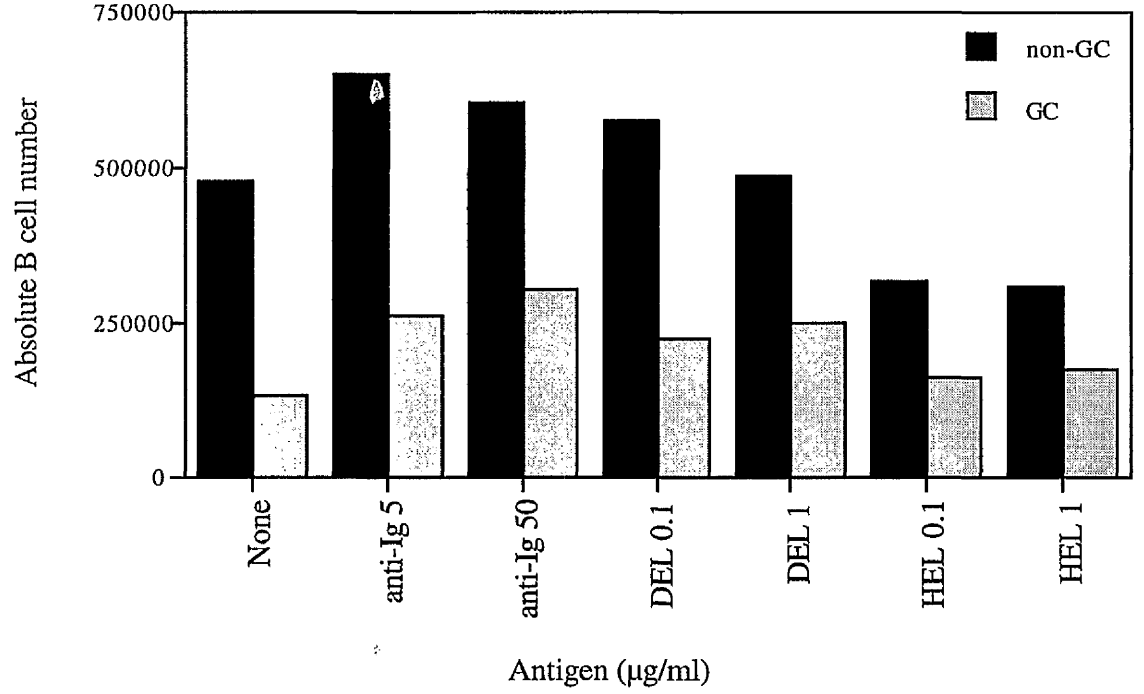
750000
500000
250000
0
Absolute B cell number
non-GC
GC
None
anti-Ig 5
anti-Ig 50
DEL 0.1
DEL 1
HEL 0.1
HEL 1
Antigen (µg/ml)

b.

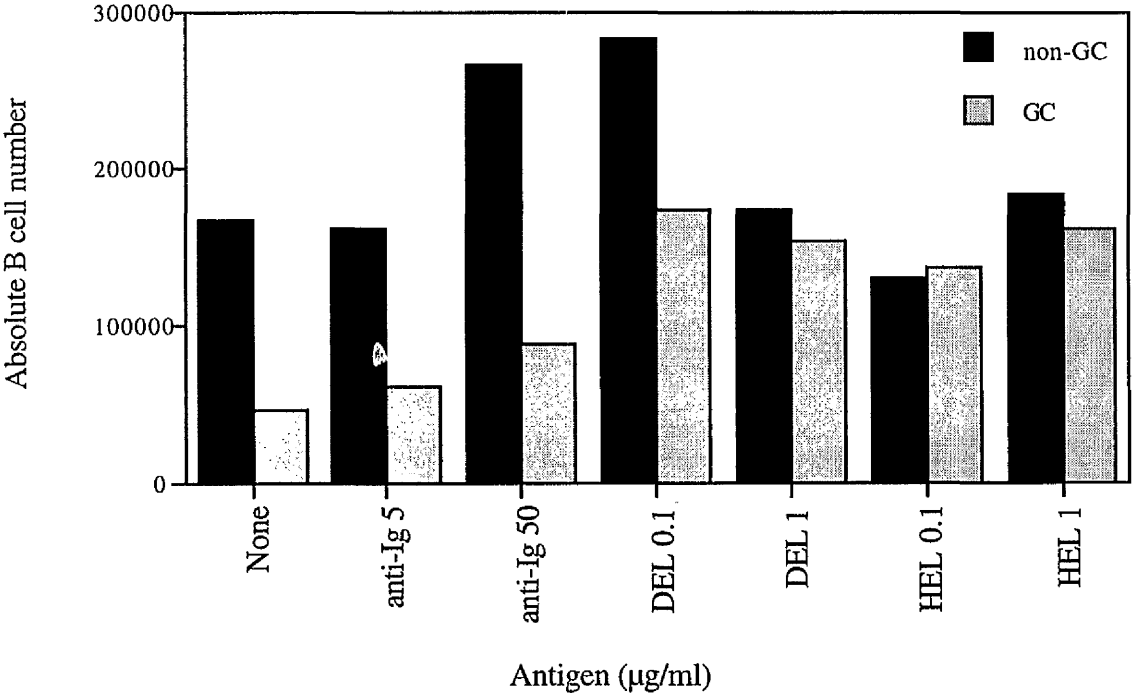
300000
200000
100000
0
Absolute B cell number
non-GC
GC
None
anti-Ig 5
anti-Ig 50
DEL 0.1
DEL 1
HEL 0.1
HEL 1
Antigen (µg/ml)

Fig. 78

Figure 78: Expansion of GC B cells in response to antigen in the spleen and in the lymph nodes. Whole spleen (a) or lymph node (b) cells (10^6 cells/sample) from MD4 mice were stimulated with anti-Ig (0-50μg/ml), DEL (0-100μg/ml) or HEL (0-100μg/ml) for 2d. Cells were counted and stained with CD19-FITC (1:20) and PNA-biotin (1:500)+streptavidin-APC (1:100). GC B cells were $CD19^+$ PNA^+ cells and non-GC the $CD19^+$ PNA^- cells.

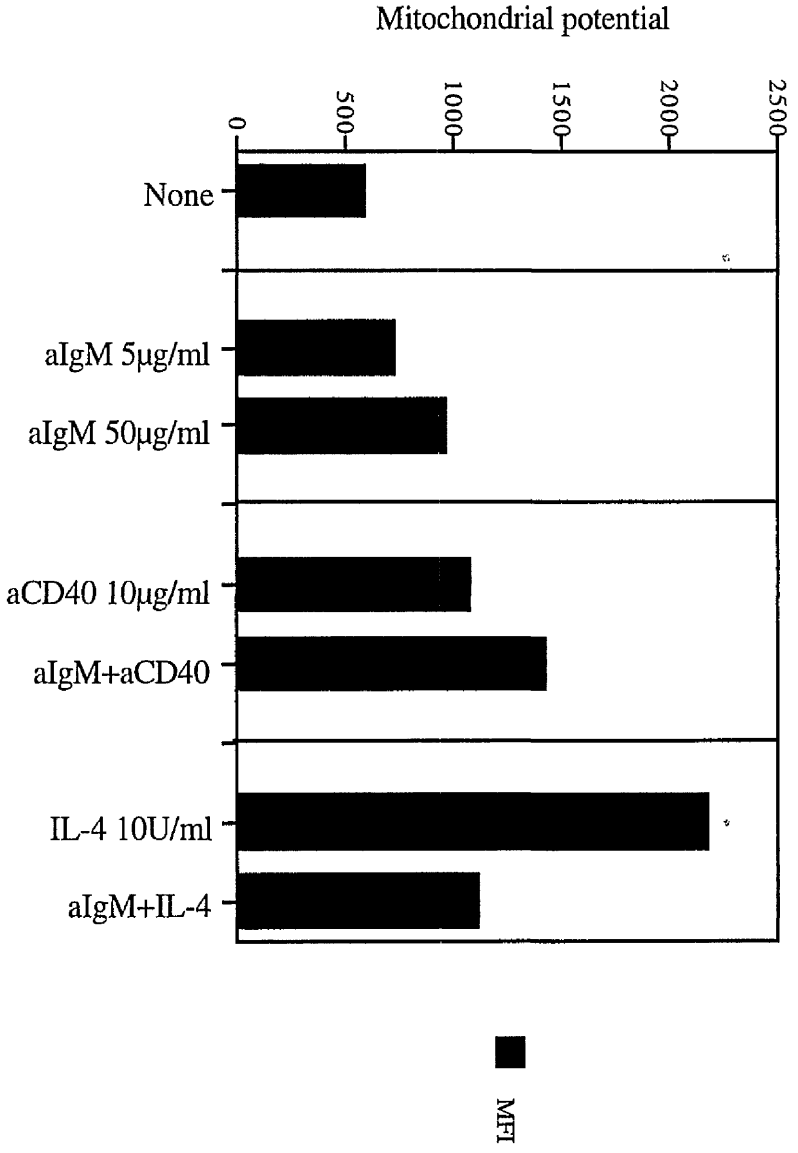
Mitochondrial potential
0
500
1000
1500
2000
2500
None
aIgM 5μg/ml
aIgM 50μg/ml
aCD40 10μg/ml
aIgM+aCD40
IL-4 10U/ml
aIgM+IL-4
MFI

Fig. 79

Figure 79: Changes in the mitochondrial potential of stimulated splenic B cells. Isolated ($CD43^-$) splenic B cells (10^6 cells/sample) were stimulated for 2d with anti-Ig (0-50µg/ml), anti-CD40 (0-15µg/ml), IL-4 (0-10U/ml) or their combinations as indicated. The cells were analysed with the mitochondrial dye $DiOC_6$ (3). The mitochondrial potential was determined by the mean fluorescence of the dye.

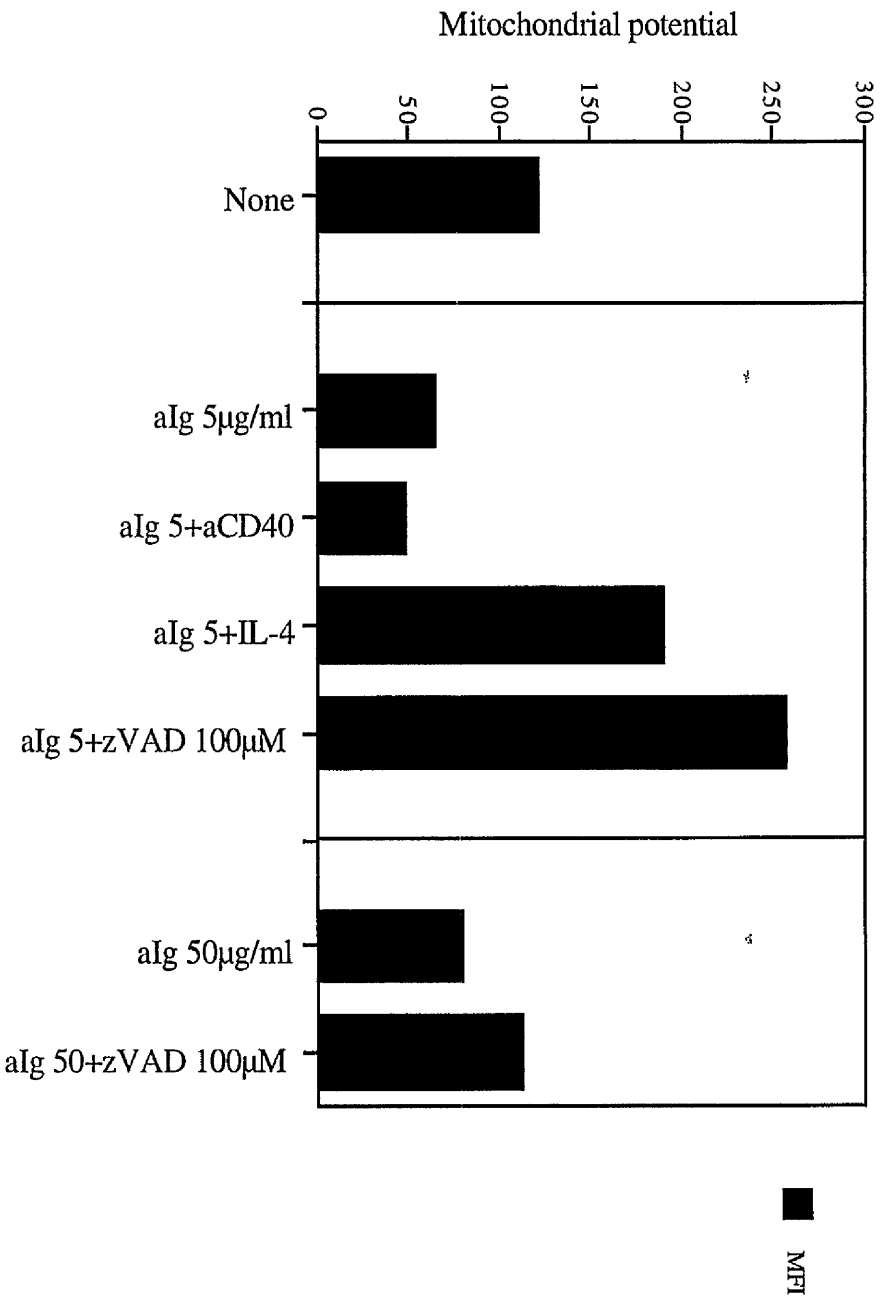
Mitochondrial potential
0
50
100
150
200
250
300
None
aIg 5µg/ml
aIg 5+aCD40
aIg 5+IL-4
aIg 5+zVAD 100µM
aIg 50µg/ml
aIg 50+zVAD 100µM
MFI

Fig. 80

Figure 80: Changes in the mitochondrial potential of Germinal Centre B cells upon stimulation. Whole spleen cells (10^6 cells/sample) were treated for 3d with 0-50μg/ml anti-Ig with or without anti-CD40 (10μg/ml), IL-4 (10U/ml) or zVAD-fmk (100μg/ml). Cells were stained with PNA-biotin (1:500)+streptavidin-APC (1:100) and then for the mitochondrial dye $DiOC_6$ (3). The mitochondrial potential of PNA^+ (GC B) cells was determined by the mean fluorescence of the dye.

a.

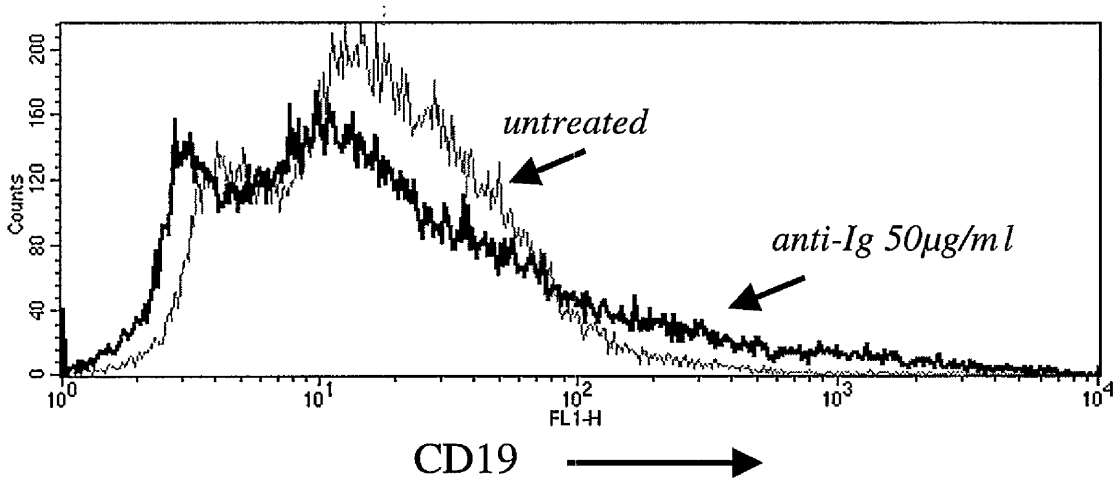
Counts
0
40
80
120
160
200
10^0
10^1
10^2
10^3
10^4
FL1-H
untreated
anti-Ig 50µg/ml
CD19

b.

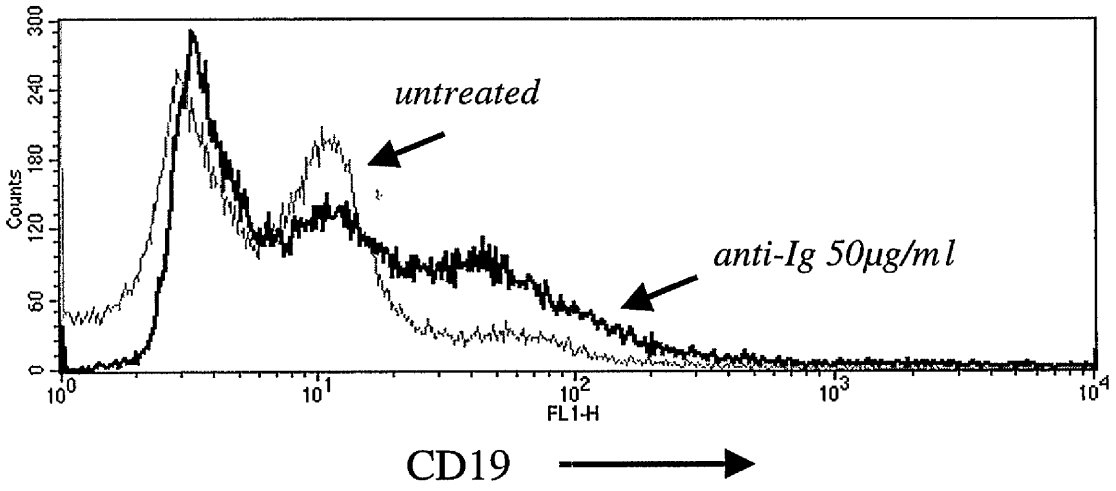
Counts
0
60
120
180
240
300
10^0
10^1
10^2
10^3
10^4
FL1-H
untreated
anti-Ig 50µg/ml
CD19

Fig. 81

Figure 81: Enhancement of CD19 expression by BCR stimulation. Whole spleen (a) or lymph node (b) cells (10^6 cells/sample) were incubated with or without 50µg/ml anti-Ig for 2d. After staining with CD19-FITC (1:20), CD19 surface expression was determined by flow cytometry.

a.

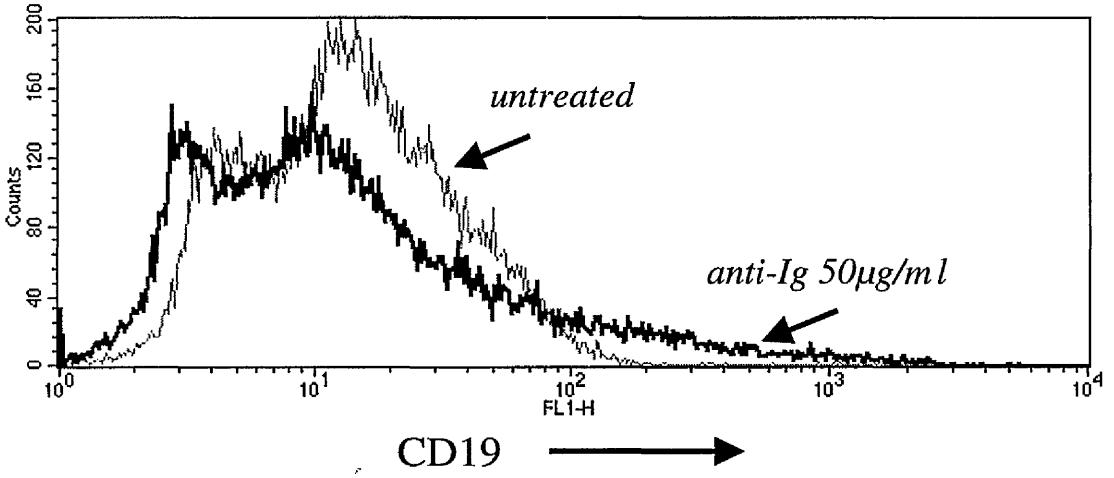
Counts
0
40
80
120
160
200
10^0
10^1
10^2
10^3
10^4
FL1-H
untreated
anti-Ig 50µg/ml
CD19

b.

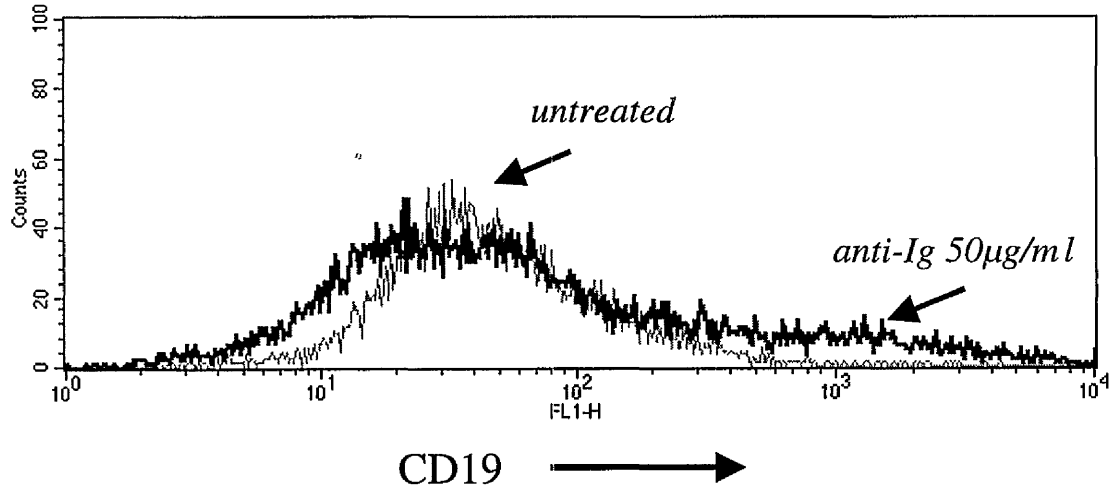
Counts
0
20
40
60
80
100
10^0
10^1
10^2
10^3
10^4
FL1-H
untreated
anti-Ig 50µg/ml
CD19

Fig. 82

Figure 82: CD19 is expressed at higher levels on GC B cells than on non-GC B cells. Whole spleen cells (10^6 cells/sample) were incubated with or without 50μg/ml anti-Ig for 2d. After staining with CD19-FITC (1:20) and PNA-biotin (1:500)+streptavidin-APC (1:100), CD19 surface expression is shown for PNA^- cells (a) and PNA^+ cells (b).

a.

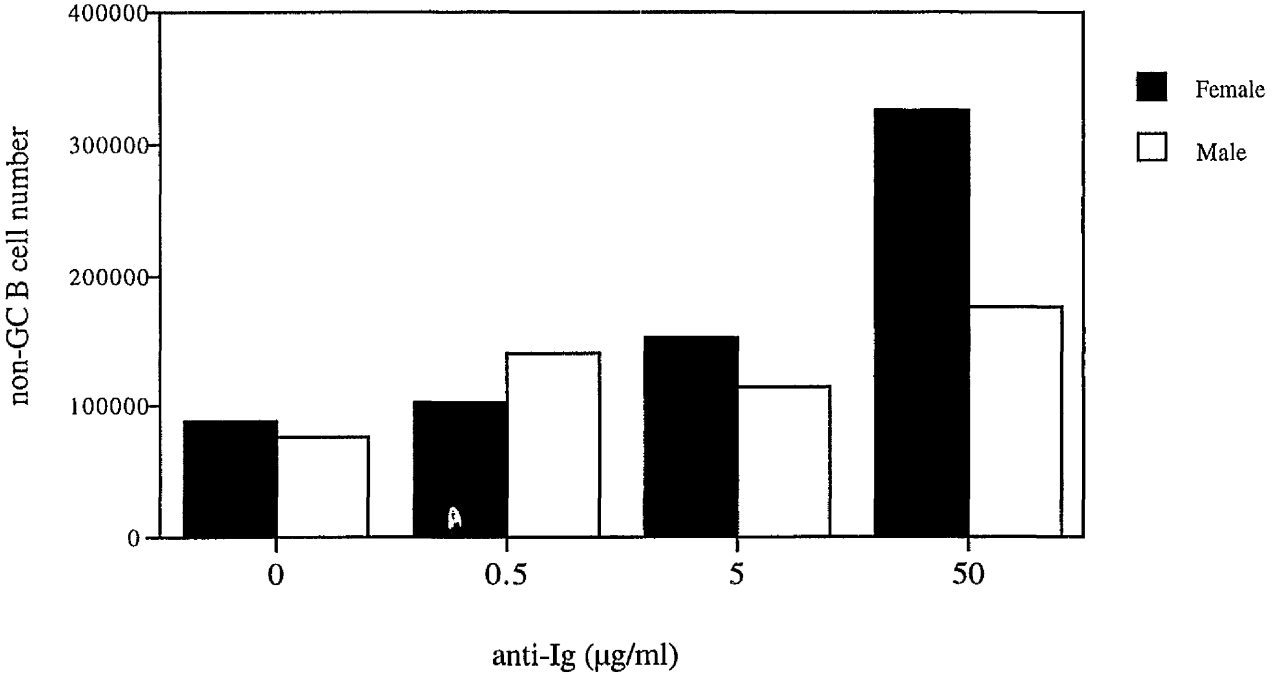
400000
300000
200000
100000
0
non-GC B cell number
0
0.5
5
50
anti-Ig (µg/ml)
Female
Male

b.

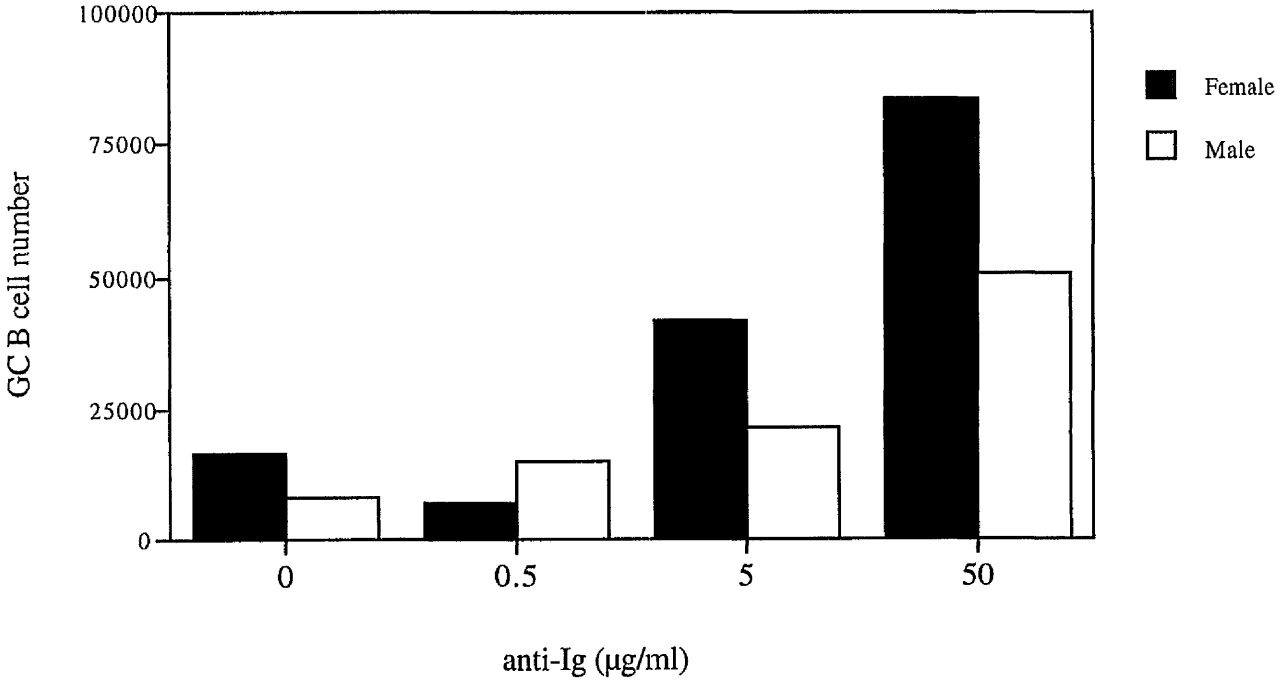
100000
75000
50000
25000
0
GC B cell number
0
0.5
5
50
anti-Ig (µg/ml)
Female
Male

Fig. 83

Figure 83: Defects in BCR induced proliferation of Xid derived splenic B cells. Whole spleen cells (10^6 cells/sample) from either female (WT) or male (*Xid*) CBA/N mice were stimulated with 0-50μg/ml anti-Igfor 2d. Cells counted and stained with CD19-FITC (1:20) and PNA-biotin (1:500)+streptavidin-APC (1:100). Non-GC B cells (a) are the $CD19^+$ PNA^- population, wheres GC B cells are the $CD19^+$ PNA^+ population (b).

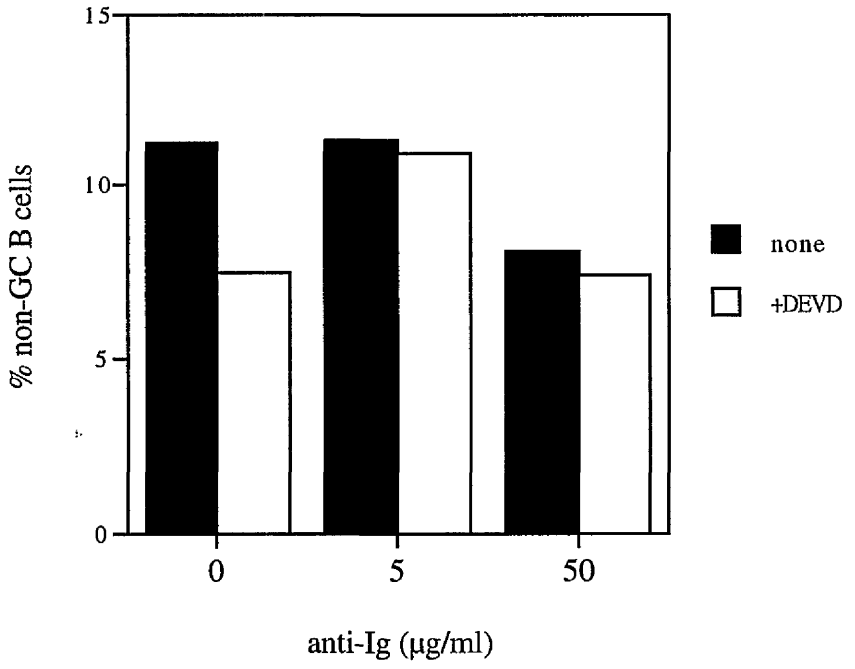
15
10
5
0
% non-GC B cells
0
5
50
anti-Ig (μg/ml)
none
+DEVD

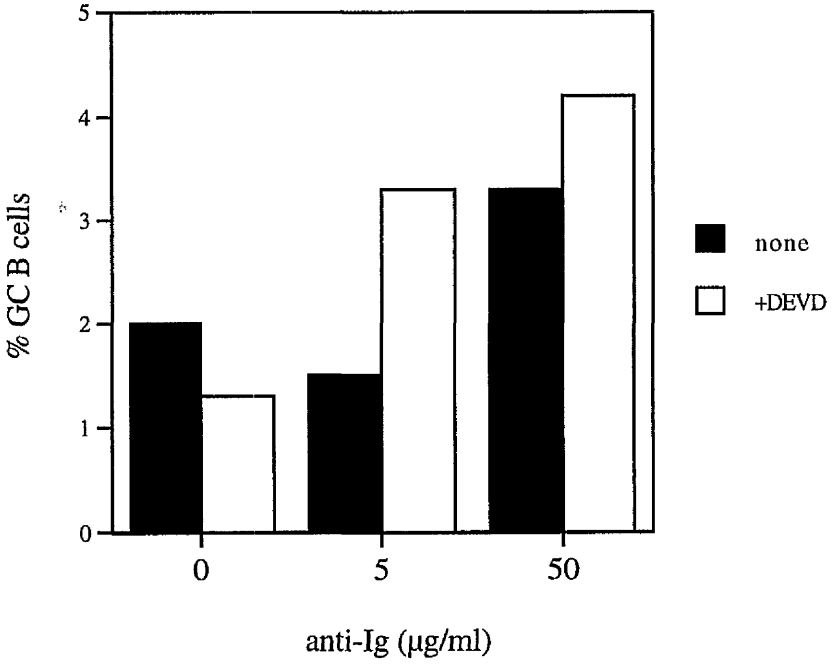
5
4
3
2
1
0
% GC B cells
0
5
50
anti-Ig (μg/ml)
none
+DEVD

Fig. 84

Figure 84: Caspase inhibition specifically supports expansion of Germinal Centre B cells in the absence of Fas. Whole lymph node cells (10^6 cells/sample) from *lpr* mice were stimulated for 2d with 0-50μg/ml anti-Ig with or without 10μM Ac-DEVD-CHO. After staining with CD19-FITC (1:20) and PNA-biotin (1:500)+streptavidin-APC (1:100), the percentage of either non-GC B cells ($CD19^+$ PNA^-) or GC B cells ($CD19^+PNA^+$) was determined by flow cytometry.

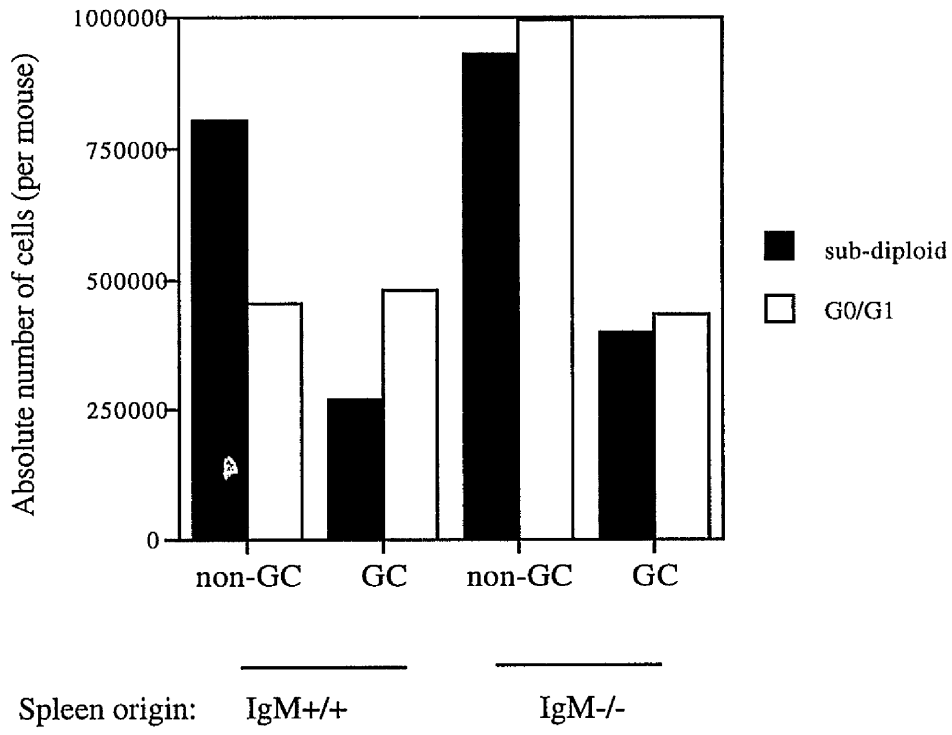
1000000
750000
500000
250000
0
Absolute number of cells (per mouse)
non-GC
GC
non-GC
GC
sub-diploid
G0/G1
Spleen origin:
IgM+/+
IgM-/-

Fig. 85

Figure 85: Enhanced apoptosis in the Germinal Gentres of $IgM^{-/-}$ derived spleens. B cell populations from the spleens of either WT or $IgM^{-/-}$ BALB/c mice were determined upon sacrifice by CD19-FITC (1:20) and PNA-biotin (1:500)+streptavidin-APC (1:100) staining and PI incorporation to determine DNA content. Germinal B cells are $CD19^+$ PNA^+ and non-GC B cells are the $CD19^+$ PNA^- population.

a.

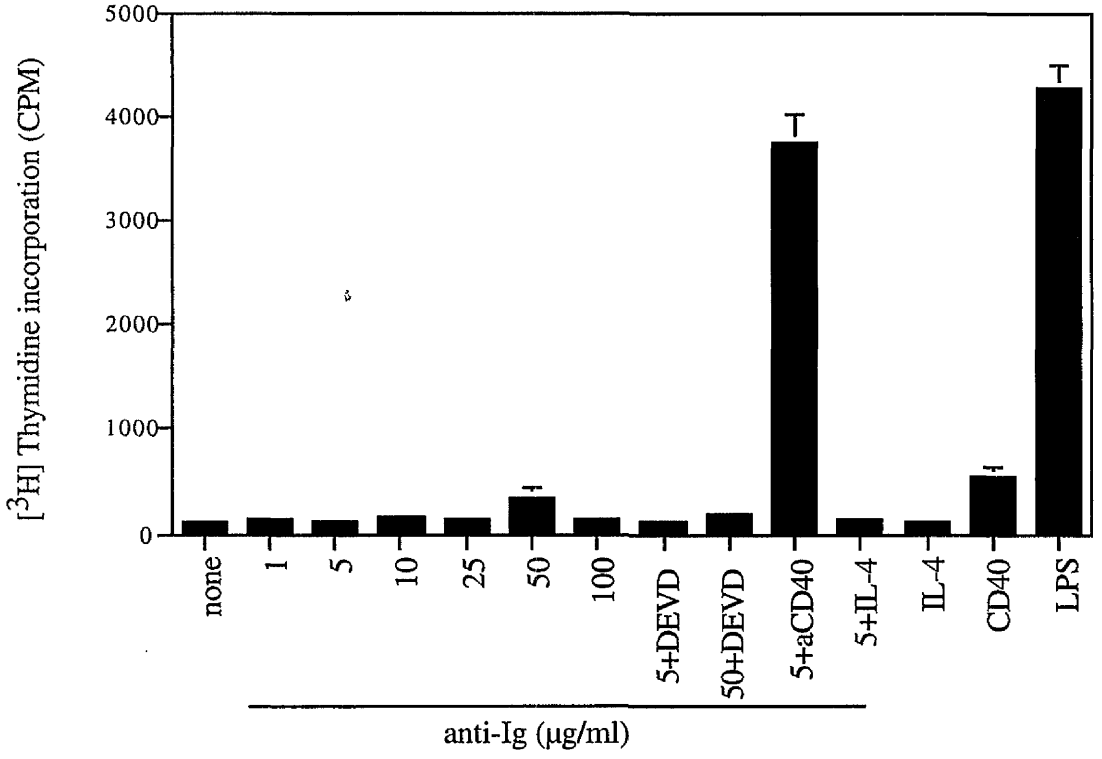
[3H] Thymidine incorporation (CPM)
5000
4000
3000
2000
1000
0
none
1
5
10
25
50
100
5+DEVD
50+DEVD
5+aCD40
5+IL-4
IL-4
CD40
LPS
anti-Ig (µg/ml)

b.

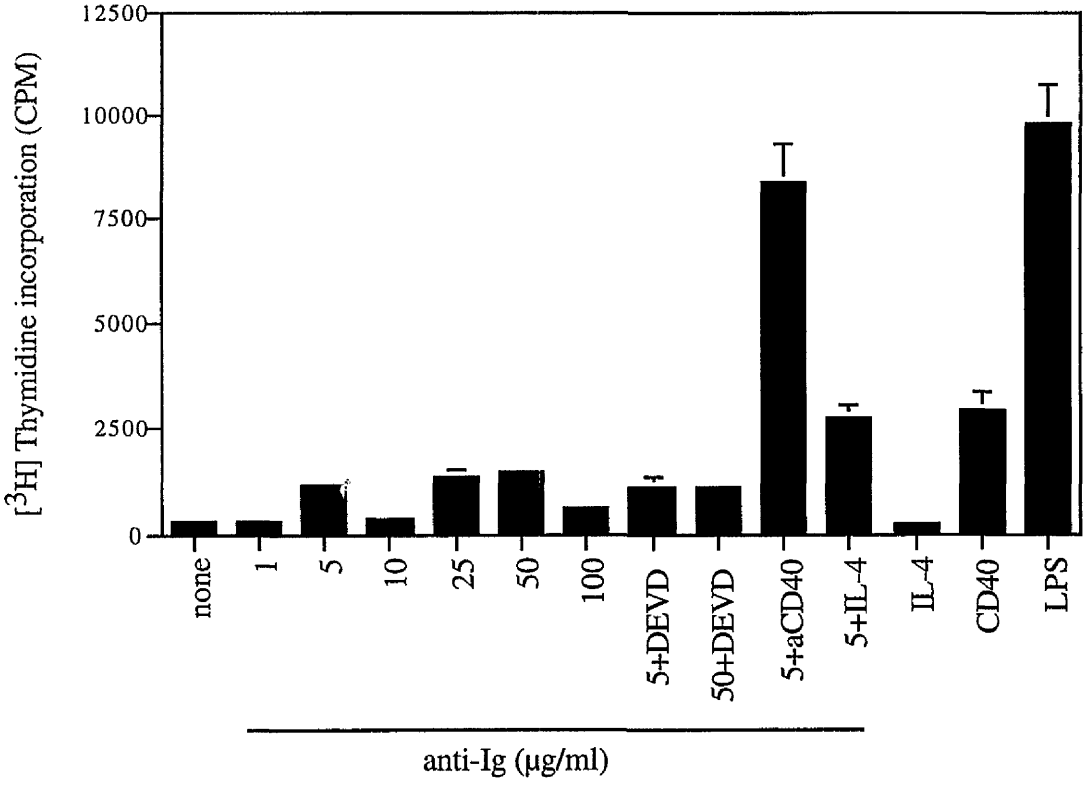
[3H] Thymidine incorporation (CPM)
12500
10000
7500
5000
2500
0
none
1
5
10
25
50
100
5+DEVD
50+DEVD
5+aCD40
5+IL-4
IL-4
CD40
LPS
anti-Ig (µg/ml)

Fig. 86

Figure 86: Responses of peripheral B cells in $IgM^{-/-}$ cultures. Proliferation in whole spleen (a) or lymph node (b) cells from $IgM^{-/-}$ BALB/c mice was assessed by measurement of DNA synthesis. Cells ($5x10^5$ cells/well) were treated for 2d with anti-Ig (0-100µg/ml), Ac-DEVD-CHO (0-10µg/ml), anti-CD40 (0-10µg/ml), IL-4 (0-10U/ml), LPS (50µg/ml) or their combinations as indicated. The levels of [^{3}H]-thymidine incorporation into DNA were measured after further 4h. Data are expressed as means ± SD (*n=3*) from a single experiment.

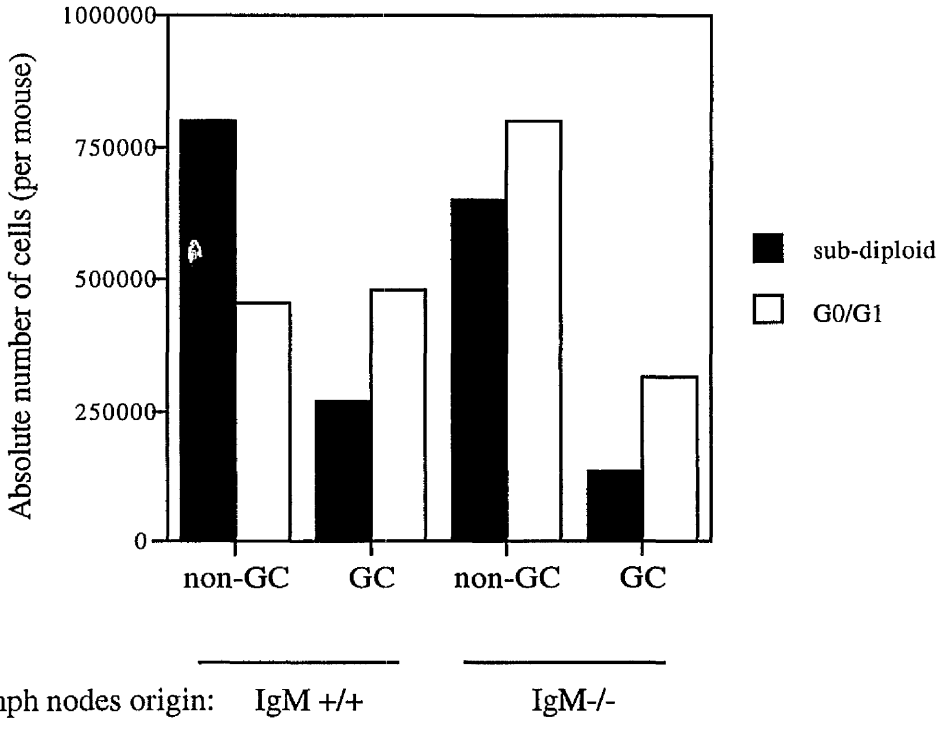
1000000
750000
500000
250000
0
Absolute number of cells (per mouse)
non-GC
GC
non-GC
GC
sub-diploid
G0/G1
Lymph nodes origin: IgM +/+
IgM-/-

Fig. 87

Figure 87: $IgM^{-/-}$ lymph nodes differ from wild-type lymph nodes in their Germinal Centre B cell content. B cell populations from the lymph nodes of either WT or $IgM^{-/-}$ BALB/c mice were determined upon sacrifice by CD19-FITC (1:20) and PNA-biotin (1:500)+streptavidin-APC (1:100) staining and PI incorporation to determine DNA content. Germinal B cells are $CD19^+$ PNA^+ and non-GC B cells are the $CD19^+$ PNA^- population.

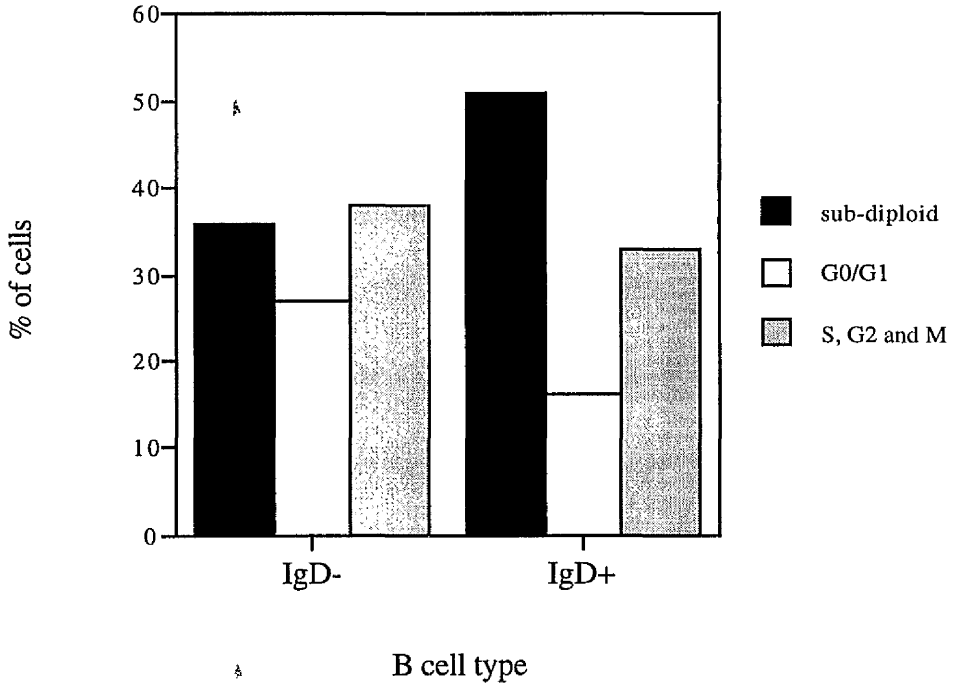
60
50
40
30
20
10
0
% of cells
IgD-
IgD+
B cell type
sub-diploid
G0/G1
S, G2 and M

Fig. 88

Figure 88: BCR responses in IgM$^{-/-}$ lymph nodes leads to cell death and not to loss of IgD expression. Whole lymph nodes from IgM$^{-/-}$ BALB/c mice were treated with 0-50µg/ml anti-Ig for 2d. B cell populations were determined upon sacrifice by anti-delta chain (1:50)+anti-rat-IgG-FITC (1:100) and anti-B200-APC (1:40) staining and PI incorporation to determine DNA content. B cells were B220^{+} cells.

a.

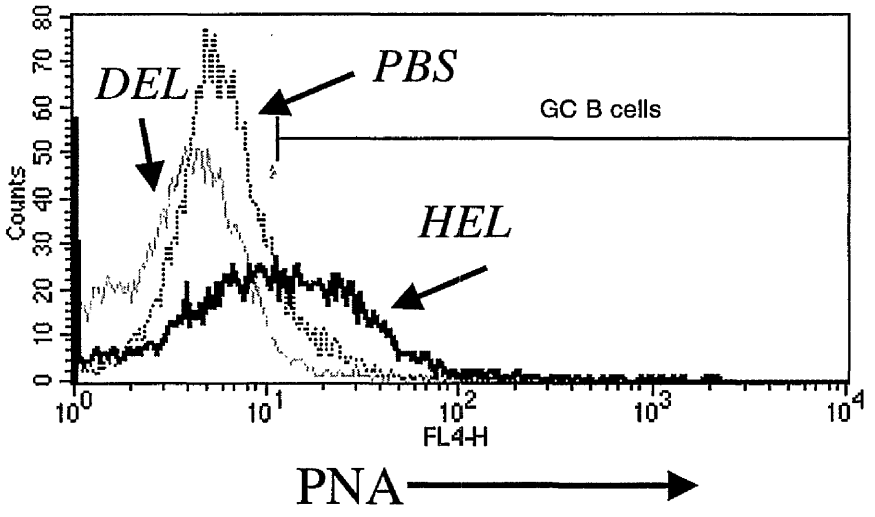
DEL
PBS
GC B cells
HEL
Counts
0
10
20
30
40
50
60
70
80
10^0
10^1
10^2
10^3
10^4
FL4-H
PNA

b.

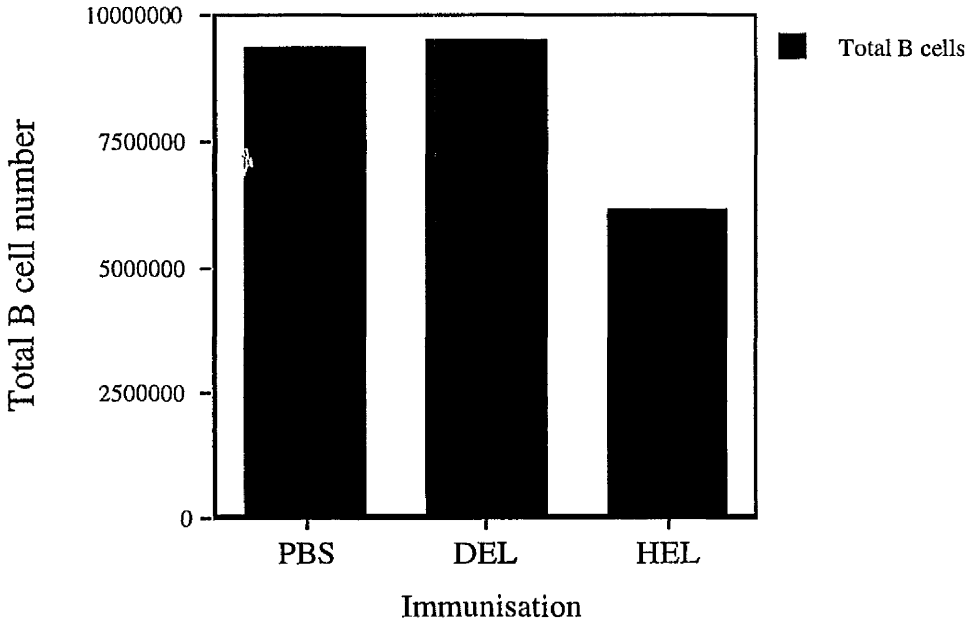
10000000
7500000
5000000
2500000
0
Total B cell number
Total B cells
PBS
DEL
HEL
Immunisation

c.

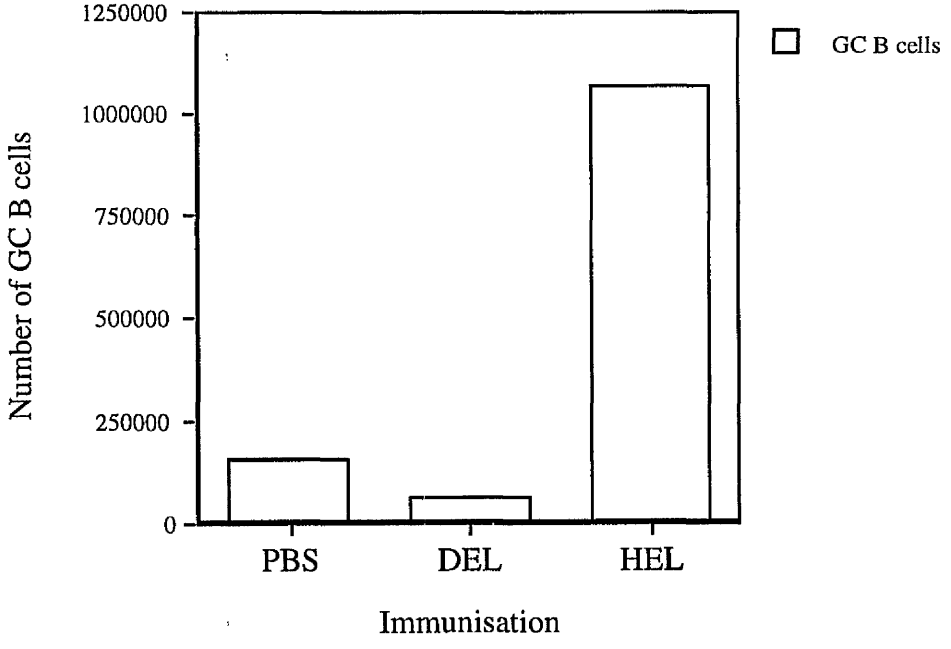
1250000
1000000
750000
500000
250000
0
Number of GC B cells
GC B cells
PBS
DEL
HEL
Immunisation

Fig. 89

Figure 89: Induction of Germinal Centres in HEL-BCR MD4 mice. MD4 mice were pre-immunised with PBS, 100μg DEL or 100μg HEL and sacrificed on day 8 when the Germinal Centre reaction is at its peak. The cells were counted and then stained with anti-CD19 (1:100)+anti-rat-FITC (1:200) and PNA-biotin (1:500)+streptavidin-APC (1:100). (a) PNA binding of $CD19^+$ B cells from each spleen. (b) Total number of splenic ($CD19^+$) B cells upon sacrifice. (c) Number of splenic ($CD19^+PNA^+$) GC B cells upon sacrifice. Similar results were observed in the lymph nodes (not shown).

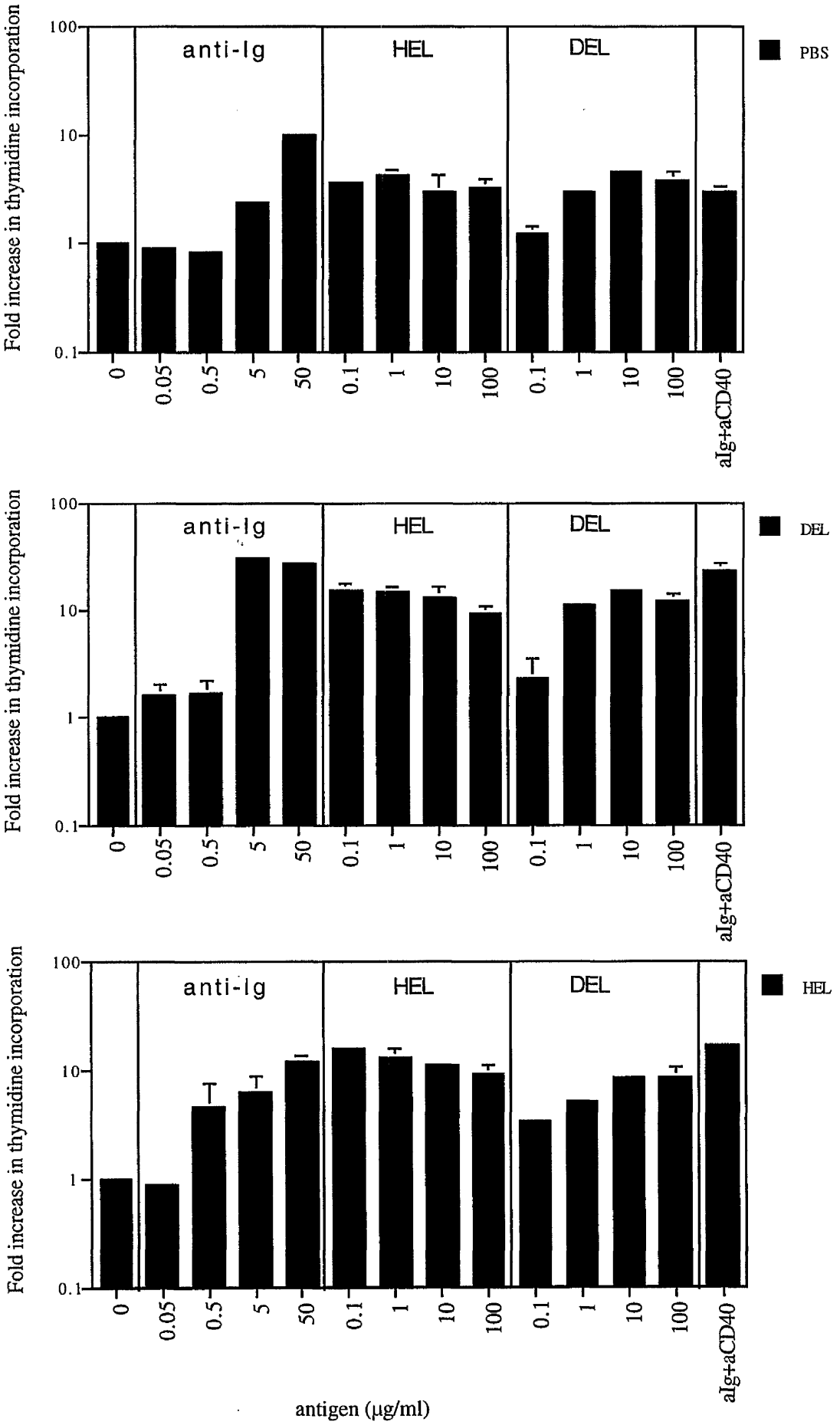
Fold increase in thymidine incorporation
100
10
1
0.1
anti-Ig
HEL
DEL
PBS
DEL
HEL
0
0.05
0.5
5
50
0.1
1
10
100
aIg+aCD40
antigen (μg/ml)

Fig. 90

Figure 90: The secondary response in the spleen of HEL-BCR mice and its effect on *in vitro* B cell stimulation. MD4 mice were pre-immunised with either PBS control, 100µg DEL or 100µg HEL. After 8d, proliferation in whole spleen cells was assessed by measurement of DNA synthesis. Cells ($5x10^5$ cells/well) were treated for 2d with anti-Ig (0-50µg/ml), DEL (0-100µg/ml), HEL (0-100µg/ml) or anti-Ig (5µg/ml)+anti-CD40 (10µg/ml). The levels of [^{3}H]-Thymidine incorporation into DNA were measured after further 4h. Data are expressed as means ± SD (*n=3*) from a single experiment.

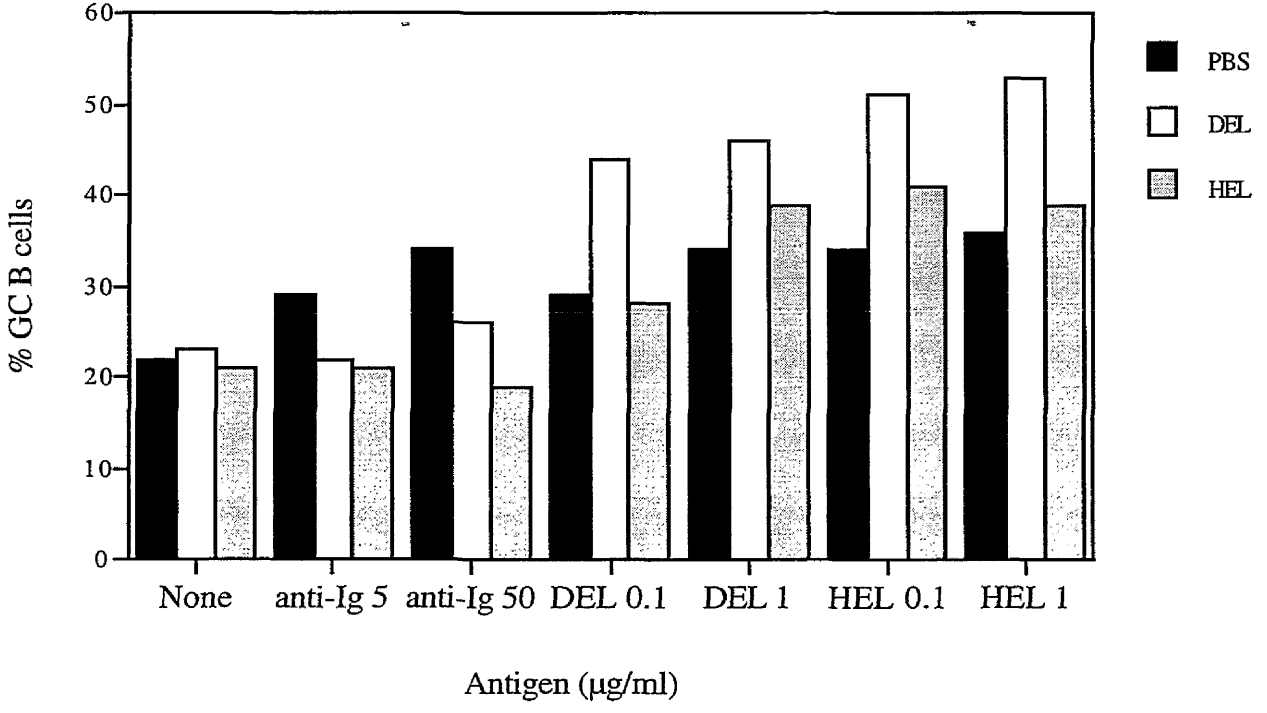
60
50
40
30
20
10
0
% GC B cells
None
anti-Ig 5
anti-Ig 50
DEL 0.1
DEL 1
HEL 0.1
HEL 1
Antigen (µg/ml)
PBS
DEL
HEL

Fig. 91

Figure 91: Expansion of GC B cells during secondary responses in the spleen. MD4 mice were pre-immunised with either PBS control, 100μg DEL or 100μg HEL. After 8d, mice were sacrified and whole spleen cells (10^6 cells/sample) stimulated for 2d with anti-Ig (0-50μg/ml), DEL (0-1μg/ml) or HEL (0-1μg/ml). Cells were counted and stained with CD19-FITC (1:20) and PNA-biotin (1:500)+streptavidin-APC (1:100). Percentage of GC B cells ($CD19^+$ PNA^+) in each sample was calculated from the number of total B cells.

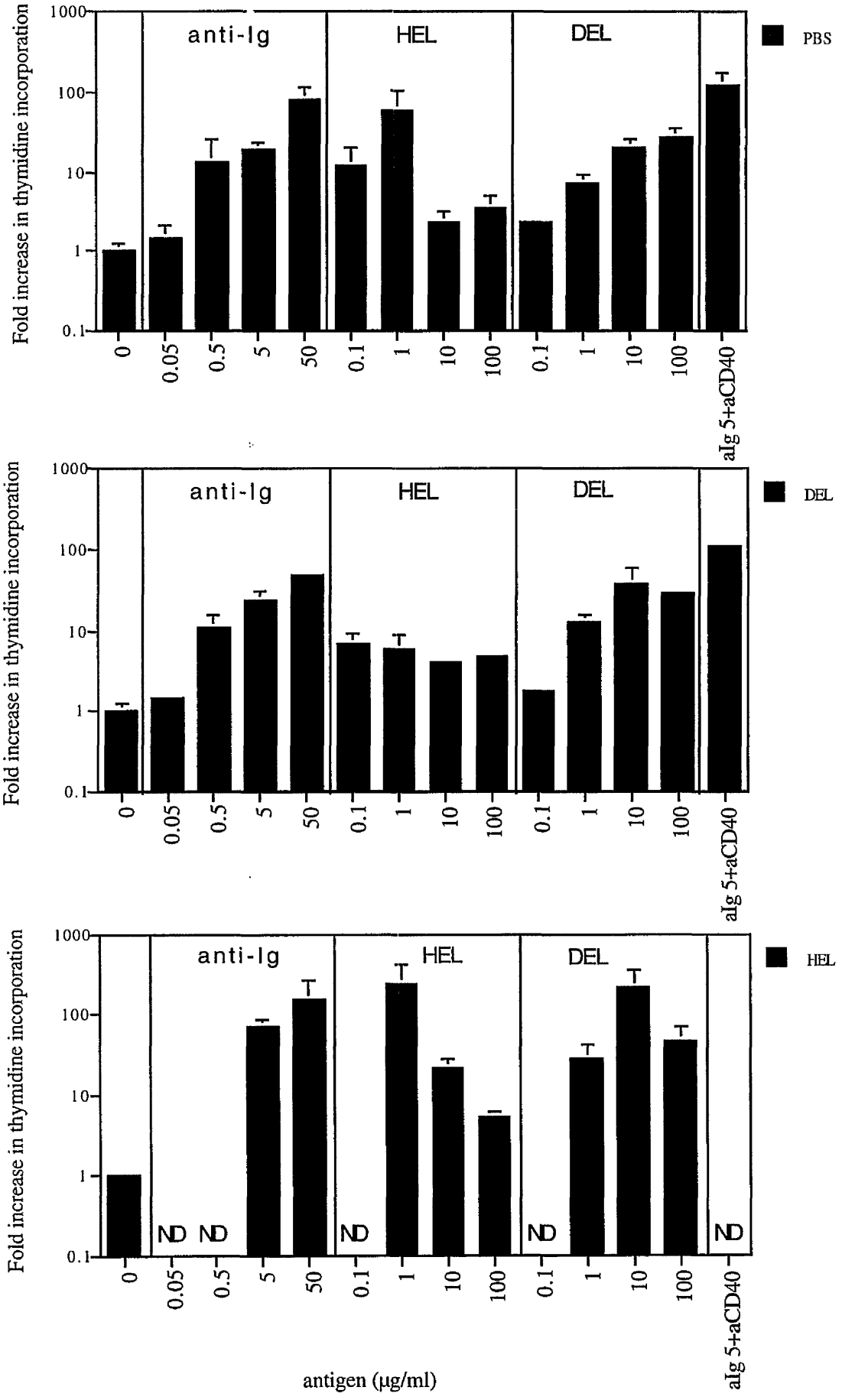
Fold increase in thymidine incorporation
1000
100
10
1
0.1
anti-Ig
HEL
DEL
PBS
DEL
HEL
0
0.05
0.5
5
50
0.1
1
10
100
aIg 5+aCD40
ND
antigen (μg/ml)

Fig. 92

Figure 92: The secondary response in the lymph nodes of HEL-BCR mice and its effect on *in vitro* B cell stimulation. MD4 mice were pre-immunised with either PBS control, 100µg DEL or 100µg HEL. After 8d, proliferation in whole lymph node cells was assessed by measurement of DNA synthesis. Cells ($5x10^5$ cells/well) were treated for 2d with anti-Ig (0-50µg/ml), DEL (0-100µg/ml), HEL (0-100µg/ml) or anti-Ig (5µg/ml)+anti-CD40 (10µg/ml). The levels of [^{3}H]-Thymidine incorporation into DNA were measured after further 4h. Data are expressed as means ± SD (*n=3*) from a single experiment. ND = not done.

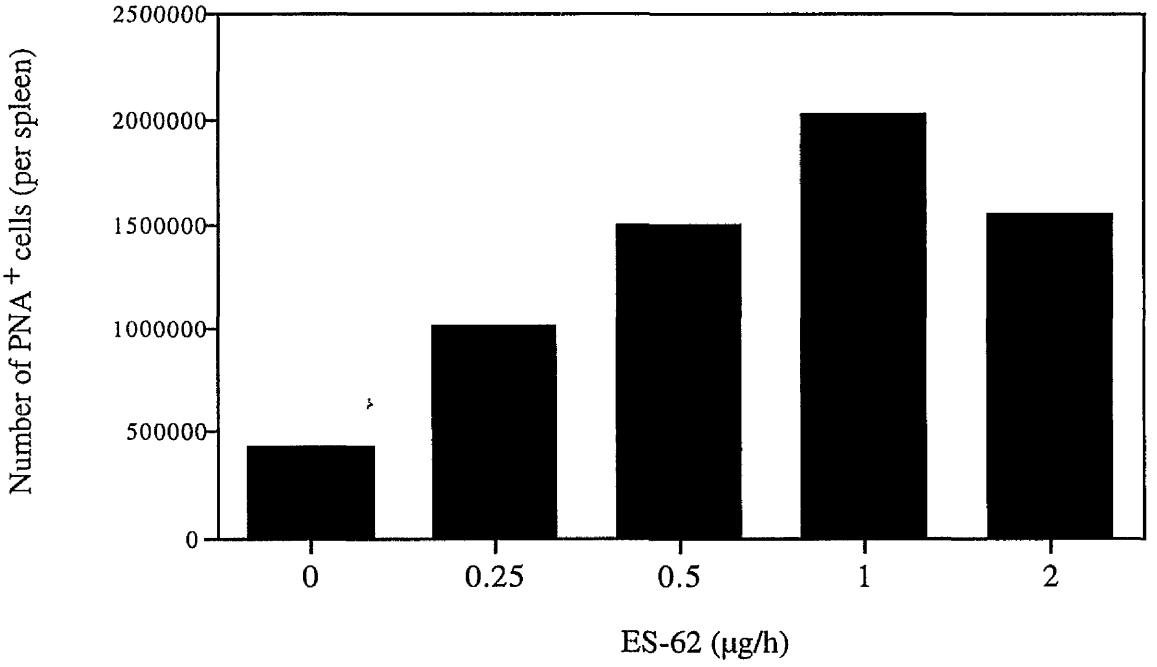
2500000
2000000
1500000
1000000
500000
0
Number of PNA + cells (per spleen)
0
0.25
0.5
1
2
ES-62 (µg/h)

Fig. 93

Figure 93: Induction of GC B cells in spleen of ES-62 treated mice. Whole spleen cells (10^6 cells/sample) from mice treated continuously with 0-2μg/h ES-62 were counted and stained upon sacrifice with PNA-FITC (1:500). Percentage of PNA^+ (GC B) cells was determined by flow cytometry.

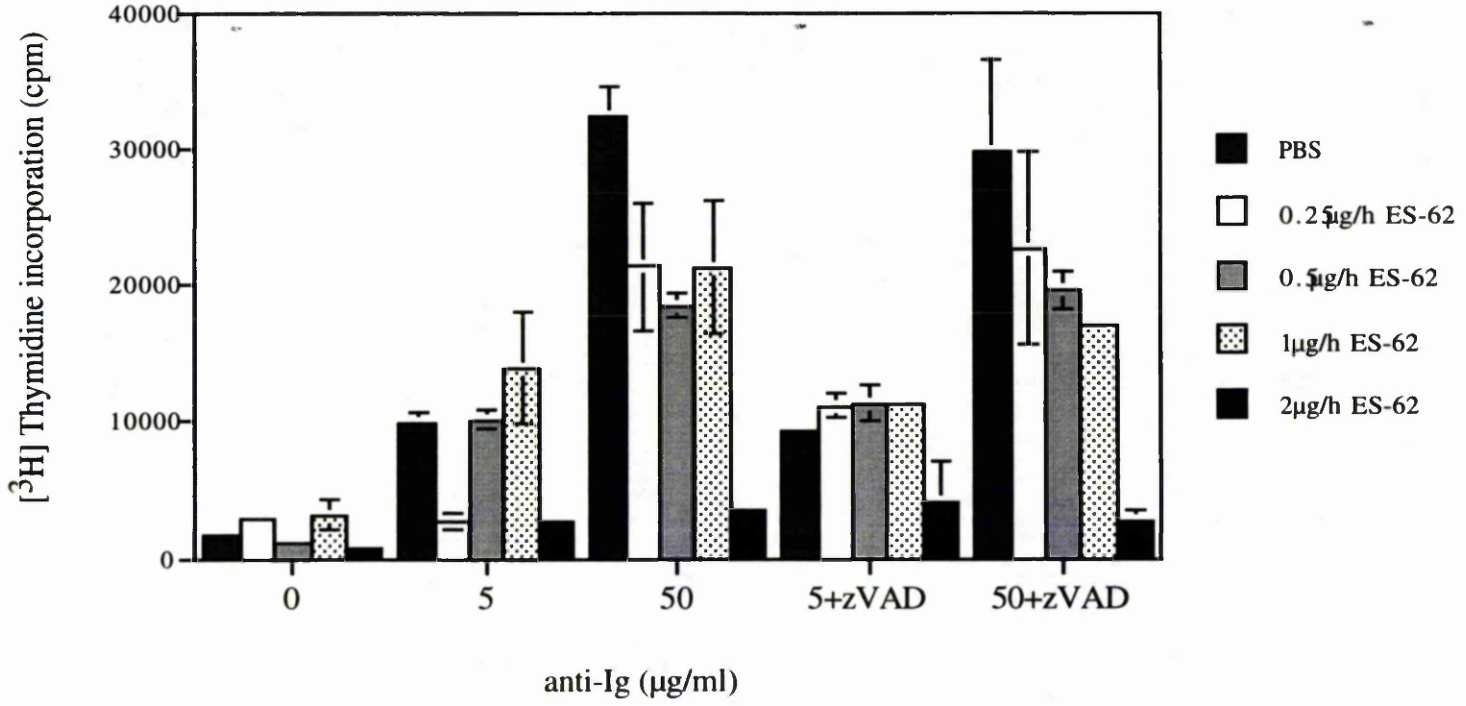
40000
30000
20000
10000
0
[3H] Thymidine incorporation (cpm)
0
5
50
5+zVAD
50+zVAD
anti-Ig (µg/ml)
PBS
0.25µg/h ES-62
0.5µg/h ES-62
1µg/h ES-62
2µg/h ES-62

Fig. 94

Figure 94: BCR stimulations of spleen cultures from ES-62 treated mice and the effect of Caspase inhibition. Proliferation in whole spleen cultures from mice exposed continuously with 0-2μg/h ES-62 ($5x10^5$ cells/well) were was assessed by measurement of DNA synthesis. Cells ($5x10^5$ cells/well) were treated for 2d with anti-Ig (0-50μg/ml) with or without 10μM zVAD-fmk. The levels of [^{3}H]-Thymidine incorporation into DNA were measured after further 4h. Data are expressed as means ± SD (*n=3*) from a single experiment.

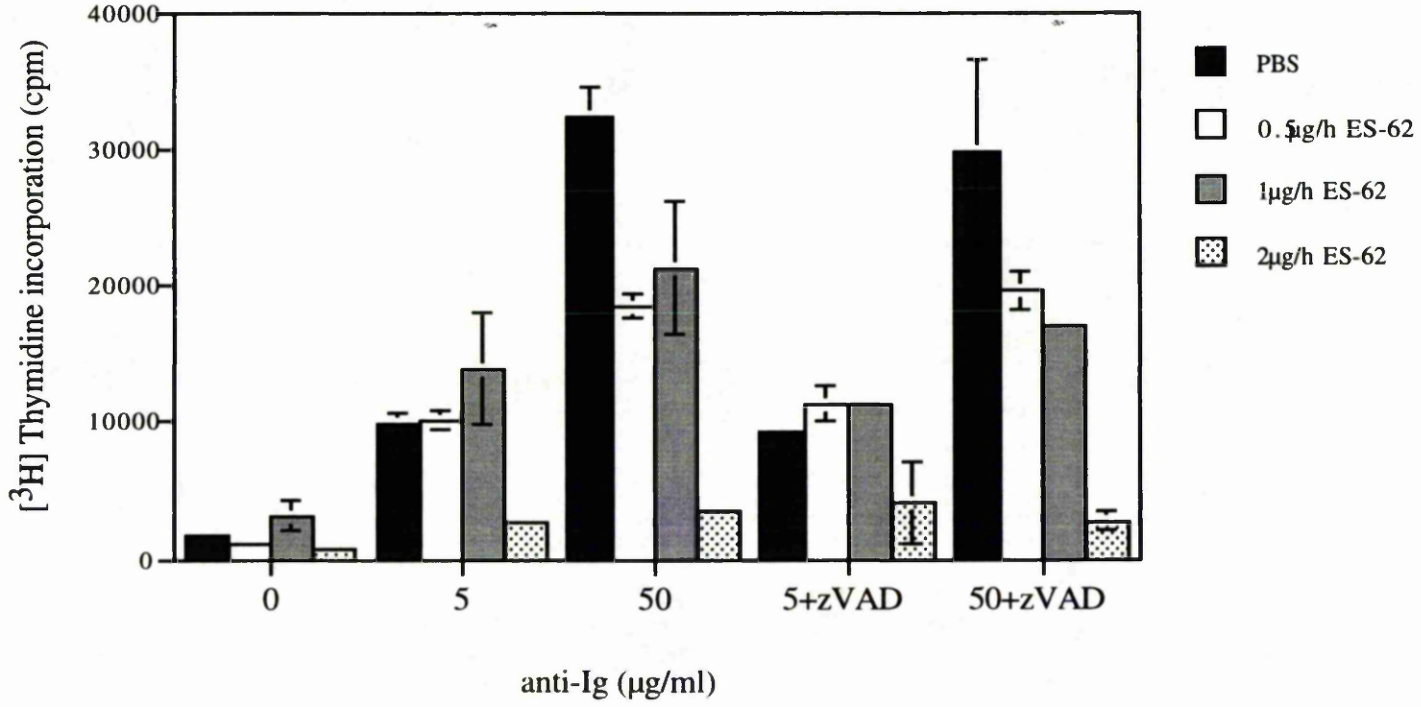
40000
30000
20000
10000
0
[3H] Thymidine incorporation (cpm)
0
5
50
5+zVAD
50+zVAD
anti-Ig (µg/ml)
PBS
0.5µg/h ES-62
1µg/h ES-62
2µg/h ES-62

Fig. 95

Figure 95: BCR stimulations of lymph node cultures from ES-62 treated mice and the effect of Caspase inhibition. Proliferation in whole lymph node cultures from mice exposed continuously with 0-2μg/h ES-62 ($5x10^5$ cells/well) were was assessed by measurement of DNA synthesis. Cells ($5x10^5$ cells/well) were treated for 2d with anti-Ig (0-50μg/ml) with or without 10μM zVAD-fmk. The levels of [^{3}H]-Thymidine incorporation into DNA were measured after further 4h. Data are expressed as means ± SD (*n=3*) from a single experiment.

a.

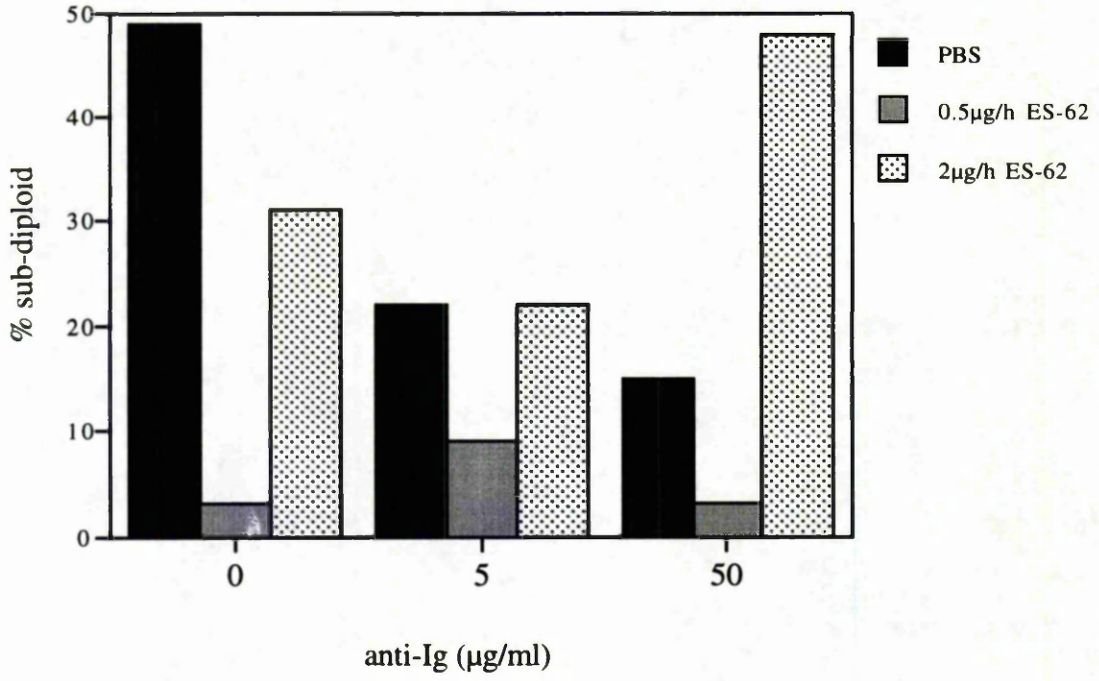
50
40
30
20
10
0
% sub-diploid
0
5
50
anti-Ig (µg/ml)
PBS
0.5µg/h ES-62
2µg/h ES-62

b.

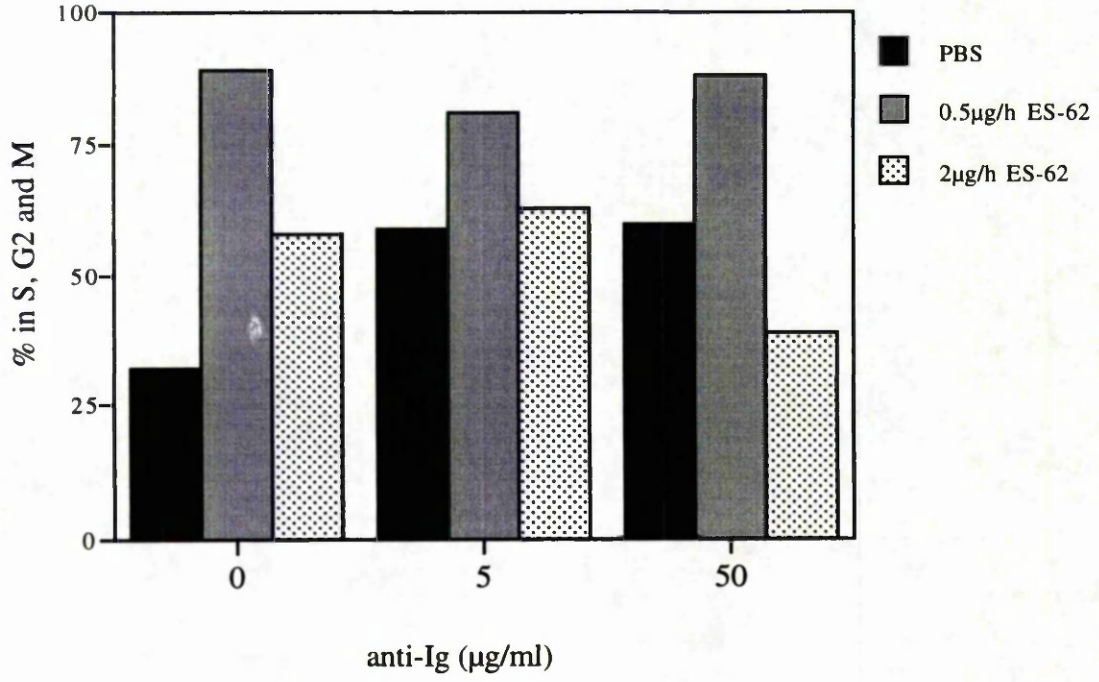
100
75
50
25
0
% in S, G2 and M
0
5
50
anti-Ig (µg/ml)
PBS
0.5µg/h ES-62
2µg/h ES-62

Fig. 96

Figure 96: Splenic Germinal Centre B cells from ES-62 treated mice - responses to BCR stimulation. Whole spleen cells (10^6 cells/sample) from mice treated continuously with 0-2μg/h ES-62 were stimulated for 18h with 0-50μg/ml anti-Ig. Cells were then stained with PNA-FITC (1:500) and subjected to PI incorporation in order to determine DNA content.

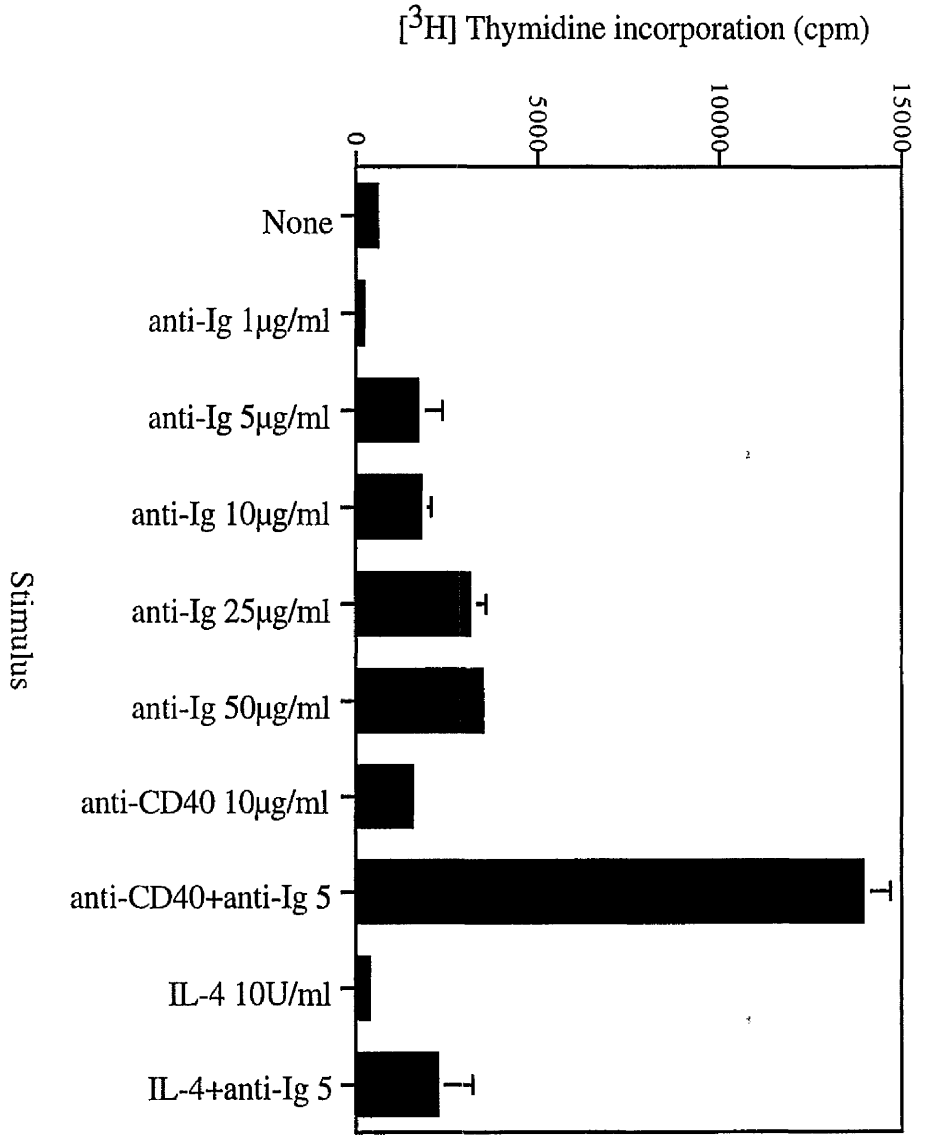
[3H] Thymidine incorporation (cpm)
0
5000
10000
15000
Stimulus
None
anti-Ig 1µg/ml
anti-Ig 5µg/ml
anti-Ig 10µg/ml
anti-Ig 25µg/ml
anti-Ig 50µg/ml
anti-CD40 10µg/ml
anti-CD40+anti-Ig 5
IL-4 10U/ml
IL-4+anti-Ig 5

Fig. 97

Figure 97: Proliferation of B-1 cells. Proliferation of peritoneal cavity B cells was assessed by measurement of DNA synthesis. Cells ($2.5x10^5$ cells/well) were treated for 2d with anti-Ig (0-50µg/ml) for 2d. The levels of [^{3}H]-Thymidine incorporation into DNA were measured after further 4h. Data are expressed as means ± SD (*n=3*) from a single experiment.

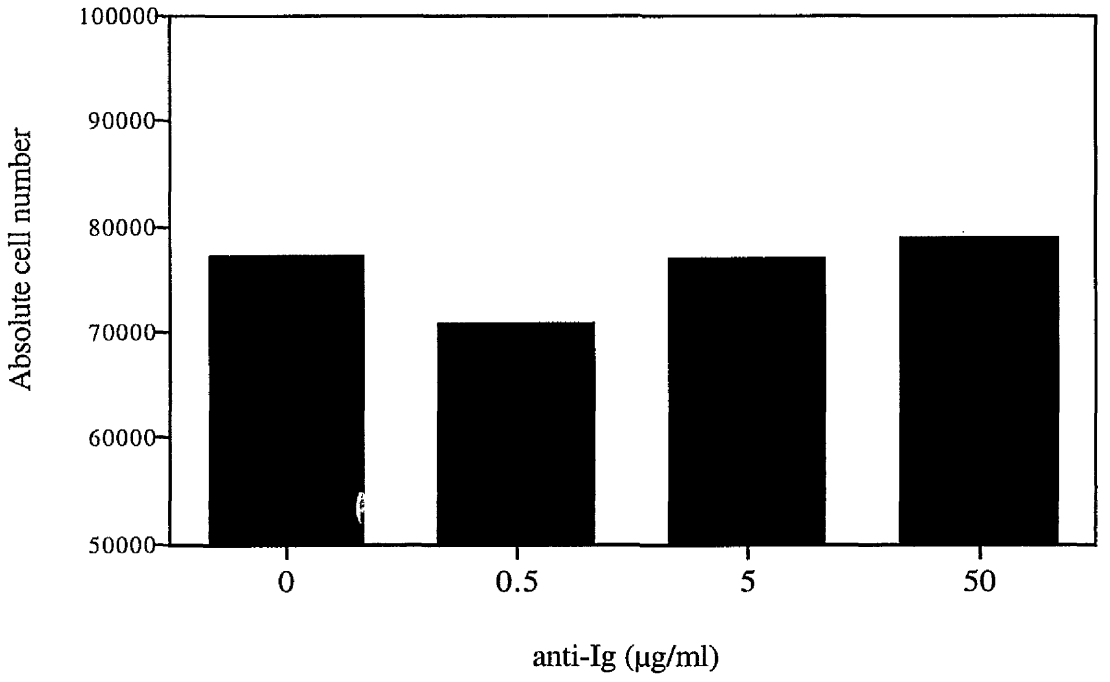
Absolute cell number
100000
90000
80000
70000
60000
50000
0
0.5
5
50
anti-Ig (µg/ml)

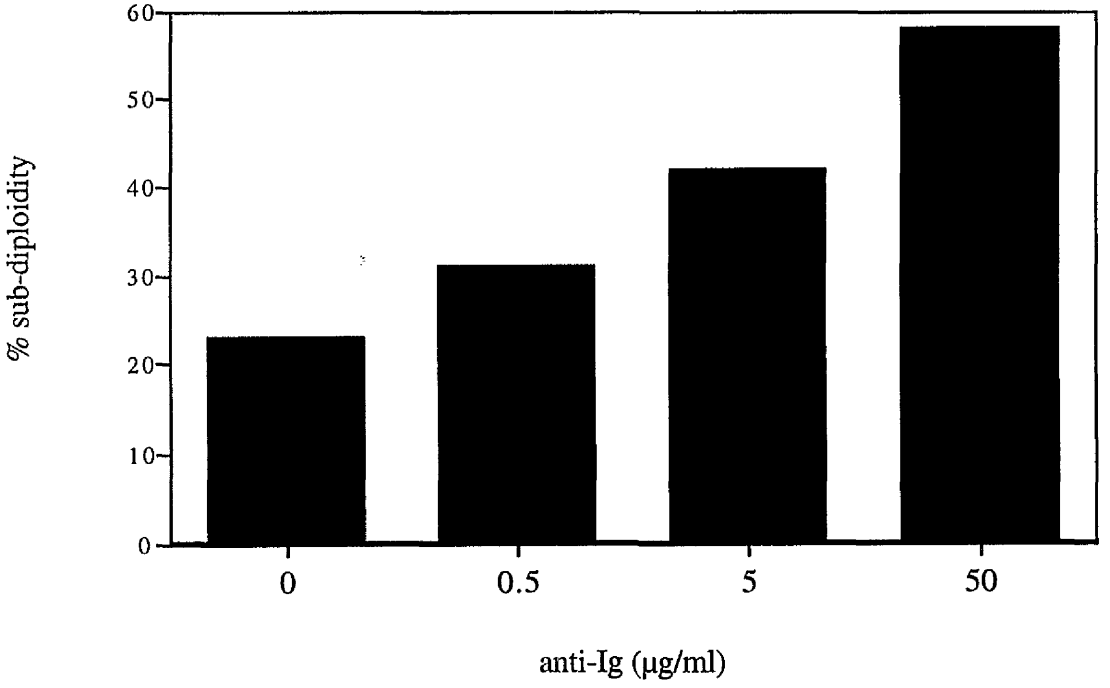
% sub-diploidity
60
50
40
30
20
10
0
0
0.5
5
50
anti-Ig (µg/ml)

Fig. 98

Figure 98: The B-1 population does not expand in response to BCR stimulation *in vitro* but undergoes apoptosis. Peritoneal cavity B cells (10^6 cells/sample) were stimulated with 0-50μg/ml anti-Ig for 2d and counted. Cells were subjected to PI incorporation and percentage of subdiploidity was determined according to cells with less than 2N DNA.

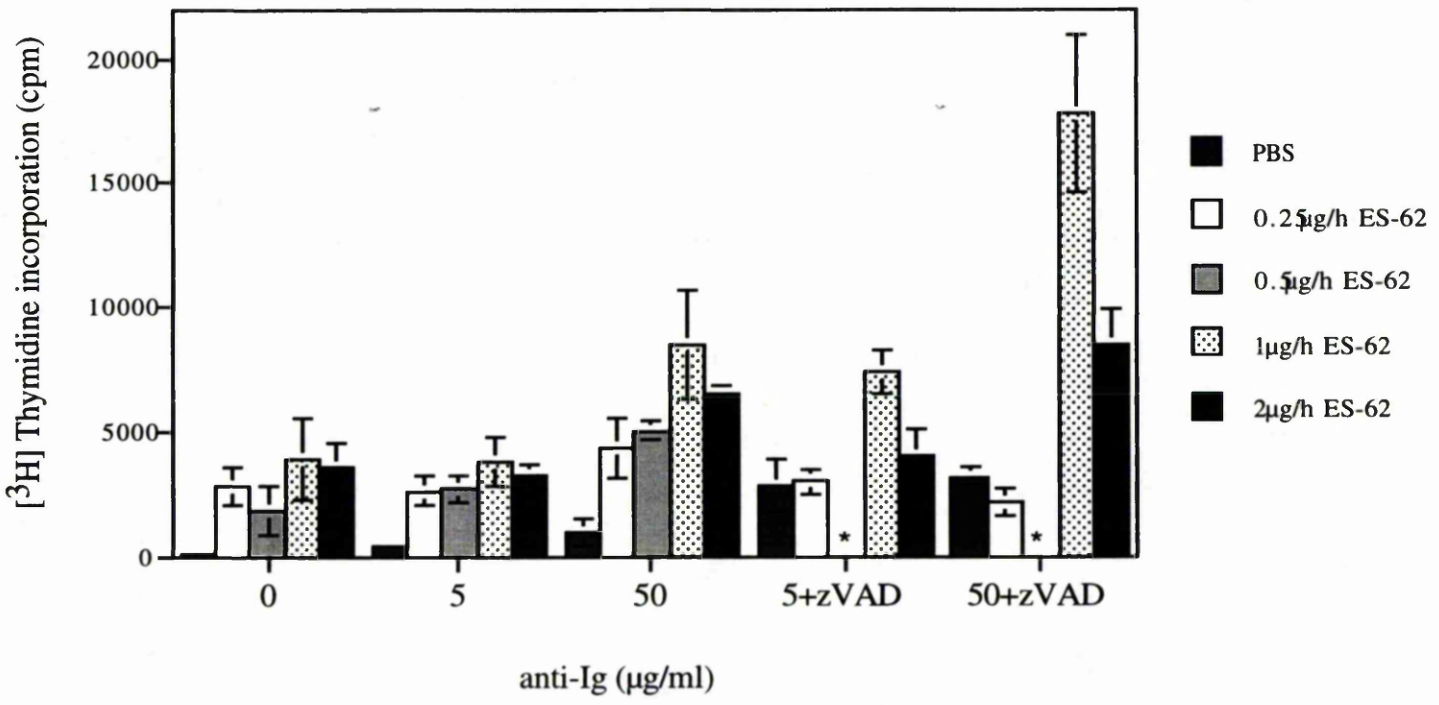

* = not done

Fig. 99

Figure 99: BCR stimulations of peritoneal cavity B cells from ES-62 treated mice and the effect of Caspase inhibition. Proliferation in peritoneal cavity B cell cultures from mice exposed continuously with 0-2μg/h ES-62 ($5x10^5$ cells/well) were assessed by measurement of DNA synthesis. Cells ($5x10^5$ cells/well) were treated for 2d with anti-Ig (0-100μg/ml) with or without 10μM zVAD-fmk. The levels of [^{3}H]-Thymidine incorporation into DNA were measured after further 4h. Data are expressed as means ± SD (*n=3*) from a single experiment.

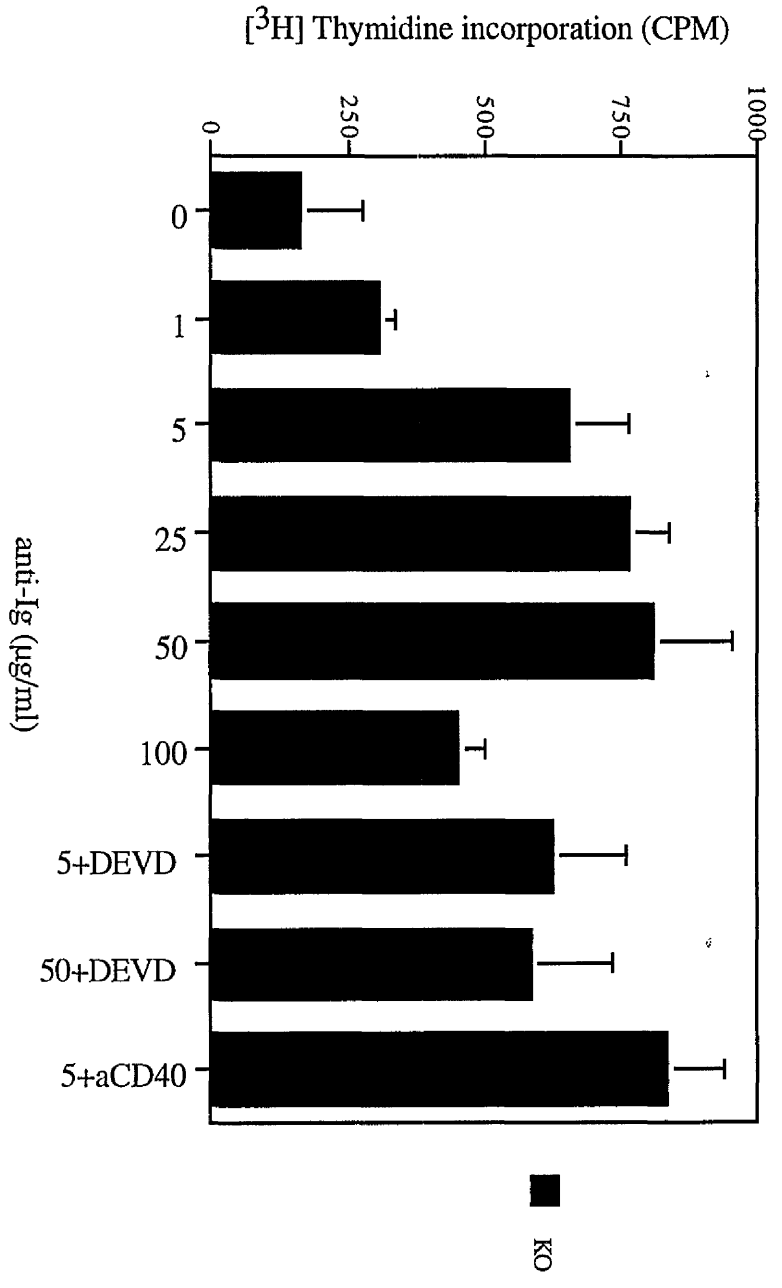
[3H] Thymidine incorporation (CPM)
0
250
500
750
1000
anti-Ig (μg/ml)
0
1
5
25
50
100
5+DEVD
50+DEVD
5+aCD40
KO

Fig. 100

Figure 100: Proliferation of peritoneal cavity B cells from $IgM^{-/-}$ mice. Proliferation of peritoneal cavity B cells from $IgM^{-/-}$ BALB/c mice was assessed by measurement of DNA synthesis. Cells ($2.5x10^5$ cells/well) were treated for 2d with anti-Ig (0-50µg/ml) with or without Ac-DEVD-CHO (10µM). The levels of [^{3}H]-Thymidine incorporation into DNA were measured after further 4h. Data are expressed as means ± SD (n=3) from a single experiment.

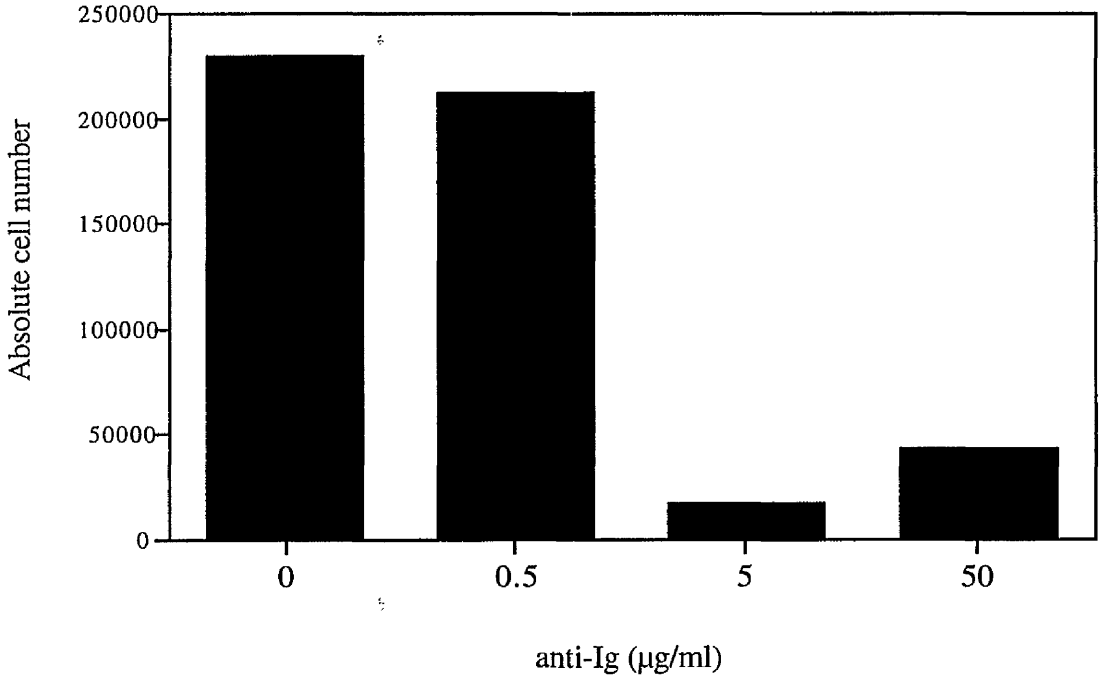
250000
200000
150000
100000
50000
0
Absolute cell number
0
0.5
5
50
anti-Ig (μg/ml)

Fig. 101

Figure 101: The anti-Ig response in peritoneal cavity B cells from Xid mice. Peritoneal cavity B cells from male Xid ($Btk^{-/-}$) mice (10^6 cells/sample) were stimulated with 0-50μg/ml anti-Ig for 2d and counted.

Chapter 6. GENERAL DISCUSSION

This thesis has focused on identifying the key cellular and molecular mechanisms underlying B cell selection. Special attention has been attributed to the selection of immature B cells using both the cell line model, WEHI-231, and experiments investigating B cell development in *ex vivo* bone marrow cultures. Comparitive experiments were also performed on bone marrow and peripheral B cell cultures to compare and contrast selection processes during other stages of B cell selection, particularly focusing on Germinal Centres and the peritoneal cavity.

6.1 The WEHI-231 cell line as a model for B cell selection

The results in chapter 3 have focused on the biochemical mechanisms involved in regulation of commitment to apoptosis of immature B cells. For these studies the immature B cell line WEHI-231 has been employed. Previous studies on this cell line have concentrated on two related areas concerned with BCR-mediated apoptosis, namely:

(i) Determination of the immediate signals downstream of the BCR, including tyrosine kinase activity and phosphorylation of target proteins [327], calcium mobilisation and PKC activation [196].

(ii) Cell cycle related events balancing the cell fate decision, as determined by BCR and CD40 signalling [98]. Contradictory evidence has arisen concerning the involvement of cyclins, cdks and ckis in these processes in WEHI-231 cells [217, 328].

Therefore, it was of interest to study the intermediate events controlling apoptosis and its inhibition in this model. Recent discoveries of mitochondrial-related events, which are crucial for such processes, provided a wide area for investigation. The mitochondria is also a focal point in terms of the Bcl-2 family and effector Caspase activity, in which have been shown to be crucial to the regulation of other types of programmed cell death in the immune system (reviewed in [50]). Therefore the mitochondria was an ideal target for investigation.

At the start of this investigation the most important evidence regarding the Bcl-2 family proteins suggested then Bcl-x_L upregulation (at the mRNA level) comprised part of the rescue signal manifested by CD40 in WEHI-231 cells [158]. Hence, initial studies concentrated on examining the effects of apoptotic and rescue siganls on protein levels of the Bcl-2 family in WEHI-231 cells. The Bcl-2 family is currently known to have more than a dozen members [61] and proteins of the three main subfamilies were found to be represented in WEHI-231 cells: anti-apoptotic (Bcl-2, Bcl-x_L, Mcl-1, A1), short pro-apoptotic (BH3-only; Bid and Bad) and long pro-apoptotic (Bax and Bak). Surprisingly, most of these proteins were induced with anti-Ig treatment alone. However, rather than a simple upregulation of expression of a particular Bcl-2 family member, the rescue signal was mapped to a bias in the balance between Bcl-2 proteins, inducing Bcl-x_L levels and blocking of Bad and Bid entry to the mitochondria (fig. 27).

A major observation was that although depolarisation of the mitochondrial potential occurs downstream of the BCR signal, it is not accompanied by cytochrome C release as in other systems (fig. 29). This evidence has been confirmed now by others [78]. This unique mitochondrial mechanism has prompted careful investigation into the role Caspases play in immature B cell deletion. Most reports which were published during the course of this work have used very high concentrations of Caspase inhibitors to block cell death [291, 328]. Using lower and more specific inhibitor concentrations has provided contradictory evidence to that of previous reports. These experiments have demonstrated that many protease inhibitors can substitute for Caspase inhibitors at such high concentrations ≥100μM (table 2). Furthermore, specific Cathepsin B activity was observed downstream of the BCR signal. Specific blockage of Cathepsin B activity, and not of Caspase activity, could rescue WEHI-231 cells from BCR-induced apoptosis (fig. 34).

Previous work in the group has shown that $cPLA_2$ is specifically expressed in lymphocytes only when they are subjected to negative selection [171]. Further studies shown here have confirmed that $cPLA_2$ plays a major role in BCR-induced apoptosis of WEHI-231 cells. This

enzyme was shown to migrate to the mitochondria as determined by both immunohistochemistry and activity assays. A detailed screening for a possible further metabolism of its product, arachidonic acid, failed to identify any candidates, which were involved in apoptosis (fig. 21-22). In contrary, the data suggested that AA was the active metabolite and that metabolism by COX or LOX pathways were utilised by rescue signals.
Interestingly, treatment of cells with arachidonic acid at a concentration that by itself is sufficient to cause apoptosis in these cells did not induce, in some cases (for example, Bcl-2 family protein expression), the same effects as IgM crosslinking, in terms of regulation. Nonetheless, both BCR-induced $cPLA_2$ activity and AA by itself do not facilitate PARP cleavage. A possible mechanism was identified here by the fact that some of the induced $cPLA_2$ activity is located in the mitochondria (fig. 19). Further results have shown that Bcl-x_L is sufficient to block AA (and anti-IgM) induced apoptosis. This may indicate that AA production serves in the mitochondrial membrane disturbance mechanism and not as a second messenger by itself.
Another important aspect of the mitochondrial participation in apoptosis is the potential involvement of calcium homeostasis. Evidence here and by others [301], has shown that cyclosporin A is suffcient to reverse apoptosis in WEHI-231 cells. This immunosupressor has been shown to have an effect on a variety of ion channels via membrane-bound cyclophillins. CsA blocks IP_3-sensitive Ca^{+2} channels in the ER as well as the mitochondrial PTP [250]. Calcium release, together with IP_3 production, are well documented events downstream of BCR stimulation. Therefore, it is possible that the mitochondria takes part in determining calcium release patterns from the ER through local buffering, as suggested for other systems. There is a whole variety of factors that may be influenced by such modeling. $cPLA_2$ is calcium dependent, suggesting a direct contribution of calcium for cell death in this cell line. It is tempting to speculate that other calcium-sensitive factors, including PKC isoforms and calcineurin [254], can also have an active role in determining cell fate, especially through regulation of transcription factors [166]. Possible links between all of these events are given in fig. 102.

The rescue of WEHI-231 cells from BCR-induced apoptosis happens in the time window between 16 and 24 hours (fig. 14). This indicates that a "point of no return" may exist, around 24h post-stimulation, when cell fate cannot by reversed by CD40 signalling. Protease activity was shown to be essential for complete effect of BCR stimulation, growth arrest and apoptosis. Although the specific protease could not be identified, it is likely to be Calpain [78]. Although blockage of Cathepsin B activity prevented BCR-mediated apoptosis, Cathepsin inhibition did not block BCR-induced growth arrest (fig. 35). It is also possible that Caspase-7 is utilised as an intiator Caspase, rather that an effector Caspase, in this model [78].

Importantly, the effect of IgM crosslinking on growth and death suggests the involvement of cell cycle regulators in this process. Earlier investigations by others used manipulated WEHI-231 cells. This evidence is not necessarily physiologically relevant, since manipulation such as over-expression of Bcl-x_L, may effect cell cycle events [66, 329]. The results presented here, however, may suggest that Mdm2 binding to p53 and its resulting degradation, is essential for the survival of these cells. This evidence further supports the theory of an innate suicide machine within the cell. That may also relate to results *in vivo* regarding a continuous signal which is essential for the survival of immature B cells.

The role of ROS in determining cell fate is not fully understood. Some evidence exists that lower levels of ROS production may contribute to proliferation. Consistent with this, observations where mitochondrial inhibitors contribute to cell cycle progression in WEHI-231 cells (fig. 13) support this speculation. Inhibitor studies suggested NO and *de novo* ceramide synthesis may have protective effect on B cell proliferation. These observation may also be linked to AA production which is documented to cause uncoupling of mitochondrial respiration and in this way to promote ROS production [330]. This may prove to be one of the missing links between the mitochondrial events and cell cycle events in apoptosis. Fresh evidence regarding p53 translocation to the mitochondria [126] and its known sensitivity to ROS [331] may provide such a link. For example it is possible that mitochondrial instability is

detected by p53, which in turn is phosphorylated in order to exert its cell fate decisions in the nucleus.

6.2 B cell selection in the bone marrow and in the periphery

The discovery of transitional B cells has questioned the classical model, which proposes that B cell selection takes place at the immature stage. Previously it was thought that immature B cells are fully selected in the bone marrow and non-self-reactive cells emigrate via the sinuses to create the naive B cell pool in the periphery. With the identification of transitional stages, some persisting in the periphery [9], this model has been challenged in some of its core assumptions:
(i) Which types of B cells are deleted?
(ii) Which types of B cells undergo receptor editing?
(iii) Does deletion occur in the periphery?
Novertheless, there is still strong evidence that most immature B cells do not eventually reach the periphery [6]. Moreover, the repertoire in the naive B cell pool is more restricted than in the bone marrow and therefore selection process must take place before entry to the naive pool.

A summary of the observations made in the *ex vivo* bone marrow cultures, and in other primary B cell cultures, is given in figure 103. Possibly, the most important finding is that even upon polyclonal stimulation, some immature B cells escape the negative selection and become mature cells. This observation may relate to suggestions of continuous stimulation ("BCR tickling") which is needed for B cell survival and even development [9, 332].
Two models of selection have been proposed based on the available data:
The instructive model
In this model the sole factor which determines the fate of B cells before entry to the naive pool is BCR specificity. Thus, exposure to selfantigens in the bone marrow instruct B cell development - if a B cell is self-reactive it will either be deleted by apoptosis or undergo a limited number of

receptor editing attempts. An interesting possibility is that while some immature B cells are deleted in the bone marrow due to selfreactivity, transitional B cells in the periphery will mainly undergo receptor editing. This model is supported by some results shown in chapter 4: 80-90% of immature B cells are deleted by BCR stimulation (fig. 39) and growth arrest has been induced in parallel to apoptosis in transitional B cells (fig. 42). Furthermore, only a small number of B cells escapes deletion via their BCR, using polyclonal stimulation. Therefore, it is feasible that B cells rely solely on BCR stimulation to determine their fate.

The stochastic model

This model proposes that specificity is not the only mechanism underlying B cell selection. For example, it is possible that competition for environmental niches in the bone marrow and the periphery plays a major role in limiting B cell numbers. Two observations made in this thesis support this model:

(i) Transitional B cells are Fas-sensitive even in the absence of strong BCR stimulation. This sensitivity has also been reported by others [8].

(ii) Some B cells escape polyclonal stimulation of the BCR - a stimulus which theoretically should delete all immature/transitional B cells.

In such a stochastic model, genetic predisposition of the immature and transitional B cells may play a part in determining which of them will ultimately survive selection. Supporting this suggestion are results in immature B cells. At least some of these bone marrow cells induce, rather than reduce, Bcl-x_L and Bcl-2 levels in response to anti-Ig treatment (fig. 41). Therefore it is possible, that surviving cells are the cells which can induce survival factors in response to BCR-stimulation.

Obviously, there are many aspects to be examined until these observations can allow the models described above to be reconciled. Two aspects may prove the most important, in relation to determination of stochastic elements in B cell selection:

Firstly, identification of factors assisting immature B cell survival in the bone marrow. Thy.1^{dull} cells, of as yet unidentified lineage, have been

identified as such a factor [12]. Moreover, Thy.1^{dull} cells interact directly with immature B cells in the bone marrow. Observations here did not support a role for CD40L or IL-4 (not shown) as possible factors involved in the rescue (rather than supporting survival) of immature or transitional B cells from apoptosis. Therefore, the nature of help from the bone marrow environment is still to be found. Moreover, it is possible that transitional B cells need another T cell dependent rescue signal, such as via MHC class II or B7.2 [313].
Secondly, the link between Fas expression and BCR stimulation is awaiting exploration. It is possible that a certain level of Ig cross-linking causes upregulation of Fas expression on the cell surface. A tempting connection to receptor editing can be made - it is possible that transitional B cells which failed this process upregulate Fas and make themselves susceptible for deletion in this manner.

Most of chapter 5 characterised the responses of B cells in the spleen and the lymph nodes. Special attention was given to the response to anti-Ig in GC and non-GC B cells at both sites. In the primary response, GC and non-GC B cells differ in their rates of proliferation and survival. Outside the GCs, resting B cells are activated quickly and proliferate within 24h. In contrast, GC B cells undergo first substantial apoptosis before the survivors start to proliferate later (48h; fig. 76). Figure 103 illustrates how B cells are selected via different mechanisms during their life span. Most notably, GC B cells appear to utilise similar BCR-induced deletion mechanisms to these of transitional B cells. The BCR signal is transduced to the mitochondria and excutes cell death in a Caspase-dependent manner (fig. 80). Nonetheless, Btk plays a different role in these developmental phases. For example, transitional B cells cannot develop further in the absence of Btk. In contrast, generation of Btk$^{-/-}$ GC B cells was accelerated and was limited mainly because of low peripheral B cell number (fig. 83). In fact, in this aspect, these GC B cells resembled Btk$^{-/-}$ immature B cells, which showed better survival than normal cells. Taken together, this evidence may suggest two independent pathways which are intiated via the BCR - a mitochondrial pathway and a Btk-

dependent pathway. In each selection step in B cell development these pathways can have different functional outcomes and therefore can differntialy determine the fate of the cell differently.

From the experiments in WEHI-231 cells one can speculate that both calcium and $cPLA_2$ may play an improtant role in the mitochondrial activity downstream of BCR stimulation *in vivo*, probably in immature B cells, which resembled overall the observations in the cell line. Although there is some evidence for differences in calcium mobilisation in a developmental-stage dependent manner [332], the implications of this evidence are not clear. Precise observations regarding calcium flux within the cell are needed to link such differences to other developmental-stage dependent mediators, such as PKCβ or c-Fos [9, 333].

6.3 Concluding remarks

In the course of this thesis, the work has progressed from dissecting a mechanism of apoptosis of immature B cells in the WEHI-231 model, to investigating the relevance of these mechanisms *in vivo*. Cell lines, such as WEHI-231, have two important advantages: availability and ease of manipulation. Therefore, the WEHI-231 model was used in all assays which required a pure cell population, such as western blotting, activity assays etc. The evidence obtained by using this system was useful in establishing the BCR stimulation of immature B cells recruits a mitochondria-dependent apoptotic process. This process involves a few components: mitochondrial phospholipase A_2 activation, disruption of mitochondrial potential and profound depletion of cellular ATP levels, but does not cause release of cytochrome C from mitochondria and is independent of Caspase activation. Although mitochondrial potential disruption is uncoupled from Caspase activation, activation of proteases such as Cathepsins does appear to play a role in the post-mitochondrial execution of apoptosis by WEHI-231 immature B cells. Development of the *ex vivo* bone marrow system has enabled to invesigate selection in primary B cells. Using this system, it was shown that polyclonal activation of immature B cells is sufficient to cause both deletion and

maturation. Transitional B cells which were produced *ex vivo* were shown to be Fas-sensitive and Btk-dependent. In addition, while BCR-induced apoptosis in immature B cells was Caspase-independent, apoptosis of transitional B cells was Caspase-dependent. Similarly to transitional B cells, BCR-induced apoptosis in GC B cells and B-1 cells was Caspase-dependent. Variation in the utilisation of pathways by BCR signalling during B cell development was demonstrated once again by the fact that GC B cells had greater rate of proliferation in the absence of Btk.

Recent progress in separation techniques will enhance future manipulation of these *ex* vivo/*in vitro* cultures. It would have been of special interest to explore two particular directions:
(i) Isolation of different primary cell populations (immature and transitional B cells, GC B cells) and stimulation *in vitro* for direct measures of cell cycle related events. Significant evidence in this direction is especially difficult to achieve using cell line models.
(ii) Sorting of B cell populations post-stimulation - comparison of protein levels (for example: of the Bcl-2 family), activity (of proteases and $cPLA_2$) and even heavy chain usage (as a measure of gene rearrangement of the BCR). Such experiments can link *ex vivo* the function of certain proteins to signalling events in each developmental stage. They can also be used to show whether the surviving cells are a genetically distinct population, for example, within the whole immature B cell population of the bone marrow.

Taken together with the possibilities encompassed in the usage of different tansgenic mice as a source for bone marrow cultures, the options for futher studies are indeed very diverse. Valuable observations can be made also in exploring possible additional signals to BCR and CD40, which are needed for transitional B cell survival. Novel data obtained here regarding peripheral B cells have also suggested some additional future directions. For example:
(i) In Germinal Centre B cells - more comparisons are needed in two different directions: between signals (BCR, CD40, IL-4 receptor and their

combinations); and between the behaviour of splenic and lymph node GC B cells.
(ii) In B-1 cells: exploration of their Caspase-dependent BCR signal. LPS is also an effctive stimulator of these cells and may help to explore the mechanism of activation of these cells.

Even from the data presented here it is already evident that comparisons from different B cell selection processes are fruitful. This is especially true in extending the understanding of possible pathways which are used during the distinct stages of B cell development to determine cell fate. Such knowledge can help in treatment of various diseases relating to the immune system. Lymphomas which could be related to a specific stage in B cell development could ultimately be treated in manner which tackles an unique pathway component used at the relevant stage of development. Recently diffuse large B cell lymphomas were recognised to be generated from both activated follicular B cells and GC B cells [334]. Such diseases could thus be treated with a specific drug which targets specifically the dysfunctional pathway, in a way which does not harm B cells of other developmental stages. In addition, clarification of the selection mechanisms preceeding entry to the naive B cell pool might assist in the treatment of various autoimmune diseases. Such information can lead, for example, to drugs or treatment which encourage reinforcement of the healthy selection processes. If selection of bone marrow B cells proves to rely heavily on a stochastic mechanism, such treatments may prove even less difficult. Such treatment could be, for instance, site-specific administration of anti-Fas antibodies to reduce transitional B cell numbers.

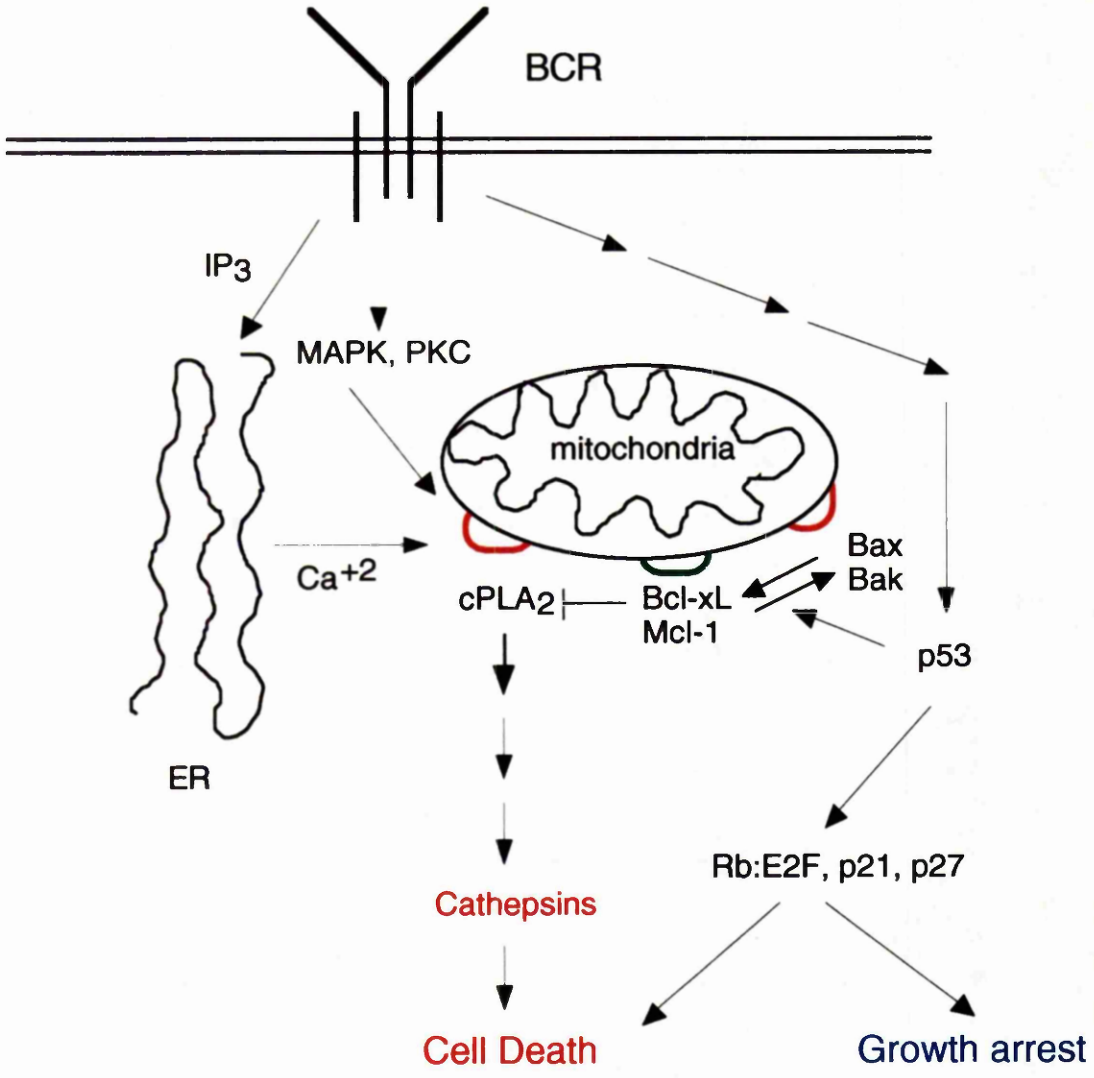
BCR
IP3
MAPK, PKC
mitochondria
Ca+2
cPLA2
Bcl-xL
Mcl-1
Bax
Bak
p53
ER
Rb:E2F, p21, p27
Cathepsins
Cell Death
Growth arrest

Fig. 102

Figure 102: Model for the role of mitochondrial events in the WEHI-231 immature B cell line model.

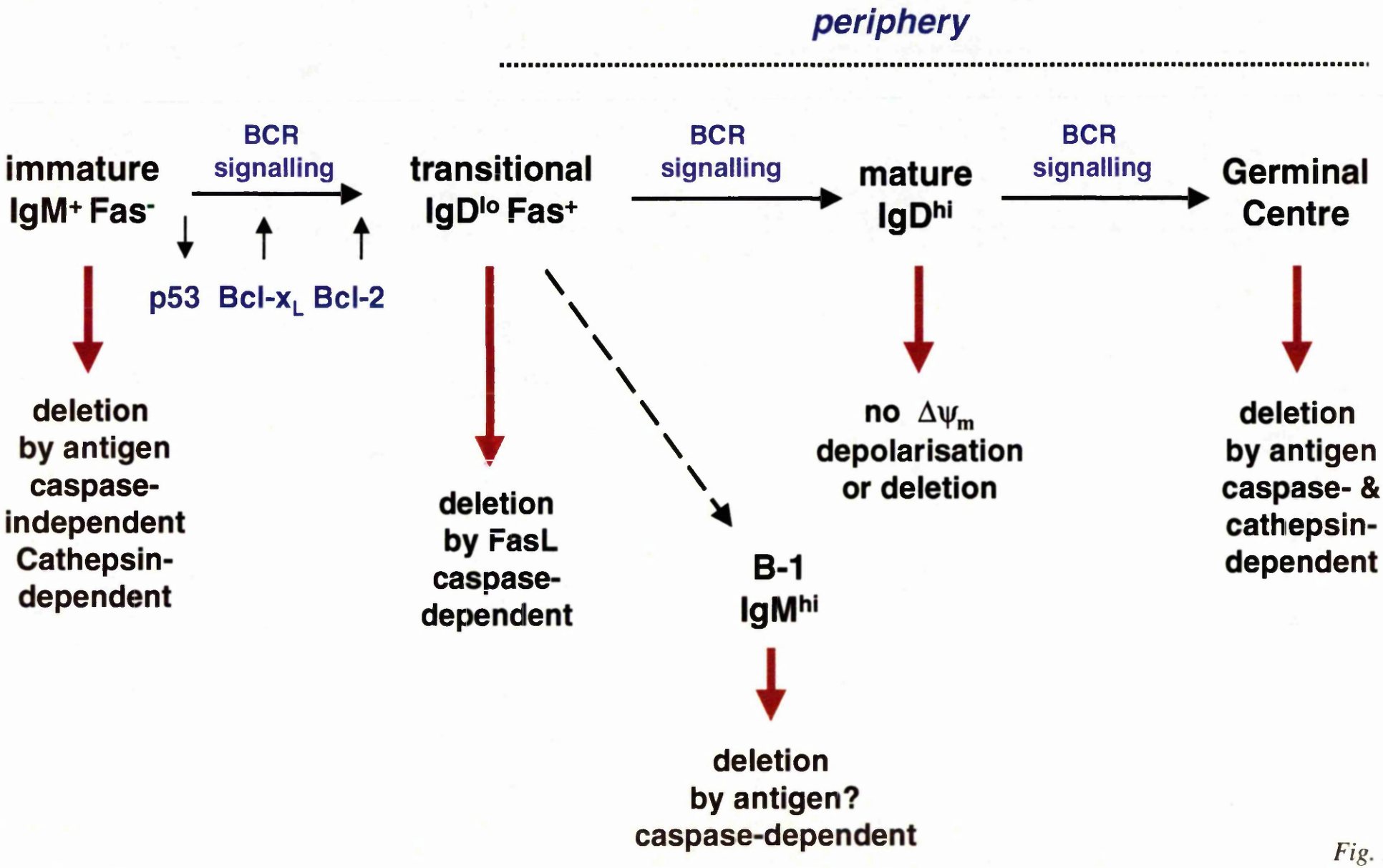
periphery
immature
IgM+ Fas-
BCR
signalling
p53 Bcl-xL Bcl-2
transitional
IgDlo Fas+
BCR
signalling
mature
IgDhi
BCR
signalling
Germinal
Centre
deletion
by antigen
caspase-
independent
Cathepsin-
dependent
deletion
by FasL
caspase-
dependent
B-1
IgMhi
deletion
by antigen?
caspase-dependent
no Δψm
depolarisation
or deletion
deletion
by antigen
caspase- &
cathepsin-
dependent

Fig. 103

Figure 103: Model for B cell selection and development - from the bone marrow to the Germinal Centre.

References

1. Busslinger, M., S.L. Nutt, and A.G. Rolink, *Lineage commitment in lymphopoiesis.* Curr Opin Immunol, 2000. **12**(2): p. 151-8.
2. Campbell, K.S., *Signal transduction from the B cell antigen-receptor.* Curr Opin Immunol, 1999. **11**(3): p. 256-64.
3. Benschop, R.J. and J.C. Cambier, *B cell development: signal transduction by antigen receptors and their surrogates.* Curr Opin Immunol, 1999. **11**(2): p. 143-51.
4. Kitamura, D., *et al., A B cell-deficient mouse by targeted disruption of the membrane exon of the immunoglobulin mu chain gene.* Nature, 1991. **350**(6317): p. 423-6.
5. Lutz, C., *et al., IgD can largely substitute for loss of IgM function in B cells.* Nature, 1998. **393**(6687): p. 797-801.
6. Pillai, S., *The chosen few? Positive selection and the generation of naive B lymphocytes.* Immunity, 1999. **10**(5): p. 493-502.
7. Hertz, M. and D. Nemazee, *BCR ligation induces receptor editing in IgM+IgD- bone marrow B cells in vitro.* Immunity, 1997. **6**(4): p. 429-36.
8. Carsetti, R., G. Köhler, and M.C. Lamers, *Transitional B cells are the target of negative selection in the B cell compartment.* J Exp Med, 1995. **181**(6): p. 2129-40.
9. Monroe, J.G., *Balancing signals for negative selection and activation of developing B lymphocytes.* Clin Immunol, 2000. **95**(1 Pt 2): p. S8-13.
10. Retter, M.W. and D. Nemazee, *Receptor editing occurs frequently during normal B cell development.* J Exp Med, 1998. **188**(7): p. 1231-8.
11. Hertz, M. and D. Nemazee, *Receptor editing and commitment in B lymphocytes.* Curr Opin Immunol, 1998. **10**(2): p. 208-13.
12. Sandel, P.C. and J.G. Monroe, *Negative selection of immature B cells by receptor editing or deletion is determined by site of antigen encounter.* Immunity, 1999. **10**(3): p. 289-99.
13. Yellen-Shaw, A. and J.G. Moroe, *Differential responsiveness of immature- mature-stage murine B cells to anti-IgM reflects both FcR-*

depdent and -independent mechanisms. Cell Immunol, 1992. **145**(2): p. 339-350.

14. Gaur, A., X.-r. Yau, and D.W. Scott, *B Cell Tolerance Induction by Cross-Linking of Membrane IgM, but not IgD, and Synergy by Cross-Linking of both Isotypes.* J Immunol, 1993. **150**(5): p. 1663-1669.

15. Goodnow, C.C., *et al.*, *Induction of self-tolerance in mature peripheral B lymphocytes.* Nature, 1989. **342**: p. 385-390.

16. Gray, D., *Regulation of immunological memory.* Curr Opin Immunol, 1994. **6**(3): p. 425-30.

17. MacLennan, I.C., *B-cell receptor regulation of peripheral B cells.* Curr Opin Immunol, 1998. **10**(2): p. 220-5.

18. Craxton, A., *et al.*, *Signal transduction pathways that regulate the fate of B lymphocytes.* Adv Immunology, 1999. **73**: p. 79-152.

19. Gray, D., K. Siepmann, and G. Wohlleben, *CD40 ligation in B cell activation, isotype switching and memory development.* Semin Immunology, 1994. **6**(5): p. 303-10.

20. Nossal, G.J.V., *The Molecular and Cellular Basis of Affinity Maturation in the Antibody Response.* Cell, 1992. **68**: p. 1-2.

21. Martin, F. and J.F. Kearney, *Positive selection from newly formed to marginal zone B cells depends on the rate of clonal production, CD19, and btk.* immunity, 2000. **12**(1): p. 39-49.

22. Han, S., *et al.*, *Distinctive characteristics of germinal center B cells.* Semin Immunol, 1997. **9**(4): p. 255-60.

23. van Rooijen, N., *Direct intrafollicular differentiation of memory B-cells into plasma cells.* Immunol Today, 1990. **11**(9): p. 154-157.

24. Gray, D., *et al.*, *Observations on memory B-cell development.* Semin Immunol, 1997. **9**(4): p. 249-54.

25. Berard, M., *et al.*, *Activation sensitizes human memory B cells to B-cell receptor-induced apoptosis.* Immunology, 1999. **98**(1): p. 47-54.

26. Dubois, B., *et al.*, *Toward a role of dendritic cells in the germinal center reaction: triggering of B cell proliferation and isotype switching.* J Immunol, 1999. **162**(6): p. 3428-36.

27. de Vinuesa, C.G., *et al.*, *Germinal centers without T cells.* J Exp Med, 2000. **191**(3): p. 485-94.

28. Liu, Y.J. and J. Banchereau, *Regulation of B-cell commitment to plasma cells or to memory B cells.* Semin Immunol, 1997. **9**(4): p. 235-40.
29. Schittek, B. and K. Rajewsky, *Maintence of B-cell memory by long-lived cells generated from proliferating precursors.* Nature, 1990. **346**: p. 749-751.
30. Hayakawa, K., *et al.*, *The Ly-1 B cell subpopulation in normal immunodefective, and autoimmune mice.* J Exp Med, 1983. **157**(1): p. 202-18.
31. Hayakawa, K., *et al.*, *Positive selection of natural autoreactive B cells.* Science, 1999. **285**(5424): p. 113-6.
32. Hayakawa, K. and R.R. Hardy, *Development and function of B-1 cells.* Curr Opin Immunol, 2000. **12**(3): p. 346-53.
33. Watanabe, N., *et al.*, *Expression levels of B cell surface immunoglobulin regulate efficiency of allelic exclusion and size of autoreactive B-1 cell compartment.* J Exp Med, 1999. **190**(4): p. 461-69.
34. Lam, K.P. and K. Rajewsky, *B cell antigen receptor specificity and surface density together determine B-1 versus B-2 cell development.* J Exp Med, 1999. **190**(4): p. 471-7.
35. Chan, V.W.F., *et al.*, *Characterization of the B Lymphocyte Populations in Lyn-Deficient Mice and the Role of Lyn in signal Intiation and Down-Regulation.* Immunity, 1997. **7**: p. 69-81.
36. Tarakhovsky, A., *Bar Mitzvah for B-1 cells: how will they grow up?* J Exp Med, 1997. **185**(6): p. 981-4.
37. Kurosaki, T., *Genetic analysis of B cell antigen receptor signaling.* Ann Rev Immunol, 1999. **17**: p. 555-92.
38. Su, I. and A. Tarakhovsky, *B-1 cells: orthodox or conformist?* Curr Opin Immunol, 2000. **12**(2): p. 191-4.
38a. Desagher, S. and J.-C. Martinou, *Mitochondria as the central point of apoptosis*, Trends Cell Biol, 2000. **10**: p. 369-377.
39. McCarthy, N., *Forever blebbing - a story of extended apoptosis.* Trends Cell Biology, 1997. **7**: p. 74.
40. Crompton, M., *The mitochondrial permeability transition pore and its role in cell death.* Biochem J, 1999. **341 (Pt 2)**: p. 233-49.

41. Cai, J. and D.P. Jones, *Superoxide in apoptosis. Mitochondrial generation triggered by cytochrome c loss.* J Biol Chem, 1998. **273**(19): p. 11401-4.

42. Wang, J.F., T.R. Jerrells, and J.J. Spitzer, *Decreased production of reactive oxygen intermediates is an early event during in vitro apoptosis of rat thymocytes.* Free Radic Biol Med, 1996. **20**(4): p. 533-42.

43. Chakraborti, T., *et al.*, *Oxidant, mitochondria and calcium: an overview.* Cell Signal, 1999. **11**(2): p. 77-85.

44. Esposti, M.D., *et al.*, *Bcl-2 and mitochondrial oxygen radicals. New approaches with reactive oxygen species-sensitive probes.* J Biol Chem, 1999. **274**(42): p. 29831-7.

45. Simbula, G., *et al.*, *Two mechanisms by which ATP depletion potentiates induction of the mitochondrial permeability transition.* Am J Physiol, 1997. **273**(2 Pt 1): p. C479-88.

46. Leist, M., *et al.*, *Intracellular adenosine triphosphate (ATP) concentration: a switch in the decision between apoptosis and necrosis.* J Exp Med, 1997. **185**(8): p. 1481-6.

47. Susin, S.A., *et al.*, *Mitochondrial release of caspase-2 and -9 during the apoptotic process.* J Exp Med, 1999. **189**(2): p. 381-94.

48. Wang, Y., *et al.*, *bcl-2 inhibits wild-type p53-triggered apoptosis but not G1 cell cycle arrest and transactivation of WAF1 and bax.* Cell Growth Differ, 1995. **6**(9): p. 1071-5.

49. Gottlieb, E. and M. Oren, *p53 facilitates pRb cleavage in IL-3-deprived cells: novel pro-apoptotic activity of p53.* EMBO J, 1998. **17**(13): p. 3587-96.

50. Rathmell, J.C. and C.B. Thompson, *The central effectors of cell death in the immune system.* Ann Review Immunol, 1999. **17**: p. 781-828.

51. Polyak, K., *et al.*, *A model for p53-induced apoptosis.* Nature, 1997. **389**(6648): p. 300-5.

52. Schuler, M., *et al.*, *p53 Induces Apoptosis by Caspase Activation through Mitochondrial Cytochrome c Release.* J Biol Chem, 2000. **275**(10): p. 7337-7342.

53. Chao, D.T. and S.J. Korsmeyer, *BCL-2 family: regulators of cell death.* Ann Rev Immunol, 1998. **16**: p. 395-419.

54. Datta, S.R., *et al.*, *Akt Phosphorylation of BAD couples Survival Signals to the Cell-Intrinsic Death Machinery.* Cell, 1997. **91**: p. 231-241.
55. Majewski, M., *et al.*, *Activation of mitochondrial Raf-1 is involved in the antiapoptotic effects of Akt.* Cancer Res, 1999. **59**(12): p. 2815-9.
56. Shimizu, S. and Y. Tsujimoto, *Proapoptotic BH3-only Bcl-2 family members induce cytochrome c release, but not mitochondrial membrane potential loss, and do not directly modulate voltage-dependent anion channel activity.* Proc Natl Acad Sci USA, 2000. **97**(2): p. 577-82.
57. Korsmeyer, S.J., *BCL-2 gene family and the regulation of programmed cell death.* Cancer Res, 1999. **59**(7 Suppl): p. 1693s-1700s.
58. Minn, A.J., *et al.*, *Bcl-xL regulates apoptosis by heterodimerization-dependent and -independent mechanisms.* EMBO J, 1999. **18**(3): p. 632-43.
59. Brenner, C., *et al.*, *Bcl-2 and Bax regulate the channel activity of the mitochondrial adenine nucleotide translocator.* Oncogene, 2000. **19**(3): p. 329-36.
60. Schendel, S., M. Montal, and J. Reed, *Bcl-2 family as ion-channels.* Cell Death Differ, 1998. **5**: p. 372-380.
61. Kelekar, A. and C.B. Thompson, *Bcl-2-family proteins: the role of the BH3 domain in apoptosis.* Trends Cell Biol, 1998. **8**(8): p. 324-30.
62. Pawlowski, J. and A.S. Kraft, *Bax-induced apoptotic cell death.* Proc Natl Acad Sci USA, 2000. **97**(2): p. 529-31.
63. Lam, M., *et al.*, *Regulation of Bcl-xl channel activity by calcium.* J Biol Chem, 1998. **273**(28): p. 17307-10.
64. Eskes, R., *et al.*, *Bid induces the oligomerization and insertion of Bax into the outer mitochondrial membrane.* Mol Cell Biol, 2000. **20**(3): p. 929-35.
65. He, H., *et al.*, *Maintenance of calcium homeostasis in the endoplasmic reticulum by Bcl-2.* J Cell Biol, 1997. **138**(6): p. 1219-28.
66. Mazel, S., D. Burtrum, and H.T. Petrie, *Regulation of Cell Division Cycle Progression by bcl-2 Expression: A potential Mechanism for Inhibition of Programmed Cell Death.* J Exp Med, 1996. **183**: p. 2219-2226.
67. Yamamoto, K., H. Ichijo, and S.J. Korsmeyer, *BCL-2 is phosphorylated and inactivated by an ASK1/Jun N-terminal protein*

kinase pathway normally activated at G(2)/M. Mol Cell Biol, 1999. **19**(12): p. 8469-78.

68. Kumar, S. and P.A. Colussi, *Prodomains--adaptors--oligomerization: the pursuit of caspase activation in apoptosis.* Trends Biochem Sci, 1999. **24**(1): p. 1-4.

69. Los, M., S. Wesselborg, and K. Schulze-Osthoff, *The role of caspases in development, immunity, and apoptotic signal transduction: lessons from knockout mice.* Immunity, 1999. **10**(6): p. 629-39.

70. Aravind, L., V.M. Dixit, and E.V. Koonin, *The domains of death: evolution of the apoptosis machinery.* Trends Biochem Sci, 1999. **24**(2): p. 47-53.

71. Roth, K.A., *et al.*, *Epistatic and independent functions of caspase-3 and Bcl-X(L) in developmental programmed cell death.* Proc Natl Acad Sci USA, 2000. **97**(1): p. 466-71.

72. Vaux, D.L., *CED-4-The Third Horseman of Apoptosis.* Cell, 1997. **90**: p. 389-390.

73. Hirata, H., *et al.*, *Caspases are activated in a branched protease cascade and control distinct downstream processes in Fas-induced apoptosis.* J Exp Med, 1998. **187**(4): p. 587-600.

74. Borner, C. and L. Monney, *Apoptosis without caspases: an inefficient molecular guillotine?* Cell Death Differ, 1999. **6**: p. 497-507.

75. Doerfler, P., K.A. Forbush, and R.M. Perlmutter, *Caspase enzyme activity is not essential for apoptosis during thymocyte development.* J Immunol, 2000. **164**(8): p. 4071-9.

76. Okuno, S., *et al.*, *Bcl-2 prevents caspase-independent cell death.* J Biol Chem, 1998. **273**(51): p. 34272-7.

77. Belaud-Rotureau, M.-A., *et al.*, *Ceramide-induced apoptosis occurs independently of caspases and is decreased by leupeptin.* Cell Death Differ, 1999. **6**: p. 788-795.

78. Ruiz-Vela, A., G. Gonzalez de Buitrago, and C. Martinez-A, *Implication of calpain in caspase activation during B cell clonal deletion.* EMBO J, 1999. **18**(18): p. 4988-98.

79. Muller, R., *Transcriptional regulation during the mammalian cell cycle.* Trends Genet, 1995. **11**(5): p. 173-8.

80. Morgan, S. and M. Kastan, *p53 and ATM: cell cycle, cell death, and cancer.* Adv Cancer Res, 1997. **71**: p. 1-25.

81. Planas-Silva, M. and R. Weinberg, *The restriction point and control of cell proliferation.* Curr Opinion Cell Biol, 1997. **9**(8): p. 738-772.

82. Sherr, C. and J. Roberts, *Inhibitors of mammalian G1 cyclin-dependent kinases.* Genes Dev, 1995. **9**(10): p. 1149-63.

83. Guo, M. and H. Bruce A, *Cell proliferation and apoptosis.* Curr Opin Cell Biol, 1999. **11**(6): p. 745-52.

84. Erhardt, J. and R. Pittman, *p21WAF1 induces permanent growth arrest and enhances differentiation, but does not alter apoptosis in PC12 cells.* Oncogene, 1998. **16**(4): p. 443-51.

85. Medema, R., *et al.*, *p21waf1 can block cells at two points in the cell cycle, but does not interfere with processive DNA-replication or stress-activated kinases.* Oncogene, 1998. **16**(4): p. 431-41.

86. Tao, W. and A.J. Levine, *P19(ARF) stabilizes p53 by blocking nucleo-cytoplasmic shuttling of Mdm2.* Proc Natl Acad Sci USA, 1999. **96**(12): p. 6937-41.

87. Pomerantz, J., *et al.*, *The Ink4a tumor suppressor gene product, p19Arf, interacts with MDM2 and neutralizes MDM2's inhibition of p53.* Cell, 1998. **92**(6): p. 713-23.

88. Møller, M.B., *et al.*, *Aberrations of the p53 pathway components p53, MDM2 and CDKN2A appear independent in diffuse large B cell lymphoma.* Leukemia, 1999. **13**(3): p. 453-9.

89. Lukas, J., *et al.*, *p16INK4a, but not constitutively active pRb, can impose a sustained G1 arrest: molecular mechanisms and implications for oncogenesis.* Oncogene, 1999. **18**(27): p. 3930-5.

90. Sanchez, I. and B. Dynlacht, *Transcriptional control of the cell cycle.* Curr Opin Cell Biol, 1996. **8**(3): p. 318-24.

91. Tao, Y., *et al.*, *Subunit composition determines E2F DNA-binding site specificity.* Mol Cell Biol, 1997. **17**(12): p. 6994-7007.

92. Kowalik, T., *et al.*, *E2F1-specific induction of apoptosis and p53 accumulation, which is blocked by Mdm2.* Cell Growth Differ, 1998. **9**(2): p. 113-8.

93. Wu, X. and A. Levine, *p53 and E2F-1 cooperate to mediate apoptosis.* Proc Natl Acad Sci USA, 1994. **91**(9): p. 3602-6.

94. Lee, C.W., *et al.*, *Functional interplay between p53 and E2F through co-activator p300.* Oncogene, 1998. **16**(21): p. 2695-710.
95. Agah, R., *et al.*, *Adenoviral delivery of E2F-1 directs cell cycle reentry and p53-independent apoptosis in postmitotic adult myocardium in vivo.* J Clin Invest, 1997. **100**(11): p. 2722-8.
96. Holmberg, C., *et al.*, *E2F-1-induced p53-independent apoptosis in transgenic mice.* Oncogene, 1998. **17**(2): p. 143-55.
97. Knudsen, E.S. and J.Y. Wang, *Dual mechanisms for the inhibition of E2F binding to RB by cyclin-dependent kinase-mediated RB phosphorylation.* Mol Cell Biol, 1997. **17**(10): p. 5771-83.
98. Scott, D., *et al.*, *Scenes from a Short Life: Checkpoints and Progression Signals for Immature B Cell Life Versus Apoptosis*, in *Lymphocyte Signalling: Mechanisms, Subversion and Manipulation*, M. Harnett and K. Rigley, Editors. 1997, John Wiely & Sons. p. 165-181.
99. Hoshikawa, Y., *et al.*, *Control of retinoblastoma protein-independent hematopoietic cell cycle by the pRB-related p130.* Proc Natl Acad Sci USA, 1998. **95**(15): p. 8574-9.
100. Liu, N., *et al.*, *A new model of cell cycle-regulated transcription: repression of the cyclin A promoter by CDF-1 and anti-repression by E2F.* Oncogene, 1998. **16**(23): p. 2957-63.
101. Mulligan, G.J., J. Wong, and T. Jacks, *p130 is dispensable in peripheral T lymphocytes: evidence for functional compensation by p107 and pRB.* Mol Cell Biol, 1998. **18**(1): p. 206-20.
102. Schrantz, N., *et al.*, *Manganese induces apoptosis of human B cells: caspase-dependent cell death blocked by bcl-2.* Cell Death Differ, 1999. **6**: p. 445-453.
103. Ferreira, R., *et al.*, *The three members of the pocket proteins family share the ability to repress E2F activity through recruitment of a histone deacetylase.* Proc Natl Acad Sci USA, 1998. **95**(18): p. 10493-8.
104. Agarwal, M., *et al.*, *The p53 network.* J Biol Chem, 1998. **273**(1): p. 1-4.
105. Levine, A., *p53, the cellular gatekeeper for growth and division.* Cell, 1997. **88**(3): p. 323-31.
106. Paulovich, A., D. Toczyski, and L. Hartwell, *When checkpoints fail.* Cell, 1997. **88**(3): p. 315-21.

107. Bian, J. and Y. Sun, *p53CP, a putative p53 competing protein that specifically binds to the consensus p53 DNA binding sites: a third member of the p53 family?* Proc Natl Acad Sci USA, 1997. **94**(26): p. 14753-8.
108. Yin, Y., *et al.*, *Involvement of p85 in p53-dependent apoptotic response to oxidative stress.* Nature, 1998. **391**(6668): p. 707-10.
109. Zhu, J., *et al.*, *The potential tumor suppressor p73 differentially regulates cellular p53 target genes.* Cancer Res, 1998. **58**(22): p. 5061-5.
110. Agami, R., *et al.*, *Interaction of c-Abl and p73alpha and their collaboration to induce apoptosis.* Nature, 1999. **399**(6738): p. 809-13.
111. Mills, A.A., *et al.*, *p63 is a p53 homologue required for limb and epidermal morphogenesis.* Nature, 1999. **398**(6729): p. 708-13.
112. Chernov, M., *et al.*, *Stabilization and activation of p53 are regulated independently by different phosphorylation events.* Proc Natl Acad Sci USA, 1998. **95**(5): p. 2284-9.
113. Liu, M., *et al.*, *Antioxidant action via p53-mediated apoptosis.* Cancer Res, 1998. **58**(8): p. 1723-9.
114. Wu, M., *et al.*, *Roles of the tumor suppressor p53 and the cyclin-dependent kinase inhibitor p21WAF1/CIP1 in receptor-mediated apoptosis of WEHI 231 B lymphoma cells.* J Exp Med, 1998. **187**(10): p. 1671-9.
115. Martinez, J.D., M.T. Craven, and M.E. Pennington, *Selective binding of different p53 response elements by p53 containing complexes.* Oncogene, 1998. **16**(4): p. 453-8.
116. Meek, D.W., *Mechanisms of switching on p53: a role for covalent modification?* Oncogene, 1999. **18**(53): p. 7666-75.
117. Dumaz, N. and D.W. Meek, *Serine15 phosphorylation stimulates p53 transactivation but does not directly influence interaction with HDM2.* EMBO J, 1999. **18**(24): p. 7002-10.
118. Perkins, N., *et al.*, *Regulation of NF-kappaB by cyclin-dependent kinases associated with the p300 coactivator.* Science, 1997. **275**(5299): p. 523-7.
119. Xie, G., *et al.*, *Requirements for p53 and the ATM gene product in the regulation of G1/S and S phase checkpoints.* Oncogene, 1998. **16**(6): p. 721-36.

120. Miyashita, T., *et al.*, *Identification of a p53-dependent negative response element in the bcl-2 gene.* Cancer Res, 1994. **54**(12): p. 3131-5.
121. Miyashita, T., *et al.*, *Tumor suppressor p53 is a regulator of bcl-2 and bax gene expression in vitro and in vivo.* Oncogene, 1994. **9**(6): p. 1799-805.
122. Miyashita, T. and J. Reed, *Tumor suppressor p53 is a direct transcriptional activator of the human bax gene.* Cell, 1995. **80**(2): p. 293-9.
123. Komarova, E., *et al.*, *Intracellular localization of p53 tumor suppressor protein in gamma-irradiated cells is cell cycle regulated and determined by the nucleus.* Cancer Res, 1997. **57**(23): p. 5217-20.
124. Hall, P. and D. Lane, *Tumor suppressors: a developing role for p53?* Curr Biol, 1997. **7**(3): p. R144-7.
125. Subbaramaiah, K., *et al.*, *Inhibition of cyclooxygenase-2 gene expression by p53.* J Biol Chem, 1999. **274**(16): p. 10911-5.
126. Marchenko, N.D., A. Zaika, and U.M. Moll, *Death signal-induced localization of p53 protein to mitochondria. A potential role in apoptotic signaling.* J Biol Chem, 2000. **275**(21): p. 16202-12.
127. Malanga, M., *et al.*, *Poly(ADP-ribose) binds to specific domains of p53 and alters its DNA binding functions.* J Biol Chem, 1998. **273**(19): p. 11839-43.
128. Ritchie, A., *et al.*, *Thrombopoietin upregulates the promoter conformation of p53 in a proliferation-independent manner coincident with a decreased expression of Bax: potential mechanisms for survival enhancing effects.* Blood, 1997. **90**(11): p. 4394-402.
129. Lane, D. and P. Hall, *MDM2--arbiter of p53's destruction.* Trends Biochem Sci, 1997. **22**(10): p. 372-4.
130. Fenteany, G. and S.L. Schreiber, *Lactacystin, proteasome function, and cell fate.* J Biol Chem, 1998. **273**(15): p. 8545-8.
131. Chang, Y., *et al.*, *mdm2 and bax, downstream mediators of the p53 response, are degraded by the ubiquitin-proteasome pathway.* Cell Growth Differ, 1998. **9**(1): p. 79-84.
132. Grimm, L., *et al.*, *Proteasomes play an essential role in thymocyte apoptosis.* EMBO J, 1996. **15**(15): p. 3835-44.
133. Tan, X. and J.Y. Wang, *The caspase-RB connection in cell death.* Trends Cell Biol, 1998. **8**(3): p. 116-20.

134. Yellen, A.J., *et al., Signalling through surface IgM in tolerance-susceptible immature murine B lymphocytes: Developmentally Regulated Differences in Transmembrane Signalling in Splenic B cells from Adult and Neonatal Mice.* J Immunol, 1991. **146**(5): p. 1446-1454.
135. Healy, J.I. and C.C. Goodnow, *Positive versus negative signaling by lymphocyte antigen receptors.* Ann Rev Immunology, 1998. **16**: p. 645-70.
136. Motyka, B., P.J. Griebel, and Reynolds, *Agents that activate protein kinase C rescue sheep ileal Preyer's patch B cells from apoptosis.* Eur J Immunol, 1993. **1993**.
137. Gold, M.R. and A.L. DeFranco, *Phorbol Esters and Dioctanoylglycerol Block Anti-IgM-Stimulated Phosphoinositide Hydrolysis in the Murine B Cell Lymphoma WEHI-231.* J Immunol, 1987. **138**(3): p. 868-876.
138. Goodnow, C.C., *et al., Altered immunoglobulin expression and functional silencing of self-reactive B lymphocytes in transgenic mice.* Nature, 1988. **334**(6184): p. 676-82.
139. Lissy, N.A., *et al., TCR antigen-induced cell death occurs from a late G1 phase cell cycle check point.* Immunity, 1998. **8**(1): p. 57-65.
140. Liu, Z., *et al., Apoptotic signals delivered through the T-cell receptor of a T-cell hybrid require the immediate-early gene nur77.* Nature, 1994. **367**(6460): p. 281-4.
141. Kuwahara, K., *et al., Cross-linking of B cell antigen receptor-related structure of pre-B cell lines induces tyrosine phosphorylation of p85 and p110 subunits and activation of phosphatidylinositol 3-kinase.* Intl Immunol, 1996. **8**(8): p. 1273-85.
142. Craxton, A., *et al., Syk and Bruton's tyrosine kinase are required for B cell antigen receptor-mediated activation of the kinase Akt.* J Biol Chem, 1999. **274**(43): p. 30644-50.
143. Schaeffer, E.M. and P.L. Schwartzberg, *Tec family kinases in lymphocyte signaling and function.* Curr Opin Immunol, 2000. **12**(3): p. 282-8.
144. Newton, A., *Regulation of protein kinase C.* Curr Opin Cell Biol, 1997. **9**(2): p. 161-7.

145. Purkerson, J. and D. Parker, *Differential coupling of membrane Ig and CD40 to the extracellularly regulated kinase signaling pathway.* J Immunol, 1998. **160**(5): p. 2121-9.
146. Marshall, A., *et al., Regulation of B-cell activation and differentiation by the phosphatidylinositol 3-kinase and phosphspholipase Cgamma pathways.* Immunol Rev, 2000. **176**: p. 30-46.
147. Tarakhovsky, A., *Xid and Xid-like immunodeficiencies from a signaling point of view.* Curr Opin Immunol, 1997. **9**(3): p. 319-23.
148. Xu, S., *et al., B cell development and activation defects resulting in xid-like immunodeficiency in BLNK/SLP-65-deficient mice.* Int Immunol, 2000. **12**(3): p. 397-404.
149. Sieckmann, D.G., *et al., Activation of mouse lymphocytes by anti-immunoglobulin. IV. Stimulation with soluble heterologous anti-delta antibodies.* Cell Immunol, 1984. **85**(1): p. 1-14.
150. Paciorkowski, N., *et al., B1 B lymphocytes play a critical role in host protection against lymphatic filarial parasites.* J Exp Med, 2000. **191**(4): p. 731-6.
151. Fultz, M.J., F.D. Finkelman, and E.S. Metcalf, *Comparison of the clonal diversity of the B cell repertoires in adult mice that differ in the expression of cell surface IgD.* Eur J Immunol, 1987. **17**(8): p. 1137-43.
152. Rigley, K.P., *et al., Analysis of signaling via surface immunoglobulin receptors on B cells from CBA/N mice.* Eur J Immunol, 1989. **19**(11): p. 2081-6.
153. Loder, F., *et al., B cell development in the spleen takes place in discrete steps and is determined by the quality of B cell receptor-derived signals.* J Exp Med, 1999. **190**(1): p. 75-89.
154. Warner, G.L. and D.W. Scott, *Lymphoma Models for B-Cell Activation and Tolerance: VII. Pathways in Anti-Ig-Mediated Growth Inhibition and Its Reversal.* Cell Immunol, 1988. **115**: p. 195-203.
155. Benhamou, L.E., P.-A. Cazenave, and P. Sarathou, *Anti-immunoglobulins induce death by apoptosis in WEHI-231 B lymphoma cells.* Eur Jounal Immunol, 1990. **20**: p. 1405-1407.
156. Ales-Martinez, J.-E., *et al., Lymphoma Models for B-Cell Activation and Tolerance: IX. Efficient Reversal of Anti-Ig-Mediated Growth*

Inhibition by an Activated T_h2 Clone. Cell Immunol, 1991. **135**: p. 402-409.

157. Scott, D.W., *et al.*, *Lymphoma Models for B-Cell Activation and Tolerance: VI. Reversal of Anti-Ig-Mediated Negative Signalling by T Cell-Derived Lymphokines.* J Immunol, 1987. **139**(12): p. 3924-3929.

158. Fang, W., *et al.*, *CD40 inhibits B cell apoptosis by upregulating bcl-xL expression and blocking oxidant accumulation.* Am J Physiol, 1997. **272**(3 Pt 1): p. C950-6.

159. Carman, J.A., R.J. Wechsler-Reya, and J.G. Monroe, *Immature Stage B stage Cells Enter but Do Not Progress Beyond the Early G1 Phase of the Cell Cycle in Response to Antigen Receptor Signalling.* J Immunol, 1996. **156**: p. 4562-4569.

160. Bonnnefoy-Bernard, N., *et al.*, *The phosphoprotein phosphatase calcineuirin controls calcium-depdent apoptosis in B cell lines.* Eur J Immunol, 1994. **24**(2): p. 325-329.

161. Sarthou, P., N. Henry-Toulme, and P. Cazenave, *Membrane IgM cross-linking is not coupled to protein kinase C translocation in WEHI-231 B lymphoma cells.* Eur J Immunol, 1989. **19**(7): p. 1247-52.

162. Genestier, L., *et al.*, *Cyclosporin A and FK506 inhibit activation-induced cell death in the murine WEHI-231 B cell line.* Cell Immunol, 1994. **155**(2): p. 283-91.

163. Healy, J.I., *et al.*, *Different nuclear signals are activated by the B cell receptor during positive versus negative signaling.* Immunity, 1997. **6**(4): p. 419-28.

164. Atsumi, G., *et al.*, *Fas-induced arachidonic acid release is mediated by Ca2+-independent phospholipase A2 but not cytosolic phospholipase A2, which undergoes proteolytic inactivation.* J Biol Chem, 1998. **273**(22): p. 13870-7.

165. He, H., *et al.*, *c-Fos degradation by the proteasome. An early, Bcl-2-regulated step in apoptosis.* J Biol Chem, 1998. **273**(39): p. 25015-9.

166. Zhu, J. and F. McKeon, *NF-AT activation requires suppression of Crm1-dependent export by calcineurin.* Nature, 1999. **398**(6724): p. 256-60.

167. Klaus, G.G. and M.M. Harnett, *Cross-talk between B cell surface immunoglobulin and interleukin 4 receptors: the role of protein kinase C and Ca2(+)-mediated signals.* Eur J Immunol, 1990. **20**(10): p. 2301-7.
168. Sarathou, P., N. Henry-Toulme, and P.-A. Cazenave, *mIgM signalling in the absence of PKC translocation.* Eur J Immunol, 1989. **19**: p. 1247-1252.
169. Hirabayashi, T., *et al.*, *Critical duration of intracellular Ca2+ response required for continuous translocation and activation of cytosolic phospholipase A2.* J Biol Chem, 1999. **274**(8): p. 5163-9.
170. Dessen, A., *et al.*, *Crystal structure of human cytosolic phospholipase A2 reveals a novel topology and catalytic mechanism.* Cell, 1999. **97**(3): p. 349-60.
171. Gilbert, J.J., *et al.*, *Antigen Receptors on Immature, but Not Mature, B and T Cells Are Coupled to Cytosolic Phospholipase A_2 Activation: Expression and Activation of Cytosolic Phospholipase A_2 Correlate with Lymphocyte Maturation.* J Immunol, 1996. **156**: p. 2054-2061.
172. Rowley, A., H. Kuhn, and T. Schewe, eds. *Eicosanoids and Related Compounds in Plants and Animals.* 1998, Portland Press: London.
173. Murakami, M., *et al.*, *Regulatory functions of phospholipase A2.* Critical Rev Immunol, 1997. **17**(3-4): p. 225-83.
174. Dennis, E.A., *Diversity of Group types, Regulation, and Function of Phospholipase A_2.* J Biol Chem, 1994. **269**(18): p. 13057-13060.
175. Serhan, C.N., J.Z. Haeggström, and C.C. Leslie, *Lipid mediator networks in cell signaling: update and impact of cytokines.* FASEB J, 1996. **10**(10): p. 1147-58.
176. Blasinde, J. and E. Dennis, *Function and Inhibition of Intracellular Calcium-independent Phospholipase A_2.* J Biol Chem, 1997. **272**(26): p. 16069-16072.
177. Murakami, M., *et al.*, *The functions of five distinct mammalian phospholipase A2S in regulating arachidonic acid release. Type IIa and type V secretory phospholipase A2S are functionally redundant and act in concert with cytosolic phospholipase A2.* J Biol Chem, 1998. **273**(23): p. 14411-23.

178. Tischfield, J.A., *A reassessment of the low molecular weight phospholipase A2 gene family in mammals.* J Biol Chem, 1997. **272**(28): p. 17247-50.

179. Zhang, J., *et al., Regulation of membrane release in apoptosis.* Biochem J, 1998. **334 (Pt 2)**: p. 479-85.

180. Leslie, C.C., *Properties and regulation of cytosolic phospholipase A2.* J Biol Chem, 1997. **272**(27): p. 16709-12.

181. Börsch-Haubold, A.G., *et al., Identification of the phosphorylation sites of cytosolic phospholipase A2 in agonist-stimulated human platelets and HeLa cells.* J Biol Chem, 1998. **273**(8): p. 4449-58.

182. Robinson, B.S., C.S. Hii, and A. Ferrante, *Activation of phospholipase A2 in human neutrophils by polyunsaturated fatty acids and its role in stimulation of superoxide production.* Biochem J, 1998. **336 (Pt 3)**: p. 611-7.

183. Sapirstein, A., *et al., Cytosolic phospholipase A2 (PLA2), but not secretory PLA2, potentiates hydrogen peroxide cytotoxicity in kidney epithelial cells.* J Biol Chem, 1996. **271**(35): p. 21505-13.

184. Crofford, L.J., *Cox-1 and Cox-2 Tissue Expression: Implications and Predictions.* Journal of Reumatology, 1997. **suppl 49**(24): p. 15-19.

185. Brown, D.M. and R.P. Phipps, *Bcl-2 Expression Inhibits Prostaglanding E2-Mediated Apoptosis in B Cell Lymphomas.* J Immunol, 1996. **157**: p. 1359-1370.

186. Sergeeva, M., *et al., Prostaglandin E2 biphasic control of lymphocyte proliferation: inhibition by picomolar concentrations.* FEBS Lett, 1997. **418**(3): p. 235-8.

187. Pica, R., *et al., Protaglandin E_2 Induces Apoptosis in Resting Immature and Mature Human Lymphocytes: A c-Myc Dependent and Bcl-2 Independent Associated Pathway.* J Pharma Exp Therap, 1996. **277**: p. 1793-1800.

188. Sheng, H., *et al., Modulation of apoptosis and Bcl-2 expression by prostaglandin E2 in human colon cancer cells.* Cancer Res, 1998. **58**(2): p. 362-6.

189. Tang, D., Y. Chen, and K. Honn, *Arachidonate lipoxygenases as essential regulators of cell survival and apoptosis.* Proc Natl Acad Sci USA, 1996. **93**(11): p. 5241-6.

190. Lin, L.-L., *et al.*, *cPLA$_2$ is Phosphorilated and Activated by MAP Kinase.* Cell, 1993. **72**: p. 269-278.
191. Basu, S. and R. Kolesnick, *Stress signals for apoptosis: ceramide and c-Jun kinase.* Oncogene, 1998. **17**(25): p. 3277-85.
192. Quintans, J., *et al.*, *Ceramide mediates the apoptotic response of WEHI 231 cells to anti-immunoglobulin, corticosteroids and irradiation.* Biochem Biophys Res Commun, 1994. **202**(2): p. 710-4.
193. Gottschalk, A.R., *et al.*, *Resistance to anti-IgM-induced apoptosis in a WEHI-231 subline is due to insufficient production of ceramide.* Eur J Immunol, 1995. **25**: p. 1032-1038.
194. Chen, L., T.J. Kim, and S. Pillai, *Inhibition of caspase activity prevents anti-IgM induced apoptosis but not ceramide generation in WEHI 231 B cells.* Molecular Immunology, 1998. **35**(4): p. 195-205.
195. Paumen, M., *et al.*, *Inhibition of carnitine palmitoyltransferase I augments sphingolipid synthesis and palmitate-induced apoptosis.* J Biol Chem, 1997. **272**(6): p. 3324-9.
196. Chmura, S., *et al.*, *Cross-talk between ceramide and PKC activity in the control of apoptosis in WEHI-231.* Adv Exp Med Biol, 1996. **406**: p. 39-55.
197. Chmura, S., *et al.*, *Protein kinase C inhibition induces apoptosis and ceramide production through activation of a neutral sphingomyelinase.* Cancer Res, 1996. **56**(12): p. 2711-4.
198. Haimovitz-Friedman, A., *et al.*, *Ionizing radiation acts on cellular membranes to generate ceramide and initiate apoptosis.* J Exp Med, 1994. **180**(2): p. 525-35.
199. Hayakawa, M., *et al.*, *Role of ceramide in stimulation of the transcription of cytosolic phospholipase A2 and cyclooxygenase 2.* Biochem Biophys Res Commun, 1996. **220**(3): p. 681-6.
200. Candela, M., S. Barker, and L. Ballou, *Sphingosine synergistically stimulates tumor necrosis factor alpha-induced prostaglandin E2 production in human fibroblasts.* J Exp Med, 1991. **174**(6): p. 1363-9.
201. Ballou, L., *et al.*, *Interleukin-1-mediated PGE2 production and sphingomyelin metabolism. Evidence for the regulation of cyclooxygenase gene expression by sphingosine and ceramide.* J Biol Chem, 1992. **267**(28): p. 20044-50.

202. Page, D.M. and A.L. DeFranco, *Antigen receptor-induced cell cycle arrest in WEHI-231 B lymphoma cells depends on the duration of signaling before the G1 phase restriction point.* Mol Cell Biol, 1990. **10**(6): p. 3003-12.

203. Zhou, B.B., *et al., Caspase-dependent activation of cyclin-dependent kinases during Fas-induced apoptosis in Jurkat cells.* Proc Natl Acad Sci USA, 1998. **95**(12): p. 6785-90.

204. Harvey, K.J., J.F. Blomquist, and D.S. Ucker, *Commitment and effector phases of the physiological cell death pathway elucidated with respect to Bcl-2 caspase, and cyclin-dependent kinase activities.* Mol Cell Biol, 1998. **18**(5): p. 2912-22.

205. Rubin, L.L., K.L. Philpott, and S.F. Brooks, *The cell cycle and cell death.* Curr Biol, 1996. **3**(6): p. 391-394.

206. Fischer, G., *et al., Lymphoma Models for B Cell Activation and Tolerance: X. Anti-mu-mediated Growth Arrest and Apoptosis of Murine B Lymphomas Is Prevented by the Stabilization of myc.* J Exp Med, 1994. **179**: p. 221-228.

207. Bouchard, C., P. Staller, and M. Eilers, *Control of cell proliferation by Myc.* Trends Cell Biol, 1998. **8**(5): p. 202-6.

208. Hoffman, B. and D.A. Liebermann, *The proto-oncogene c-myc and apoptosis.* Oncogene, 1998. **17**(25): p. 3351-7.

209. Joseph, L.F., S. Ezhevsky, and D.W. Scott, *Lymphoma models for B-cell activation and tolerance: anti-immunoglobulin M treatment induces growth arrest by preventing the formation of an active kinase complex which phosphorylates retinoblastoma gene product in G1.* Cell Growth Differ, 1995. **6**(1): p. 51-7.

210. Obaya, A.J., M.K. Mateyak, and J.M. Sedivy, *Mysterious liaisons: the relationship between c-Myc and the cell cycle.* Oncogene, 1999. **18**(19): p. 2934-41.

211. Takase, K., *et al., Control of cell cycle entry and progression in mitogen stimulated human B lymphocytes.* J Cell Physiol, 1995. **162**(2): p. 246-55.

212. Ishida, T., *et al., CD40 Signalling-Mediated Induction of Bcl-x_L, cdk4, and cdk 6: Implication of Their Cooperation in Selective B Cell Growth.* J Immunol, 1995. **155**: p. 5527-5535.

213. Ku, P.T., M. You, and H.R.J. Bose, *Role and regulation of Rel/NF-kappaB activity in anti-immunoglobulin-induced apoptosis in WEHI-231 B lymphoma cells.* Cell Signal, 2000. **12**(4): p. 245-53.
214. Zuo, Z., N.M. Dean, and R.E. Honkanen, *Serine/threonine protein phosphatase type 5 acts upstream of p53 to regulate the induction of p21(WAF1/Cip1) and mediate growth arrest.* J Biol Chem, 1998. **273**(20): p. 12250-8.
215. Russo, T., *et al.*, *A p53-independent pathway for activation of WAF1/CIP1 expression following oxidative stress.* J Biol Chem, 1995. **270**(49): p. 29386-91.
216. Zhang, W., *et al.*, *p53-independent induction of WAF1/CIP1 in human leukemia cells is correlated with growth arrest accompanying monocyte/macrophage differentiation.* Cancer Res, 1995. **55**(3): p. 668-74.
217. Ezhevsky, S.A., *et al.*, *Role of cyclin A and p27 in anti-IgM induced G1 growth arrest of murine B-cell lymphomas.* Mol Biol Cell, 1996. **7**(4): p. 553-64.
218. Han, H., *et al.*, *Differential modulation of cyclin-dependent kinase inhibitor p27Kip1 by negative signaling via the antigen receptor of B cells and positive signaling via CD40.* Eur J Immunol, 1996. **26**(10): p. 2425-32.
219. Pushkareva, M., *et al.*, *Stereoselectivity of induction of the retinoblastoma gene product (pRb) dephosphorylation by D-erythro-sphingosine supports a role for pRb in growth suppression by sphingosine.* Biochemistry, 1995. **34**(6): p. 1885-92.
220. Lam, E.W., *et al.*, *Modulation of E2F activity via signaling through surface IgM and CD40 receptors in WEHI-231 B lymphoma cells.* J Biol Chem, 1998. **273**(16): p. 10051-7.
221. van der Sman, J., N.S. Thomas, and E.W. Lam, *Modulation of E2F complexes during G0 to S phase transition in human primary B-lymphocytes.* J Biol Chem, 1999. **274**(17): p. 12009-16.
222. Hartley, S., *et al.*, *Elimination of self-reactive B lymphocytes proceeds in two stages: arrested development and cell death.* Cell, 1993. **72**(3): p. 325-35.
223. Wolf, B.B. and D.R. Green, *Suicidal tendencies: apoptotic cell death by caspase family proteinases.* J Biol Chem, 1999. **274**(29): p. 20049-52.

224. Scaffidi, C., *et al.*, *Apoptosis signaling in lymphocytes.* Curr Opin Immunol, 1999. **11**(3): p. 277-85.
225. Osborne, B.A., *Apoptosis and the maintenance of homoeostasis in the immune system.* Curr Opin Immunol, 1996. **8**(2): p. 245-54.
226. Winoto, A., *Cell death in the regulation of immune responses.* Curr Opin Immunol, 1997. **9**(3): p. 365-70.
227. Wyllie, A.H., *Apoptosis (The 1992 Frank Rose Memorial Lecture).* British J Cancer, 1993. **67**: p. 205-208.
228. Miller, D., *The role of the Caspase family of cysteine proteases in apoptosis.* Semin Immunol, 1997. **9**(1): p. 35-49.
229. Villa, P., S. Kaufmann, and W. Earnshaw, *Caspases and caspase inhibitors.* Trends Biochem Sci, 1997. **22**(10): p. 388-93.
230. Kuida, K., *et al.*, *Decreased apoptosis in the brain and premature lethality in CPP32-deficient mice.* Nature, 1996. **384**(6607): p. 368-72.
231. Kuida, K., *et al.*, *Reduced apoptosis and cytochrome c-mediated caspase activation in mice lacking caspase 9.* Cell, 1998. **94**(3): p. 325-37.
232. Lesage, S., *et al.*, *CD4+ CD8+ thymocytes are preferentially induced to die following CD45 cross-linking, through a novel apoptotic pathway.* J Immunol, 1997. **159**(10): p. 4762-71.
233. Hirsch, T., *et al.*, *The apoptosis-necrosis paradox. Apoptogenic proteases activated after mitochondrial permeability transition determine the mode of cell death.* Oncogene, 1997. **15**(13): p. 1573-81.
234. Green, D. and G. Kroemer, *The central executioners of apoptosis: caspases or mitochondria?* Trends Cell Biol, 1998. **8**(7): p. 267-71.
235. Shimizu, S., *et al.*, *Bcl-2 prevents apoptotic mitochondrial dysfunction by regulating proton flux.* Proc Natl Acad Sci USA1998. **95**(4): p. 1455-9.
236. Green, D.R. and J.C. Reed, *Mitochondria and apoptosis.* Science, 1998. **281**(5381): p. 1309-12.
237. Garland, J.M. and C. Rudin, *Cytochrome c induces caspase-dependent apoptosis in intact hematopoietic cells and overrides apoptosis suppression mediated by bcl-2, growth factor signaling, MAP-kinase-kinase, and malignant change.* Blood, 1998. **92**(4): p. 1235-46.

238. Adachi, S., *et al., Bcl-2 and the outer mitochondrial membrane in the inactivation of cytochrome c during Fas-mediated apoptosis.* J Biol Chem, 1997. **272**(35): p. 21878-82.
239. Jurgensmeier, J.M., *et al., Bax directly induces release of cytochrome c from isolated mitochondria.* Proc Natl Acad Sci USA, 1998. **95**(9): p. 4997-5002.
240. Marzo, I., *et al., The permeability transition pore complex: a target for apoptosis regulation by caspases and bcl-2-related proteins.* J Exp Med, 1998. **187**(8): p. 1261-71.
241. Marzo, I., *et al., Bax and adenine nucleotide translocator cooperate in the mitochondrial control of apoptosis.* Science, 1998. **281**(5385): p. 2027-31.
242. Susin, S.A., N. Zamzami, and G. Kroemer, *Mitochondria as regulators of apoptosis: doubt no more.* Biochim Biophys Acta, 1998. **1366**(1-2): p. 151-65.
243. Vander Heiden, M.G., *et al., Bcl-xL regulates the membrane potential and volume homeostasis of mitochondria.* Cell, 1997. **91**(5): p. 627-37.
244. Lenardo, M., *et al., Mature T lymphocyte apoptosis--immune regulation in a dynamic and unpredictable antigenic environment.* Annual Review of Immunology, 1999. **17**: p. 221-53.
245. Green, D.R., *Apoptotic pathways: the roads to ruin.* Cell, 1998. **94**(6): p. 695-8.
246. Metivier, D., *et al., Cytofluorometric detection of mitochondrial alterations in early CD95/Fas/APO-1-triggered apoptosis of Jurkat T lymphoma cells. Comparison of seven mitochondrion-specific fluorochromes.* Immunol Lett, 1998. **61**(2-3): p. 157-63.
247. Zoratti, M. and I. Szabo, *The mitochondrial permeability transition.* Biochim Biophys Acta, 1995. **1241**(2): p. 139-76.
248. Eguchi, Y., *et al., ATP-dependent steps in apoptotic signal transduction.* Cancer Res, 1999. **59**(9): p. 2174-81.
249. Matsuyama, S., *et al., The Mitochondrial F0F1-ATPase proton pump is required for function of the proapoptotic protein Bax in yeast and mammalian cells.* Mol Cell, 1998. **1**(3): p. 327-36.

250. Szabo, I. and M. Zoratti, *The giant channel of the inner mitochondrial membrane is inhibited by cyclosporin A.* J Biol Chem, 1991. **266**(6): p. 3376-9.
251. Michel, T. and O. Feron, *Nitric oxide synthases: Which, where, how, and why?* Journal Of Clinical Investigation, 1997. **100**(9): p. 2146-2152.
252. Nathan, C. and Q. Xie, *Nitric oxide synthases: roles, tolls, and controls.* Cell, 1994. **78**(6): p. 915-8.
253. Harrison, D.G., *Cellular and Molecular Mechanisms of Endothelial Cell Dysfunction.* J Clin Invest, 1997. **100**(9): p. 2153-2157.
254. Hattori, Y. and N. Nakanishi, *Effects of cyclosporin A and FK506 on nitric oxide and tetrahydrobiopterin synthesis in bacterial lipopolysaccharide-treated J774 macrophages.* Cell Immunol, 1995. **165**(1): p. 7-11.
255. Mohr, S., T.S. McCormick, and E.G. Lapetina, *Macrophages resistant to endogenously generated nitric oxide-mediated apoptosis are hypersensitive to exogenously added nitric oxide donors: dichotomous apoptotic response independent of caspase 3 and reversal by the mitogen-activated protein kinase kinase (MEK) inhibitor PD 098059.* Proc Natl Acad Sci USA, 1998. **95**(9): p. 5045-50.
256. Genaro, A., *et al.*, *Splenic B lymphocyte programmed cell death is prevented by nitric oxide release through mechanisms involving sustained Bcl-2 levels.* J Clin Invest, 1995. **95**(4): p. 1884-90.
257. Gunter, T.E. and D.R. Pfeiffer, *Mechanisms by which mitochondria transport calcium.* Am J Physiol, 1990. **258**(5 Pt 1): p. C755-86.
258. Kinnally, K.W., Y.N. Antonenko, and D.B. Zorov, *Modulation of inner mitochondrial membrane channel activity.* J Bioenerg Biomembr, 1992. **24**(1): p. 99-110.
259. Kristal, B.S., B.K. Park, and B.P. Yu, *4-Hydroxyhexenal is a potent inducer of the mitochondrial permeability transition.* J Biol Chem, 1996. **271**(11): p. 6033-8.
260. Gilbert, J.J., *The role of lipid siganalling in lymphocyte activation, maturation and cell death*, in *Department of Biochemistry*. 1995, University of Glasgow: Glasgow. p. 229.

261. Tsujii, M. and R. DuBois, *Alterations in cellular adhesion and apoptosis in epithelial cells overexpressing prostaglandin endoperoxide synthase 2.* Cell, 1995. **83**(3): p. 493-501.
262. Mor, F. and I.R. Cohen, *IL-2 Rescuse Antigen-Specific T Cells from Radiation or Dexamethasone-Induced Apoptosis: Correlation with Induction of Bcl-2.* J Immunol, 1996. **156**: p. 515-522.
263. Ristimaki, A., K. Narko, and T. Hla, *Down-regulation of cytokine-induced cyclo-oxygenase-2 transcript isoforms by dexamethasone: evidence for post-transcriptional regulation.* Biochem J, 1996. **318 (Pt 1)**: p. 325-31.
264. Goetzl, E., S. An, and W. Smith, *Specificity of expression and effects of eicosanoid mediators in normal physiology and human diseases.* FASEB J, 1995. **9**(11): p. 1051-8.
265. Brash, A.R., *Lipoxygenases: occurrence, functions, catalysis, and acquisition of substrate.* J Biol Chem, 1999. **274**(34): p. 23679-82.
266. Brinckmann, R., *et al., Membrane translocation of 15-lipoxygenase in hematopoietic cells is calcium-dependent and activates the oxygenase activity of the enzyme.* Blood, 1998. **91**(1): p. 64-74.
267. Jayadev, S., C. Linardic, and Y. Hannun, *Identification of arachidonic acid as a mediator of sphingomyelin hydrolysis in response to tumor necrosis factor alpha.* J Biol Chem, 1994. **269**(8): p. 5757-63.
268. Kroemer, G., *The proto-oncogene Bcl-2 and its role in regulating apoptosis.* Nat Med, 1997. **3**(6): p. 614-20.
269. Fang, W., *et al., Bcl-xL rescues WEHI 231 B lymphocytes from oxidant-mediated death following diverse apoptotic stimuli.* J Immunol, 1995. **155**(1): p. 66-75.
270. Simbulan-Rosenthal, C.M., *et al., Transient poly(ADP-ribosyl)ation of nuclear proteins and role of poly(ADP-ribose) polymerase in the early stages of apoptosis.* J Biol Chem, 1998. **273**(22): p. 13703-12.
271. Fujita, N., *et al., Acceleration of apoptotic cell death after the cleavage of Bcl-XL protein by caspase-3-like proteases.* Oncogene, 1998. **17**(10): p. 1295-304.
272. Qi, X., *et al., Baculovirus p35 and Z-VAD-fmk inhibit thapsigargin-induced apoptosis of breast cancer cells.* Oncogene, 1997. **15**(10): p. 1207-12.

273. Hara, H., *et al., Inhibition of interleukin 1beta converting enzyme family proteases reduces ischemic and excitotoxic neuronal damage.* Proc Natl Acad Sci USA, 1997. **94**(5): p. 2007-12.
274. Faleiro, L., *et al., Multiple species of CPP32 and Mch2 are the major active caspases present in apoptotic cells.* EMBO J, 1997. **16**(9): p. 2271-81.
275. van Eijk, M. and C. de Groot, *Germinal center B cell apoptosis requires both caspase and cathepsin activity.* J Immunol, 1999. **163**(5): p. 2478-82.
276. Graña, X., J. Garriga, and X. Mayol, *Role of the retinoblastoma protein family, pRB, p107 and p130 in the negative control of cell growth.* Oncogene, 1998. **17**(25): p. 3365-83.
277. Zou, H., *et al., Apaf-1, a human protein homologous to C. elegans CED-4, participates in cytochrome c-dependent activation of caspase-3.* Cell, 1997. **90**(3): p. 405-13.
278. Choi, M.S., *et al., The role of bcl-x_L in CD40-mediated rescue from anti-mu-induced apoptosis in WEHI-231 B lymphoma cells.* Eur J Immunol, 1995. **25**(5): p. 1352-1357.
279. Dorward, A., *et al., Mitochondrial contributions to cancer cell physiology: redox balance, cell cycle, and drug resistance.* J Bioenerg Biomembr, 1997. **29**(4): p. 385-92.
280. Kamata, H. and H. Hirata, *Redox regulation of cellular signalling.* Cell Signal, 1999. **11**(1): p. 1-14.
281. Grillot, D., *et al., bcl-x exhibits regulated expression during B cell development and activation and modulates lymphocyte survival in transgenic mice.* J Exp Med, 1996. **183**(2): p. 381-91.
282. Zhou, P., *et al., Mcl-1 in transgenic mice promotes survival in a spectrum of hematopoietic cell types and immortalization in the myeloid lineage.* Blood, 1998. **92**(9): p. 3226-39.
283. Heiden, M.G., *et al., Bcl-xL prevents cell death following growth factor withdrawal by facilitating mitochondrial ATP/ADP exchange.* Mol Cell, 1999. **3**(2): p. 159-67.
284. Huang, D., S. Cory, and A. Strasser, *Bcl-2, Bcl-XL and adenovirus protein E1B19kD are functionally equivalent in their ability to inhibit cell death.* Oncogene, 1997. **14**(4): p. 405-14.

285. Kuss, A.W., *et al., A1 expression is stimulated by CD40 in B cells and rescues WEHI 231 cells from anti-IgM-induced cell death.* european J Immunol, 1999. **29**(10): p. 3077-88.
286. Craxton, A., *et al., The CD40-inducible Bcl-2 family member A1 protects B cells from antigen receptor-mediated apoptosis.* Cell Immunol, 2000. **200**(1): p. 56-62.
287. Fang, W., *et al., Self-reactive B lymphocytes overexpressing Bcl-xL escape negative selection and are tolerized by clonal anergy and receptor editing.* Immunity, 1998. **9**(1): p. 35-45.
288. Gottschalk, A.R., *et al., Physiological cell death in B lymphocytes: I. Differential susceptibility of WEHI-231 sublines to anti-Ig induced physiological cell death and lack of correlation with bcl-2 expression.* Intl Immunol, 1994. **6**(1): p. 121-130.
289. Liu, Y., *et al., Germinal center cells express bcl-2 protein after activation by signals which prevent their entry into apoptosis.* Eur J Immunol, 1991. **21**(8): p. 1905-10.
290. Smith, K.G., *et al., bcl-2 transgene expression inhibits apoptosis in the germinal center and reveals differences in the selection of memory B cells and bone marrow antibody-forming cells.* J Exp Med, 2000. **191**(3): p. 475-84.
291. Graves, J.D., *et al., A comparison of signaling requirements for apoptosis of human B lymphocytes induced by the B cell receptor and CD95/Fas.* J Immunol, 1998. **161**(1): p. 168-74.
292. Doi, T., *et al., Death signals from the B cell antigen receptor target mitochondria, activating necrotic and apoptotic death cascades in a murine B cell line, WEHI-231.* Intl Immunol, 1999. **11**(6): p. 933-41.
293. Chang, T. and H. Eisen, *Effects of N-tosyl-L-lysyl-chloromethylketone on the activity of cytolytic T lymphocytes.* J Immunol, 1980. **124**: p. 1028.
294. Squier, M. and J. Cohen, *Calpain and cell death.* Cell Death Differ, 1996. **3**: p. 275.
295. Deiss, L.P., *et al., Cathepsin D protease mediates programmed cell death induced by interferon-gamma, Fas/APO-1 and TNF-alpha.* EMBO J, 1996. **15**(15): p. 3861-70.

296. Nakamura, N. and Y. Wada, *Properties of DNA fragmentation activity generated by ATP depletion.* Cell Death Differ, 2000. **7**: p. 477-484.
297. Eguchi, Y., S. Shimizu, and Y. Tsujimoto, *Intracellular ATP levels determine cell death fate by apoptosis or necrosis.* Cancer Res, 1997. **57**(10): p. 1835-40.
298. Sweet, S. and G. Singh, *Accumulation of human promyelocytic leukemic (HL-60) cells at two energetic cell cycle checkpoints.* Cancer Res, 1995. **55**(22): p. 5164-7.
299. Hakem, R., *et al.*, *Differential requirement for caspase 9 in apoptotic pathways in vivo.* Cell, 1998. **94**(3): p. 339-52.
300. Schievella, A.R., *et al.*, *Calcium-mediated translocation of cytosolic phospholipase A2 to the nuclear envelope and endoplasmic reticulum.* J Biol Chem, 1995. **270**(51): p. 30749-54.
301. Gottschalk, A.R. and J. Quintáns, *Apoptosis in B lymphocytes: the WEHI-231 perspective.* Immunol Cell Biol, 1995. **73**(1): p. 8-16.
302. LeBien, T.W., *B-cell lymphopoiesis in mouse and man.* Curr Opin Immunol, 1998. **10**(2): p. 188-95.
303. Carsetti, R., *The development of B cells in the bone marrow is controlled by the balance between cell-autonomous mechanisms and signals from the microenvironment.* J Exp Med, 2000. **191**(1): p. 5-8.
304. Janani, R., *et al.*, *Effect of a bcl-2 transgene on production and localization of precursor B cells in mouse bone marrow.* Exp Hematol, 1998. **26**(10): p. 982-90.
305. Nishimoto, N., *et al.*, *Normal pre-B cells express a receptor complex of mu heavy chains and surrogate light-chain proteins.* Proc Natl Acad Sci USA, 1991. **88**: p. 6284-6288.
306. Rathmell, J.C., *et al.*, *CD95 (Fas)-dependent elimination of self-reactive B cells upon interaction with CD4+ T cells.* Nature, 1995. **376**(6536): p. 181-4.
307. Rubio, C.F., *et al.*, *Analysis of central B cell tolerance in autoimmune-prone MRL/lpr mice bearing autoantibody transgenes.* J Immunol, 1996. **157**(1): p. 65-71.
308. Klaus, G.G., *et al.*, *A re-evaluation of the effects of X-linked immunodeficiency (xid) mutation on B cell differentiation and function in the mouse.* Eur J Immunol, 1997. **27**(11): p. 2749-56.

309. Behrens, T.W. and D.L. Mueller, *Bcl-x and the Regulation of Survival in the Immune System.* Immunol Res, 1997. **16**(2): p. 149-160.
310. Merino, R., *et al.*, *Developmental regulation of the Bcl-2 protein and susceptibility to cell death in B lymphocytes.* EMBO J, 1994. **13**(3): p. 683-691.
311. Deehan, M., M. Harnett, and W. Harnett, *A filarial nematode secreted product differentially modulates expression and activation of protein kinase C isoforms in B lymphocytes.* J Immunol, 1997. **159**(12): p. 6105-11.
312. Brink, R., *et al.*, *Immunoglobulin M and D antigen receptors are both capable of mediating B lymphocyte activation, deletion, or anergy after interaction with specific antigen.* J Exp Med, 1992. **176**(4): p. 991-1005.
313. Marshall-Clarke, S., L. Tasker, and R.M. Parkhouse, *Immature B lymphocytes from adult bone marrow exhibit a selective defect in induced hyperexpression of major histocompatibility complex class II and fail to show B7.2 induction.* Immunology, 2000. **100**(2): p. 141-51.
314. Cariappa, A., T.J. Kim, and S. Pillai, *Accelerated emigration of B lymphocytes in the Xid mouse.* J Immunol, 1999. **162**(8): p. 4417-23.
315. Fulcher, D.A. and A. Basten, *B cell life span: a review.* Immunology Cell Biol, 1997. **75**(5): p. 446-55.
316. McHeyzer-Williams, L.J., M. Cool, and M.G. McHeyzer-Williams, *Antigen-specific B cell memory: expression and replenishment of a novel b220(-) memory B cell compartment.* J Exp Med, 2000. **191**(7): p. 1149-66.
317. Grammer, A.C., *et al.*, *Expression, regulation, and function of B cell-expressed CD154 in germinal centers.* J Immunol, 1999. **163**(8): p. 4150-9.
318. Inaoki, M., *et al.*, *CD19-regulated signaling thresholds control peripheral tolerance and autoantibody production in B lymphocytes.* J Exp Med, 1997. **186**(11): p. 1923-31.
319. Mason, D.Y., M. Jones, and C.C. Goodnow, *Development and follicular localization of tolerant B lymphocytes in lysozyme/anti-lysozyme IgM/IgD transgenic mice.* Intl Immunol, 1992. **4**(2): p. 163-75.
320. Smith-Gill, S.J., *et al.*, *Mapping the antigenic epitope for a monoclonal antibody against lysozyme.* J Immunol, 1982. **128**(1): p. 314-22.

321. Lavoie, T.B., W.N. Drohan, and S.J. Smith-Gill, *Experimental analysis by site-directed mutagenesis of somatic mutation effects on affinity and fine specificity in antibodies specific for lysozyme.* J Immunol, 1992. **148**(2): p. 503-13.
322. Pals, S.T., *et al.*, *Regulation of adhesion and migration in the germinal center microenvironment.* Cell Adhes Comm, 1998. **6**(2-3): p. 111-6.
323. van den Brink, M.R., *et al.*, *The extracellular signal-regulated kinase pathway is required for activation-induced cell death of T cells.* J Biol Chem, 1999. **274**(16): p. 11178-85.
324. Bouchon, A., P.H. Krammer, and H. Walczak, *Critical role for mitochondria in B cell receptor-mediated apoptosis.* Eur J Immunol, 2000. **30**(1): p. 69-77.
325. Shinall, S.M., *et al.*, *Identification of murine germinal center B cell subsets defined by the expression of surface isotypes and differentiation antigens.* J Immunol, 2000. **164**(11): p. 5729-38.
326. Tarlinton, D., *Germinal centers: form and function.* Curr Opin Immunol, 1998. **10**(3): p. 245-51.
327. Saouaf, S.J., *et al.*, *Temporal differences in the activation of three classes of non-transmembrane protein tyrosine kinases following B-cell antigen receptor surface engagement.* Proc Natl Acad Sci USA, 1994. **91**(20): p. 9524-8.
328. Bras, A., *et al.*, *Caspase activation by BCR cross-linking in immature B cells: differential effects on growth arrest and apoptosis.* FASEB J, 1999. **13**(8): p. 931-44.
329. Lind, E.F., *et al.*, *Bcl-2-induced changes in E2F regulatory complexes reveal the potential for integrated cell cycle and cell death functions.* J Immunol, 1999. **162**(9): p. 5374-9.
330. Cocco, T., *et al.*, *Arachidonic acid interaction with the mitochondrial electron transport chain promotes reactive oxygen species generation.* Free Rad Biol Med, 1999. **27**(1-2): p. 51-9.
331. Li, P.F., R. Dietz, and R. von Harsdorf, *p53 regulates mitochondrial membrane potential through reactive oxygen species and induces cytochrome c-independent apoptosis blocked by Bcl-2.* EMBO J, 1999. **18**(21): p. 6027-36.

332. Benschop, R.J., *et al.*, *Distinct signal thresholds for the unique antigen receptor-linked gene expression programs in mature and immature B cells.* J Exp Med, 1999. **190**(6): p. 749-56.
333. Monroe, J., *Up-regulation of c-fos expression is a component of the mIg signal transduction mechanism but is not indicative of competence for proliferation.* J Immunol, 1988. **140**(5): p. 1454-60.
334. Alizadeh, A.A., *et al.*, *Distinct types of diffuse large B-cell lymphoma identified by gene expression profiling.* Nature, 2000. **403**(6769): p. 503-11.